Acknowledgements:
Numerous physics colleagues who have educated me over the years

Parity Violation at Jefferson Lab and Beyond

Probing Nuclear and Nucleon Structure with PVES
Lecture IV

Krishna Kumar
University of Massachusetts, Amherst

CNUGS26, Jefferson Lab
June 5, 2026

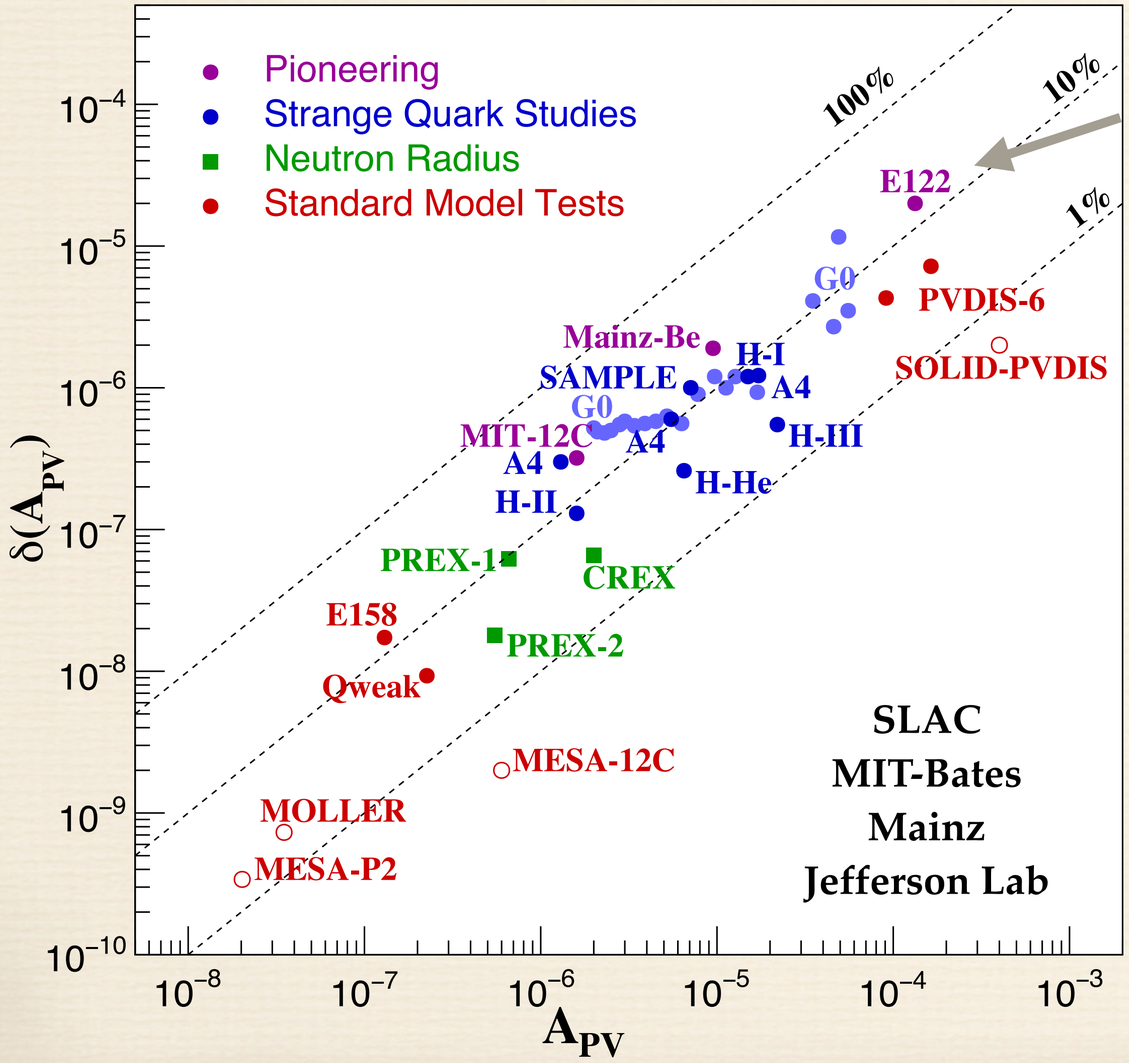
Lecture 4 Outline

- Strange Quark Content of the Proton
- Neutron Skin of a Heavy Nucleus
- PVES at the Electron Ion Collider
- Summary

Continuous interplay between probing hadron structure and electroweak physics

5 Decades of Progress

Parity-violating electron scattering has become a precision tool



Pioneering electron-quark PV DIS experiment SLAC E122

photocathodes, polarimetry, high power cryotargets, novel spectrometer concepts, nanometer beam stability, precision beam diagnostics, low noise electronics, radiation hard detectors

State-of-the-art:

- *sub-part per billion statistical reach and systematic control*
- *sub-1% normalization control*

Remainder of the Lecture

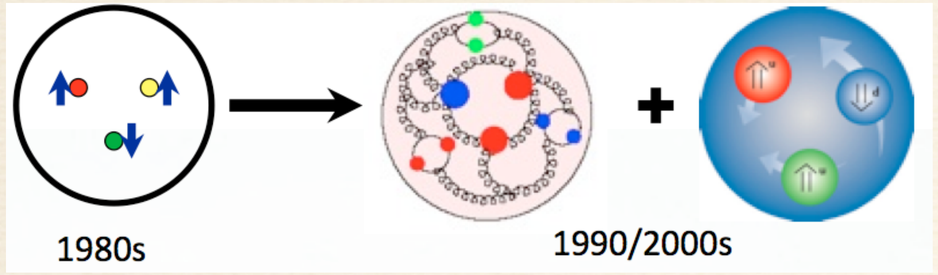
- *Strange Quark Form Factors*
- *Neutron Radius Measurements*
- *EIC Potential*

Strange Quark Content of the Proton

Late 1970's onwards, Quantum Chromodynamics (QCD) began to tackle the challenge of fundamental understanding of nuclear systems

Sea Quarks in the Proton

It became clear that proton is an extraordinarily complex object at small length scales

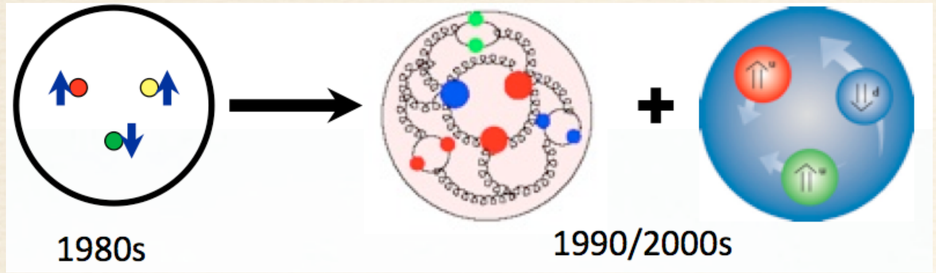




Late 1970's onwards, Quantum Chromodynamics (QCD) began to tackle the challenge of fundamental understanding of nuclear systems

Sea Quarks in the Proton

It became clear that proton is an extraordinarily complex object at small length scales





Nucleon charge and magnetization distributions:

$G_E(Q^2)$, $G_M(Q^2)$ — *electric and magnetic form factors*

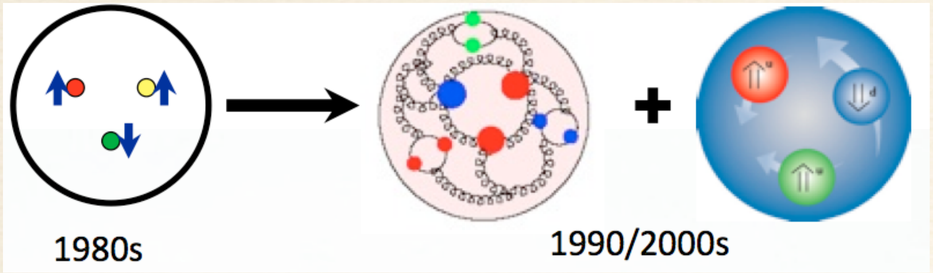
$G_E^p(0) = 1$ $\quad$ $G_M^p(0) = +2.79 \equiv \mu_p$

$G_E^n(0) = 0$ $\quad$ $G_M^n(0) = -1.91 \equiv \mu_n$

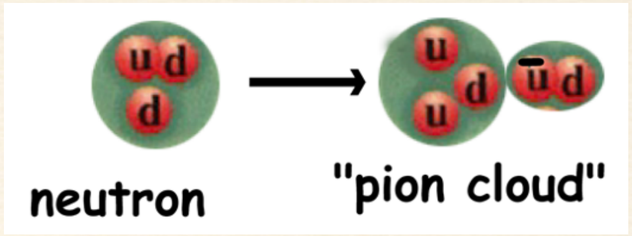
Late 1970's onwards, Quantum Chromodynamics (QCD) began to tackle the challenge of fundamental understanding of nuclear systems

Sea Quarks in the Proton

It became clear that proton is an extraordinarily complex object at small length scales







Possible models to explain the electric charge form factor of the neutron were being explored

Nucleon charge and magnetization distributions:

$G_E(Q^2)$, $G_M(Q^2)$

electric and magnetic form factors

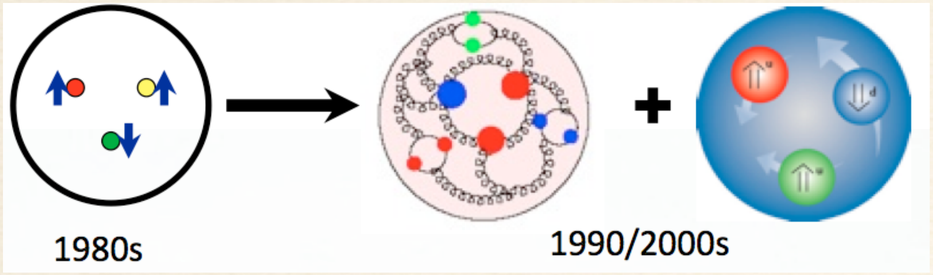
$G_E^p(0) = 1$ $\quad G_M^p(0) = +2.79 \equiv \mu_p$

$G_E^n(0) = 0$ $\quad G_M^n(0) = -1.91 \equiv \mu_n$

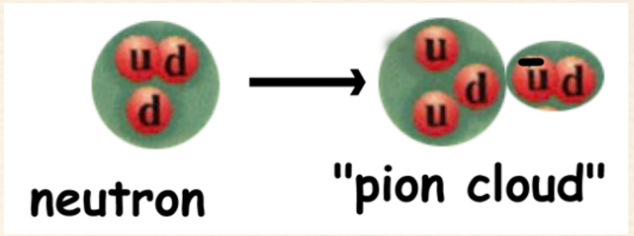
Late 1970's onwards, Quantum Chromodynamics (QCD) began to tackle the challenge of fundamental understanding of nuclear systems

Sea Quarks in the Proton

It became clear that proton is an extraordinarily complex object at small length scales







Possible models to explain the electric charge form factor of the neutron were being explored



Polarized lepton scattering off polarized protons showed that only 25% of the proton spin was being carried by valence quarks!

Nucleon charge and magnetization distributions:

$G_E(Q^2)$, $G_M(Q^2)$ — *electric and magnetic form factors*

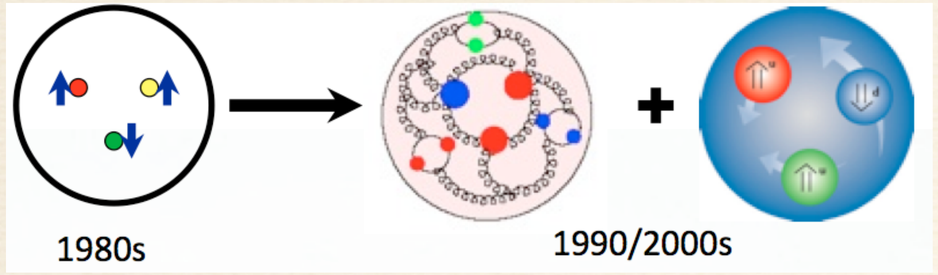
$G_E^p(0) = 1$ $\quad G_M^p(0) = +2.79 \equiv \mu_p$

$G_E^n(0) = 0$ $\quad G_M^n(0) = -1.91 \equiv \mu_n$

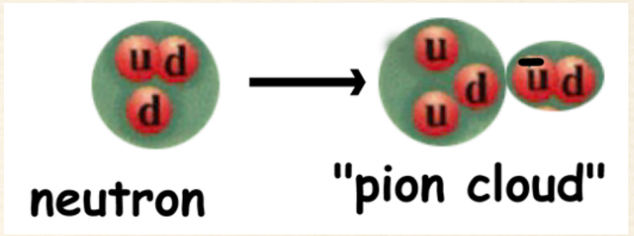
Late 1970's onwards, Quantum Chromodynamics (QCD) began to tackle the challenge of fundamental understanding of nuclear systems

Sea Quarks in the Proton

It became clear that proton is an extraordinarily complex object at small length scales







Possible models to explain the electric charge form factor of the neutron were being explored



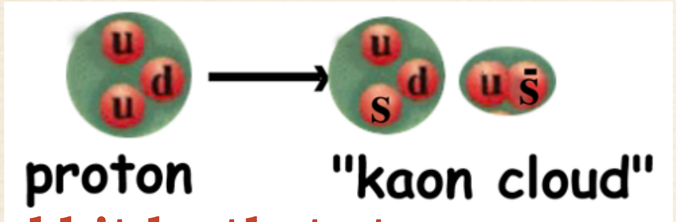
Polarized lepton scattering off polarized protons showed that only 25% of the proton spin was being carried by valence quarks!

Nucleon charge and magnetization distributions:

$G_E(Q^2)$, $G_M(Q^2)$ — *electric and magnetic form factors*

$G_E^p(0) = 1$ $\quad G_M^p(0) = +2.79 \equiv \mu_p$

$G_E^n(0) = 0$ $\quad G_M^n(0) = -1.91 \equiv \mu_n$

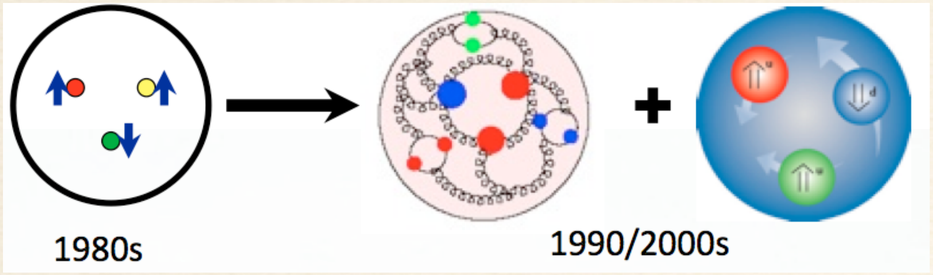


Could it be that strange sea quarks also affect proton properties?

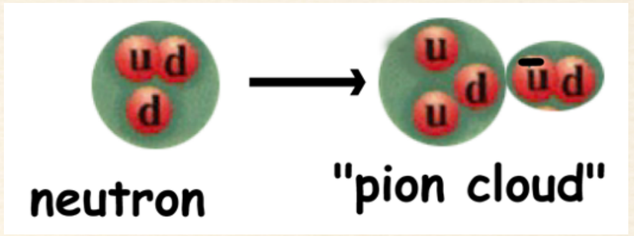
Late 1970's onwards, Quantum Chromodynamics (QCD) began to tackle the challenge of fundamental understanding of nuclear systems

Sea Quarks in the Proton

It became clear that proton is an extraordinarily complex object at small length scales







Possible models to explain the electric charge form factor of the neutron were being explored



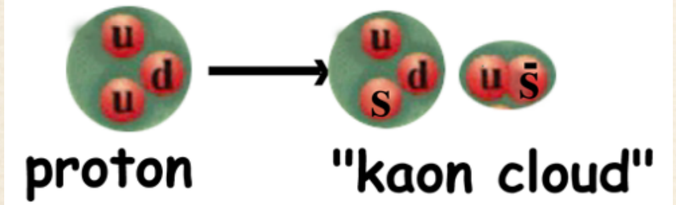
Polarized lepton scattering off polarized protons showed that only 25% of the proton spin was being carried by valence quarks!

Nucleon charge and magnetization distributions:

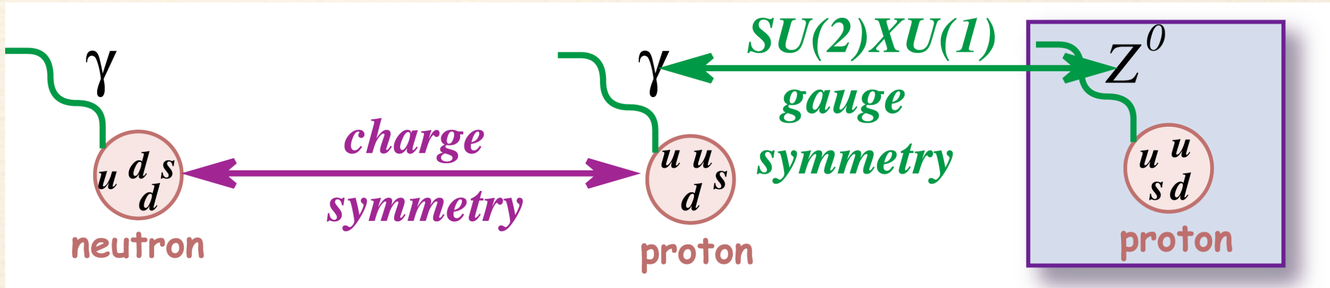
$G_E(Q^2), G_M(Q^2)$ — *electric and magnetic form factors*

$G_E^p(0) = 1$ $\quad G_M^p(0) = +2.79 \equiv \mu_p$

$G_E^n(0) = 0$ $\quad G_M^n(0) = -1.91 \equiv \mu_n$



Could it be that strange sea quarks also affect proton properties?



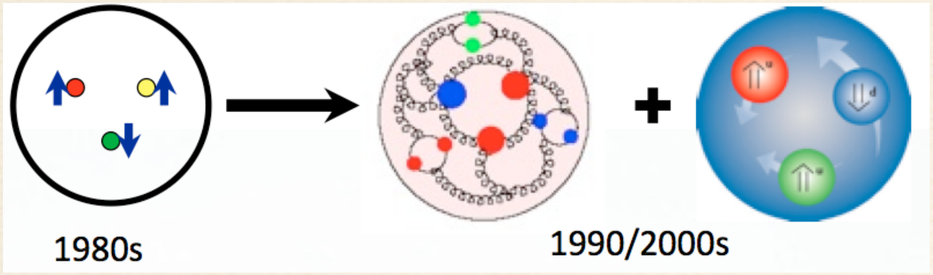
$$G_p^Z \sim (1 - 4\sin^2\theta_W)\, G_p^\gamma - G_n^\gamma - G_s$$

⇨ $G_E^s(Q^2), G_M^s(Q^2)$

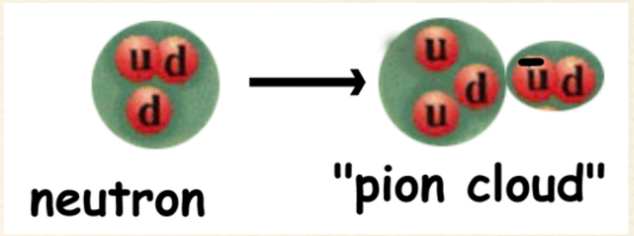
Late 1970's onwards, Quantum Chromodynamics (QCD) began to tackle the challenge of fundamental understanding of nuclear systems

Sea Quarks in the Proton

It became clear that proton is an extraordinarily complex object at small length scales







Possible models to explain the electric charge form factor of the neutron were being explored



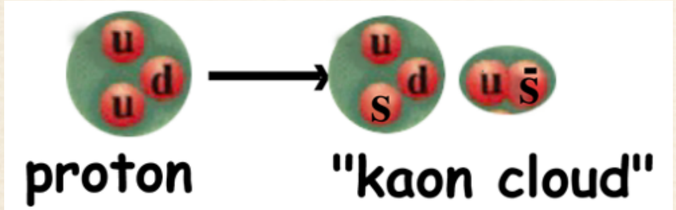
Polarized lepton scattering off polarized protons showed that only 25% of the proton spin was being carried by valence quarks!

Nucleon charge and magnetization distributions:

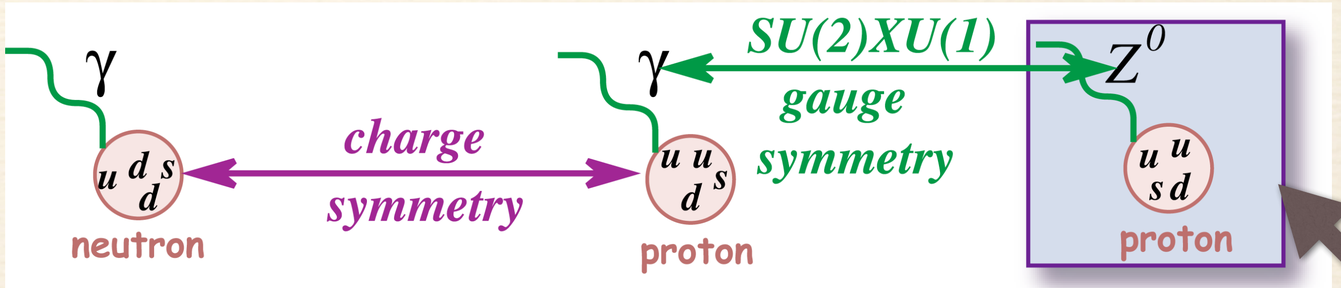
$G_E(Q^2), G_M(Q^2)$ — *electric and magnetic form factors*

$G_E^p(0) = 1$ $\quad G_M^p(0) = +2.79 \equiv \mu_p$

$G_E^n(0) = 0$ $\quad G_M^n(0) = -1.91 \equiv \mu_n$



Could it be that strange sea quarks also affect proton properties?

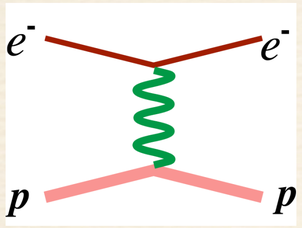


$$G_p^Z \sim (1 - 4\sin^2\theta_W)\, G_p^\gamma - G_n^\gamma - G_s$$

Parity-violating electron scattering

$\Rightarrow$ $G_E^s(Q^2), G_M^s(Q^2)$

Forward and Backward PV Elastic Scattering



A_{PV} for elastic e-p scattering:

$$A = \left[\frac{-G_F Q^2}{4\pi\alpha\sqrt{2}}\right]\frac{A_E + A_M + A_A}{\sigma_p}$$

$$A_E = \epsilon\, G_E^p G_E^Z \qquad A_M = \tau\, G_M^p G_M^Z \qquad A_A = (1 - 4\sin^2\theta_W)\epsilon'\, G_M^p \tilde{G}_A$$

Forward angle | Backward angle

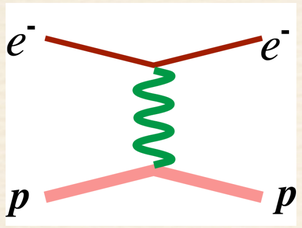
Spin=0,T=0 (^{4}He): G^s_E only!

nuclear corrections require
forward angle, low Q^2 only

Deuterium QE (back-angle):

Enhanced G_A

Forward and Backward PV Elastic Scattering



A_{PV} for elastic e-p scattering:

$$A = \left[\frac{-G_F Q^2}{4\pi\alpha\sqrt{2}}\right]\frac{A_E + A_M + A_A}{\sigma_p}$$

$$A_E = \epsilon\, G_E^p G_E^Z \qquad A_M = \tau\, G_M^p G_M^Z \qquad A_A = (1 - 4\sin^2\theta_W)\epsilon'\, G_M^p \tilde{G}_A$$

Forward angle | Backward angle

Spin=0,T=0 (^{4}He): G^s_E only!

nuclear corrections require forward angle, low Q^2 only

Deuterium QE (back-angle):

Enhanced G_A

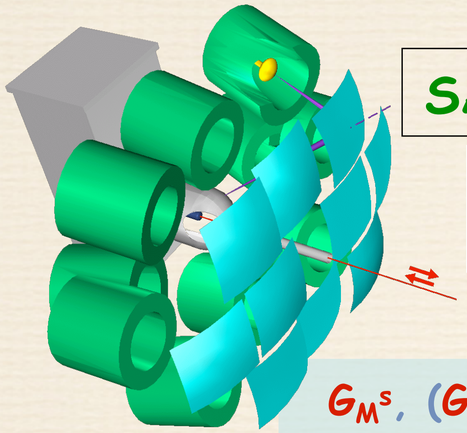
$$G_E^{p,Z} = \left(1 - \frac{8}{3}\sin^2\theta_W\right) G_E^u - \left(1 - \frac{4}{3}\sin^2\theta_W\right) G_E^d - \left(1 - \frac{4}{3}\sin^2\theta_W\right) G_E^s$$

PV Electron-Nucleon Elastic Scattering: The Experiments

1990s - 2010s

PV Electron-Nucleon Elastic Scattering: The Experiments

1990s - 2010s



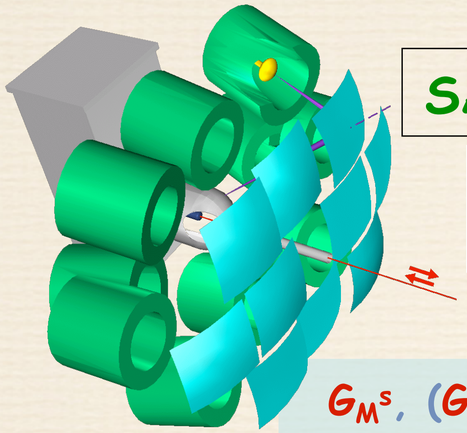
SAMPLE at MIT-Bates

open geometry, integrating

G_M^s, (G_A) at Q^2 = 0.1 GeV^2

PV Electron-Nucleon Elastic Scattering: The Experiments

1990s - 2010s



SAMPLE at MIT-Bates

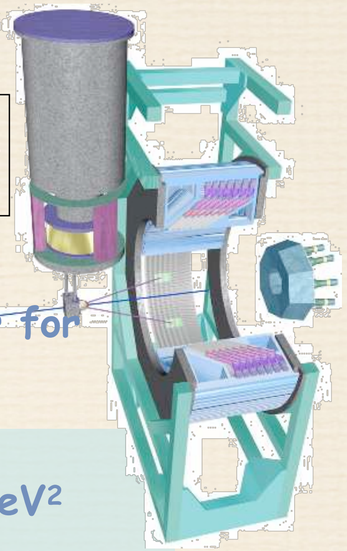
open geometry, integrating

G_M^s, (G_A) at Q^2 = 0.1 GeV^2

A4 at Mainz

Open geometry

Fast counting calorimeter for background rejection



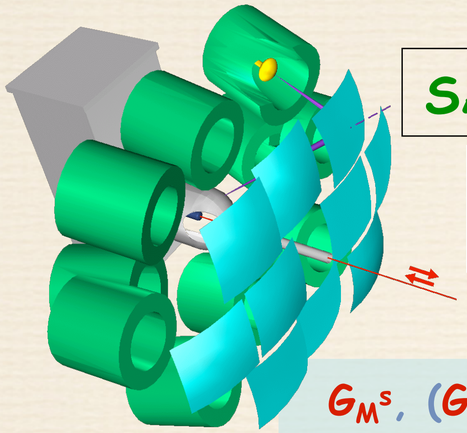
G_E^s + 0.23 G_M^s at Q^2 = 0.23 GeV^2

G_E^s + 0.10 G_M^s at Q^2 = 0.1 GeV^2

G_M^s, G_A^e at Q^2 = 0.23 GeV^2

PV Electron-Nucleon Elastic Scattering: The Experiments

1990s - 2010s

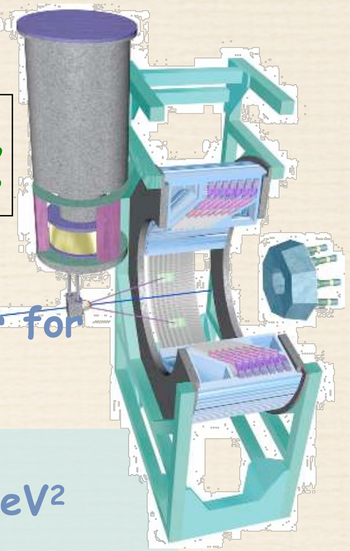


SAMPLE at MIT-Bates

open geometry, integrating

G_M^s, (G_A) at Q^2 = 0.1 GeV^2

A4 at Mainz



Open geometry

Fast counting calorimeter for background rejection

G_E^s + 0.23 G_M^s at Q^2 = 0.23 GeV^2

G_E^s + 0.10 G_M^s at Q^2 = 0.1 GeV^2

G_M^s, G_A^e at Q^2 = 0.23 GeV^2

HAPPEX at Jefferson Lab

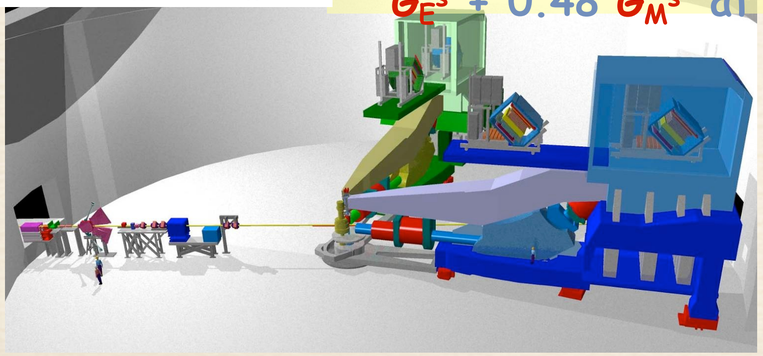
Precision spectrometer, integrating

G_E^s + 0.39 G_M^s at Q^2 = 0.48 GeV^2

G_E^s + 0.08 G_M^s at Q^2 = 0.1 GeV^2

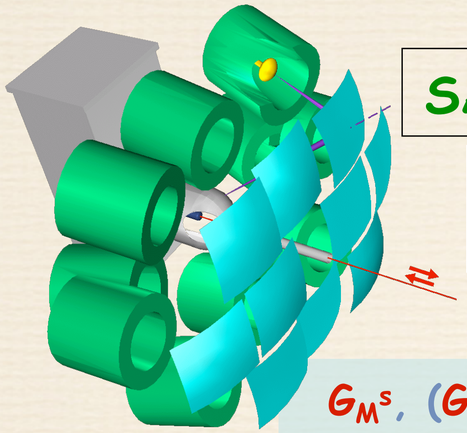
G_E^s at Q^2 = 0.1 GeV^2 (^{4}He)

G_E^s + 0.48 G_M^s at Q^2 = 0.62 GeV^2



PV Electron-Nucleon Elastic Scattering: The Experiments

1990s - 2010s

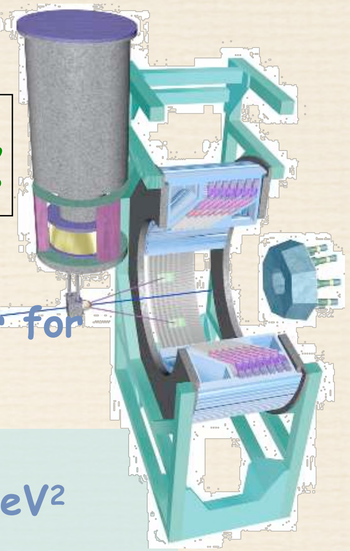


SAMPLE at MIT-Bates

open geometry, integrating

G_M^s, (G_A) at Q^2 = 0.1 GeV^2

A4 at Mainz



Open geometry

Fast counting calorimeter for background rejection

G_E^s + 0.23 G_M^s at Q^2 = 0.23 GeV^2

G_E^s + 0.10 G_M^s at Q^2 = 0.1 GeV^2

G_M^s, G_A^e at Q^2 = 0.23 GeV^2

HAPPEX at Jefferson Lab

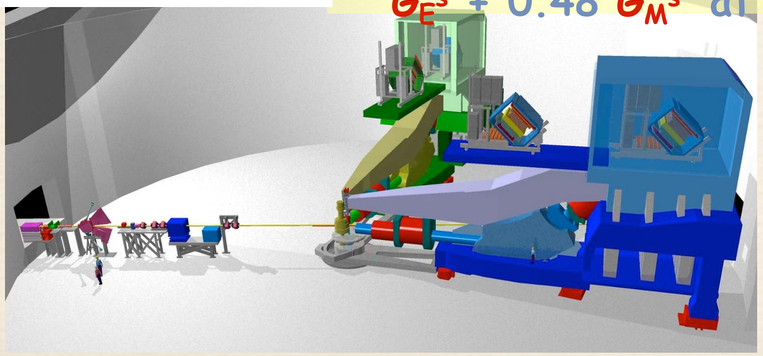
Precision spectrometer, integrating

G_E^s + 0.39 G_M^s at Q^2 = 0.48 GeV^2

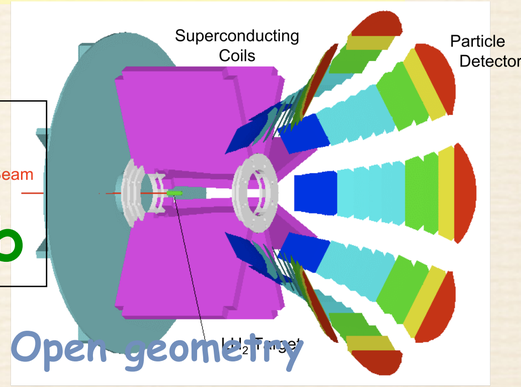
G_E^s + 0.08 G_M^s at Q^2 = 0.1 GeV^2

G_E^s at Q^2 = 0.1 GeV^2 (^{4}He)

G_E^s + 0.48 G_M^s at Q^2 = 0.62 GeV^2



G0 at Jefferson Lab



Open geometry

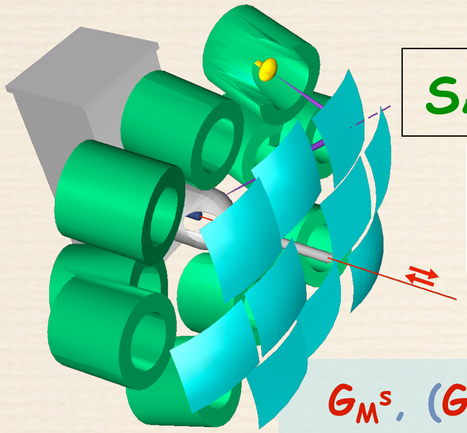
Fast counting with magnetic spectrometer + TOF for background rejection

G_E^s + η G_M^s over Q^2 = [0.12,1.0] GeV^2

G_M^s, G_A^e at Q^2 = 0.23, 0.62 GeV^2

PV Electron-Nucleon Elastic Scattering: The Experiments

1990s - 2010s

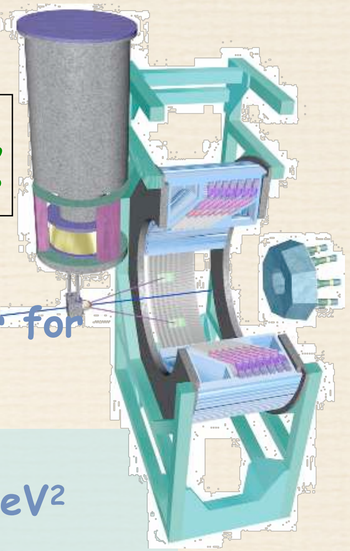


SAMPLE at MIT-Bates

open geometry, integrating

G_M^s, (G_A) at Q^2 = 0.1 GeV^2

A4 at Mainz



Open geometry

Fast counting calorimeter for background rejection

G_E^s + 0.23 G_M^s at Q^2 = 0.23 GeV^2

G_E^s + 0.10 G_M^s at Q^2 = 0.1 GeV^2

G_M^s, G_A^e at Q^2 = 0.23 GeV^2

HAPPEX at Jefferson Lab

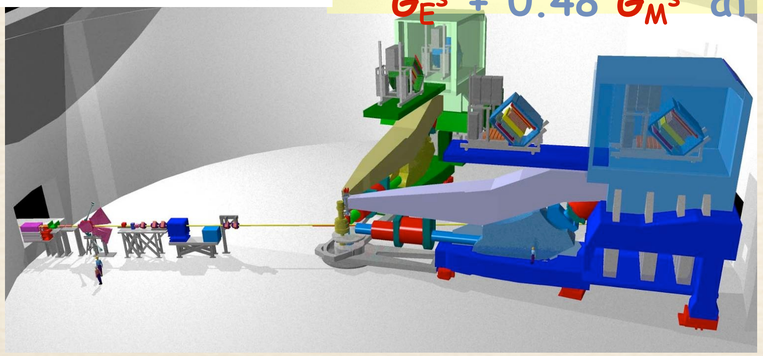
Precision spectrometer, integrating

G_E^s + 0.39 G_M^s at Q^2 = 0.48 GeV^2

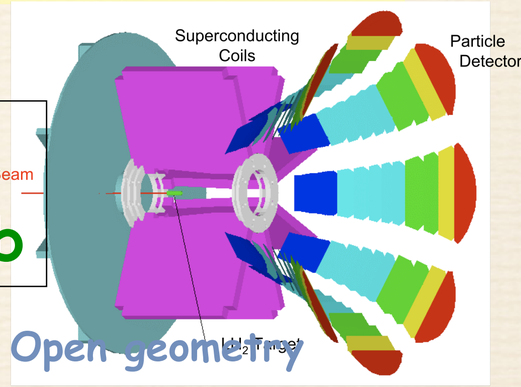
G_E^s + 0.08 G_M^s at Q^2 = 0.1 GeV^2

G_E^s at Q^2 = 0.1 GeV^2 (^{4}He)

G_E^s + 0.48 G_M^s at Q^2 = 0.62 GeV^2



G0 at Jefferson Lab



Open geometry

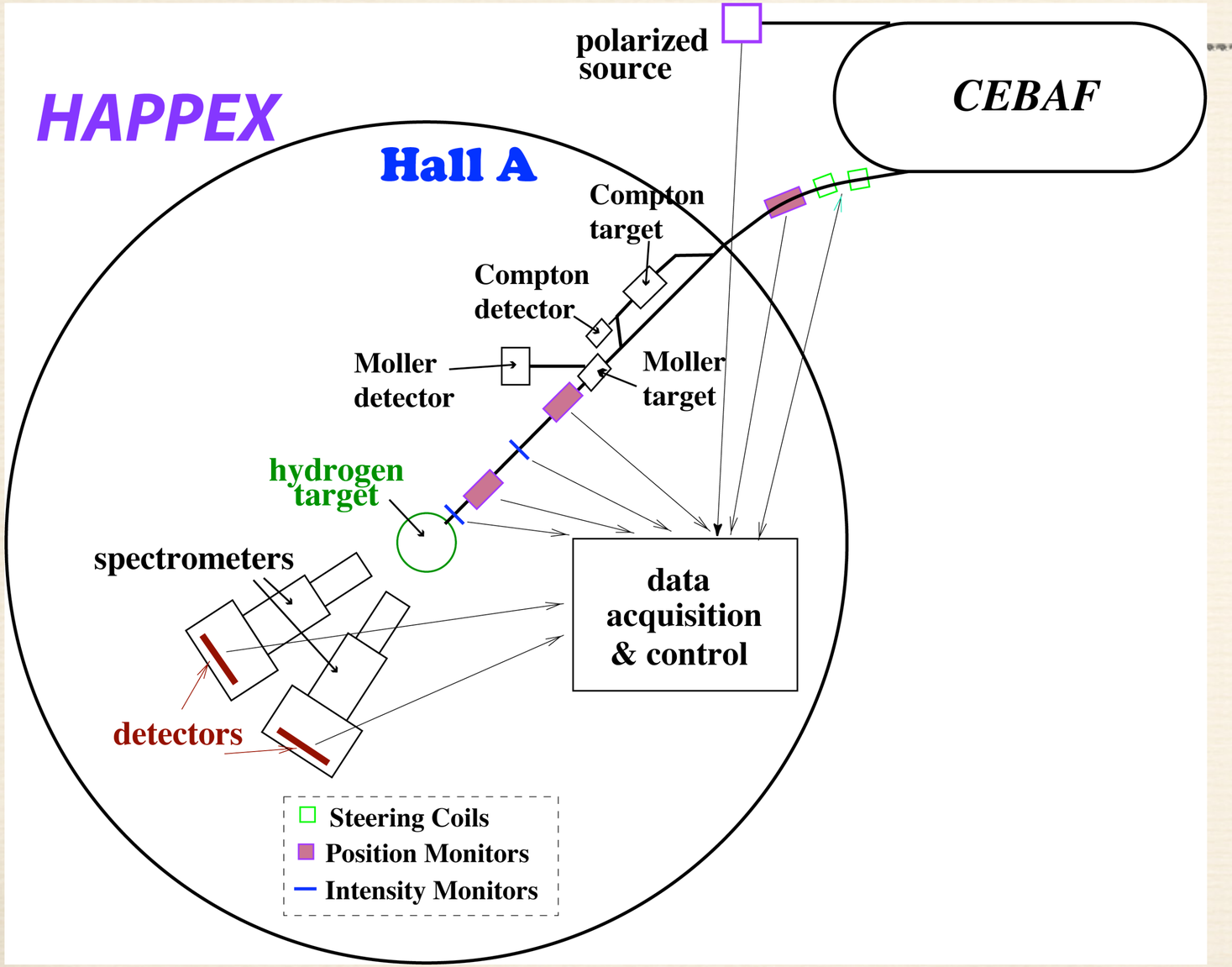
Fast counting with magnetic spectrometer + TOF for background rejection

G_E^s + η G_M^s over Q^2 = [0.12,1.0] GeV^2

G_M^s, G_A^e at Q^2 = 0.23, 0.62 GeV^2

Typical asymmetries: 10's of ppm

HAPPEX in Hall A



1998-99: Q^2=0.5 GeV^2, ^{1}H

2004-05: Q^2=0.1 GeV^2, ^{1}H, ^{4}He

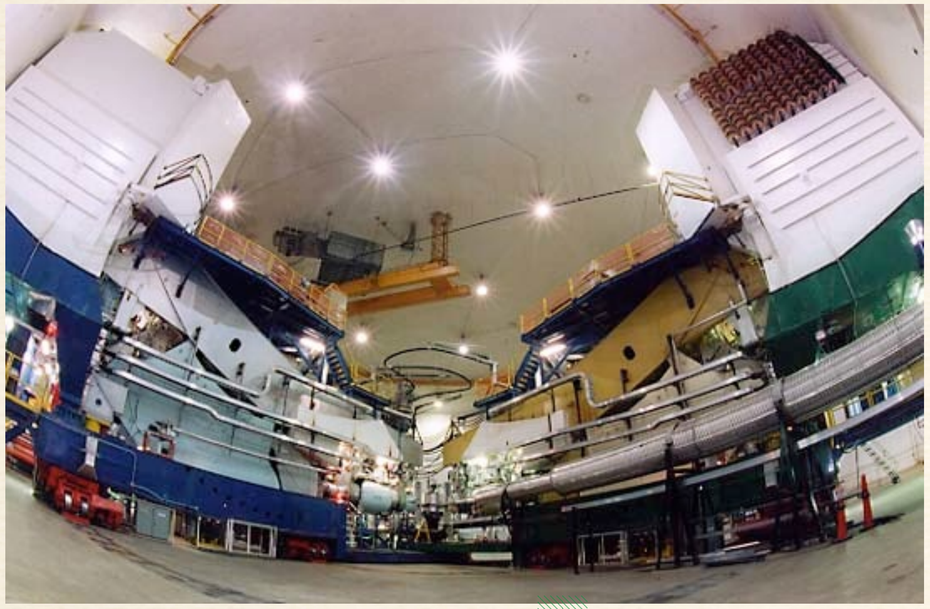
Scattering angle 12.5^o to 6^o with addition of septum magnets

The HAPPEX Collaboration

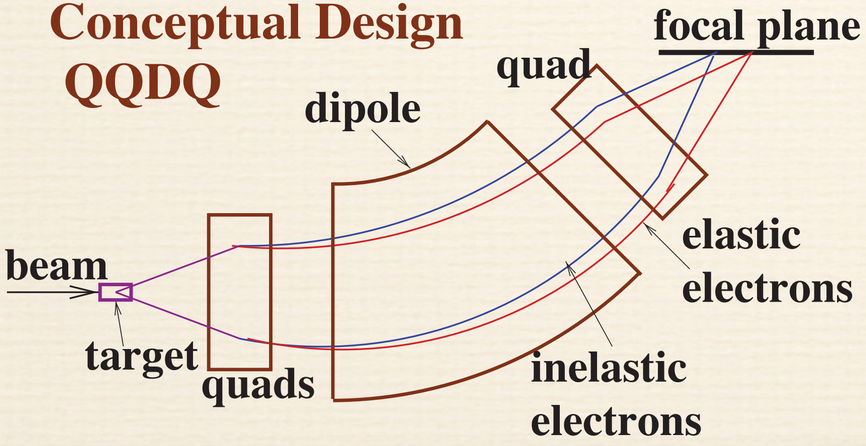
Thomas Jefferson National Accelerator Facility – Argonne National Laboratory – CSU, Los Angeles -William and Mary – Duke –
DSM/DAPNIA/SPhN CEA Saclay - FIU – Harvard - INFN, Rome - INFN, Bari – IAE, Beijing –
IPT Kharkov - Jozef Stefan Institute – Kent State - MIT – NPIRAS, St. Petersburg – ODU – Rutgers - Smith College – Syracuse – Temple – U. Blaise Pascal – U. of Illinois Urbana-Champagne – UMass, Amherst –
U. of Kentucky – U. of Virginia – UST, Heifei

late 1990's

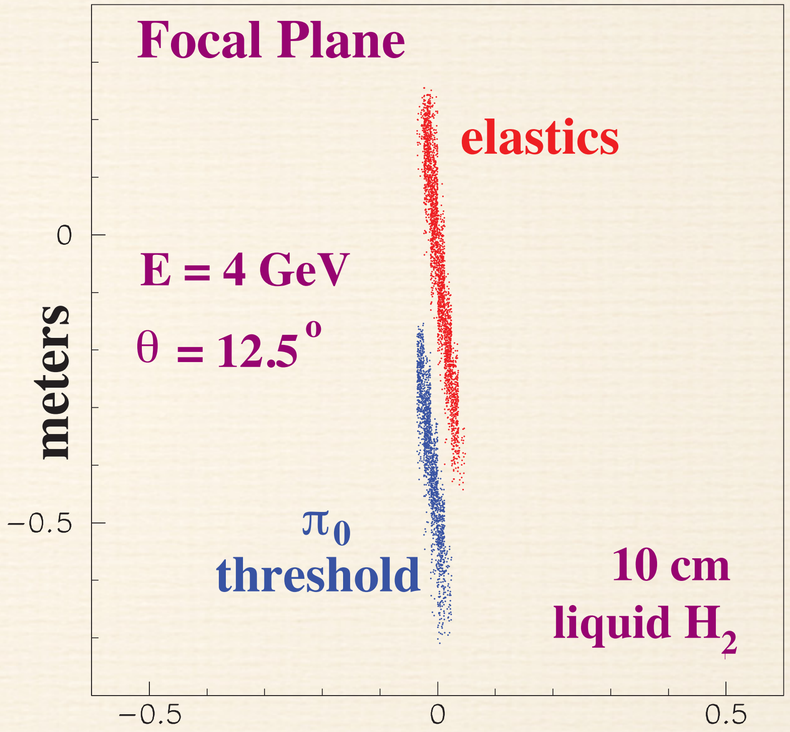
HRS in Hall A

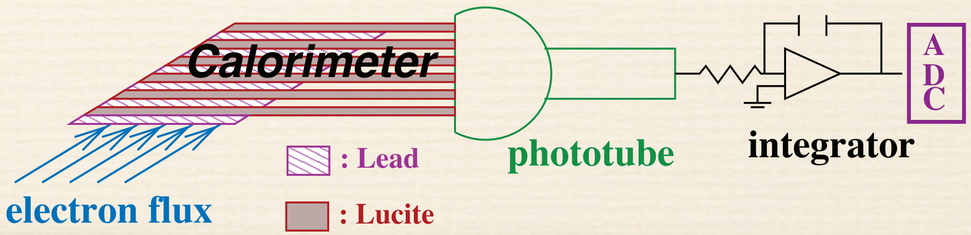


Conceptual Design
QQDQ

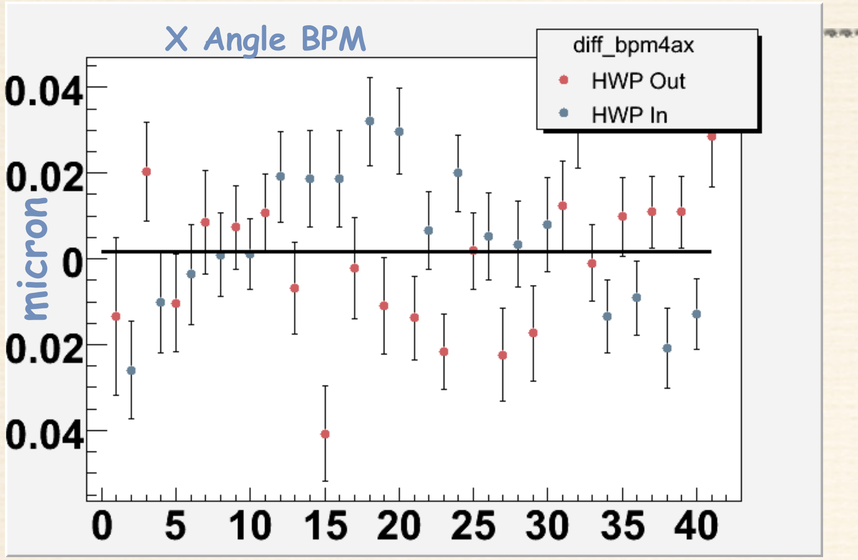


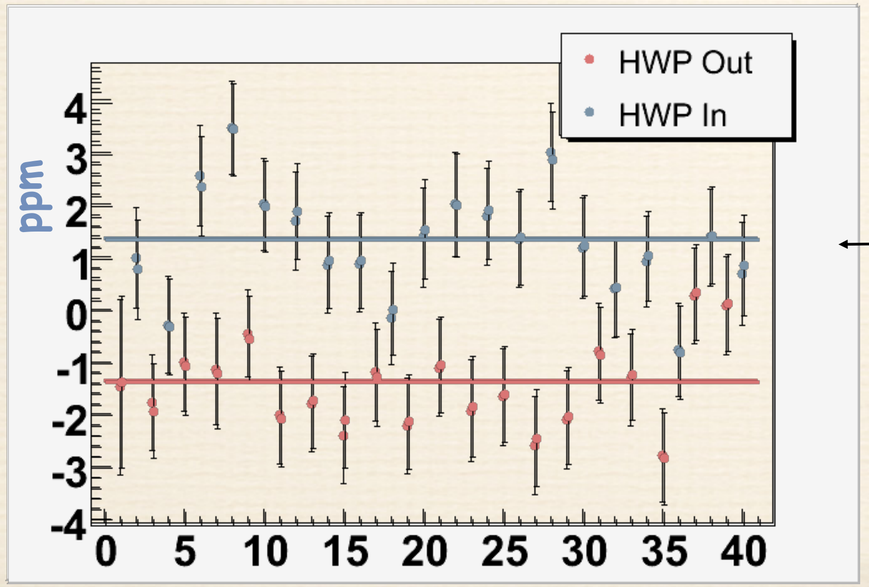
e^- Distribution at Detectors





HAPPEXII Final Results





Surpassed Beam Asymmetry Goals for Hydrogen Run

Energy: -0.25 ppb

X Target: 1 nm

X Angle: 2 nm

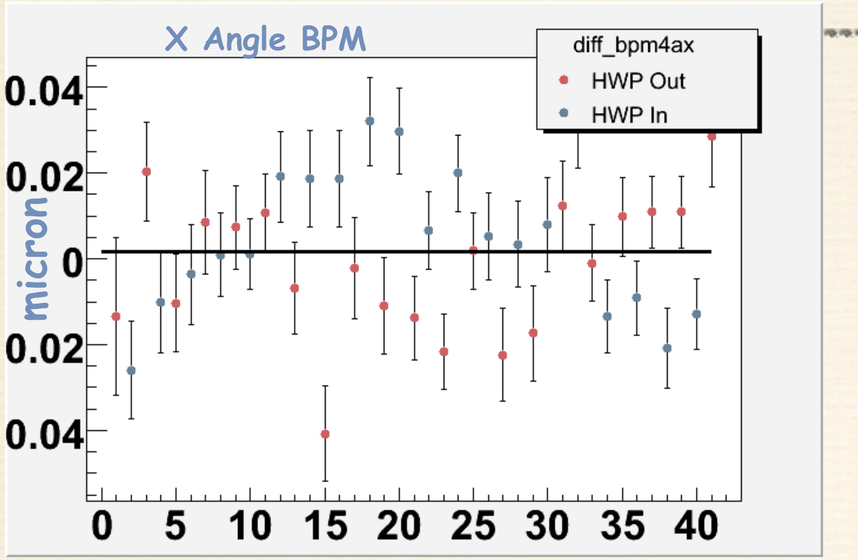
Y Target : 1 nm

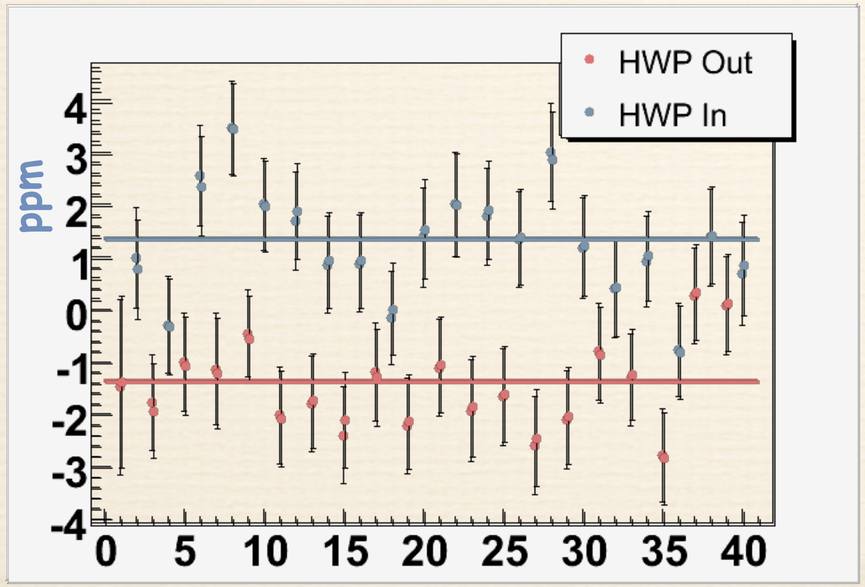
Y Angle: <1 nm

Corrected and Raw, Left arm alone, Superimposed!

Total correction for beam position asymmetry on Left, Right, or ALL detector: 10 ppb

HAPPEXII Final Results





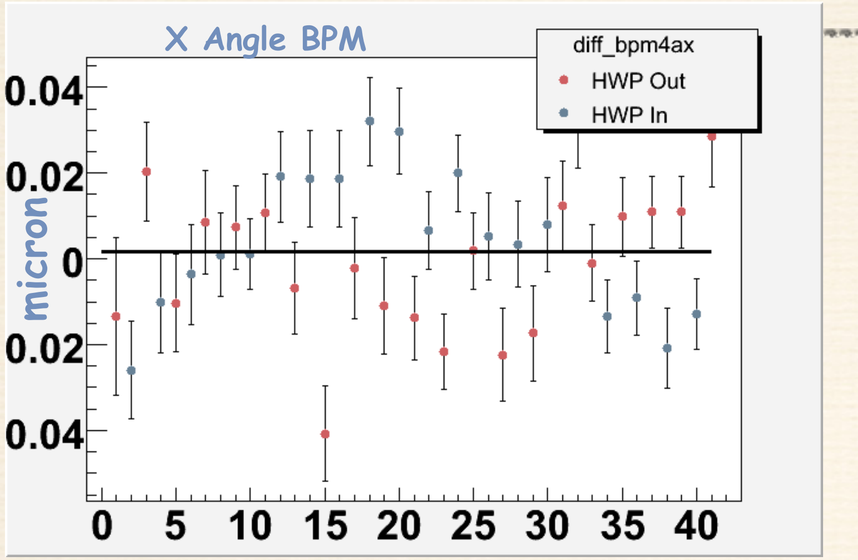
Hydrogen

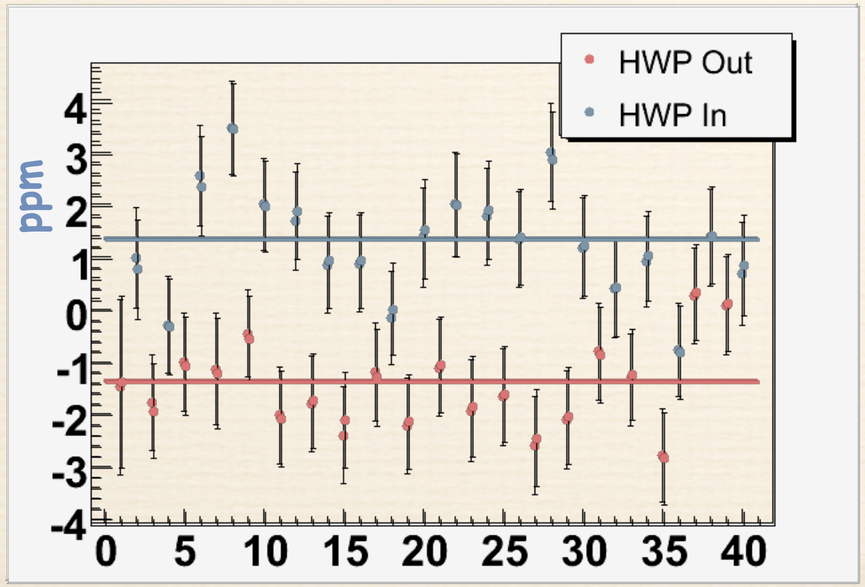
Systematic control ~ 10^{-8}

A_{PV} = -1.58 ± 0.12 *(stat)* ± 0.04 *(syst)* *ppm*

$A(G^s=0)$ = -1.66 ppm ± 0.05 ppm

HAPPEXII Final Results





Hydrogen

Systematic control ~ 10^{-8}

A_{PV} = -1.58 ± 0.12 *(stat)* ± 0.04 *(syst)* *ppm*

$A(G^s=0)$ = -1.66 ppm ± 0.05 ppm

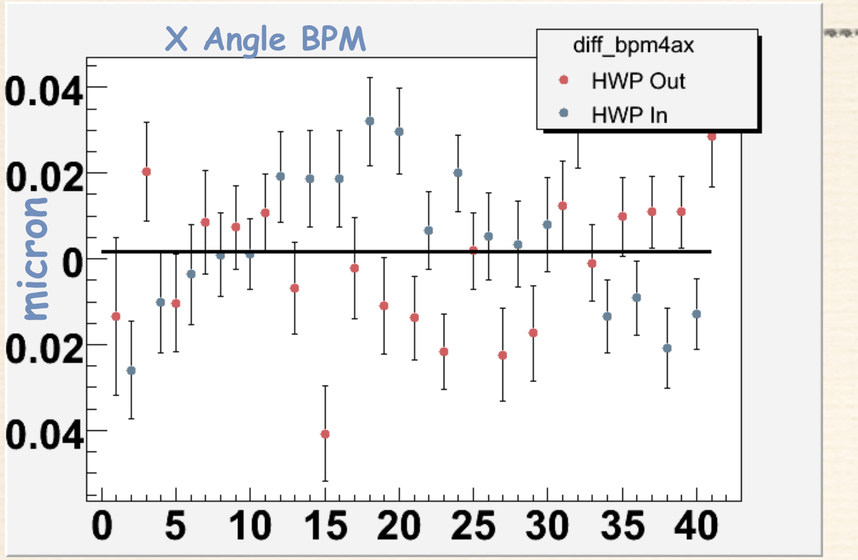
Helium

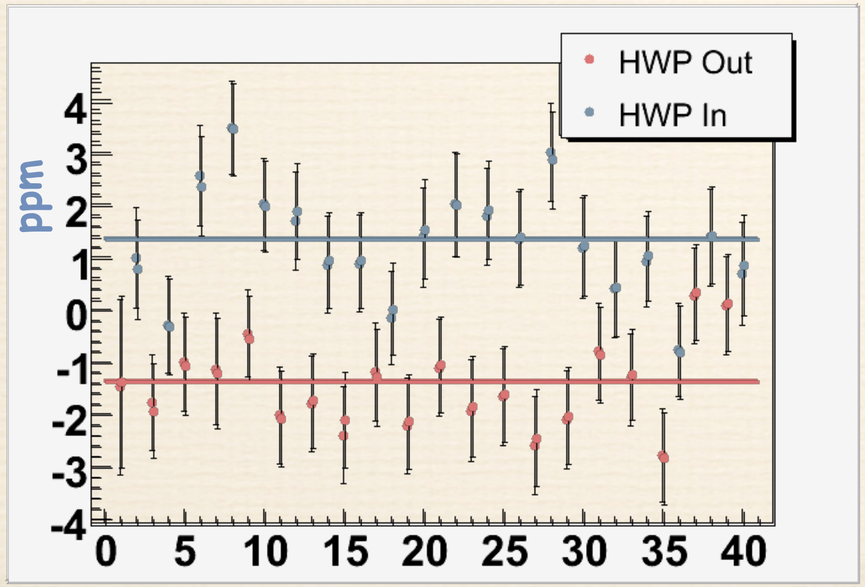
Normalization control ~ 2%

A_{PV} = +6.40 ± 0.23 *(stat)* ± 0.12 *(syst)* *ppm*

$A(G^s=0)$ = +6.37 ppm

HAPPEXII Final Results





Hydrogen

Systematic control ~ 10^{-8}

A_{PV} = -1.58 ± 0.12 *(stat)* ± 0.04 *(syst)* *ppm*

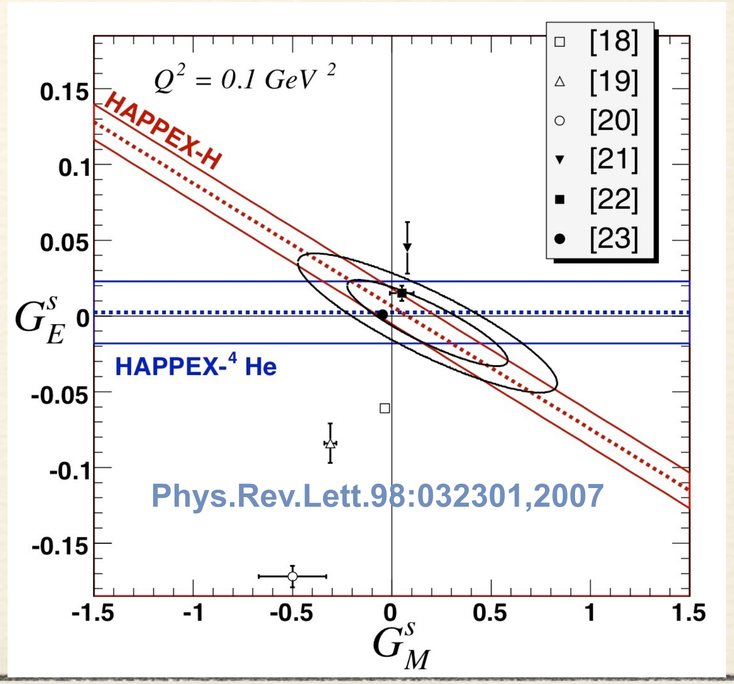
$A(G^s=0)$ = -1.66 ppm ± 0.05 ppm

Helium

Normalization control ~ 2%

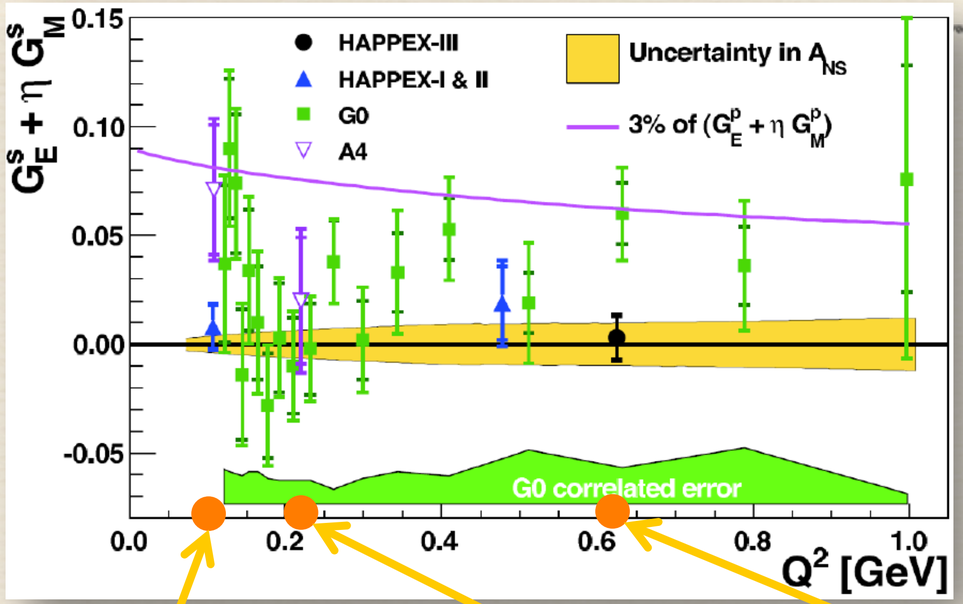
A_{PV} = +6.40 ± 0.23 *(stat)* ± 0.12 *(syst)* *ppm*

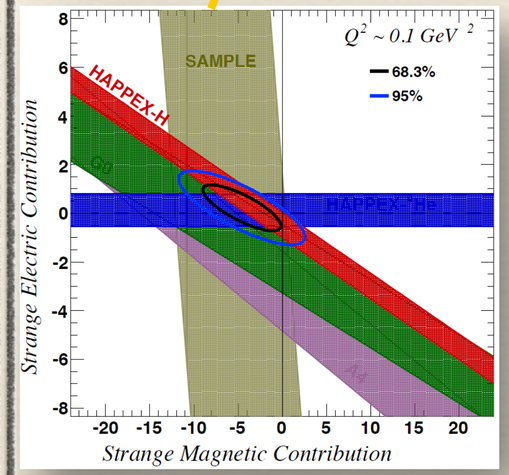
$A(G^s=0)$ = +6.37 ppm

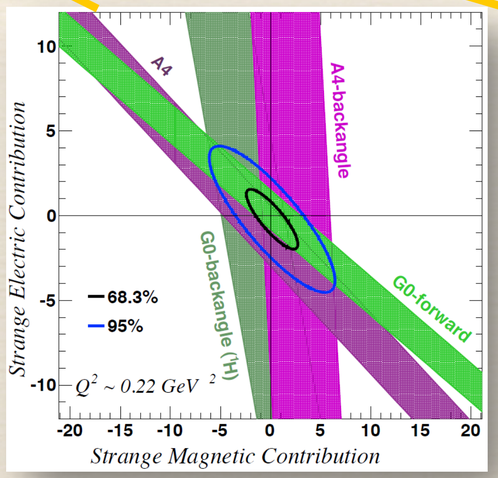


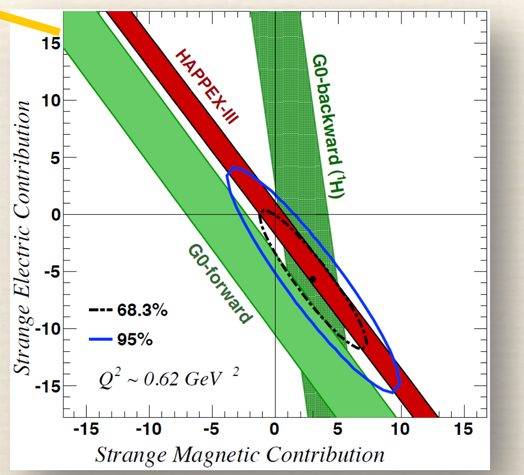
1990 - 2010

What have we learnt?



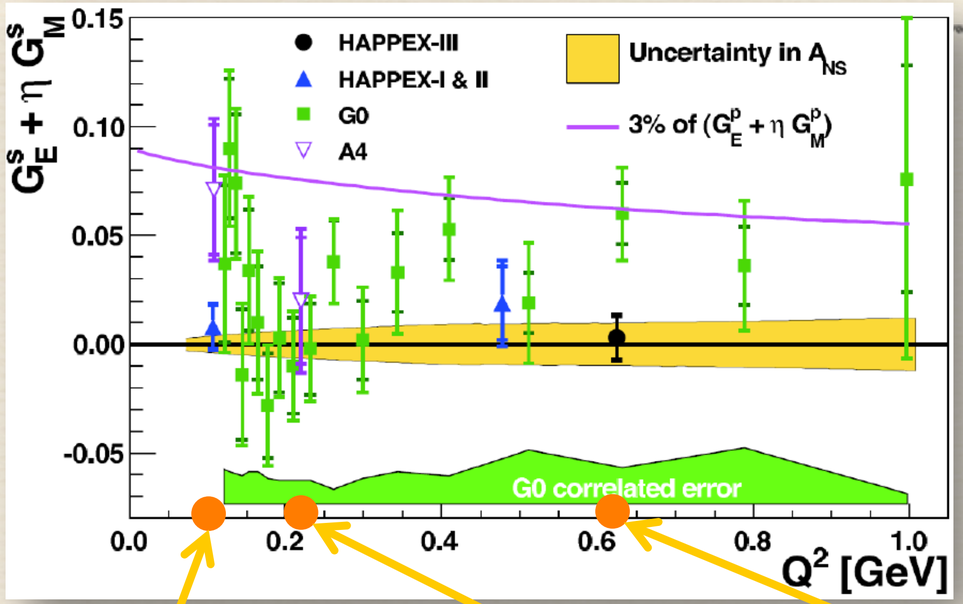




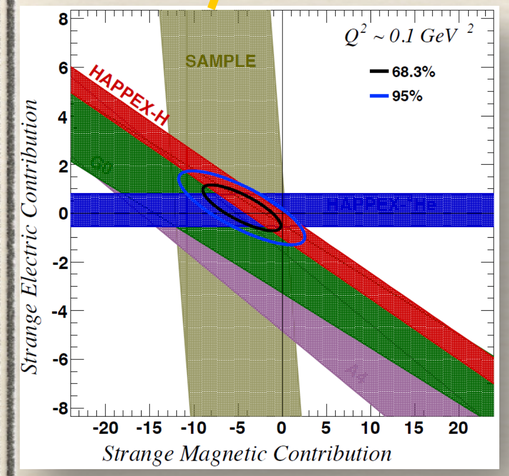


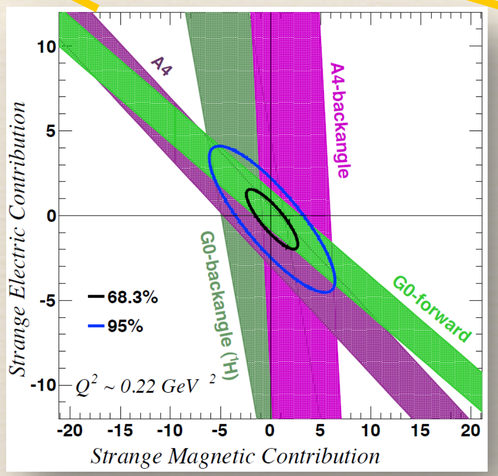
1990 - 2010

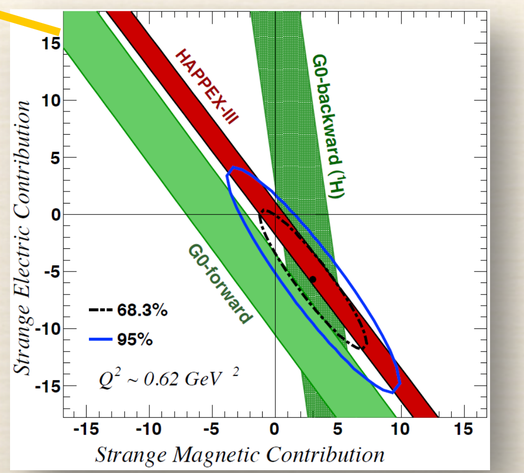
What have we learnt?



- Sensitive Flavor separation at three Q^2 values
- Strange quarks are no more than a few % of the proton's electromagnetic structure
- Modern lattice QCD results are in agreement

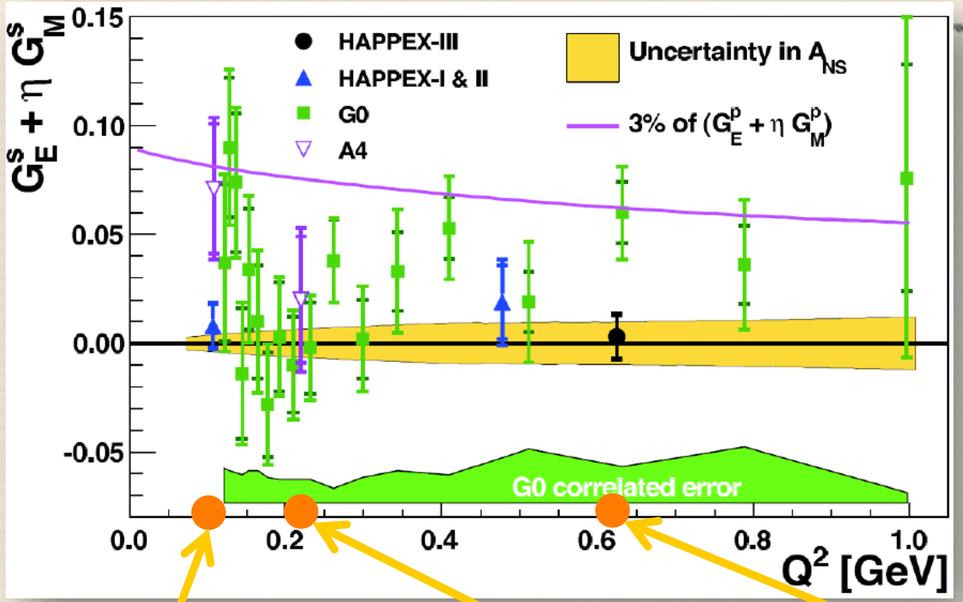




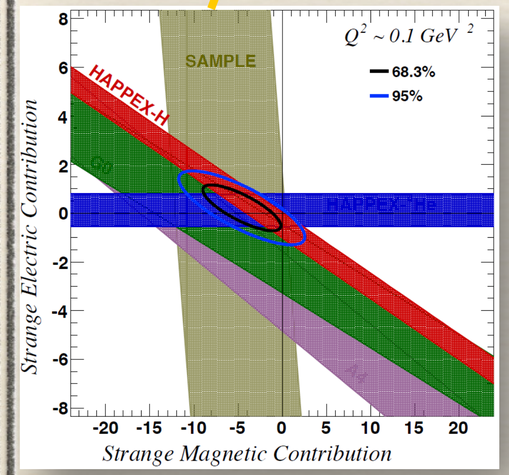


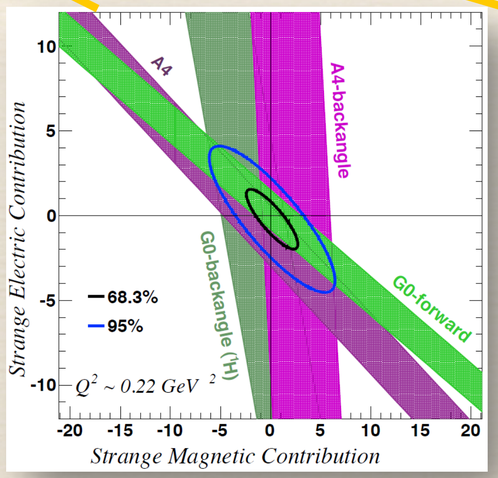
1990 - 2010

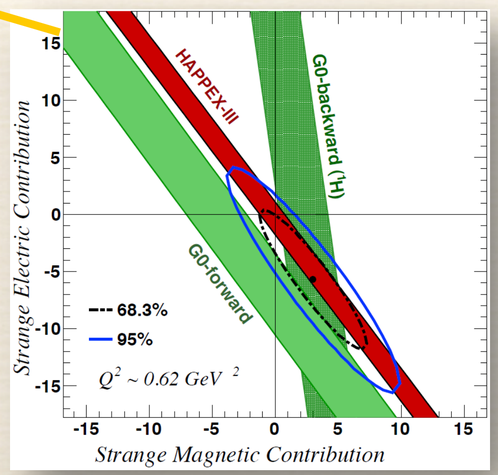
What have we learnt?



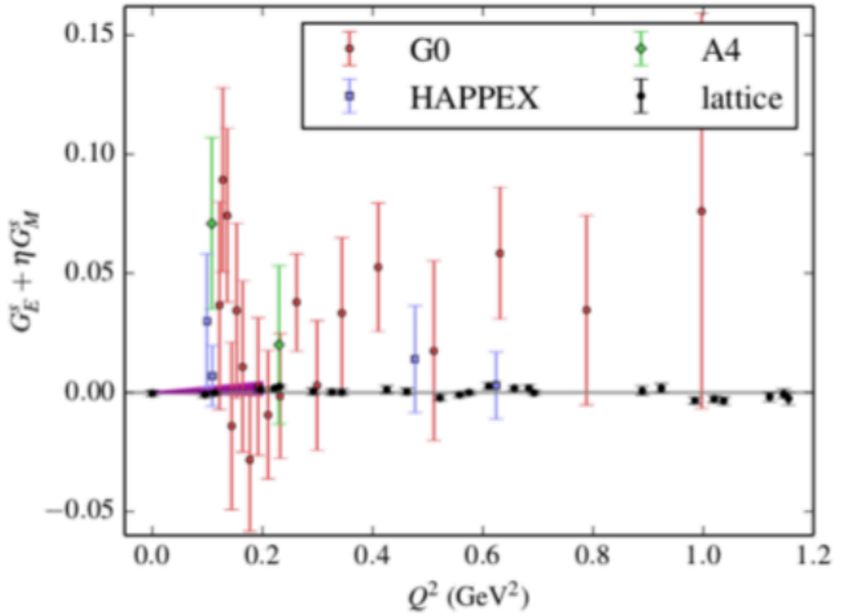
- Sensitive Flavor separation at three Q^2 values
- Strange quarks are no more than a few % of the proton's electromagnetic structure
- Modern lattice QCD results are in agreement





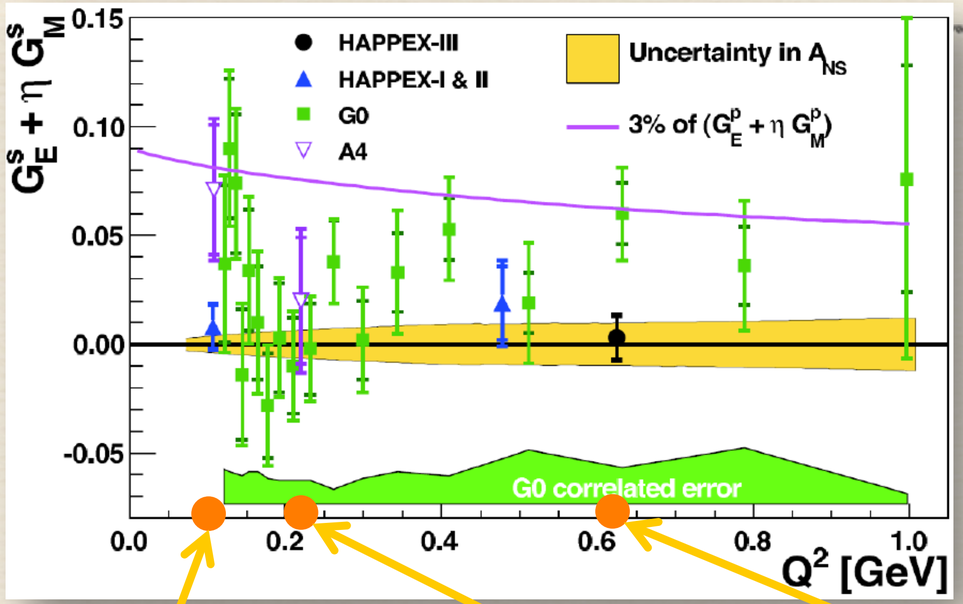


J.Green etal, 2015



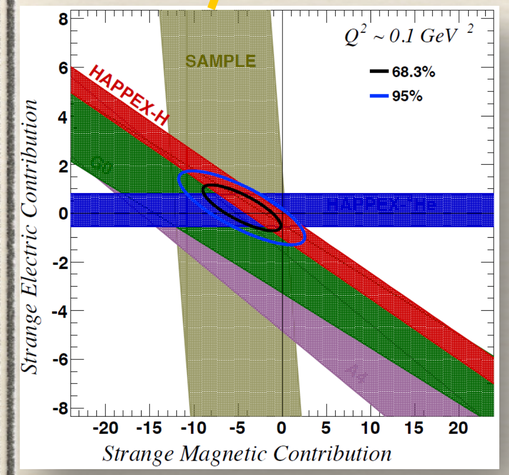
1990 - 2010

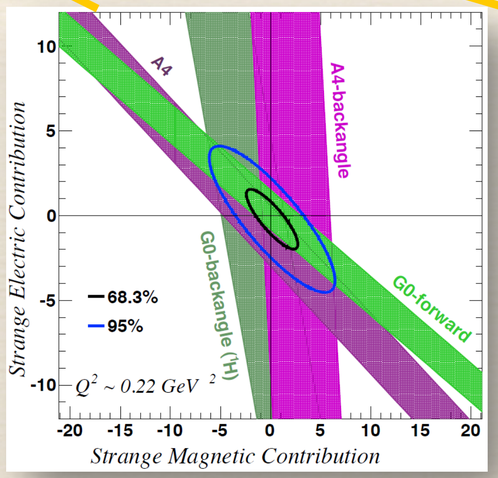
What have we learnt?

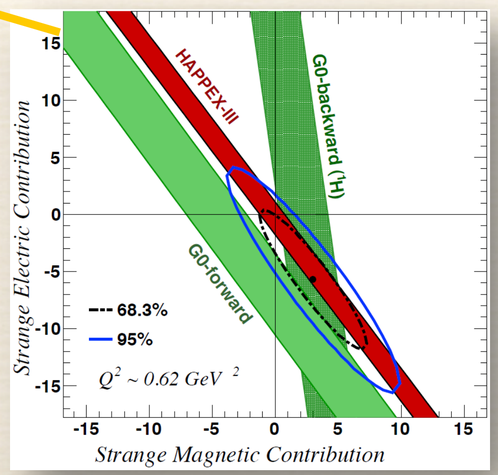


- Sensitive Flavor separation at three Q^2 values
- Strange quarks are no more than a few % of the proton's electromagnetic structure
- Modern lattice QCD results are in agreement

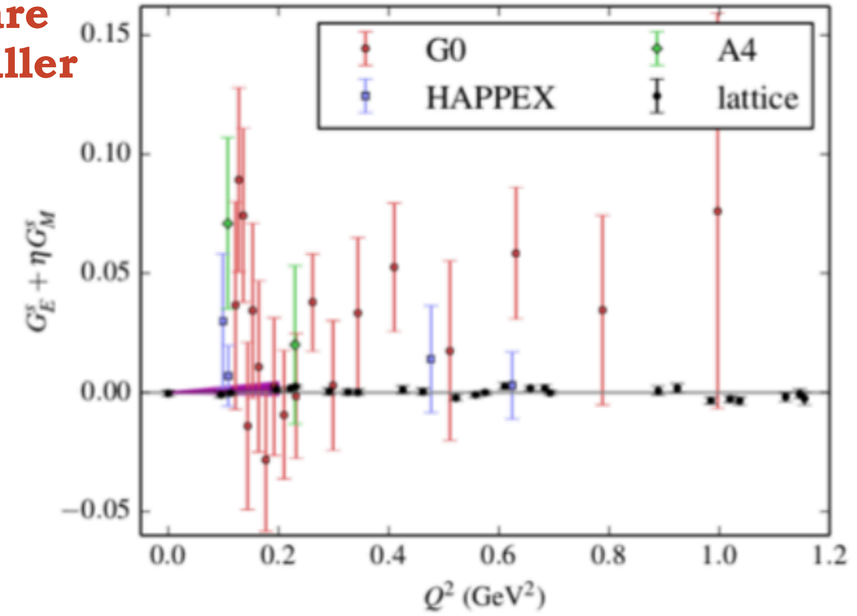
Latest lattice calculations say strange quark form factors are indeed non-zero but they are an order of magnitude smaller than these uncertainties



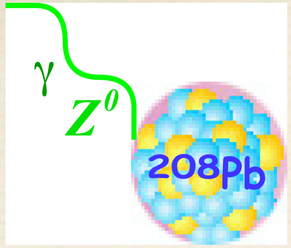




J.Green etal, 2015



Neutron Skin of a Heavy Nucleus

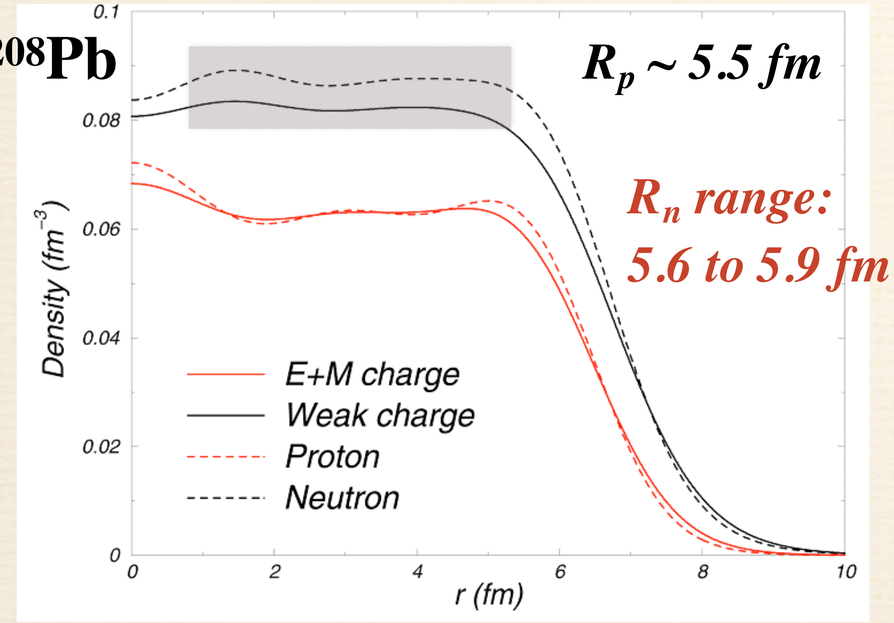


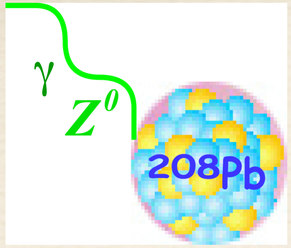
PV Elastic Scattering off Heavy Nuclei: Neutron Densities

2010's

Photon Exchange

$$M^{EM} = \frac{4\pi\alpha}{Q^2} F_p\left(Q^2\right)$$



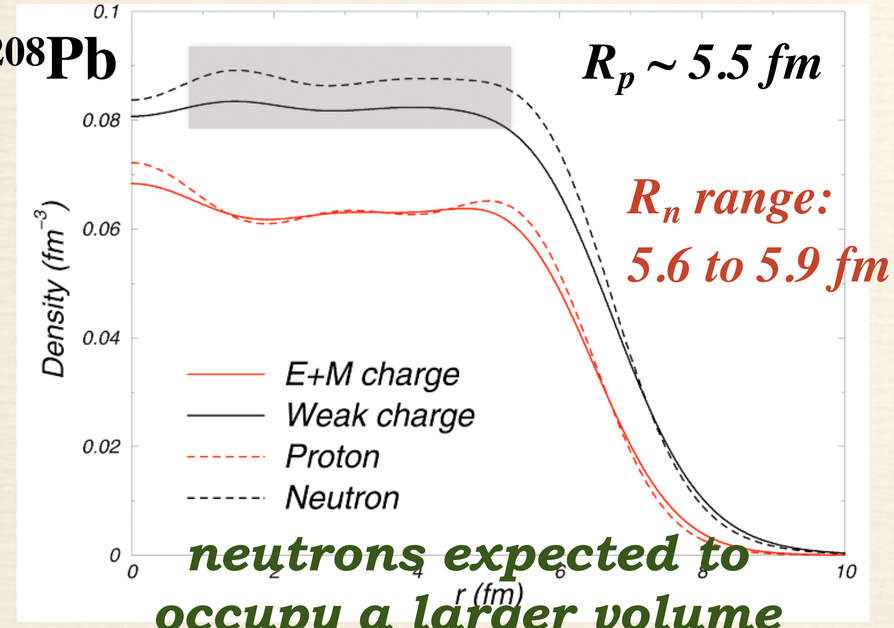


PV Elastic Scattering off Heavy Nuclei: Neutron Densities

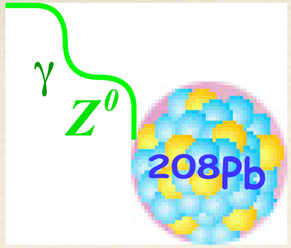
2010's

Photon Exchange

$$M^{EM} = \frac{4\pi\alpha}{Q^2} F_p\left(Q^2\right)$$



neutrons expected to occupy a larger volume



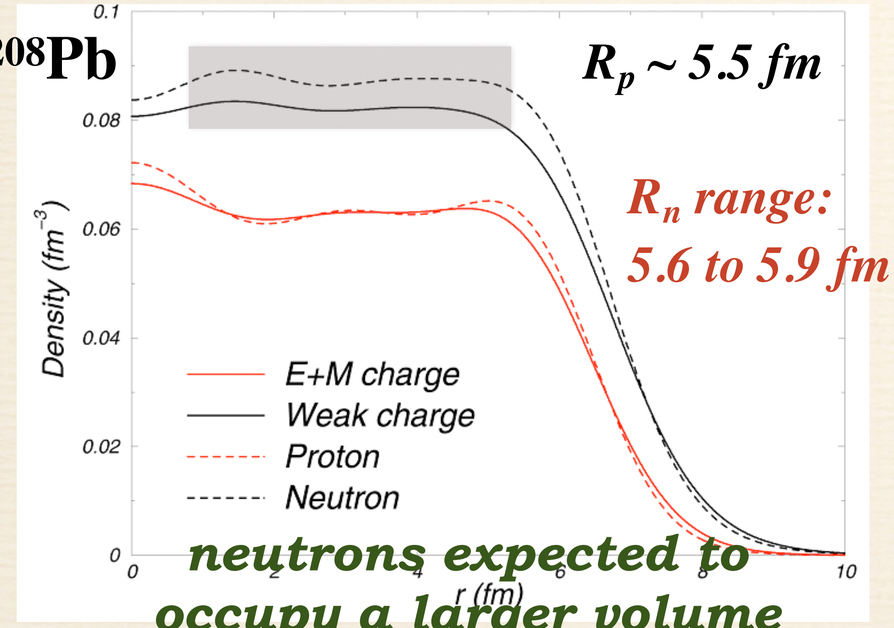
PV Elastic Scattering off Heavy Nuclei: Neutron Densities

2010's

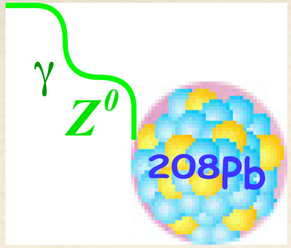
Photon Exchange

$$M^{EM} = \frac{4\pi\alpha}{Q^2} F_p\left(Q^2\right)$$

$Q^p_{EM} \sim 1$ $Q^n_{EM} \sim 0$ $Q^n_W \sim -1$ $Q^p_W \sim 1 - 4\sin^2\theta_W$



neutrons expected to occupy a larger volume



PV Elastic Scattering off Heavy Nuclei: Neutron Densities

2010's

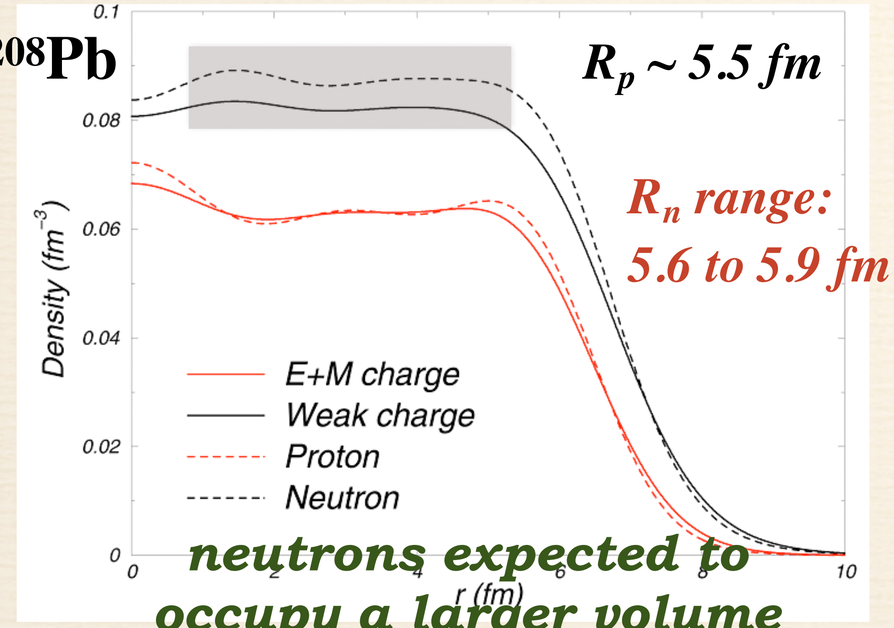
Photon Exchange

$$M^{EM} = \frac{4\pi\alpha}{Q^2} F_p\left(Q^2\right)$$

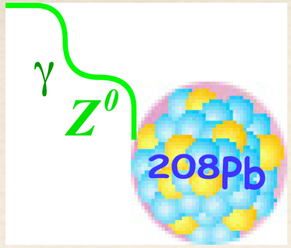
$Q^p_{EM} \sim 1$ $Q^n_{EM} \sim 0$ $Q^n_W \sim -1$ $Q^p_W \sim 1 - 4\sin^2\theta_W$

Z_0 exchange

$$M^{NC}_{PV} = \frac{G_F}{\sqrt{2}}\left[\left(1 - 4\sin^2\theta_W\right)F_p\left(Q^2\right) - F_n\left(Q^2\right)\right]$$



neutrons expected to occupy a larger volume



PV Elastic Scattering off Heavy Nuclei: Neutron Densities

2010's

$$A_{PV} \approx \frac{G_F Q^2}{4\pi\alpha\sqrt{2}} \frac{F_n\left(Q^2\right)}{F_p\left(Q^2\right)}$$

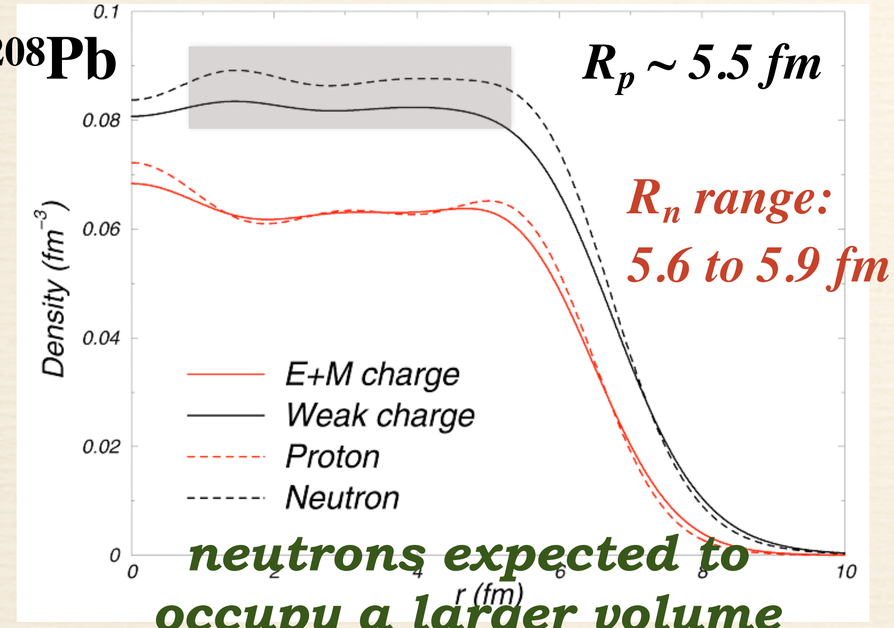
Photon Exchange

$$M^{EM} = \frac{4\pi\alpha}{Q^2} F_p\left(Q^2\right)$$

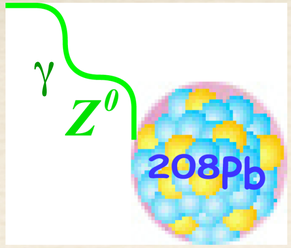
$Q^p_{EM} \sim 1$ $Q^n_{EM} \sim 0$ $Q^n_W \sim -1$ $Q^p_W \sim 1 - 4\sin^2\theta_W$

Z_0 exchange

$$M^{NC}_{PV} = \frac{G_F}{\sqrt{2}}\left[\left(1 - 4\sin^2\theta_W\right)F_p\left(Q^2\right) - F_n\left(Q^2\right)\right]$$



neutrons expected to occupy a larger volume



PV Elastic Scattering off Heavy Nuclei: Neutron Densities

2010's

$$A_{PV} \approx \frac{G_F Q^2}{4\pi\alpha\sqrt{2}} \frac{F_n\left(Q^2\right)}{F_p\left(Q^2\right)}$$

Photon Exchange

$$M^{EM} = \frac{4\pi\alpha}{Q^2} F_p\left(Q^2\right)$$

$Q^p_{EM} \sim 1$ $Q^n_{EM} \sim 0$ $Q^n_W \sim -1$ $Q^p_W \sim 1 - 4\sin^2\theta_W$

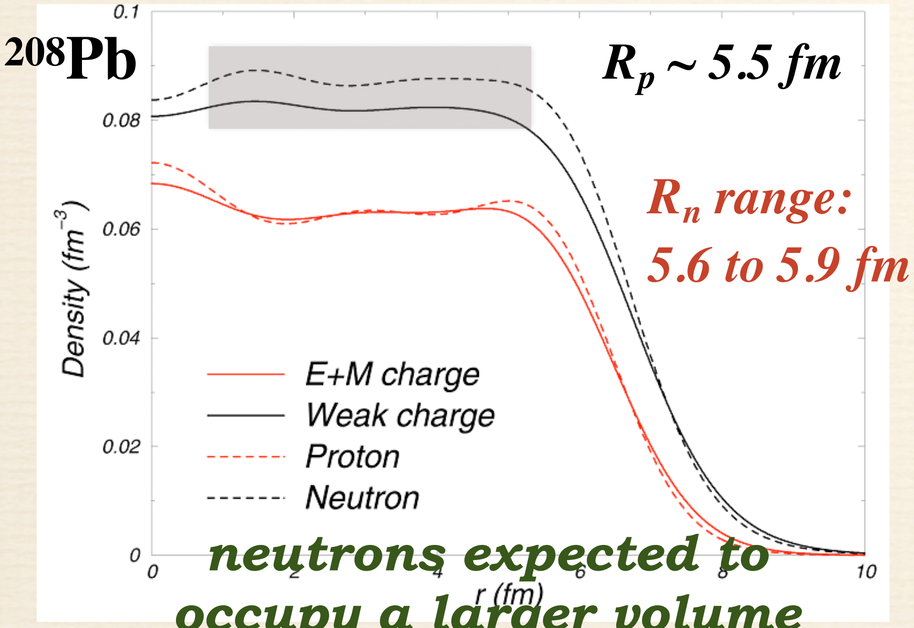
Z_0 exchange

$$M^{NC}_{PV} = \frac{G_F}{\sqrt{2}}\left[\left(1 - 4\sin^2\theta_W\right)F_p\left(Q^2\right) - F_n\left(Q^2\right)\right]$$

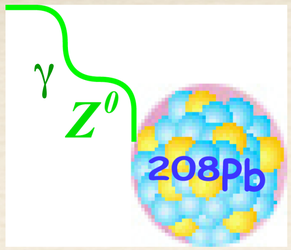
$\delta(A_{PV})/A_{PV} \sim 3\%$

$\delta(R_n)/R_n \sim 1\%$

$\delta(R_n)$: ± 0.07 fm (^{208}Pb)
± 0.03 fm (^{48}Ca)



neutrons expected to occupy a larger volume



PV Elastic Scattering off Heavy Nuclei: Neutron Densities

2010's

Photon Exchange

$$M^{EM} = \frac{4\pi\alpha}{Q^2} F_p\left(Q^2\right)$$

Z_0 exchange

$$M_{PV}^{NC} = \frac{G_F}{\sqrt{2}}\left[\left(1-4\sin^2\theta_W\right)F_p\left(Q^2\right) - F_n\left(Q^2\right)\right]$$

$$A_{PV} \approx \frac{G_F Q^2}{4\pi\alpha\sqrt{2}} \frac{F_n\left(Q^2\right)}{F_p\left(Q^2\right)}$$

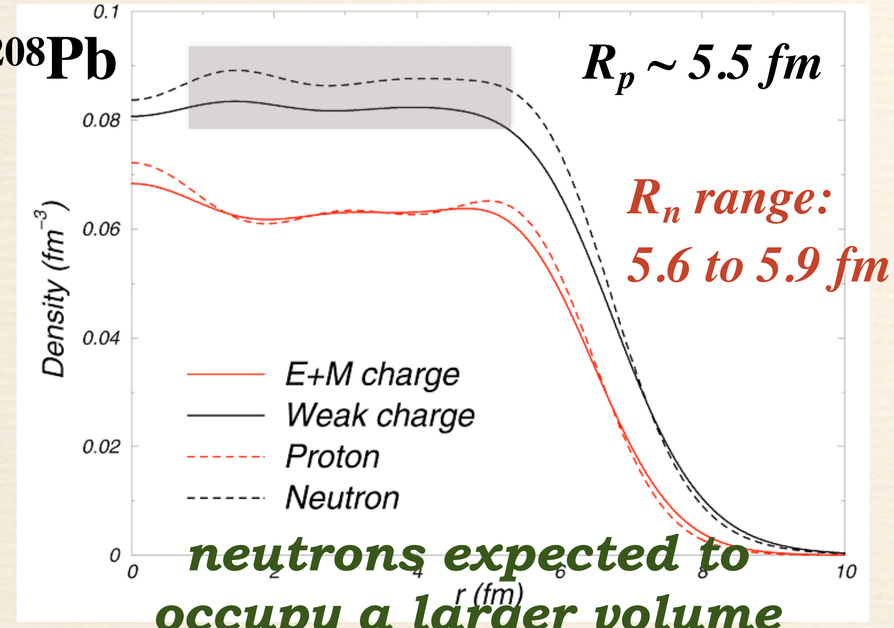
$Q^p_{EM} \sim 1$ $\quad Q^n_{EM} \sim 0$ $\quad Q^n_W \sim -1$ $\quad Q^p_W \sim 1 - 4\sin^2\theta_W$

$\delta(A_{PV})/A_{PV} \sim 3\%$

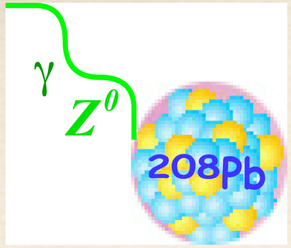
$\delta(R_n)/R_n \sim 1\%$

$\delta(R_n)$: ± 0.07 fm (^{208}Pb)
± 0.03 fm (^{48}Ca)

PREX ^{208}Pb
&
CREX ^{48}Ca



neutrons expected to occupy a larger volume



PV Elastic Scattering off Heavy Nuclei: Neutron Densities

2010's

Photon Exchange

$$M^{EM} = \frac{4\pi\alpha}{Q^2} F_p\left(Q^2\right)$$

Z_0 exchange

$$M_{PV}^{NC} = \frac{G_F}{\sqrt{2}}\left[\left(1-4\sin^2\theta_W\right)F_p\left(Q^2\right) - F_n\left(Q^2\right)\right]$$

$$A_{PV} \approx \frac{G_F Q^2}{4\pi\alpha\sqrt{2}} \frac{F_n\left(Q^2\right)}{F_p\left(Q^2\right)}$$

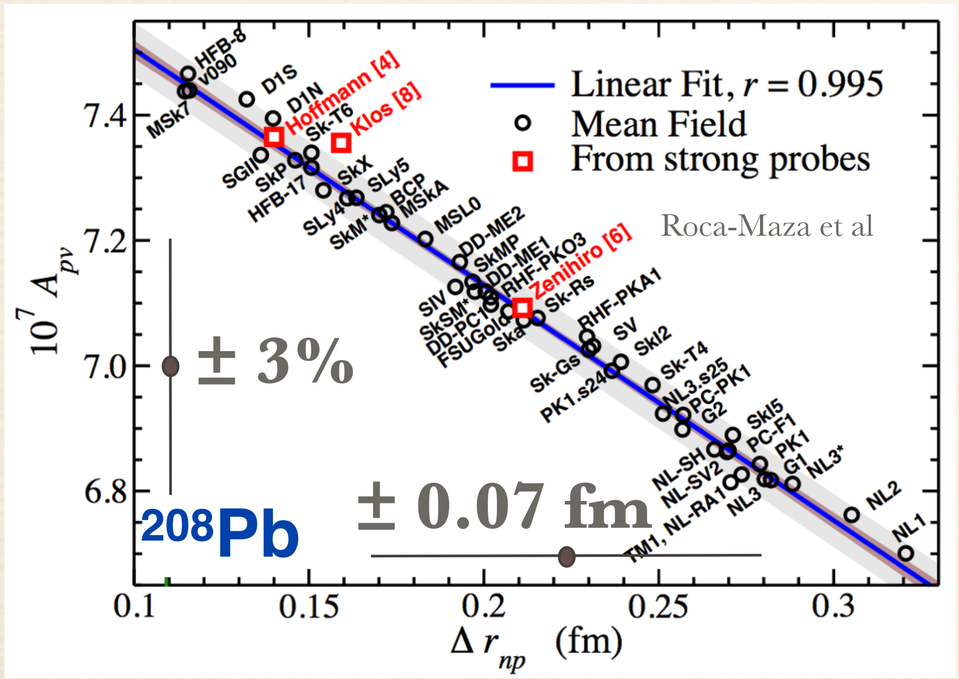
$Q^p_{EM} \sim 1$ $\quad Q^n_{EM} \sim 0$ $\quad Q^n_W \sim -1$ $\quad Q^p_W \sim 1 - 4\sin^2\theta_W$

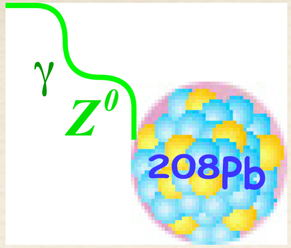
$\delta(A_{PV})/A_{PV} \sim 3\%$

$\delta(R_n)/R_n \sim 1\%$

$\delta(R_n)$: ± 0.07 fm (^{208}Pb)
± 0.03 fm (^{48}Ca)

PREX ^{208}Pb
&
CREX ^{48}Ca





PV Elastic Scattering off Heavy Nuclei: Neutron Densities

2010's

$$A_{PV} \approx \frac{G_F Q^2}{4\pi\alpha\sqrt{2}} \frac{F_n\left(Q^2\right)}{F_p\left(Q^2\right)}$$

Photon Exchange

$$M^{EM} = \frac{4\pi\alpha}{Q^2} F_p\left(Q^2\right)$$

$Q^p_{EM} \sim 1$ $Q^n_{EM} \sim 0$ $Q^n_W \sim -1$ $Q^p_W \sim 1 - 4\sin^2\theta_W$

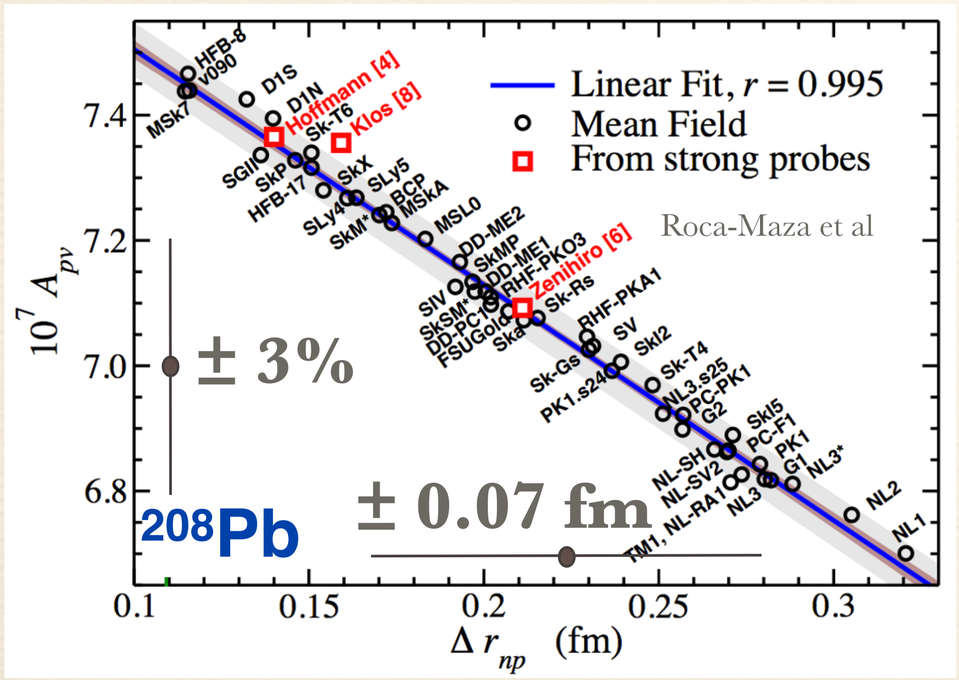
Z_0 exchange

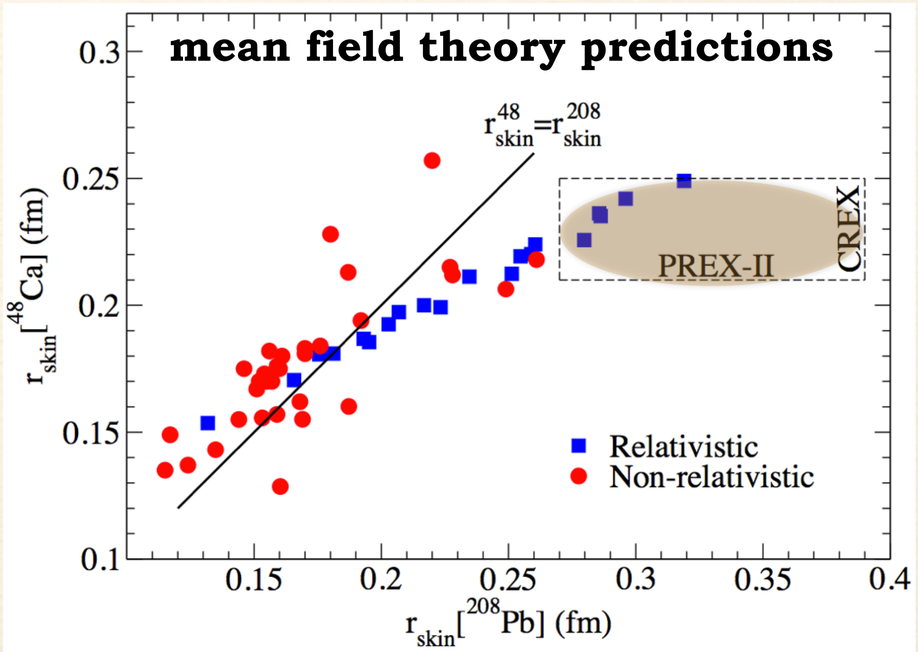
$$M^{NC}_{PV} = \frac{G_F}{\sqrt{2}}\left[\left(1 - 4\sin^2\theta_W\right)F_p\left(Q^2\right) - F_n\left(Q^2\right)\right]$$

$\delta(A_{PV})/A_{PV} \sim 3\%$

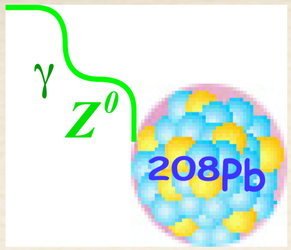
$\delta(R_n)/R_n \sim 1\%$

$\delta(R_n)$: ± 0.07 fm (^{208}Pb)
± 0.03 fm (^{48}Ca)





PREX ^{208}Pb
&
CREX ^{48}Ca



PV Elastic Scattering off Heavy Nuclei: Neutron Densities

2010's

$$A_{PV} \approx \frac{G_F Q^2}{4\pi\alpha\sqrt{2}} \frac{F_n\left(Q^2\right)}{F_p\left(Q^2\right)}$$

Photon Exchange

$$M^{EM} = \frac{4\pi\alpha}{Q^2} F_p\left(Q^2\right)$$

$Q^p_{EM} \sim 1$ $Q^n_{EM} \sim 0$ $Q^n_W \sim -1$ $Q^p_W \sim 1 - 4\sin^2\theta_W$

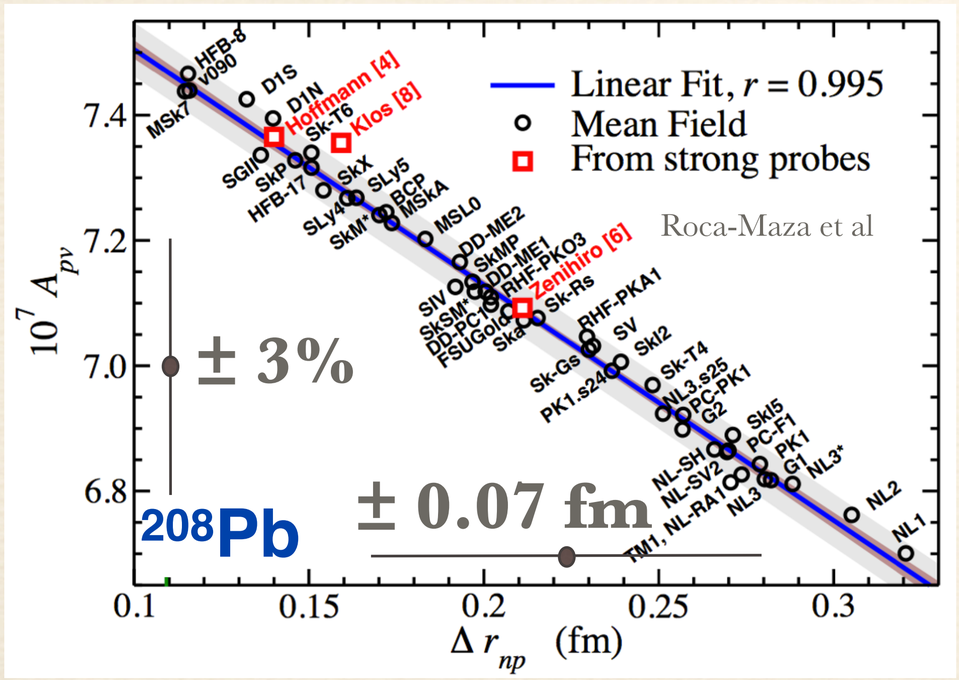
Z_0 exchange

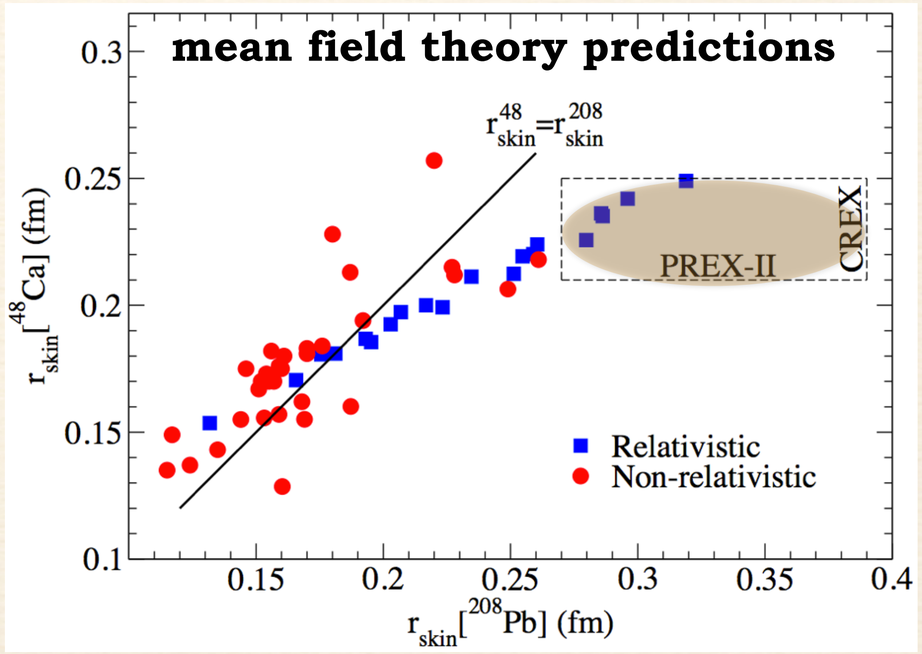
$$M^{NC}_{PV} = \frac{G_F}{\sqrt{2}}\left[\left(1 - 4\sin^2\theta_W\right)F_p\left(Q^2\right) - F_n\left(Q^2\right)\right]$$

$\delta(A_{PV})/A_{PV} \sim 3\%$

$\delta(R_n)/R_n \sim 1\%$

$\delta(R_n)$: ± 0.07 fm (^{208}Pb)
± 0.03 fm (^{48}Ca)





PREX ^{208}Pb
&
CREX ^{48}Ca

PREX-2 Run:
Summer 2019

CREX runs:
Dec 19 to Sep 20
(Despite lockdowns!)

^{208}Pb PREX/CREX Overview and Data ^{48}Ca

$Q^2 \sim 0.006$ GeV^2

$A_{PV} \sim 0.6$ ppm

Rate ~ 4 GHz

$\Delta(A_{PV}) \sim 16$ ppb

$\Delta(R_n) \sim 0.07$ fm

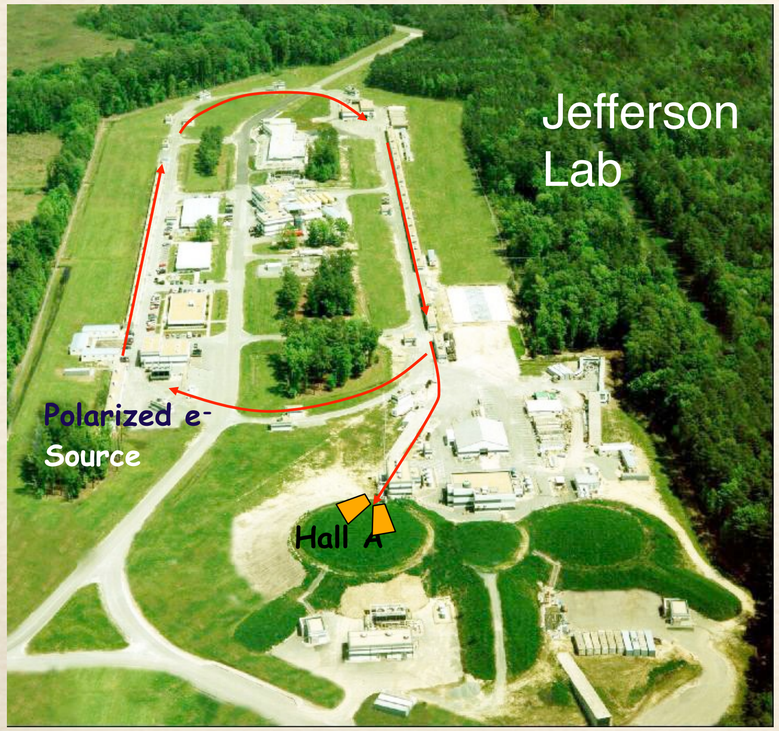
$Q^2 \sim 0.03$ GeV^2

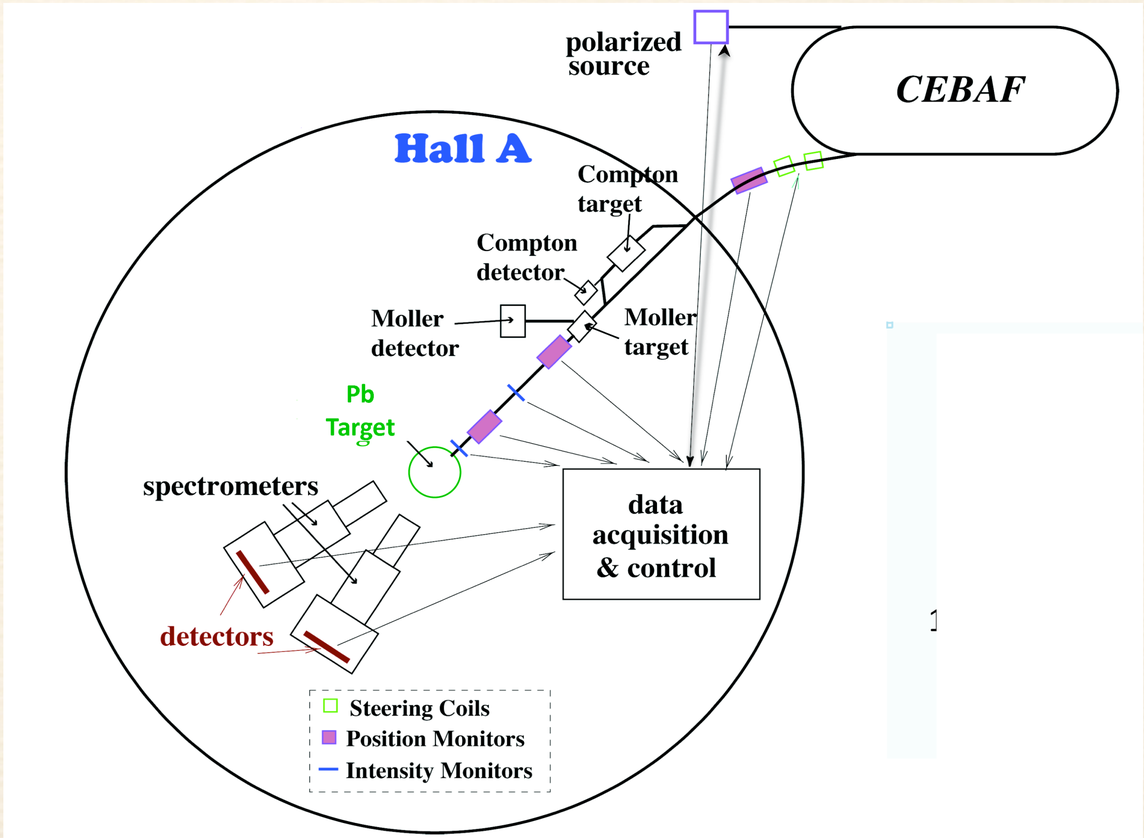
$A_{PV} \sim 2$ ppm

Rate ~ 56 MHz

$\Delta(A_{PV}) \sim 100$ ppb

$\Delta(R_n) \sim 0.03$ fm





^{208}Pb PREX/CREX Overview and Data ^{48}Ca

$Q^2 \sim 0.006$ GeV^2

$A_{PV} \sim 0.6$ ppm

Rate ~ 4 GHz

$\Delta(A_{PV}) \sim 16$ ppb

$\Delta(R_n) \sim 0.07$ fm

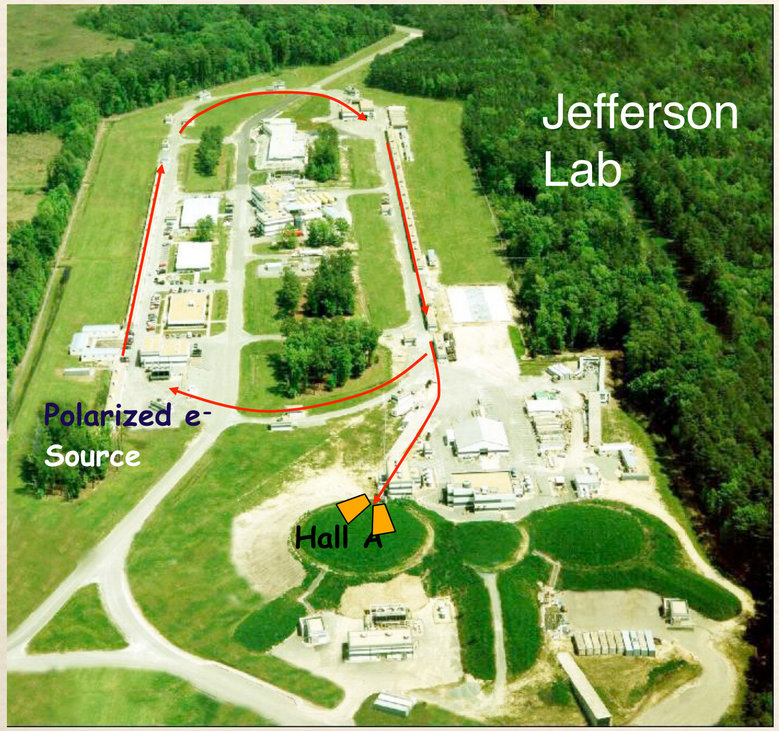
$Q^2 \sim 0.03$ GeV^2

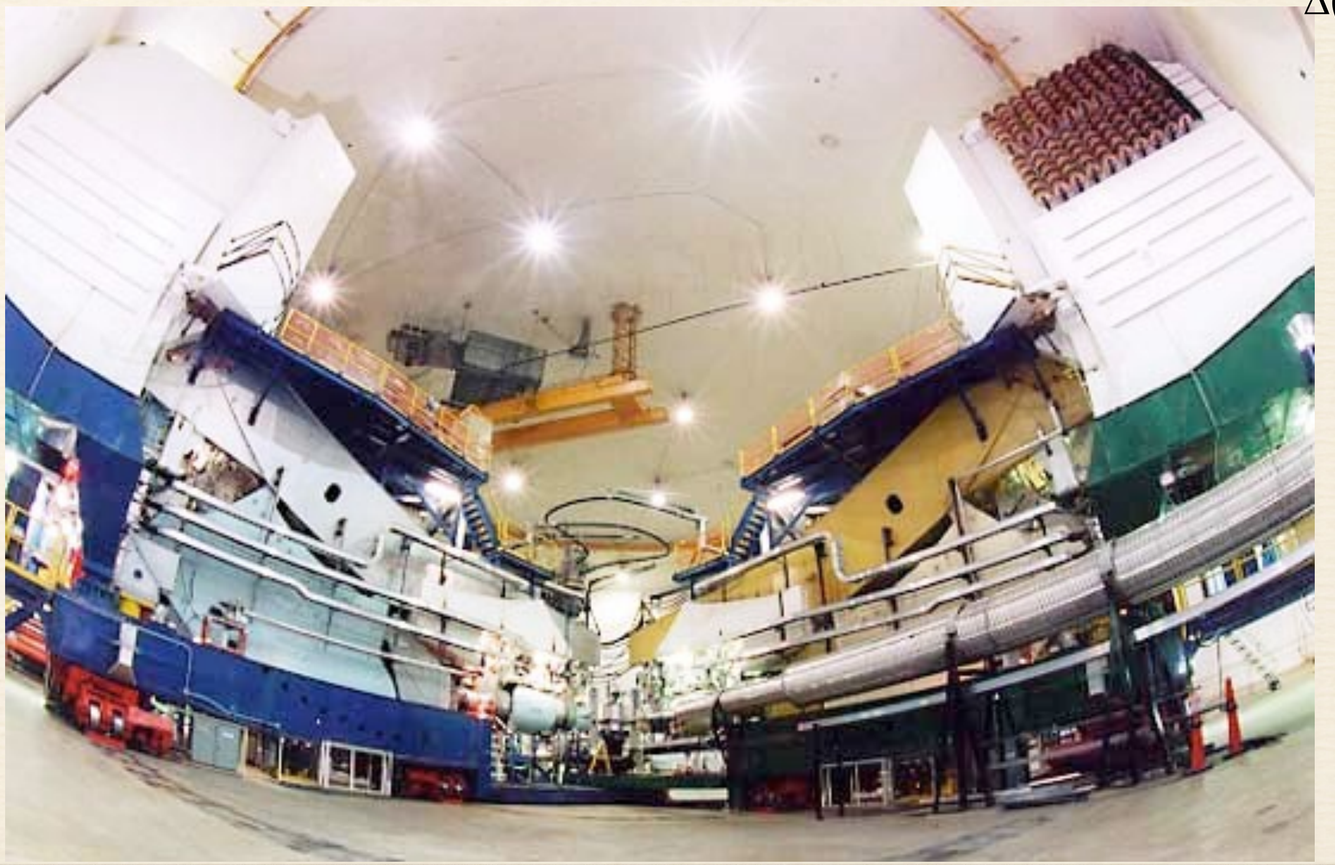
$A_{PV} \sim 2$ ppm

Rate ~ 56 MHz

$\Delta(A_{PV}) \sim 100$ ppb

$\Delta(R_n) \sim 0.03$ fm





^{208}Pb PREX/CREX Overview and Data ^{48}Ca

$Q^2 \sim 0.006$ GeV^2

$A_{PV} \sim 0.6$ ppm

Rate ~ 4 GHz

$\Delta(A_{PV}) \sim 16$ ppb

$\Delta(R_n) \sim 0.07$ fm

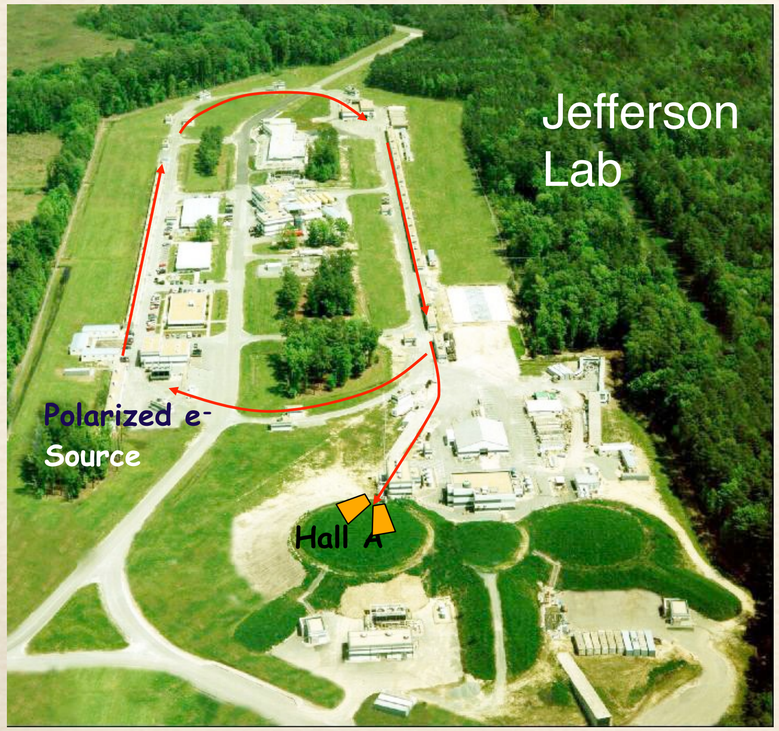
$Q^2 \sim 0.03$ GeV^2

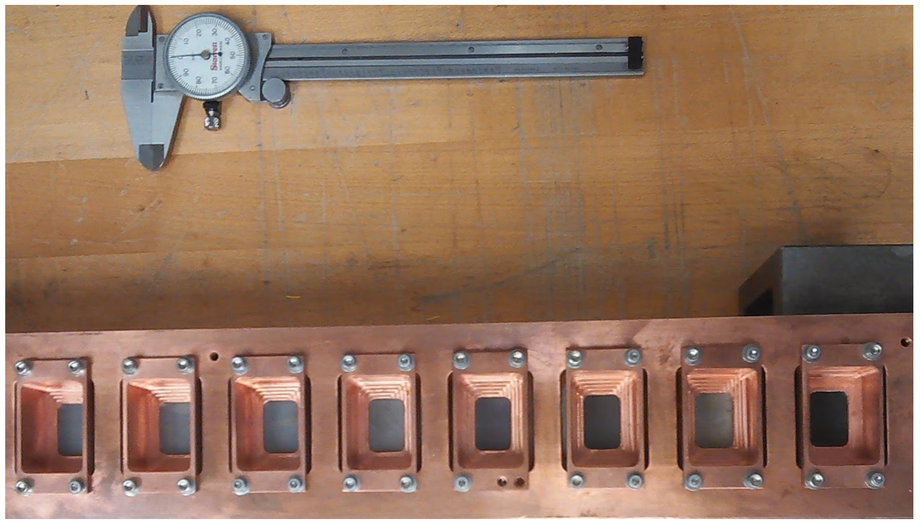
$A_{PV} \sim 2$ ppm

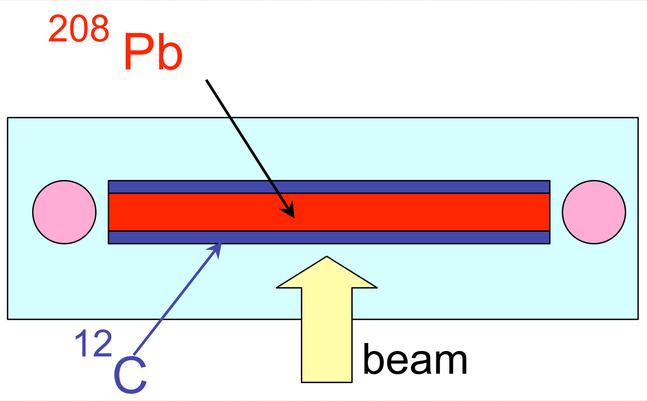
Rate ~ 56 MHz

$\Delta(A_{PV}) \sim 100$ ppb

$\Delta(R_n) \sim 0.03$ fm







^{208}Pb PREX/CREX Overview and Data ^{48}Ca

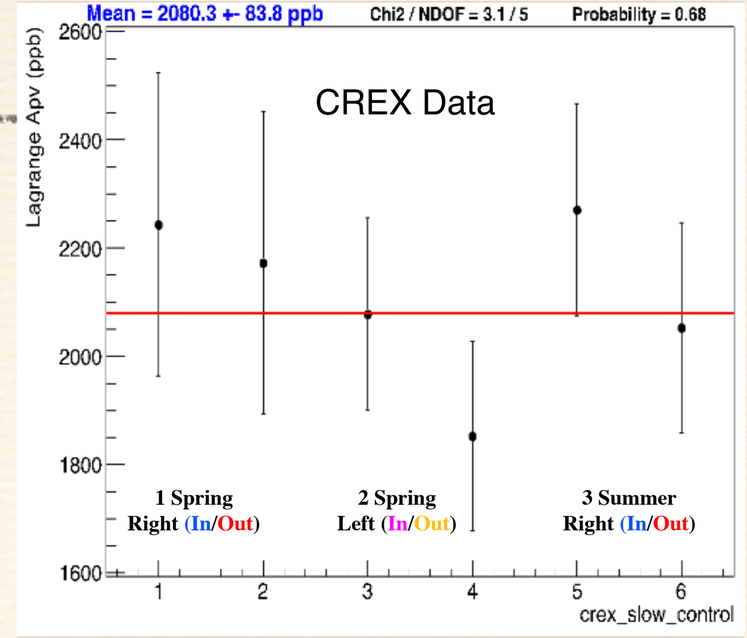
$Q^2 \sim 0.006$ GeV^2

$A_{PV} \sim 0.6$ ppm

Rate ~ 4 GHz

$\Delta(A_{PV}) \sim 16$ ppb

$\Delta(R_n) \sim 0.07$ fm



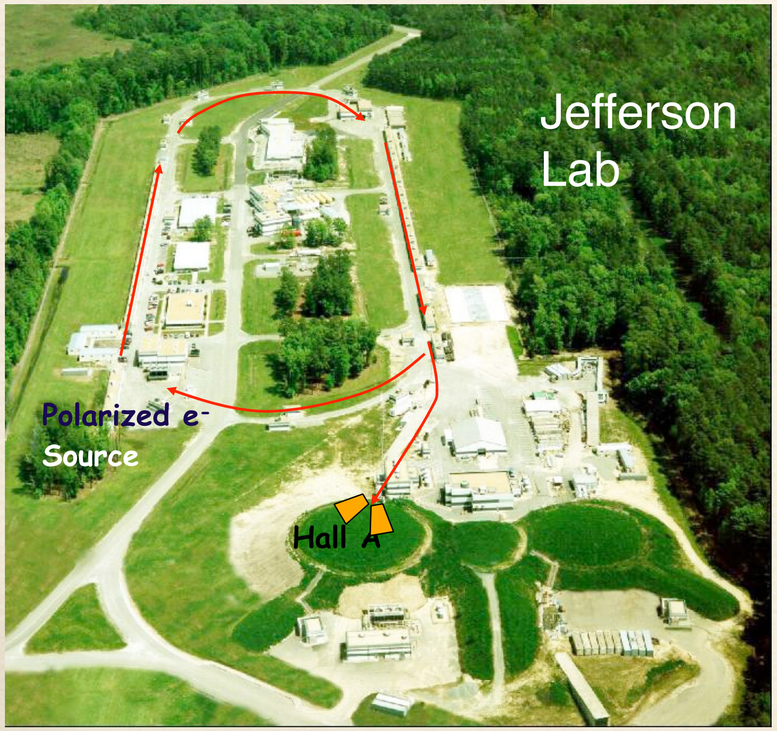
$Q^2 \sim 0.03$ GeV^2

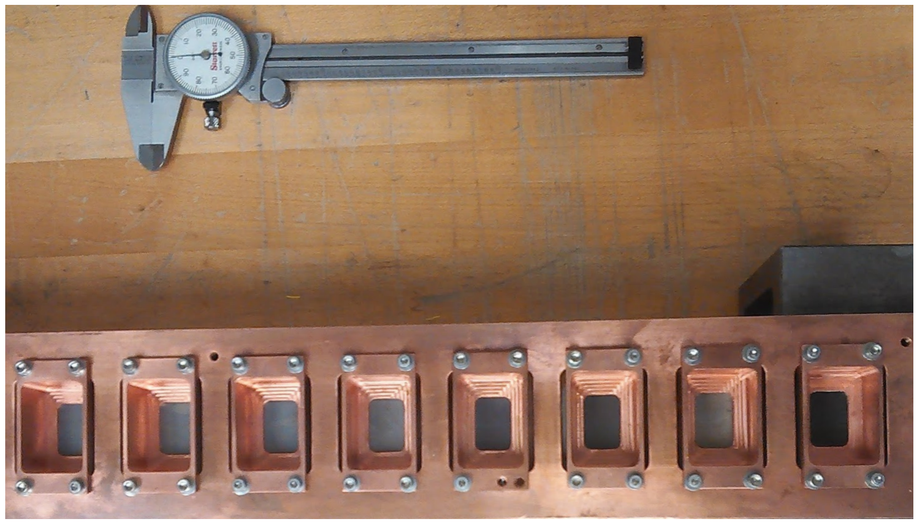
$A_{PV} \sim 2$ ppm

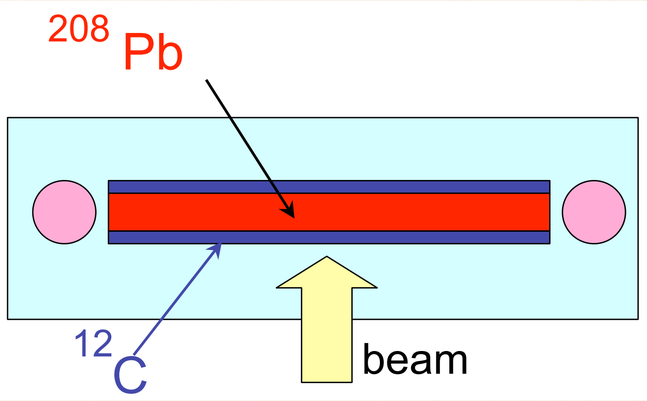
Rate ~ 56 MHz

$\Delta(A_{PV}) \sim 100$ ppb

$\Delta(R_n) \sim 0.03$ fm







^{208}Pb PREX/CREX Overview and Data ^{48}Ca

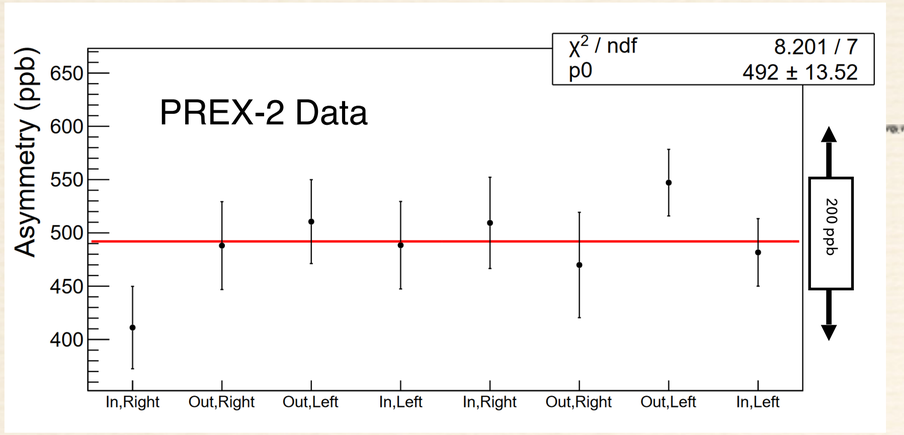
Q^2 ~ 0.006 GeV^2

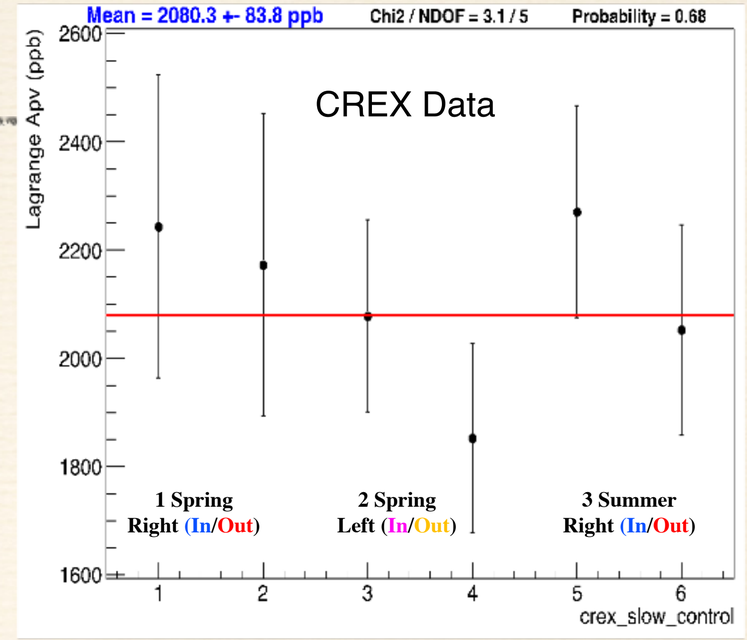
A_{PV} ~ 0.6 ppm

Rate ~ 4 GHz

$\Delta(A_{PV})$ ~ 16 ppb

$\Delta(R_n)$ ~ 0.07 fm





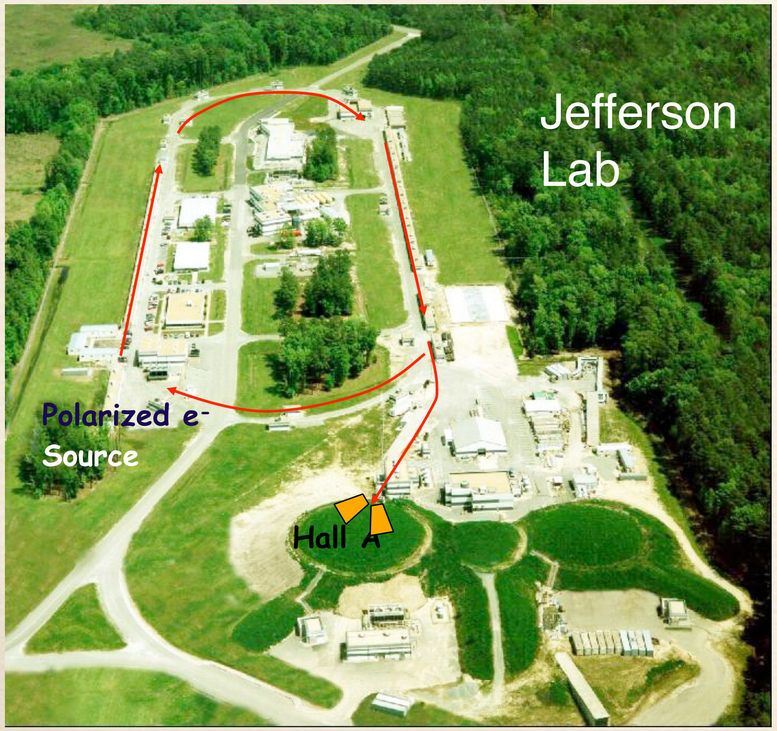
Q^2 ~ 0.03 GeV^2

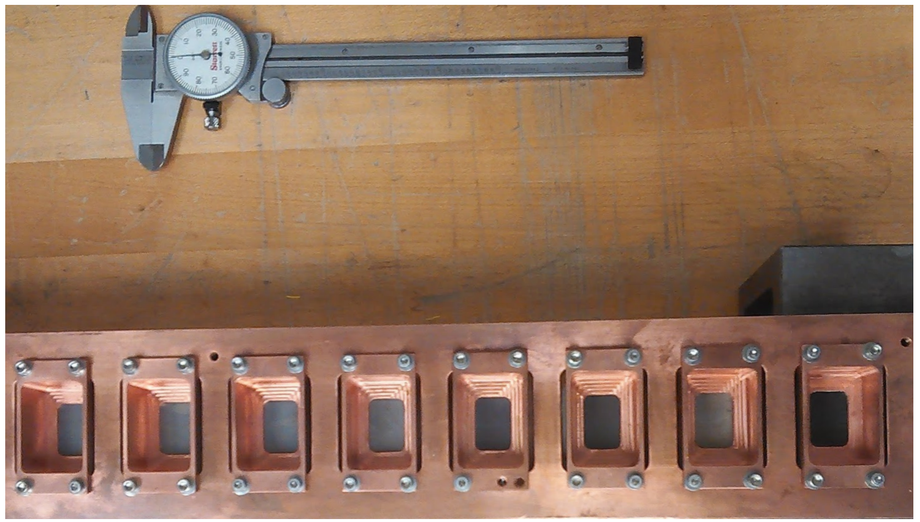
A_{PV} ~ 2 ppm

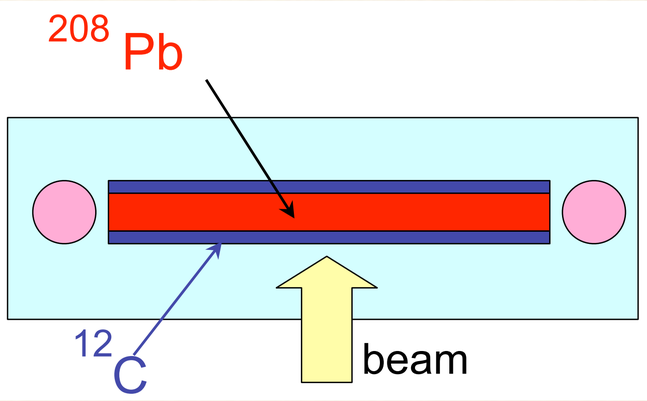
Rate ~ 56 MHz

$\Delta(A_{PV})$ ~ 100 ppb

$\Delta(R_n)$ ~ 0.03 fm







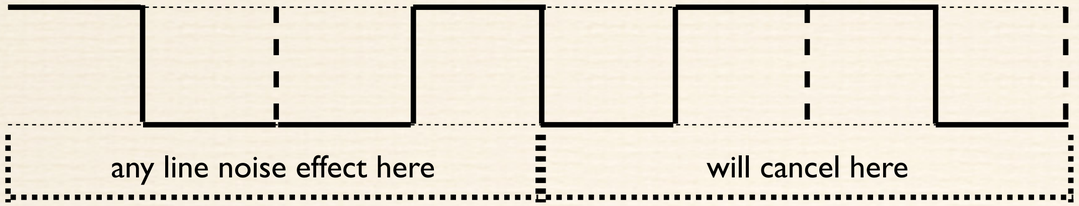
CW electron beam: scattered signal rate ~ 3 GHz

Flux Integration

10 ppb (average 3.3×10^6 s)

sequence of "window multiplets"

Example: at 240 Hz reversal



$$A_{pair} = \frac{F_R - F_L}{F_R + F_L}$$

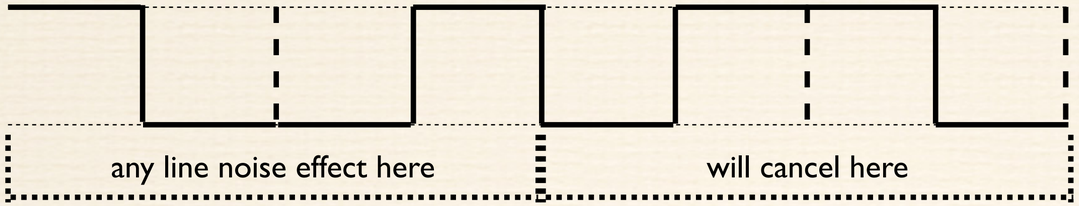
Detector D, Current I: F = D/I $A_{pair} = \frac{\Delta F}{2F} + \Delta A$

CW electron beam: scattered signal rate ~ 3 GHz

Flux Integration

30 Hz Stat. Width: 100 ppm → N = 100 M: 10 ppb (average 3.3×10^6 s)

sequence of "window multiplets" Example: at 240 Hz reversal



$$A_{pair} = \frac{F_R - F_L}{F_R + F_L}$$

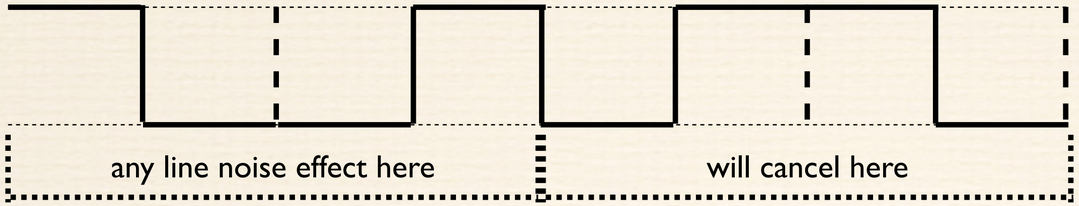
Detector D, Current I: F = D/I $A_{pair} = \frac{\Delta F}{2F} + \Delta A$

CW electron beam: scattered signal rate ~ 3 GHz

Flux Integration

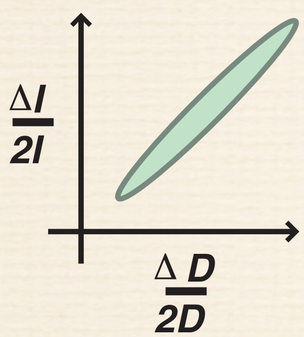
30 Hz Stat. Width: 100 ppm → N = 100 M: 10 ppb (average 3.3×10^6 s)

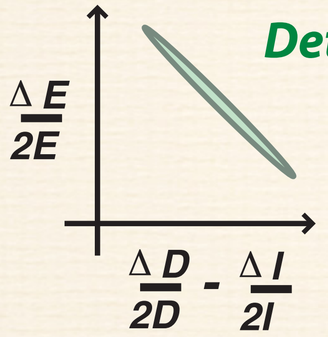
sequence of "window multiplets" Example: at 240 Hz reversal



$$A_{pair} = \frac{F_R - F_L}{F_R + F_L}$$

Detector D, Current I: F = D/I $A_{pair} = \frac{\Delta F}{2F} + \Delta A$





I order: $x, y, \theta_x, \theta_y, E$

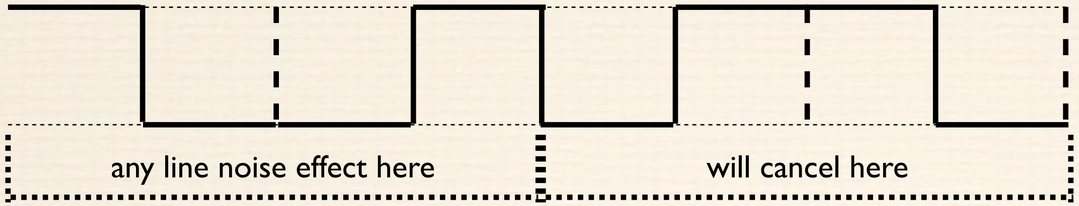
II order: e.g. spot-size

CW electron beam: scattered signal rate ~ 3 GHz

Flux Integration

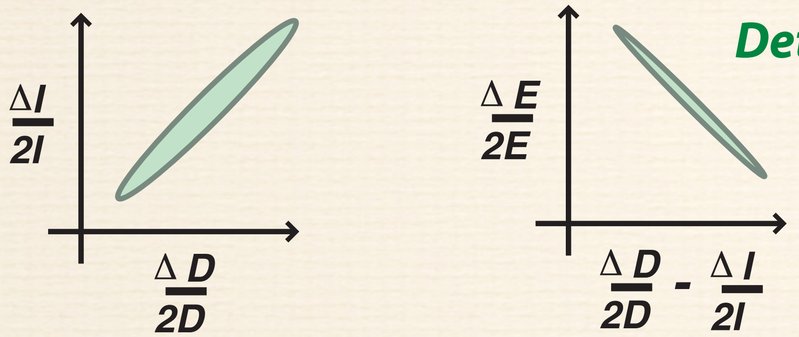
30 Hz Stat. Width: 100 ppm → N = 100 M: 10 ppb (average 3.3×10^6 s)

sequence of "window multiplets" Example: at 240 Hz reversal



$$A_{pair} = \frac{F_R - F_L}{F_R + F_L}$$

Detector D, Current I: F = D/I $A_{pair} = \frac{\Delta F}{2F} + \Delta A$



I order: $x, y, \theta_x, \theta_y, E$
II order: e.g. spot-size

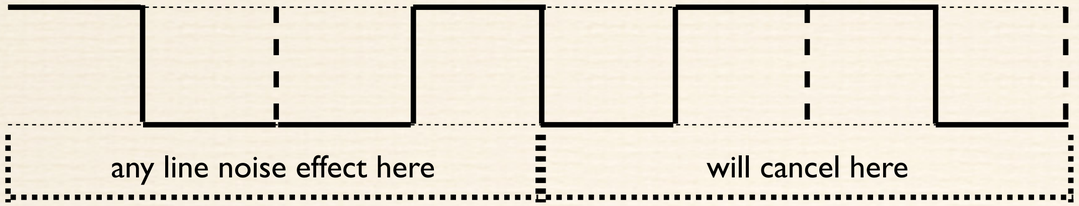
Must minimize (both) random and helicity-correlated fluctuations in average window-pair response of electron beam trajectory, energy and spot-size.

CW electron beam: scattered signal rate ~ 3 GHz

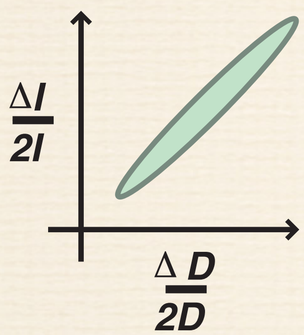
Flux Integration

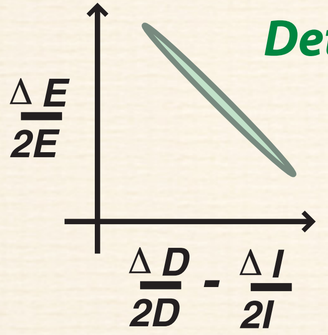
30 Hz Stat. Width: 100 ppm ➡ N = 100 M: 10 ppb (average 3.3×10^6 s)

sequence of "window multiplets" Example: at 240 Hz reversal



$$A_{pair} = \frac{F_R - F_L}{F_R + F_L}$$





Detector D, Current I: $F = D/I$ $A_{pair} = \frac{\Delta F}{2F} + \Delta A$

I order: $x, y, \theta_x, \theta_y, E$
II order: e.g. spot-size

Must minimize (both) random and helicity-correlated fluctuations in average window-pair response of electron beam trajectory, energy and spot-size.

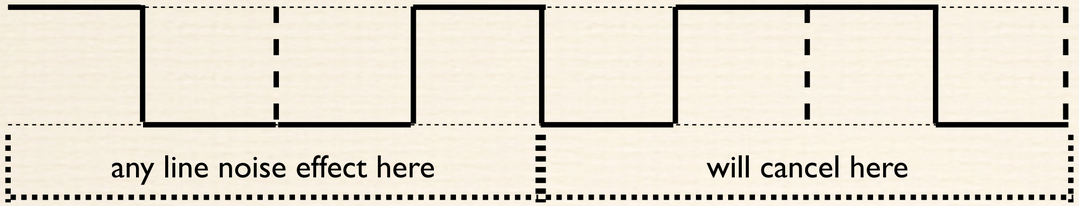
After corrections, variance of A_{pair} must get as close to counting statistics as possible: ~ 100 ppm at 30 Hz; central value then reflects A_{phys}

CW electron beam: scattered signal rate ~ 3 GHz

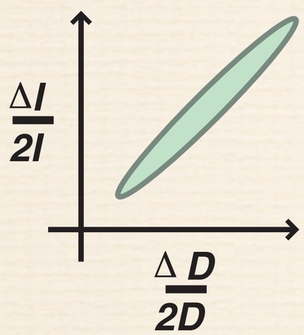
Flux Integration

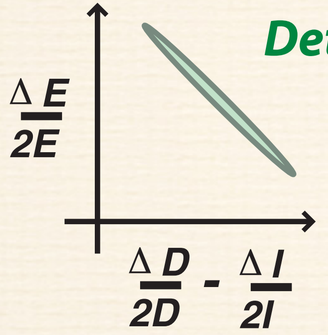
30 Hz Stat. Width: 100 ppm → N = 100 M: 10 ppb (average 3.3×10^6 s)

sequence of "window multiplets" Example: at 240 Hz reversal



$$A_{pair} = \frac{F_R - F_L}{F_R + F_L}$$





Detector D, Current I: $F = D/I$ $A_{pair} = \frac{\Delta F}{2F} + \Delta A$

I order: $x, y, \theta_x, \theta_y, E$
II order: e.g. spot-size

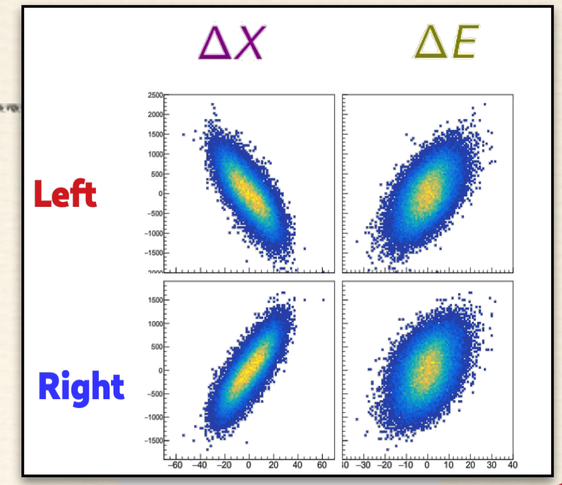
Must minimize (both) random and helicity-correlated fluctuations in average window-pair response of electron beam trajectory, energy and spot-size.

After corrections, variance of A_{pair} must get as close to counting statistics as possible: ~ 100 ppm at 30 Hz; central value then reflects A_{phys}

Goal: corrections no bigger than statistical uncertainty: ~ppm, microns over minutes, ~ppb, nm over days,

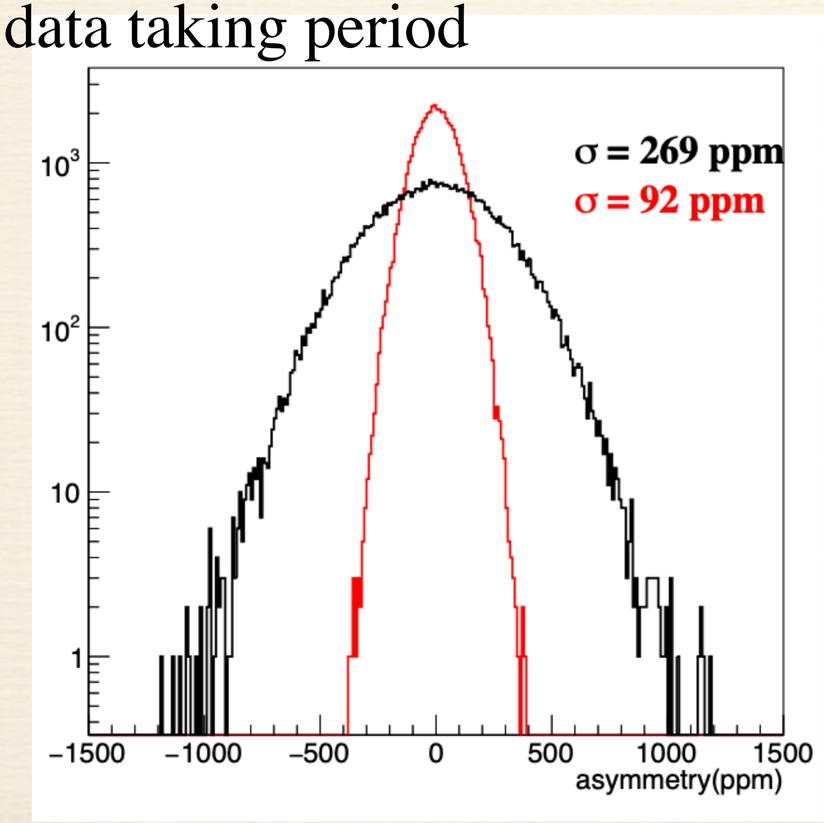
Corrections for Beam Fluctuations

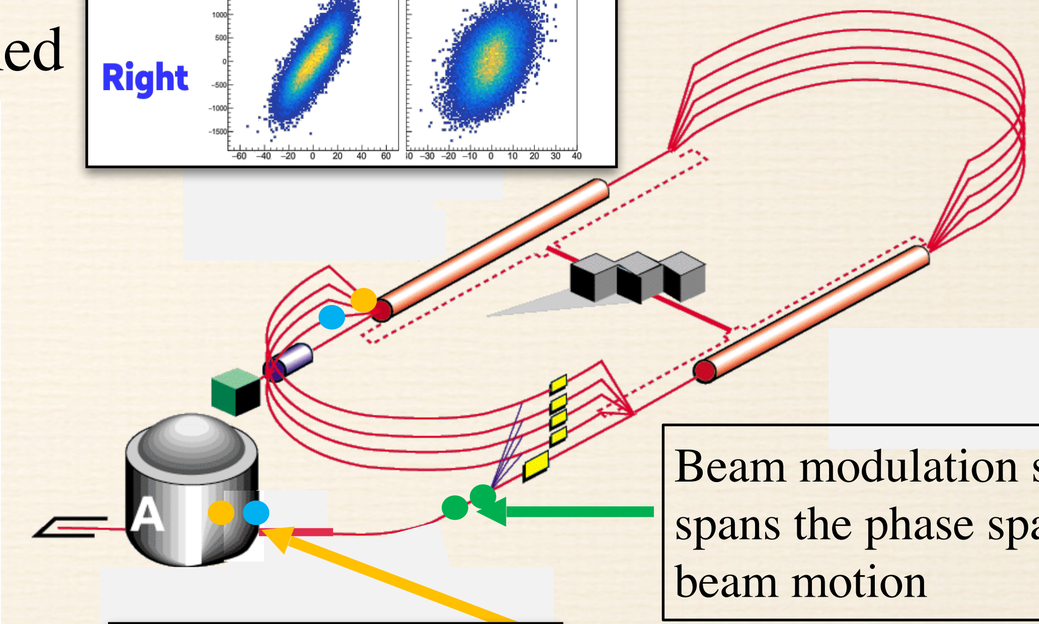
- To span the 5 dimension phase space of beam motion at the target (position, angle, energy) we made use of a set of 6 coils and an energy vernier
  - This modulation is automated and was performed throughout the data taking period



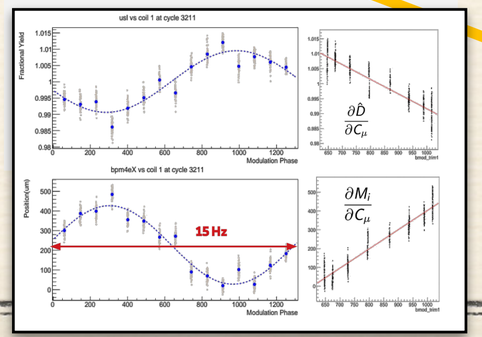
$A_{corr} = A_{det} - A_Q + \alpha \Delta_E + \Sigma \beta_i \Delta x_i$

$A_{corr} \sim 500$ ppb



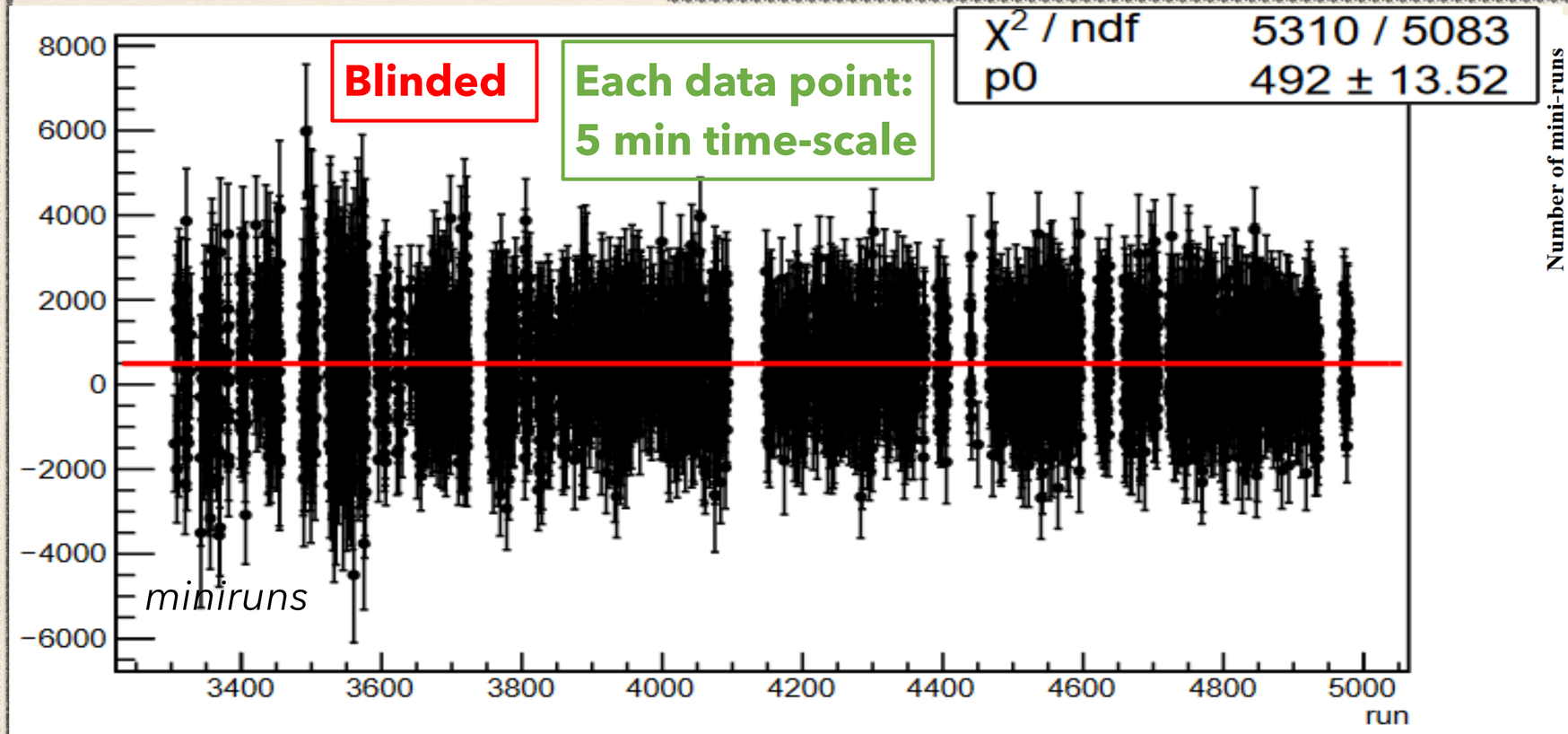


Beam modulation system spans the phase space of beam motion

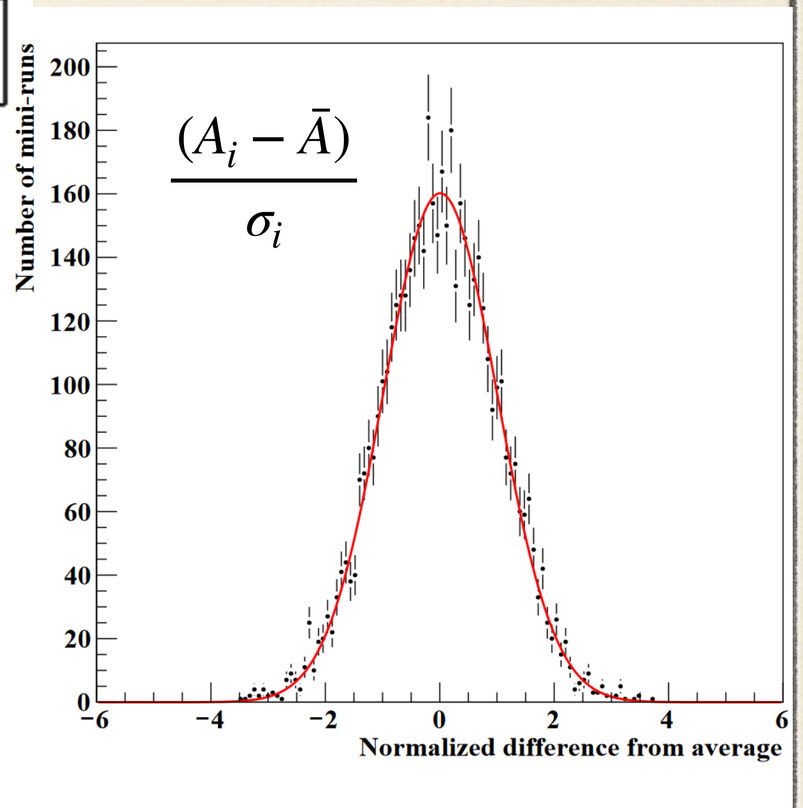


Beam monitors determine trajectory and parameters onto target

5 minute time scale

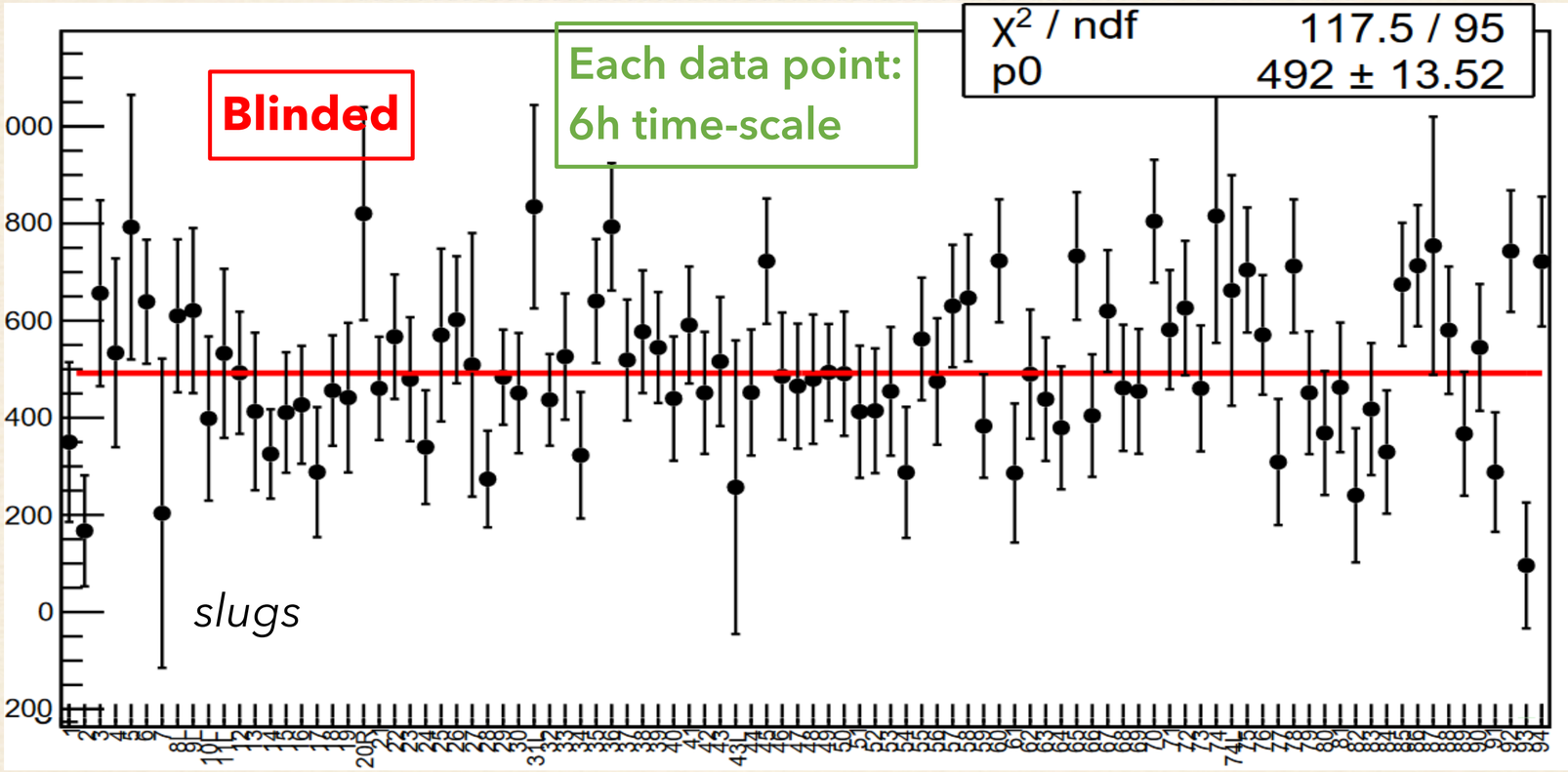


"pull" plot



- The corrected asymmetry removed effects from beam asymmetries and noise
- Still to come: polarization and background corrections

6 hour time scale

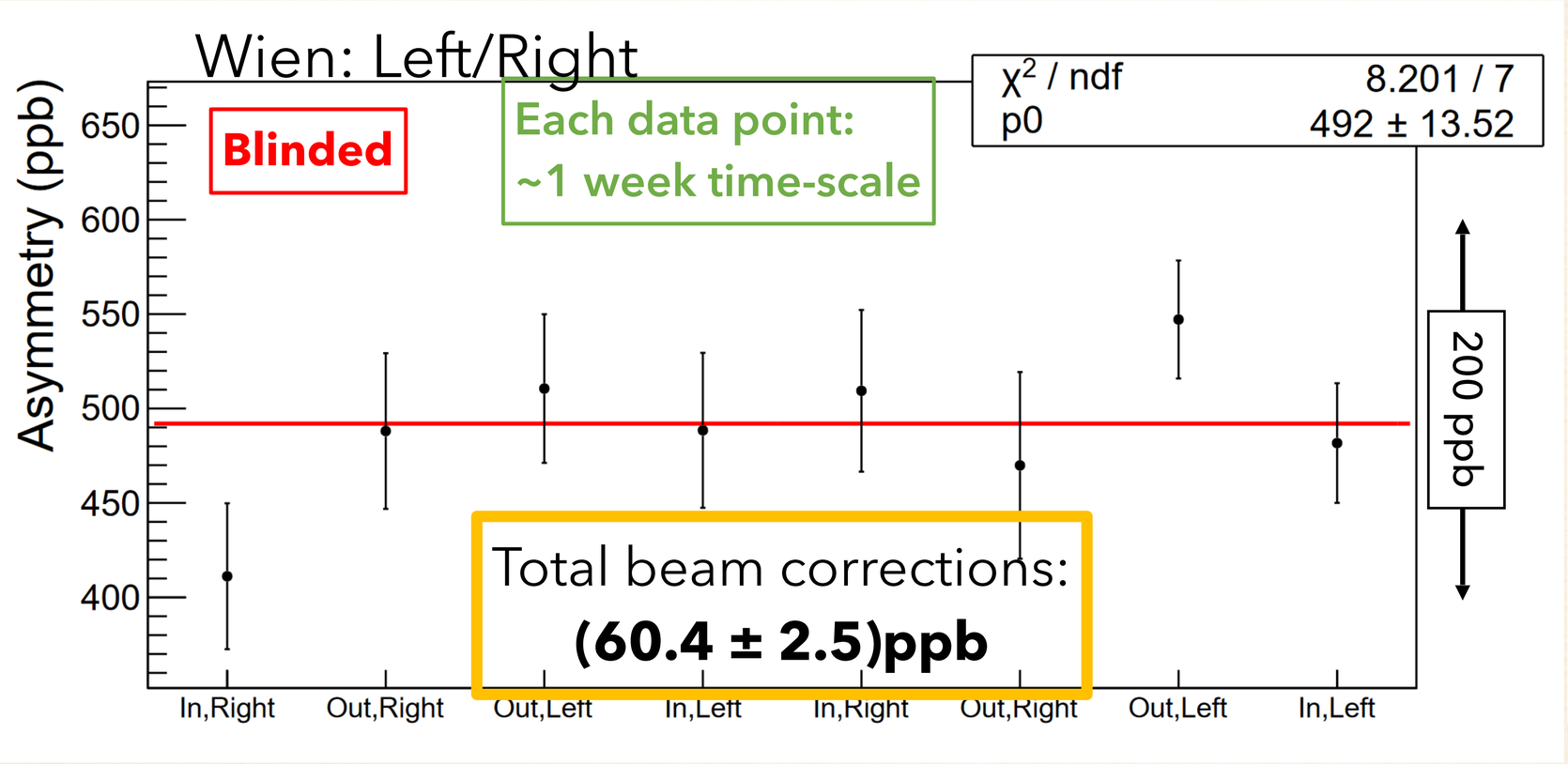


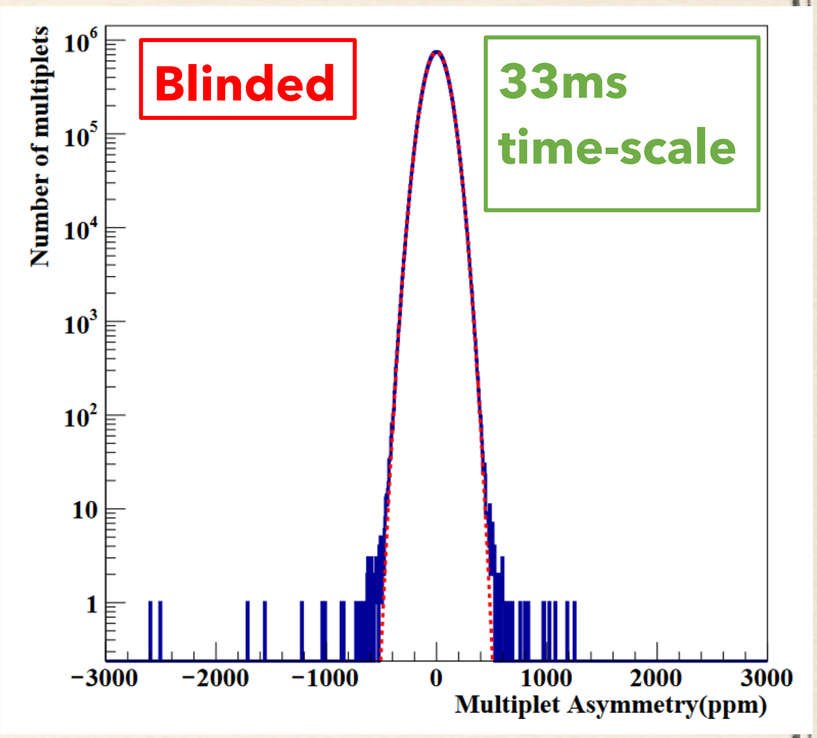
- The corrected asymmetry removed effects from beam asymmetries and noise
- Still to come: polarization and background corrections

Data Overview: Corrected Asymmetry

Half Wave Plate: IN/OUT

Wien: Left/Right

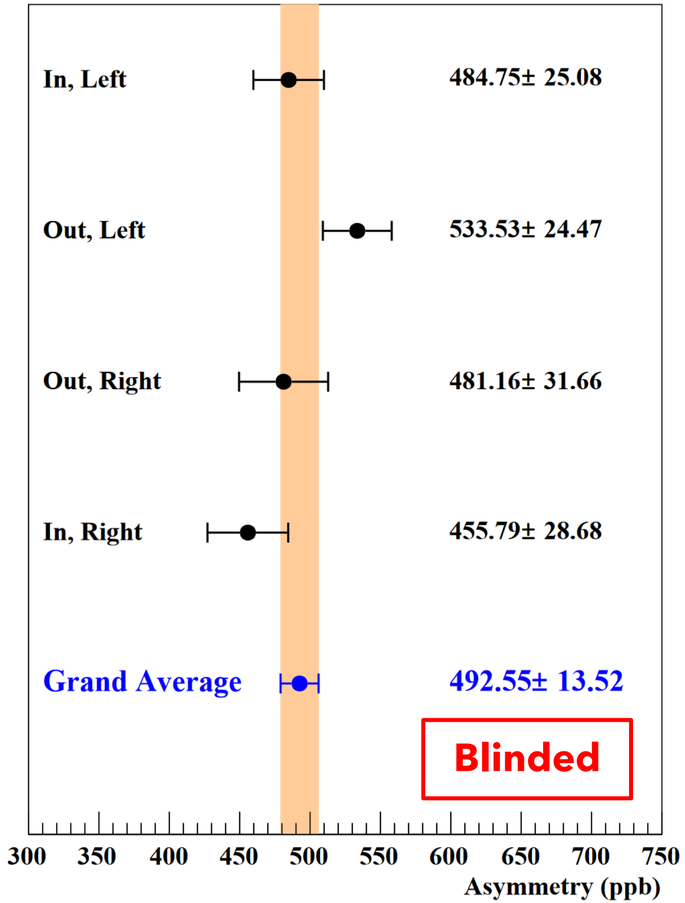




- The corrected asymmetry removed effects from beam asymmetries and noise
- Still to come: polarization and background corrections

Summary of Systematics

The final result is dominated by counting statistics



$$A_{PV} = R_{acceptNorm}\frac{A_{corr}/P_e - \sum_i A_i f_i}{1 - \sum_i f_i}$$

$$A_{corr} = A_{raw} + A_{beam} + A_{nonLin} - A_{blind}$$

Blinded A_{PV}:

(549.4 ± 16.1)ppb

	A_{PV} uncertainty contribution [ppb]	A_{PV} uncertainty contribution [%]
Polarization	5.23	0.95%
Acceptance normalization	4.56	0.83%
Beam correction	2.98	0.54%
Non-linear detector response	2.69	0.49%
Carbon dilution	1.45	0.26%
Charge correction	0.25	0.04%
Inelastic contamination	0.12	0.02%
Total	**8.16**	**1.48%**

When taken all into account the experimental systematic uncertainty comes to just shy of 1.5%

Unblinding

Blinded A_{PV}:

(549.4 ± 16.1)ppb

"Blinding box": an additive term on every octet asymmetry, randomly selected (flat) at the start of the run,

from ± 160 ppb

Unblinding

Blinded A_{PV}:
(549.4 ± 16.1)ppb

Unblinded A_{PV}:
(550.0 ± 16.1)ppb

"Blinding box": an additive term on every octet asymmetry, randomly selected (flat) at the start of the run,
from ± 160 ppb

Blinding term turned out to be 0.5313 ppb !!!

Unblinding

Blinded A_{PV}:
(549.4 ± 16.1)ppb

Unblinded A_{PV}:
(550.0 ± 16.1)ppb

"Blinding box": an additive term on every octet asymmetry, randomly selected (flat) at the start of the run,
from ± 160 ppb

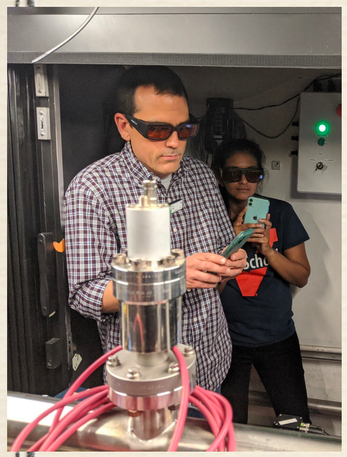
Blinding term turned out to be 0.5313 ppb !!!

This is entirely just luck-of-the-draw 🙄

	Blindedasym - rawasym (ppb)	
ops	0.5313	Roadkill stew sounds mighty good right NOW. --- Unspecified collaborator
test1	6.0223	Roadlife stew sounds mighty good right NOW. --- Unspecified collaborator
test2	-96.6812	Porkbean stew sounds mighty good right NOW. --- Unspecified collaborator
test3	53.2091	Suspicious stew sounds mighty good right NOW. --- Unspecified collaborator
test4	-121.4924	Road-kill stew sounds mighty good right NOW. --- Unspecified collaborator

Congratulations to the PREX crew

Students: **Devi Adhikari**, Devaki Bhatta Pathak, Quinn Campagna, Yufan Chen, **Cameron Clarke**, Catherine Feldman, **Iris Halilovic**, **Siyu Jian**, **Eric King**, Carrington Metts, Marisa Petrusky, **Amali Premathilake**, **Victoria Owen**, **Robert Radloff**, **Sakib Rahman**, **Ryan Richards**, Ezekiel Wertz, **Tao Ye**, **Adam Zec**, **Weibin Zhang**








Post-docs and Run Coordinators: Rakitha Beminiwattha, Juan Carlos Cornejo, Mark-Macrae Dalton, Ciprian Gal, Chandan Ghosh, Donald Jones, Tyler Kutz, Hanjie Liu, Juliette Mammei, Dustin McNulty, Caryn Palatchi, Sanghwa Park, Ye Tian, Jinlong Zhang

Spokespeople: Kent Paschke (contact), Krishna Kumar, Robert Michaels, Paul A. Souder, Guido M. Urciuoli

Thanks to the Hall A techs, Machine Control, Yves Roblin, Jay Benesch and other Jefferson Lab staff

Special thanks to: Charles Horowitz and Jorge Piekarewicz for support and insightful conversations
Especially Chuck and grad student Brendan Reed who have worked to help us interpret our results

PREX and CREX Final Results

697 citations

^{208}Pb

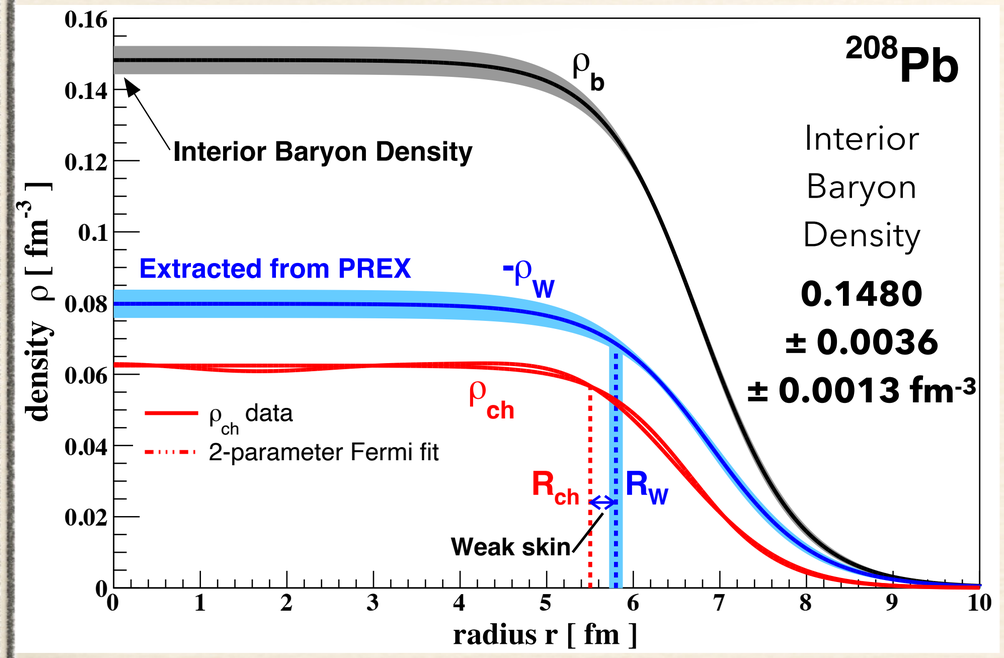
Phys.Rev.Lett. 126 (2021) 17, 172502

$$A_{\rm PV} = 550 \pm 16({\rm stat}) \pm 8\ ({\rm syst})\ \ {\rm ppb}$$

$F_W (Q^2 = 0.00616\ GeV^2) = 0.368 \pm 0.013$

Implied neutron skin thickness PREX-1 and PREX-2

$$R_n - R_p = 0.283 \pm 0.071\ {\rm fm}$$



PREX and CREX Final Results

697 citations

^{208}Pb

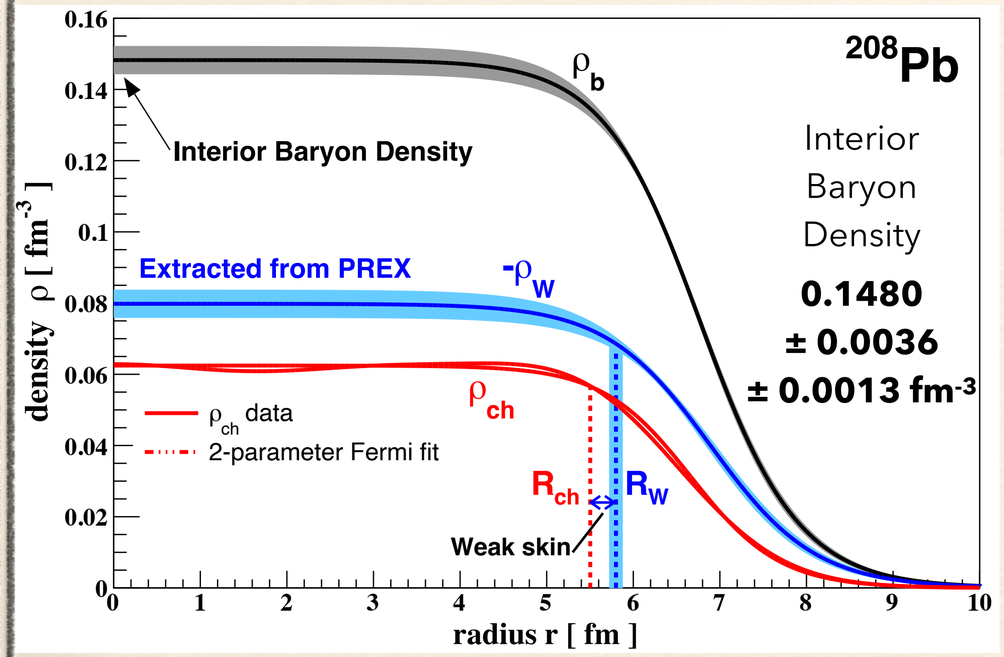
Phys.Rev.Lett. 126 (2021) 17, 172502

$$A_{PV} = 550 \pm 16(\text{stat}) \pm 8\ (\text{syst})\ \text{ppb}$$

F_W (Q^2 = 0.00616 GeV^2) = 0.368 ± 0.013

Implied neutron skin thickness PREX-1 and PREX-2

$$R_n - R_p = 0.283 \pm 0.071\ \text{fm}$$



340 citations

^{48}Ca

Phys.Rev.Lett. 129 (2022) 4, 042501

$$A_{PV} = 2668 \pm 106\ (\text{stat}) \pm 40\ (\text{sys})\ \text{ppb}$$

F_W (Q^2 = 0.0297 GeV^2) = 0.1304 ± 0.0055

Implied neutron skin thickness from CREX

$$R_n - R_p = 0.121 \pm 0.026\ (\text{exp}) \pm 0.024\ (\text{model})$$

PREX and CREX Final Results

697 citations

^{208}Pb

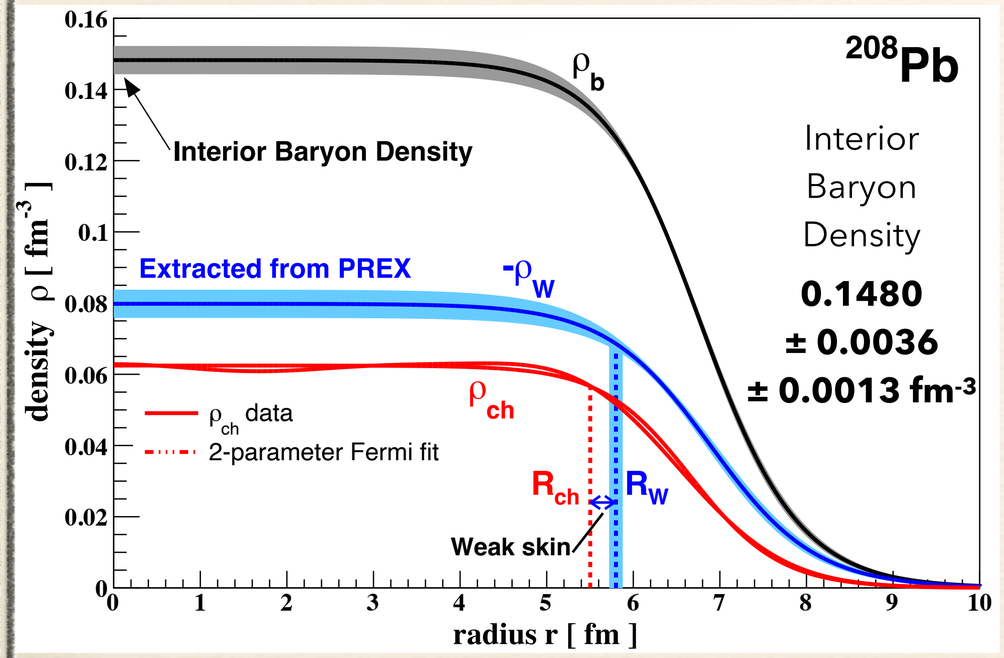
Phys.Rev.Lett. 126 (2021) 17, 172502

$$A_{PV} = 550 \pm 16(\text{stat}) \pm 8\ (\text{syst})\ \text{ppb}$$

$F_W (Q^2 = 0.00616\ \text{GeV}^2) = 0.368 \pm 0.013$

Implied neutron skin thickness PREX-1 and PREX-2

$$R_n - R_p = 0.283 \pm 0.071\ \text{fm}$$



340 citations

^{48}Ca

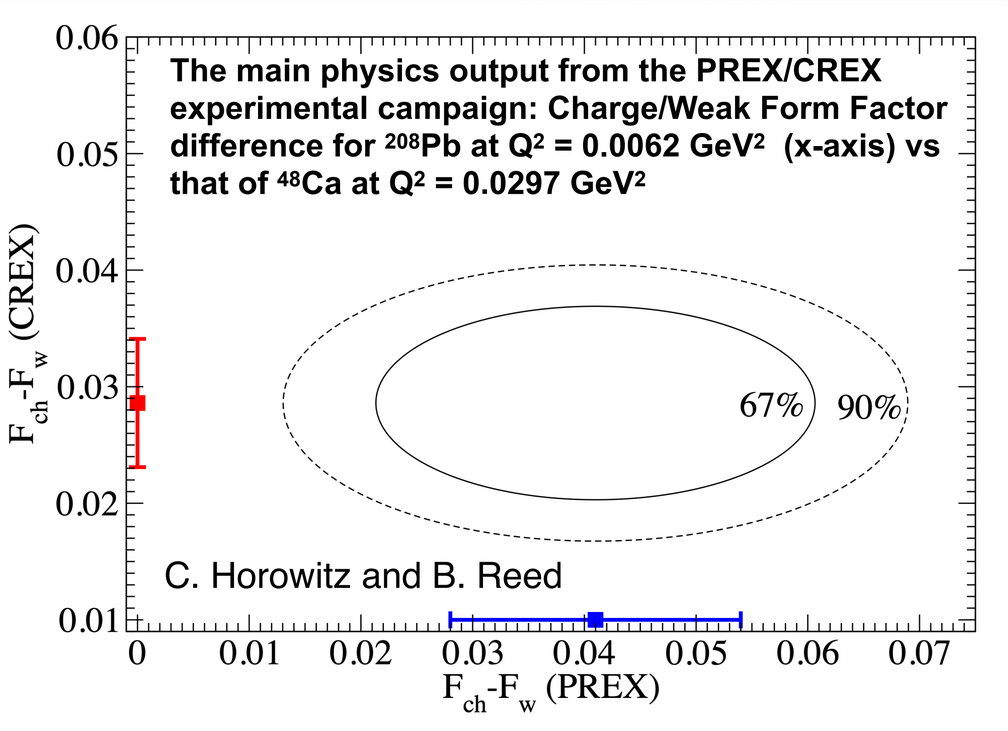
Phys.Rev.Lett. 129 (2022) 4, 042501

$$A_{PV} = 2668 \pm 106\ (\text{stat}) \pm 40\ (\text{sys})\ \text{ppb}$$

$F_W (Q^2 = 0.0297\ \text{GeV}^2) = 0.1304 \pm 0.0055$

Implied neutron skin thickness from CREX

$$R_n - R_p = 0.121 \pm 0.026\ (\text{exp}) \pm 0.024\ (\text{model})$$



PREX and CREX Final Results

^{208}Pb

697 citations

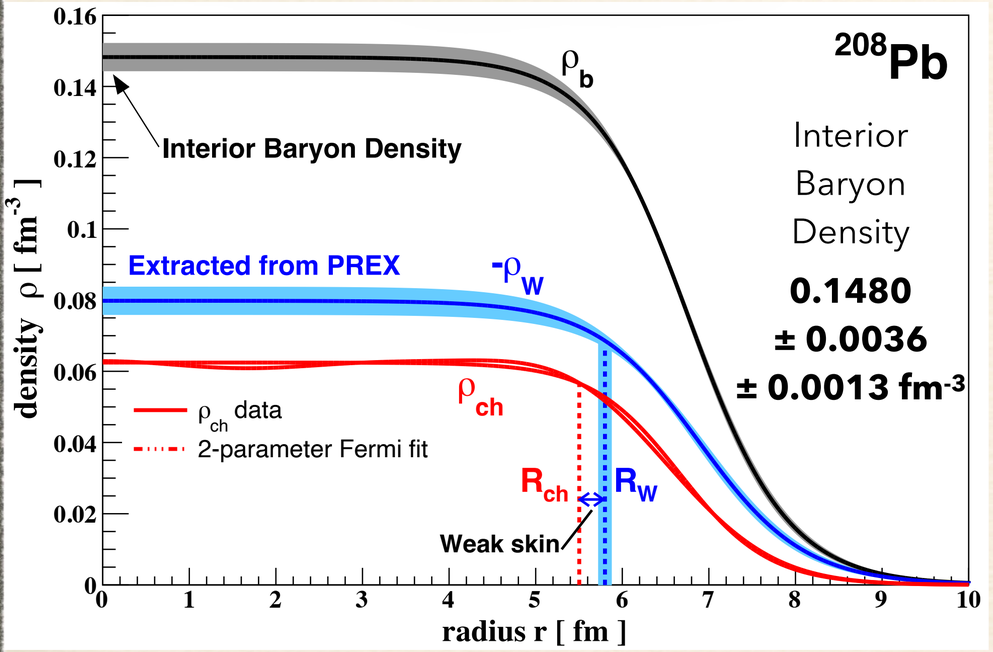
Phys.Rev.Lett. 126 (2021) 17, 172502

$$A_{PV} = 550 \pm 16(\text{stat}) \pm 8\ (\text{syst})\ \text{ppb}$$

F_W (Q^2 = 0.00616 GeV^2) = 0.368 ± 0.013

Implied neutron skin thickness PREX-1 and PREX-2

$$R_n - R_p = 0.283 \pm 0.071\ \text{fm}$$



^{48}Ca

340 citations

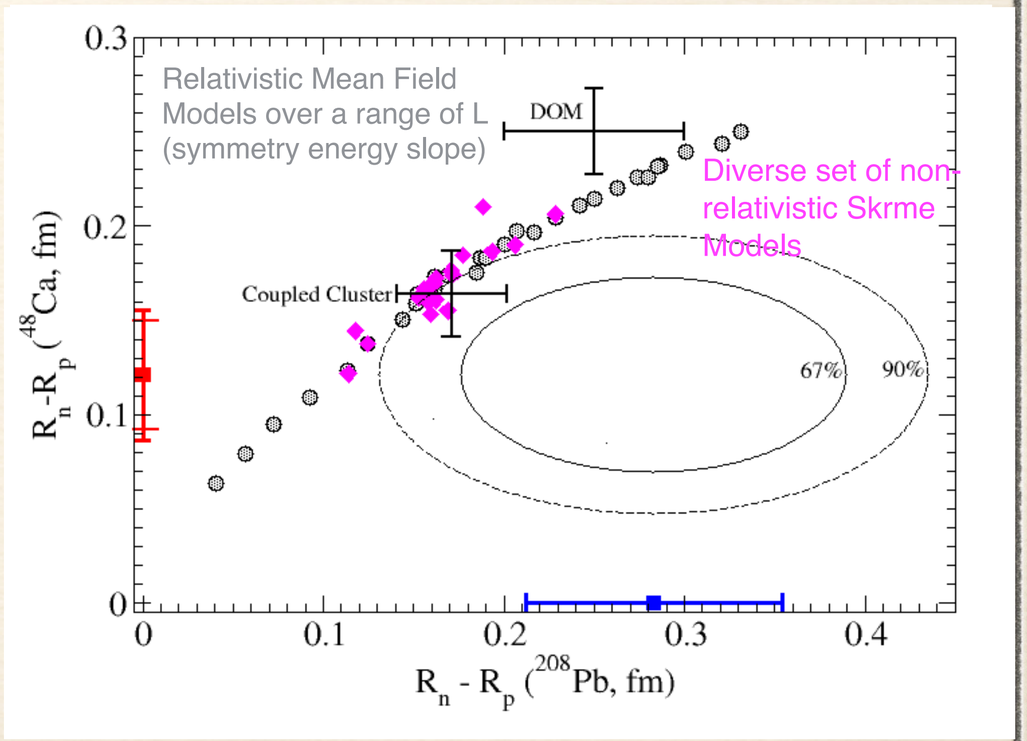
Phys.Rev.Lett. 129 (2022) 4, 042501

$$A_{PV} = 2668 \pm 106\ (\text{stat}) \pm 40\ (\text{sys})\ \text{ppb}$$

F_W (Q^2 = 0.0297 GeV^2) = 0.1304 ± 0.0055

Implied neutron skin thickness from CREX

$$R_n - R_p = 0.121 \pm 0.026\ (\text{exp}) \pm 0.024\ (\text{model})$$



PREX and CREX Final Results

697 citations

^{208}Pb

Phys.Rev.Lett. 126 (2021) 17, 172502

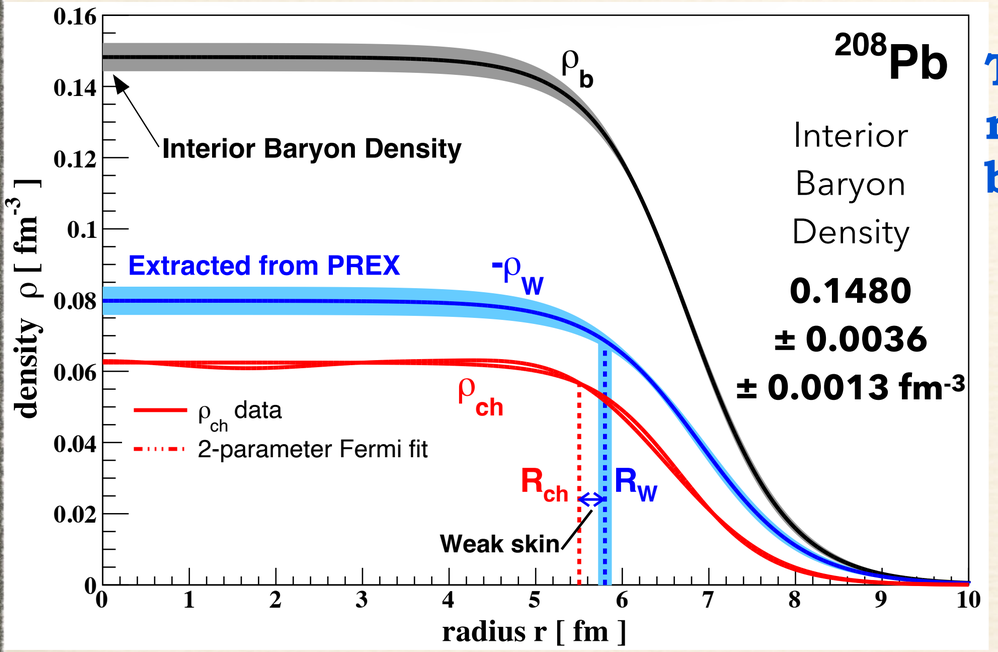
$$A_{PV} = 550 \pm 16(\text{stat}) \pm 8\ (\text{syst})\ \text{ppb}$$

F_W (Q^2 = 0.00616 GeV^2) = 0.368 ± 0.013

Implied neutron skin thickness PREX-1 and PREX-2

$$R_n - R_p = 0.283 \pm 0.071\ \text{fm}$$

The PREX ^{208}Pb measurement has very little model uncertainty



340 citations

^{48}Ca

Phys.Rev.Lett. 129 (2022) 4, 042501

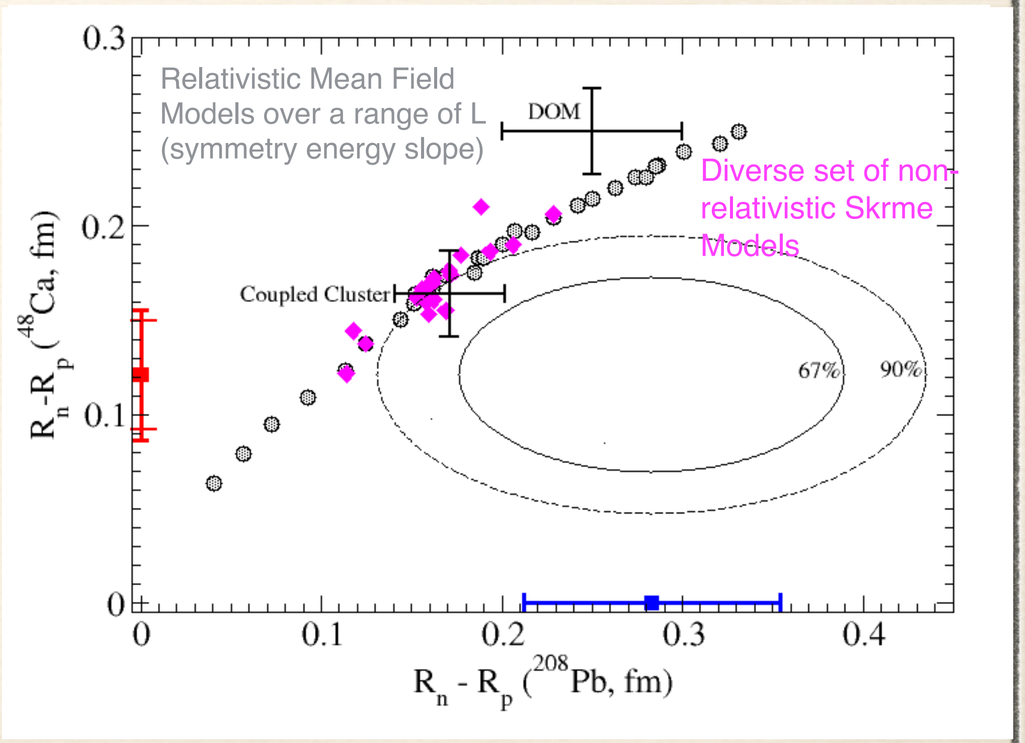
$$A_{PV} = 2668 \pm 106\ (\text{stat}) \pm 40\ (\text{sys})\ \text{ppb}$$

F_W (Q^2 = 0.0297 GeV^2) = 0.1304 ± 0.0055

Implied neutron skin thickness from CREX

$$R_n - R_p = 0.121 \pm 0.026\ (\text{exp}) \pm 0.024\ (\text{model})$$

The CREX ^{48}Ca measurement will be hard to improve



PREX and CREX Final Results

^{208}Pb

697 citations

Phys.Rev.Lett. 126 (2021) 17, 172502

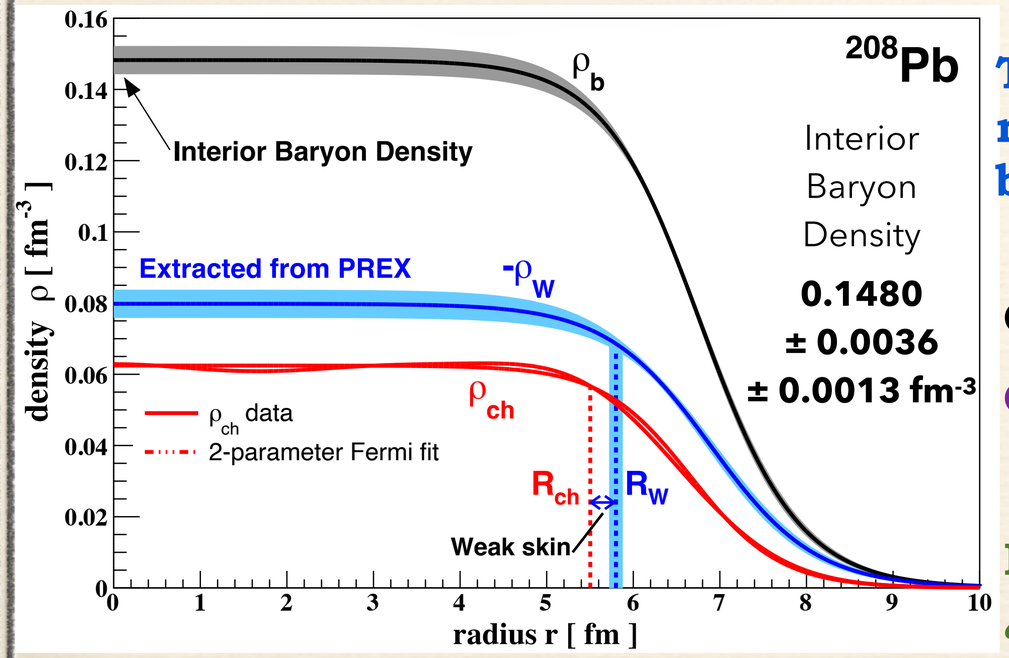
$$A_{PV} = 550 \pm 16(\text{stat}) \pm 8\ (\text{syst})\ \text{ppb}$$

F_W (Q^2 = 0.00616 GeV^2) = 0.368 ± 0.013

Implied neutron skin thickness PREX-1 and PREX-2

$$R_n - R_p = 0.283 \pm 0.071\ \text{fm}$$

The PREX ^{208}Pb measurement has very little model uncertainty



^{48}Ca

340 citations

Phys.Rev.Lett. 129 (2022) 4, 042501

$$A_{PV} = 2668 \pm 106\ (\text{stat}) \pm 40\ (\text{sys})\ \text{ppb}$$

F_W (Q^2 = 0.0297 GeV^2) = 0.1304 ± 0.0055

Implied neutron skin thickness from CREX

$$R_n - R_p = 0.121 \pm 0.026\ (\text{exp}) \pm 0.024\ (\text{model})$$

The CREX ^{48}Ca measurement will be hard to improve

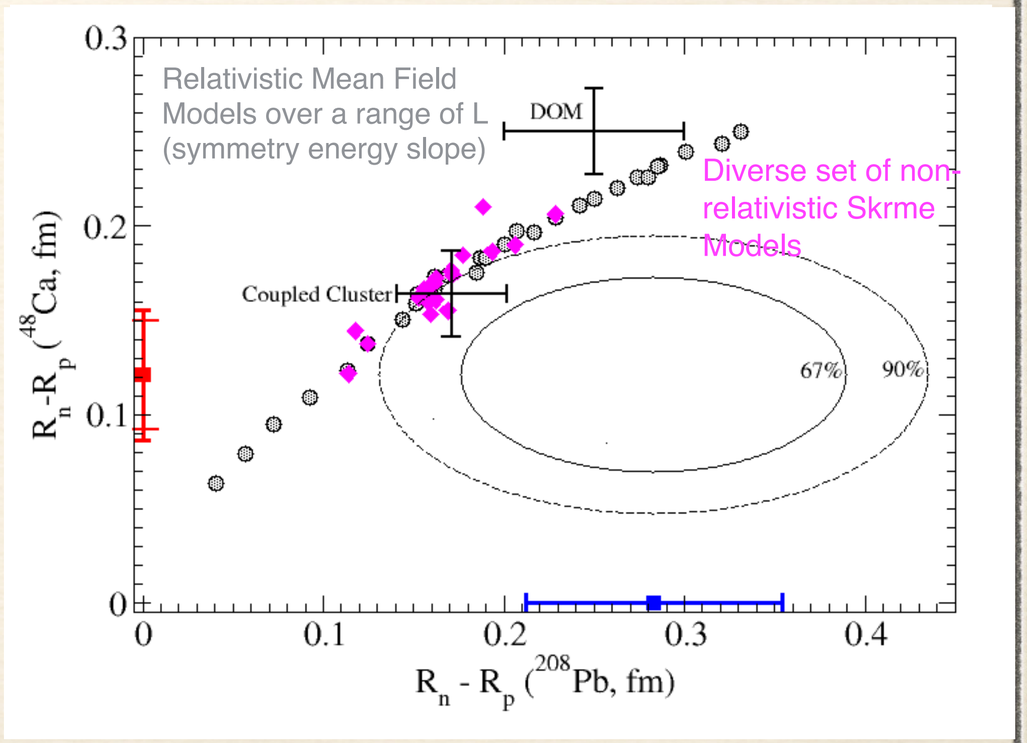
Community "Lore":

Ca-48 skin:

"too thin"

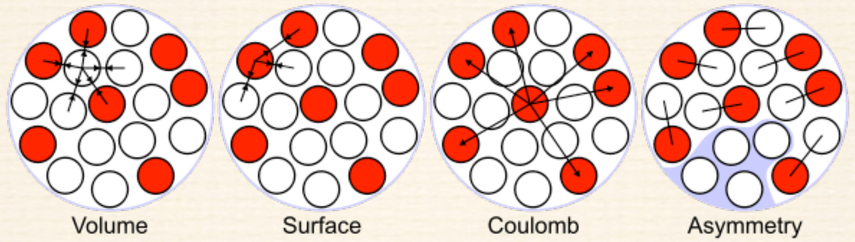
Pb-208 skin:

"too thick"



Neutron Radius: Broader Context

- *Nuclear Structure Physics*
- *Neutron Star Physics*
- *Atomic Parity Violation*
- *Coherent Neutrino Scattering*



pressure pushes against surface tension

Equation of state (EOS) of dense nuclear matter

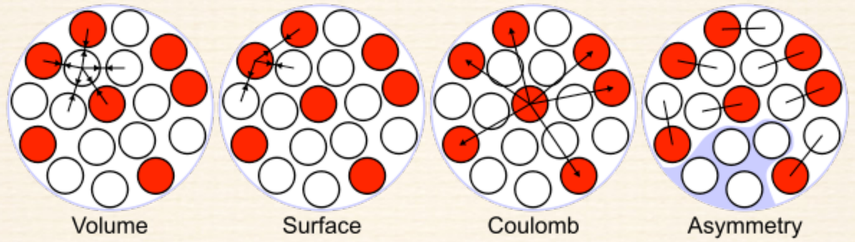
$$E(\rho,\delta) = E_0(\rho,\delta=0) + S(\rho)\delta^2$$

$$\delta = \frac{(\rho_n - \rho_p)}{\rho}$$

Symmetry Energy

Neutron Radius: Broader Context

- *Nuclear Structure Physics*
- *Neutron Star Physics*
- *Atomic Parity Violation*
- *Coherent Neutrino Scattering*



pressure pushes against surface tension

Equation of state (EOS) of dense nuclear matter

$$E(\rho,\delta) = E_0(\rho,\delta=0) + S(\rho)\delta^2$$

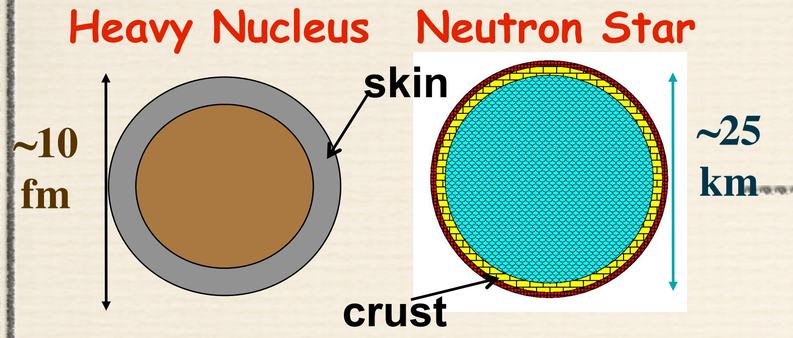
Symmetry Energy

size of neutron skin

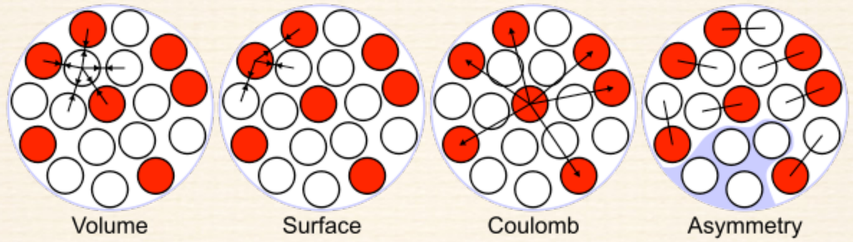
↓

pressure → density dependence of symmetry energy at subnuclear densities

Neutron Radius: Broader Context



- *Nuclear Structure Physics*
- *Neutron Star Physics*
- *Atomic Parity Violation*
- *Coherent Neutrino Scattering*



pressure pushes against surface tension

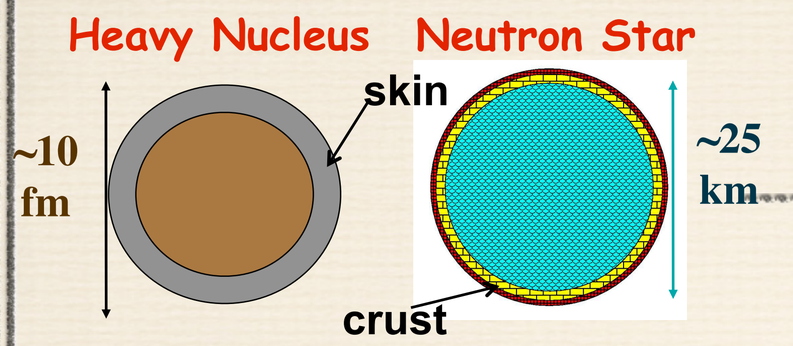
Equation of state (EOS) of dense nuclear matter

$$E(\rho,\delta) = E_0(\rho,\delta=0) + S(\rho)\delta^2$$

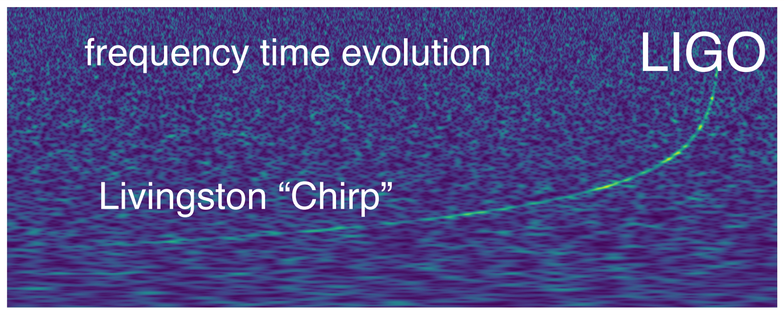
Symmetry Energy

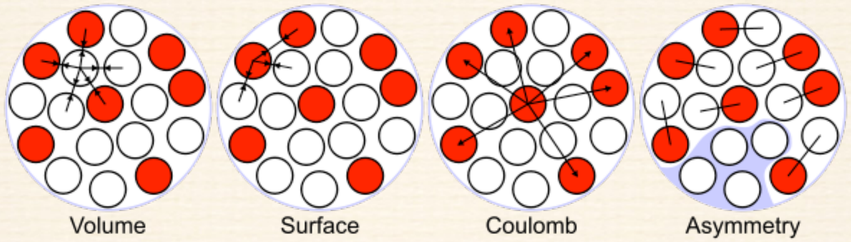
size of neutron skin → pressure → density dependence of symmetry energy at subnuclear densities

Neutron Radius: Broader Context

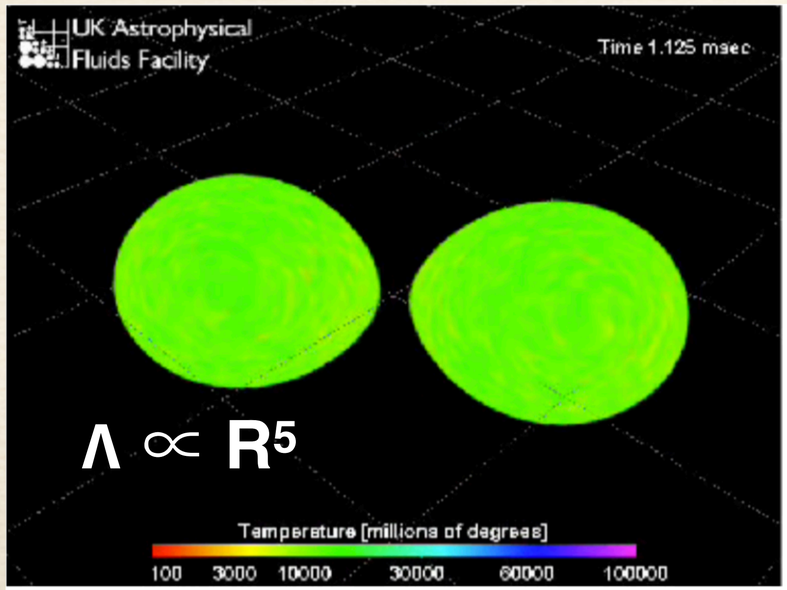


- *Nuclear Structure Physics*
- *Neutron Star Physics*
- *Atomic Parity Violation*
- *Coherent Neutrino Scattering*





pressure pushes against surface tension



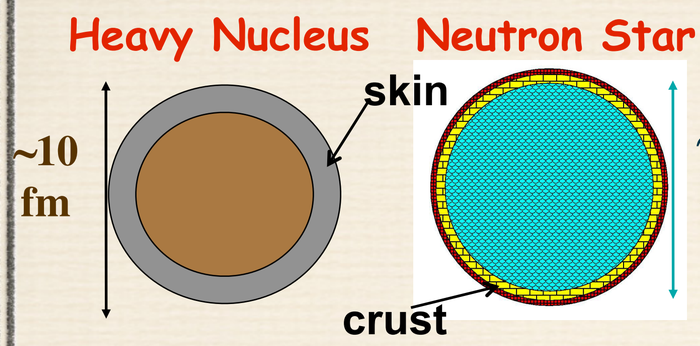
Equation of state (EOS) of dense nuclear matter

$$E(\rho,\delta) = E_0(\rho,\delta=0) + S(\rho)\delta^2$$

Symmetry Energy

size of neutron skin → pressure → density dependence of symmetry energy at subnuclear densities

Neutron Radius: Broader Context

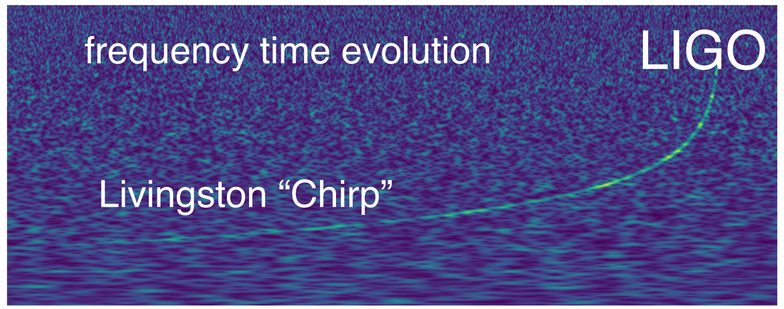


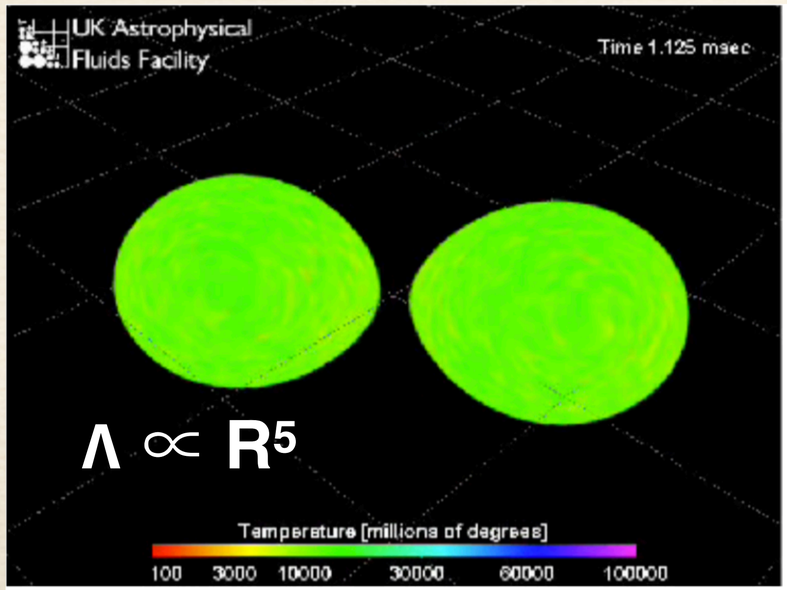
- *Nuclear Structure Physics*
- *Neutron Star Physics*
- *Atomic Parity Violation*
- *Coherent Neutrino Scattering*

LIGO Binary Inspiral Tidal Deformability

Neutron Star Radius

NICER Measurements of Pulsar X-rays





^{208}Pb Neutron Skin

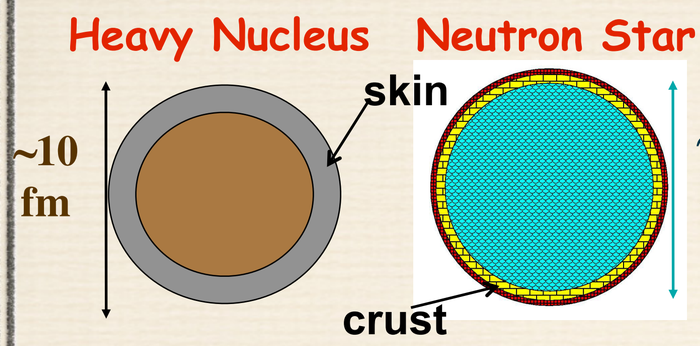
Equation of state (EOS) of dense nuclear matter

$$E(\rho,\delta) = E_0(\rho,\delta=0) + S(\rho)\delta^2$$

Symmetry Energy

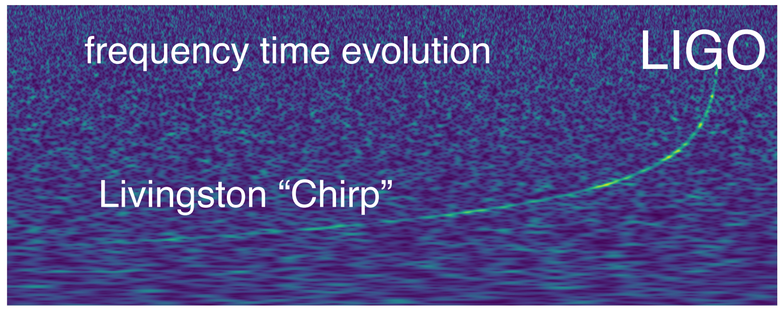
size of neutron skin → pressure → density dependence of symmetry energy at subnuclear densities

Neutron Radius: Broader Context



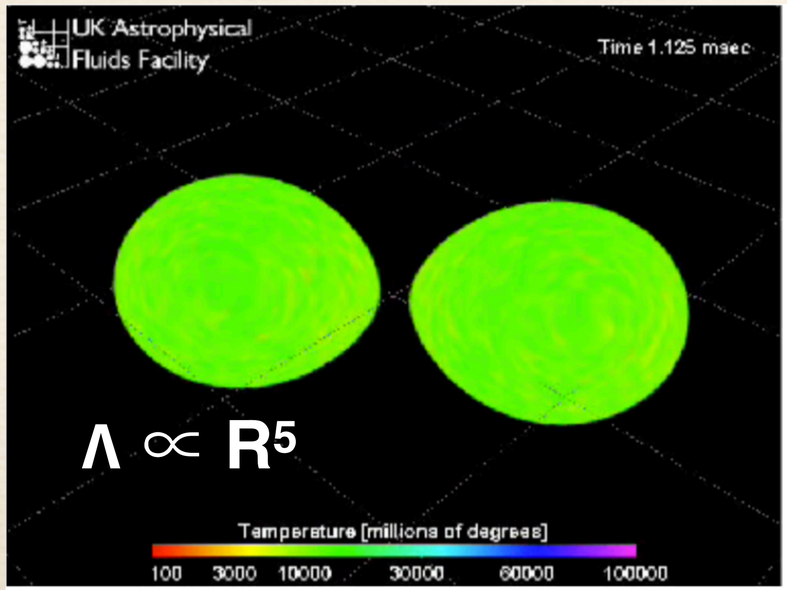
- *Nuclear Structure Physics*
- *Neutron Star Physics*
- *Atomic Parity Violation*
- *Coherent Neutrino Scattering*

LIGO Binary Inspiral Tidal Deformability ⟷ **Neutron Star Radius** ⟷ *NICER Measurements of Pulsar X-rays*



MREX at MESA: *Use of a solenoidal spectrometer with a 200 MeV beam*

→ $\delta(A_{PV})/A_{PV} \sim 1.5\%$ → $\delta(R_n)$: ± 0.03 fm



^{208}Pb Neutron Skin

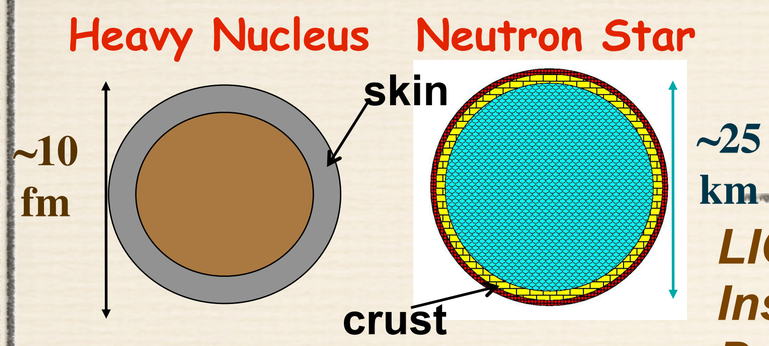
Equation of state (EOS) of dense nuclear matter

$$E(\rho,\delta) = E_0(\rho,\delta=0) + S(\rho)\delta^2$$

Symmetry Energy

size of neutron skin → pressure → density dependence of symmetry energy at subnuclear densities

Neutron Radius: Broader Context

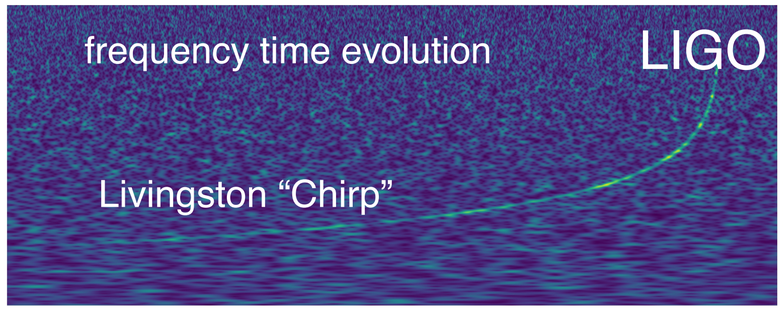


- *Nuclear Structure Physics*
- *Neutron Star Physics*
- *Atomic Parity Violation*
- *Coherent Neutrino Scattering*

LIGO Binary Inspiral Tidal Deformability

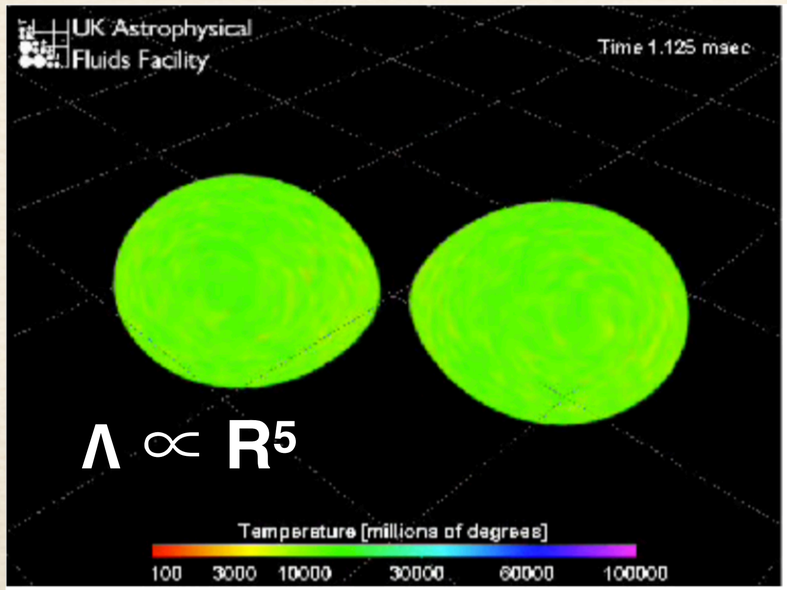
Neutron Star Radius

NICER Measurements of Pulsar X-rays



MREX at MESA: *Use of a solenoidal spectrometer with a 200 MeV beam*

$\delta(A_{PV})/A_{PV} \sim 1.5\%$ → $\delta(R_n)$: ± 0.03 fm



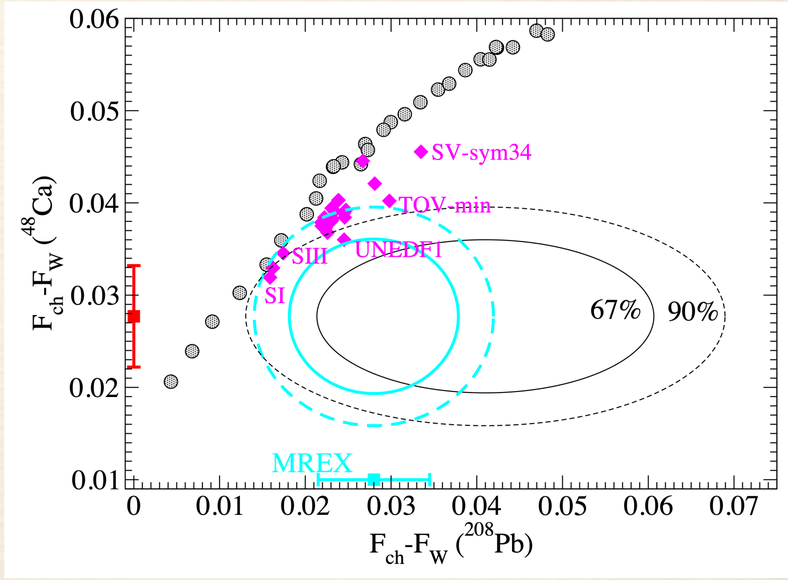
^{208}Pb Neutron Skin

Equation of state (EOS) of dense nuclear matter

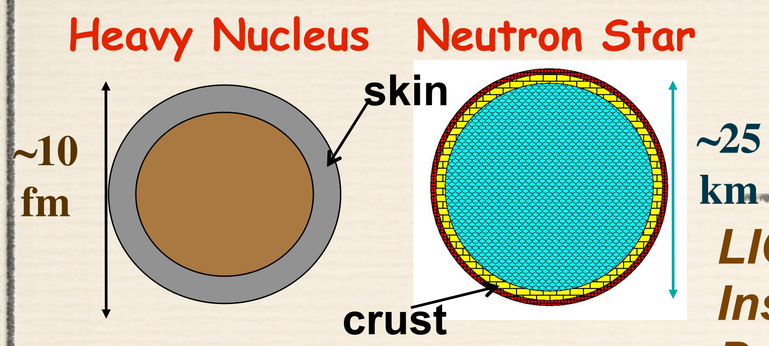
$$E(\rho,\delta) = E_0(\rho,\delta=0) + S(\rho)\delta^2$$

Symmetry Energy

size of neutron skin → pressure → density dependence of symmetry energy at subnuclear densities

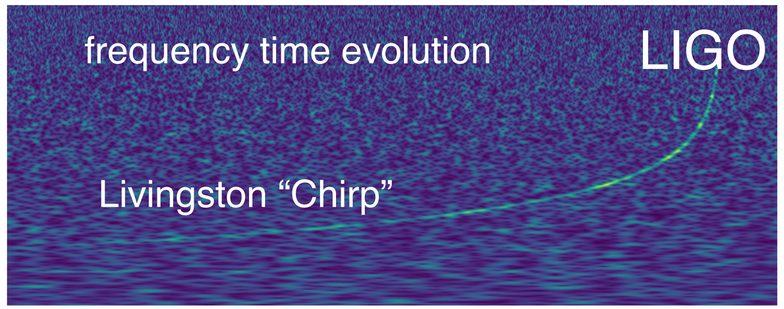


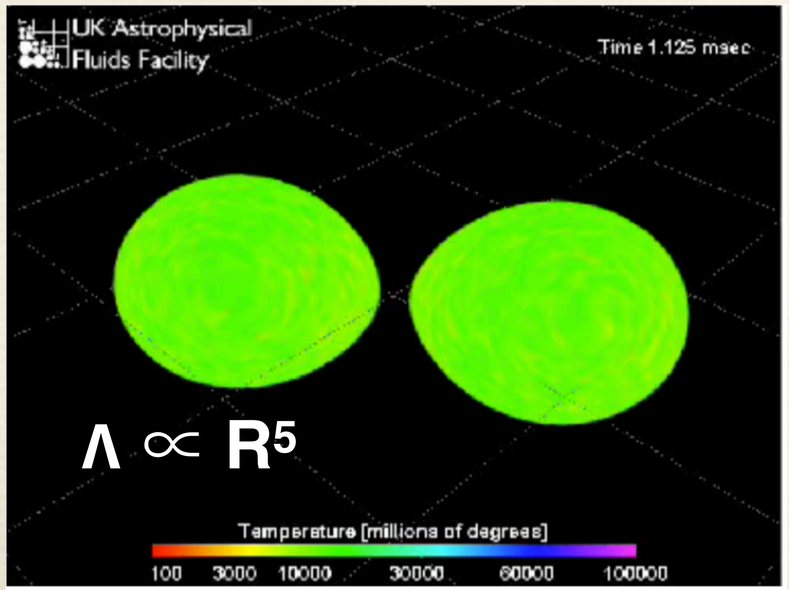
Neutron Radius: Broader Context



- *Nuclear Structure Physics*
- *Neutron Star Physics*
- *Atomic Parity Violation*
- *Coherent Neutrino Scattering*

LIGO Binary Inspiral Tidal Deformability ⟷ **Neutron Star Radius** ⟷ *NICER Measurements of Pulsar X-rays*





^{208}Pb Neutron Skin

Equation of state (EOS) of dense nuclear matter

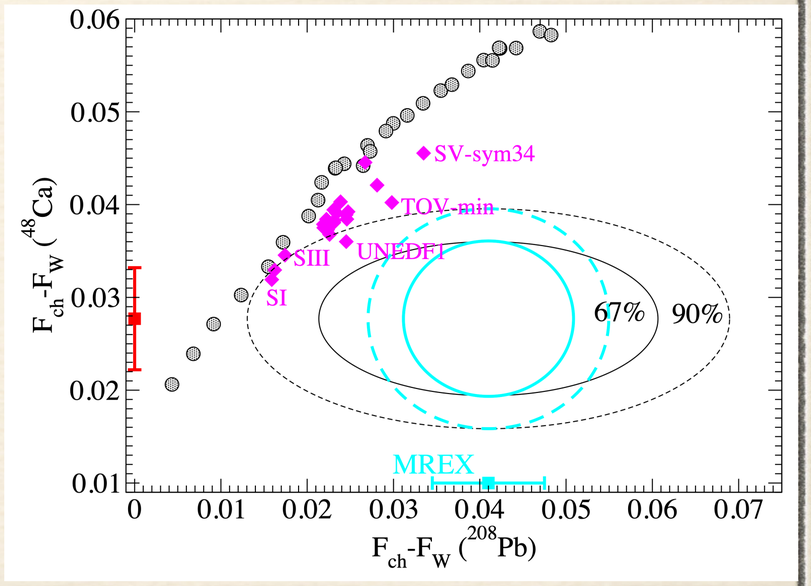
$$E(\rho,\delta) = E_0(\rho,\delta=0) + S(\rho)\delta^2$$

Symmetry Energy

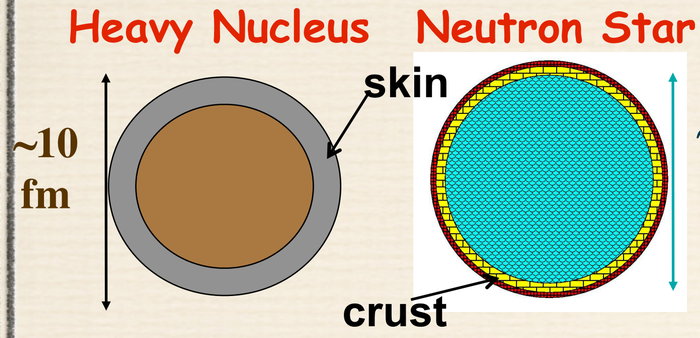
size of neutron skin ↓ pressure → density dependence of symmetry energy at subnuclear densities

MREX at MESA: *Use of a solenoidal spectrometer with a 200 MeV beam*

$\delta(A_{PV})/A_{PV} \sim 1.5\%$ → $\delta(R_n)$: ± 0.03 fm

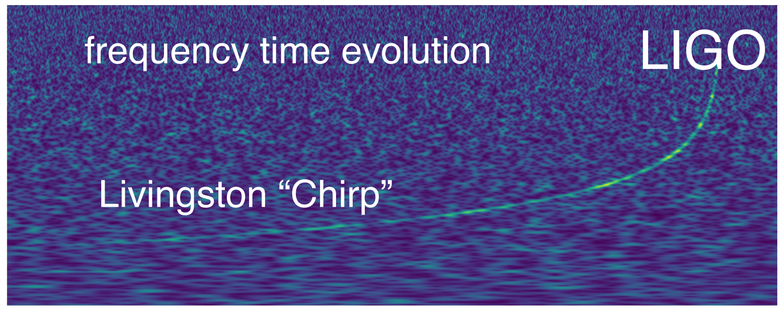


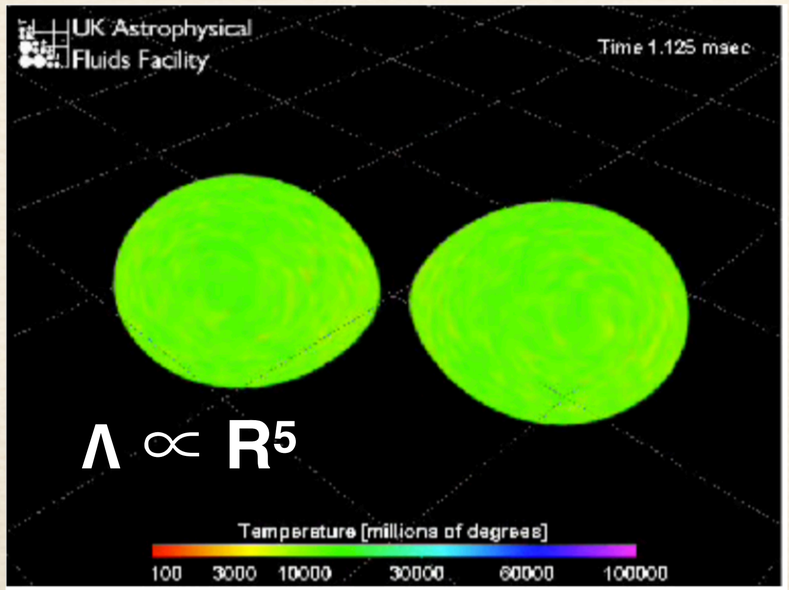
Neutron Radius: Broader Context



- *Nuclear Structure Physics*
- *Neutron Star Physics*
- *Atomic Parity Violation*
- *Coherent Neutrino Scattering*

LIGO Binary Inspiral Tidal Deformability ⟷ **Neutron Star Radius** ⟷ *NICER Measurements of Pulsar X-rays*





MREX at MESA: *Use of a solenoidal spectrometer with a 200 MeV beam*

$\delta(A_{PV})/A_{PV} \sim 1.5\%$ → $\delta(R_n)$: ± 0.03 fm

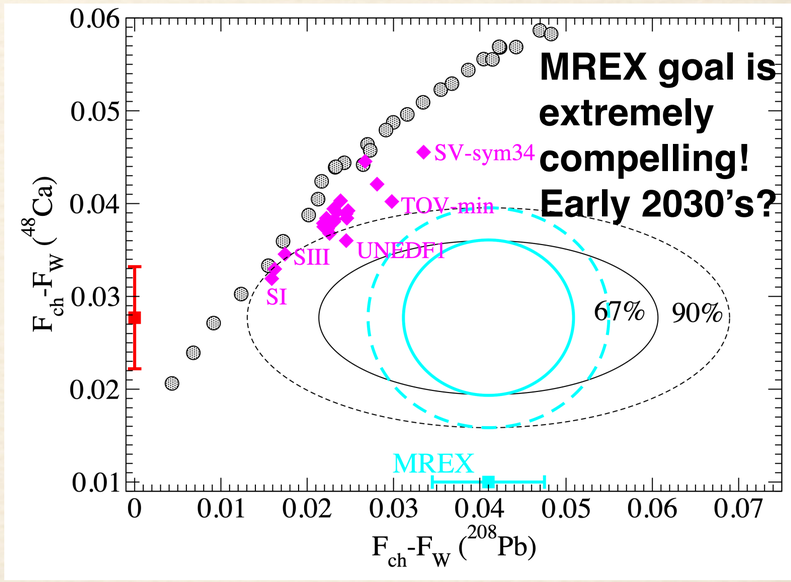
^{208}Pb Neutron Skin

Equation of state (EOS) of dense nuclear matter

$$E(\rho,\delta) = E_0(\rho,\delta=0) + S(\rho)\delta^2$$

Symmetry Energy

size of neutron skin → pressure → density dependence of symmetry energy at subnuclear densities



PVES at the EIC

The Electron Ion Collider

•***Ultimate EIC Performance Parameters:***

- High Luminosity: L= 10^{33} – 10^{34}cm^{-2}sec^{-1}
- Highly Polarized Beams: 70%
- Large Center of Mass Energy Range: Ecm = 28 – 140 GeV
- Large Ion Species Range: protons – Uranium
- Large Detector Forward Acceptance and Low-Background Conditions
- Possibility to Implement a **Second Interaction Region (IR)**

Accelerator Status at a glance:

✓ Polarized ion/proton source

✓ Ion injection and initial acceleration systems – Linac (200 MeV), Booster (1.5 GeV), AGS (25 GeV)

UPGRADE Hadron Storage Ring (40-275 GeV) – HSR

NEW Electron Pre-Injector (750 MeV linac)

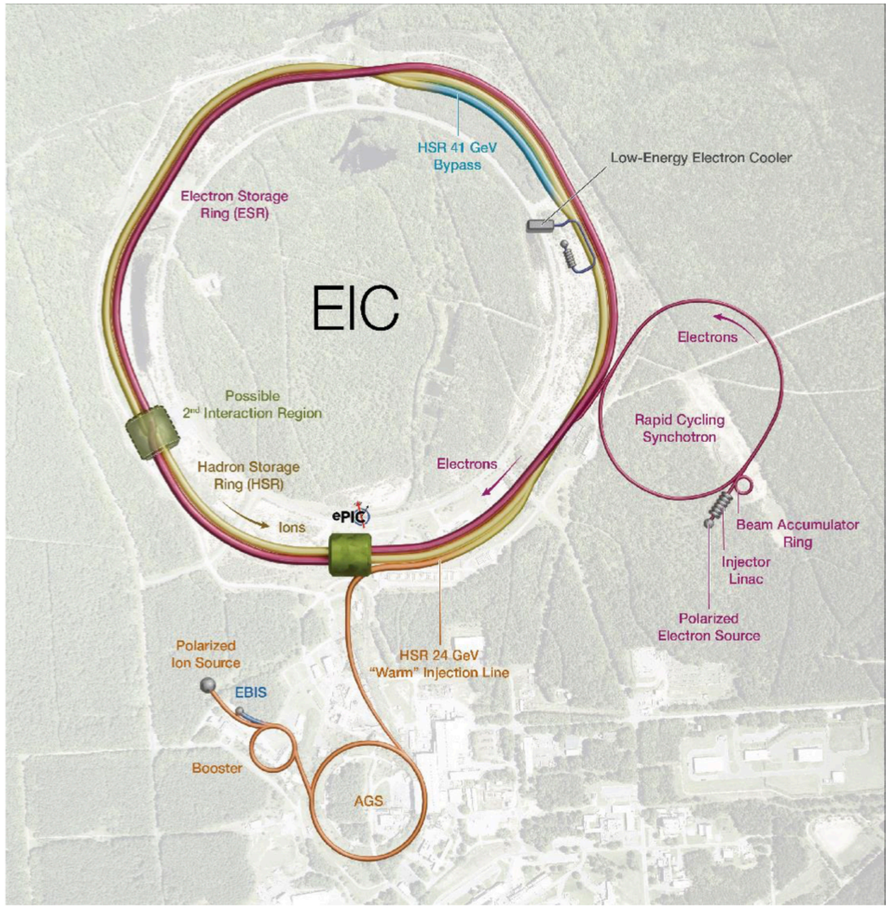
NEW Beam Accumulation Ring (750 MeV) – BAR

NEW Electron Rapid Cycling Synchrotron (0.75 GeV – top energy) – RCS

NEW Electron Storage Ring (5 GeV – 18 GeV) – ESR

NEW Interaction Region(s) – IR

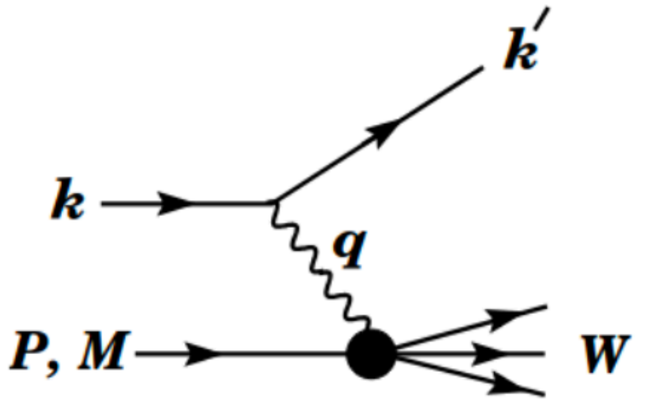
NEW Hadron Cooling System

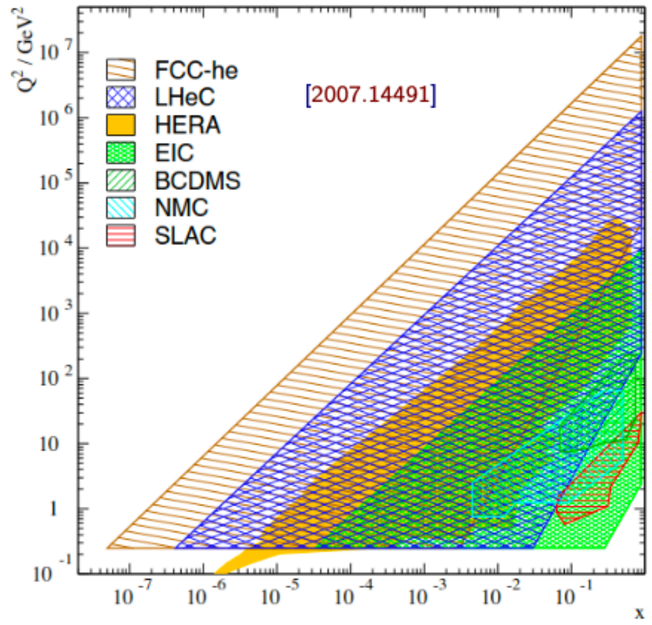


Protons: ~40 – 275 GeV
Electrons: 5 – 18 GeV

Deep Inelastic Scattering

Deep Inelastic Scattering: Kinematics





In the nucleon's rest frame

- $\nu = \frac{q\cdot P}{M} = E - E'$: lepton's energy loss
- $Q^2 = -q^2 = 2(EE' - \vec{k}\cdot\vec{k}') - m_\ell^2 - m_{\ell'}^2 \approx 2EE'(1-\cos\theta)$: photon virtuality (momentum transfer)
- $x = \frac{Q^2}{2M\nu}$: Bjorken x, parton momentum fraction at the LO
- $y = \frac{q\cdot P}{k\cdot P} = \frac{\nu}{E} = 1 - \frac{E'}{E}$: inelasticity, lepton's energy loss fraction
- $W^2 = (P+q)^2 = M^2 + 2M\nu - Q^2$: squared mass of the X system
- $s = (k+P)^2 = \frac{Q^2}{xy} + M^2 + m_\ell^2$: center-of-mass energy square

DIS conditions:

- Deep: $Q^2 \gg M^2$
- Inelastic: $W^2 \gg M^2$ with a lower bound $(M+m_\pi)^2$

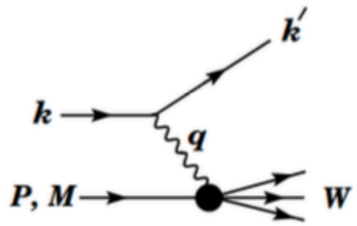
Photon, W and Z exchange

Structure Functions

Keping Xie

Schematically

$$d\sigma \sim \sum_X \left| \quad \right|^2 \sim L^{\mu\nu} W_{\mu\nu}$$



- $L^{\mu\nu}$ Leptonic tensor, calculable with the electroweak interaction
- $W_{\mu\nu}$ Hadronic tensor, constrained by Lorentz invariance

Cross section

$$\frac{d^2\sigma^i}{dx\,dy} = \underbrace{\frac{4\pi\alpha^2}{xyQ^2}\,\eta^i}_{\text{Leptonic}} \underbrace{\left\{\left(1-y-\frac{x^2y^2M^2}{Q^2}\right)F_2^i + y^2 xF_1^i \mp \left(y-\frac{y^2}{2}\right)xF_3^i\right\}}_{\text{Hadronic}}$$

- Neutral Current: $\eta^{\rm NC} = 1$ for unpolarized $e^\pm$,

$$F_2^{\rm NC} = F_2^\gamma - (g_V^e \pm \lambda g_A^e)\,\eta_{\gamma Z}\,F_2^{\gamma Z} + \left({g_V^e}^2 + {g_A^e}^2 \pm 2\lambda g_V^e g_A^e\right)\eta_Z\,F_2^Z$$

$$xF_3^{\rm NC} = -(g_A^e \pm \lambda g_V^e)\,\eta_{\gamma Z}\,xF_3^{\gamma Z} + \left[2g_V^e g_A^e \pm \lambda\left({g_V^e}^2 + {g_A^e}^2\right)\right]\eta_Z\,xF_3^Z$$

- Charged Current: $\eta^{\rm CC} = (1\pm\lambda)^2\eta_W$

$$F_1^{\rm CC} = F_1^W, \quad F_2^{\rm CC} = F_2^W, \quad xF_3^{\rm CC} = xF_3^W$$

New Structure Functions

Keping Xie

Neutral Current Couplings in S(2)XU(1): $g_V = T^3 - 2q\sin^2\theta_W \qquad g_A = T^3$

Neutral Current Cross-section: Pure photon exchange, weak-electromagnetic interference and pure Z exchange

Bjorken Scaling: In the Bjorken limit $Q^2, \nu \to \infty$, $F_i(x, Q^2) \to F_i(x)$

- Neutral Current

$$\left[F_2^\gamma, F_2^{\gamma Z}, F_2^Z\right] = x\sum_q \left[e_q^2,\, 2e_q g_V^q,\, (g_V^q)^2 + (g_A^q)^2\right](q+\bar{q}),$$

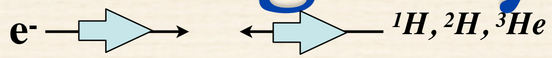
$$\left[F_3^\gamma, F_3^{\gamma Z}, F_3^Z\right] = \sum_q \left[0,\, 2e_q g_A^q,\, 2g_V^q g_A^q\right](q-\bar{q}),$$

- Charged Current

$$F_2^{W^-} = 2x\left(u + \bar{d} + \bar{s} + c\ldots\right),$$
$$F_3^{W^-} = 2\left(u - \bar{d} - \bar{s} + c\ldots\right),$$

- Callan-Gross relation: $F_2^i = 2xF_1^i$.

Parity-Violating Asymmetries



EIC neutral current event kinematics very clean: can very cleanly separate y-independent and y-dependent pieces and study Q^2 evolution

polarized electron, unpolarized hadron

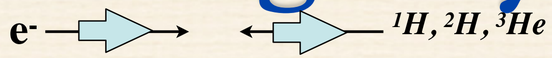
$$A_{PV} = \frac{G_F Q^2}{2\sqrt{2}\pi\alpha}\left[g_A \frac{F_1^{\gamma Z}}{F_1^{\gamma}} + g_V \frac{f(y)}{2}\frac{F_3^{\gamma Z}}{F_1^{\gamma}}\right]$$

unpolarized electron, polarized hadron

$$A_{TPV} = \frac{G_F Q^2}{2\sqrt{2}\pi\alpha}\left[g_V \frac{g_5^{\gamma Z}}{F_1^{\gamma}} + g_A f(y)\frac{g_1^{\gamma Z}}{F_1^{\gamma}}\right]$$

proton	deuteron
$F_1^{\gamma Z} \propto u + d + s$	$F_1^{\gamma Z} \propto u + d + 2s$
$F_3^{\gamma Z} \propto 2u_v + d_v$	$F_3^{\gamma Z} \propto u_v + d_v$
$g_1^{\gamma Z} \propto \Delta u + \Delta d + \Delta s$	$g_1^{\gamma Z} \propto \Delta u + \Delta d + \Delta s$
$g_5^{\gamma Z} \propto 2\Delta u_v + \Delta d_v$	$g_5^{\gamma Z} \propto \Delta u_v + \Delta d_v$

Parity-Violating Asymmetries



EIC neutral current event kinematics very clean: can very cleanly separate y-independent and y-dependent pieces and study Q^2 evolution

polarized electron, unpolarized hadron

$$A_{PV} = \frac{G_F Q^2}{2\sqrt{2}\pi\alpha}\left[g_A \frac{F_1^{\gamma Z}}{F_1^{\gamma}} + g_V \frac{f(y)}{2}\frac{F_3^{\gamma Z}}{F_1^{\gamma}}\right]$$

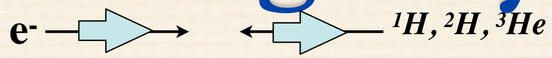
unpolarized electron, polarized hadron

$$A_{TPV} = \frac{G_F Q^2}{2\sqrt{2}\pi\alpha}\left[g_V \frac{g_5^{\gamma Z}}{F_1^{\gamma}} + g_A f(y)\frac{g_1^{\gamma Z}}{F_1^{\gamma}}\right]$$

proton	deuteron
$F_1^{\gamma Z} \propto u + d + s$	$F_1^{\gamma Z} \propto u + d + 2s$
$F_3^{\gamma Z} \propto 2u_v + d_v$	$F_3^{\gamma Z} \propto u_v + d_v$
$g_1^{\gamma Z} \propto \Delta u + \Delta d + \Delta s$	$g_1^{\gamma Z} \propto \Delta u + \Delta d + \Delta s$
$g_5^{\gamma Z} \propto 2\Delta u_v + \Delta d_v$	$g_5^{\gamma Z} \propto \Delta u_v + \Delta d_v$

- **Electron Asymmetries are sensitive to the weak mixing angle**

Parity-Violating Asymmetries



EIC neutral current event kinematics very clean: can very cleanly separate y-independent and y-dependent pieces and study Q^2 evolution

polarized electron, unpolarized hadron

$$A_{PV} = \frac{G_F Q^2}{2\sqrt{2}\pi\alpha}\left[g_A \frac{F_1^{\gamma Z}}{F_1^{\gamma}} + g_V \frac{f(y)}{2}\frac{F_3^{\gamma Z}}{F_1^{\gamma}}\right]$$

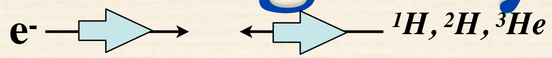
unpolarized electron, polarized hadron

$$A_{TPV} = \frac{G_F Q^2}{2\sqrt{2}\pi\alpha}\left[g_V \frac{g_5^{\gamma Z}}{F_1^{\gamma}} + g_A f(y)\frac{g_1^{\gamma Z}}{F_1^{\gamma}}\right]$$

proton	deuteron
$F_1^{\gamma Z} \propto u + d + s$	$F_1^{\gamma Z} \propto u + d + 2s$
$F_3^{\gamma Z} \propto 2u_v + d_v$	$F_3^{\gamma Z} \propto u_v + d_v$
$g_1^{\gamma Z} \propto \Delta u + \Delta d + \Delta s$	$g_1^{\gamma Z} \propto \Delta u + \Delta d + \Delta s$
$g_5^{\gamma Z} \propto 2\Delta u_v + \Delta d_v$	$g_5^{\gamma Z} \propto \Delta u_v + \Delta d_v$

- **Electron Asymmetries are sensitive to the weak mixing angle**
  - *Deuteron is very clean but need a large data set going to be even part of the program*

Parity-Violating Asymmetries



EIC neutral current event kinematics very clean: can very cleanly separate y-independent and y-dependent pieces and study Q^2 evolution

polarized electron, unpolarized hadron

$$A_{PV} = \frac{G_F Q^2}{2\sqrt{2}\pi\alpha}\left[g_A \frac{F_1^{\gamma Z}}{F_1^{\gamma}} + g_V \frac{f(y)}{2}\frac{F_3^{\gamma Z}}{F_1^{\gamma}}\right]$$

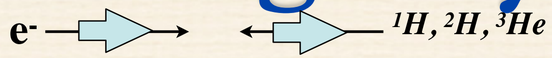
unpolarized electron, polarized hadron

$$A_{TPV} = \frac{G_F Q^2}{2\sqrt{2}\pi\alpha}\left[g_V \frac{g_5^{\gamma Z}}{F_1^{\gamma}} + g_A f(y)\frac{g_1^{\gamma Z}}{F_1^{\gamma}}\right]$$

proton	deuteron
$F_1^{\gamma Z} \propto u + d + s$	$F_1^{\gamma Z} \propto u + d + 2s$
$F_3^{\gamma Z} \propto 2u_v + d_v$	$F_3^{\gamma Z} \propto u_v + d_v$
$g_1^{\gamma Z} \propto \Delta u + \Delta d + \Delta s$	$g_1^{\gamma Z} \propto \Delta u + \Delta d + \Delta s$
$g_5^{\gamma Z} \propto 2\Delta u_v + \Delta d_v$	$g_5^{\gamma Z} \propto \Delta u_v + \Delta d_v$

- **Electron Asymmetries are sensitive to the weak mixing angle**
  - *Deuteron is very clean but need a large data set going to be even part of the program*
  - *Must control pdf uncertainties well enough to use proton events (the main data sample at EIC)*

Parity-Violating Asymmetries



EIC neutral current event kinematics very clean: can very cleanly separate y-independent and y-dependent pieces and study Q^2 evolution

polarized electron, unpolarized hadron

$$A_{PV} = \frac{G_F Q^2}{2\sqrt{2}\pi\alpha}\left[g_A \frac{F_1^{\gamma Z}}{F_1^{\gamma}} + g_V \frac{f(y)}{2}\frac{F_3^{\gamma Z}}{F_1^{\gamma}}\right]$$

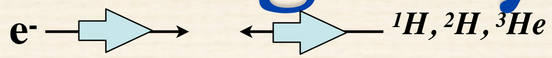
unpolarized electron, polarized hadron

$$A_{TPV} = \frac{G_F Q^2}{2\sqrt{2}\pi\alpha}\left[g_V \frac{g_5^{\gamma Z}}{F_1^{\gamma}} + g_A f(y)\frac{g_1^{\gamma Z}}{F_1^{\gamma}}\right]$$

proton	deuteron
$F_1^{\gamma Z} \propto u + d + s$	$F_1^{\gamma Z} \propto u + d + 2s$
$F_3^{\gamma Z} \propto 2u_v + d_v$	$F_3^{\gamma Z} \propto u_v + d_v$
$g_1^{\gamma Z} \propto \Delta u + \Delta d + \Delta s$	$g_1^{\gamma Z} \propto \Delta u + \Delta d + \Delta s$
$g_5^{\gamma Z} \propto 2\Delta u_v + \Delta d_v$	$g_5^{\gamma Z} \propto \Delta u_v + \Delta d_v$

- **Electron Asymmetries are sensitive to the weak mixing angle**
  - *Deuteron is very clean but need a large data set going to be even part of the program*
  - *Must control pdf uncertainties well enough to use proton events (the main data sample at EIC)*
  - *Studies are required to use both low Q^2 (well-understood) and high Q^2*

Parity-Violating Asymmetries



EIC neutral current event kinematics very clean: can very cleanly separate y-independent and y-dependent pieces and study Q^2 evolution

polarized electron, unpolarized hadron

$$A_{PV} = \frac{G_F Q^2}{2\sqrt{2}\pi\alpha}\left[g_A \frac{F_1^{\gamma Z}}{F_1^{\gamma}} + g_V \frac{f(y)}{2}\frac{F_3^{\gamma Z}}{F_1^{\gamma}}\right]$$

unpolarized electron, polarized hadron

$$A_{TPV} = \frac{G_F Q^2}{2\sqrt{2}\pi\alpha}\left[g_V \frac{g_5^{\gamma Z}}{F_1^{\gamma}} + g_A f(y)\frac{g_1^{\gamma Z}}{F_1^{\gamma}}\right]$$

proton	deuteron
$F_1^{\gamma Z} \propto u + d + s$	$F_1^{\gamma Z} \propto u + d + 2s$
$F_3^{\gamma Z} \propto 2u_v + d_v$	$F_3^{\gamma Z} \propto u_v + d_v$
$g_1^{\gamma Z} \propto \Delta u + \Delta d + \Delta s$	$g_1^{\gamma Z} \propto \Delta u + \Delta d + \Delta s$
$g_5^{\gamma Z} \propto 2\Delta u_v + \Delta d_v$	$g_5^{\gamma Z} \propto \Delta u_v + \Delta d_v$

- **Electron Asymmetries are sensitive to the weak mixing angle**
  - *Deuteron is very clean but need a large data set going to be even part of the program*
  - *Must control pdf uncertainties well enough to use proton events (the main data sample at EIC)*
  - *Studies are required to use both low Q^2 (well-understood) and high Q^2*
  - *Over the next few years, QED and QCD radiative corrections will require a careful look*

Parity-Violating Asymmetries



EIC neutral current event kinematics very clean: can very cleanly separate y-independent and y-dependent pieces and study Q^2 evolution

polarized electron, unpolarized hadron

$$A_{PV} = \frac{G_F Q^2}{2\sqrt{2}\pi\alpha}\left[g_A \frac{F_1^{\gamma Z}}{F_1^{\gamma}} + g_V \frac{f(y)}{2}\frac{F_3^{\gamma Z}}{F_1^{\gamma}}\right]$$

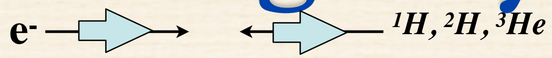
unpolarized electron, polarized hadron

$$A_{TPV} = \frac{G_F Q^2}{2\sqrt{2}\pi\alpha}\left[g_V \frac{g_5^{\gamma Z}}{F_1^{\gamma}} + g_A f(y)\frac{g_1^{\gamma Z}}{F_1^{\gamma}}\right]$$

proton	deuteron
$F_1^{\gamma Z} \propto u + d + s$	$F_1^{\gamma Z} \propto u + d + 2s$
$F_3^{\gamma Z} \propto 2u_v + d_v$	$F_3^{\gamma Z} \propto u_v + d_v$
$g_1^{\gamma Z} \propto \Delta u + \Delta d + \Delta s$	$g_1^{\gamma Z} \propto \Delta u + \Delta d + \Delta s$
$g_5^{\gamma Z} \propto 2\Delta u_v + \Delta d_v$	$g_5^{\gamma Z} \propto \Delta u_v + \Delta d_v$

- **Electron Asymmetries are sensitive to the weak mixing angle**
  - *Deuteron is very clean but need a large data set going to be even part of the program*
  - *Must control pdf uncertainties well enough to use proton events (the main data sample at EIC)*
  - *Studies are required to use both low Q^2 (well-understood) and high Q^2*
  - *Over the next few years, QED and QCD radiative corrections will require a careful look*
- **Hadron Asymmetries**

Parity-Violating Asymmetries



EIC neutral current event kinematics very clean: can very cleanly separate y-independent and y-dependent pieces and study Q^2 evolution

polarized electron, unpolarized hadron

$$A_{PV} = \frac{G_F Q^2}{2\sqrt{2}\pi\alpha}\left[g_A \frac{F_1^{\gamma Z}}{F_1^{\gamma}} + g_V \frac{f(y)}{2}\frac{F_3^{\gamma Z}}{F_1^{\gamma}}\right]$$

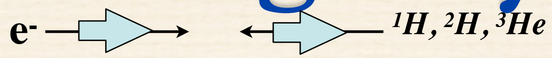
unpolarized electron, polarized hadron

$$A_{TPV} = \frac{G_F Q^2}{2\sqrt{2}\pi\alpha}\left[g_V \frac{g_5^{\gamma Z}}{F_1^{\gamma}} + g_A f(y)\frac{g_1^{\gamma Z}}{F_1^{\gamma}}\right]$$

proton	deuteron
$F_1^{\gamma Z} \propto u + d + s$	$F_1^{\gamma Z} \propto u + d + 2s$
$F_3^{\gamma Z} \propto 2u_v + d_v$	$F_3^{\gamma Z} \propto u_v + d_v$
$g_1^{\gamma Z} \propto \Delta u + \Delta d + \Delta s$	$g_1^{\gamma Z} \propto \Delta u + \Delta d + \Delta s$
$g_5^{\gamma Z} \propto 2\Delta u_v + \Delta d_v$	$g_5^{\gamma Z} \propto \Delta u_v + \Delta d_v$

- **Electron Asymmetries are sensitive to the weak mixing angle**
  - *Deuteron is very clean but need a large data set going to be even part of the program*
  - *Must control pdf uncertainties well enough to use proton events (the main data sample at EIC)*
  - *Studies are required to use both low Q^2 (well-understood) and high Q^2*
  - *Over the next few years, QED and QCD radiative corrections will require a careful look*
- **Hadron Asymmetries**
  - *Access to entirely new set of structure functions*

Parity-Violating Asymmetries



EIC neutral current event kinematics very clean: can very cleanly separate y-independent and y-dependent pieces and study Q^2 evolution

polarized electron, unpolarized hadron

$$A_{PV} = \frac{G_F Q^2}{2\sqrt{2}\pi\alpha}\left[g_A \frac{F_1^{\gamma Z}}{F_1^{\gamma}} + g_V \frac{f(y)}{2}\frac{F_3^{\gamma Z}}{F_1^{\gamma}}\right]$$

unpolarized electron, polarized hadron

$$A_{TPV} = \frac{G_F Q^2}{2\sqrt{2}\pi\alpha}\left[g_V \frac{g_5^{\gamma Z}}{F_1^{\gamma}} + g_A f(y)\frac{g_1^{\gamma Z}}{F_1^{\gamma}}\right]$$

proton	deuteron
$F_1^{\gamma Z} \propto u + d + s$	$F_1^{\gamma Z} \propto u + d + 2s$
$F_3^{\gamma Z} \propto 2u_v + d_v$	$F_3^{\gamma Z} \propto u_v + d_v$
$g_1^{\gamma Z} \propto \Delta u + \Delta d + \Delta s$	$g_1^{\gamma Z} \propto \Delta u + \Delta d + \Delta s$
$g_5^{\gamma Z} \propto 2\Delta u_v + \Delta d_v$	$g_5^{\gamma Z} \propto \Delta u_v + \Delta d_v$

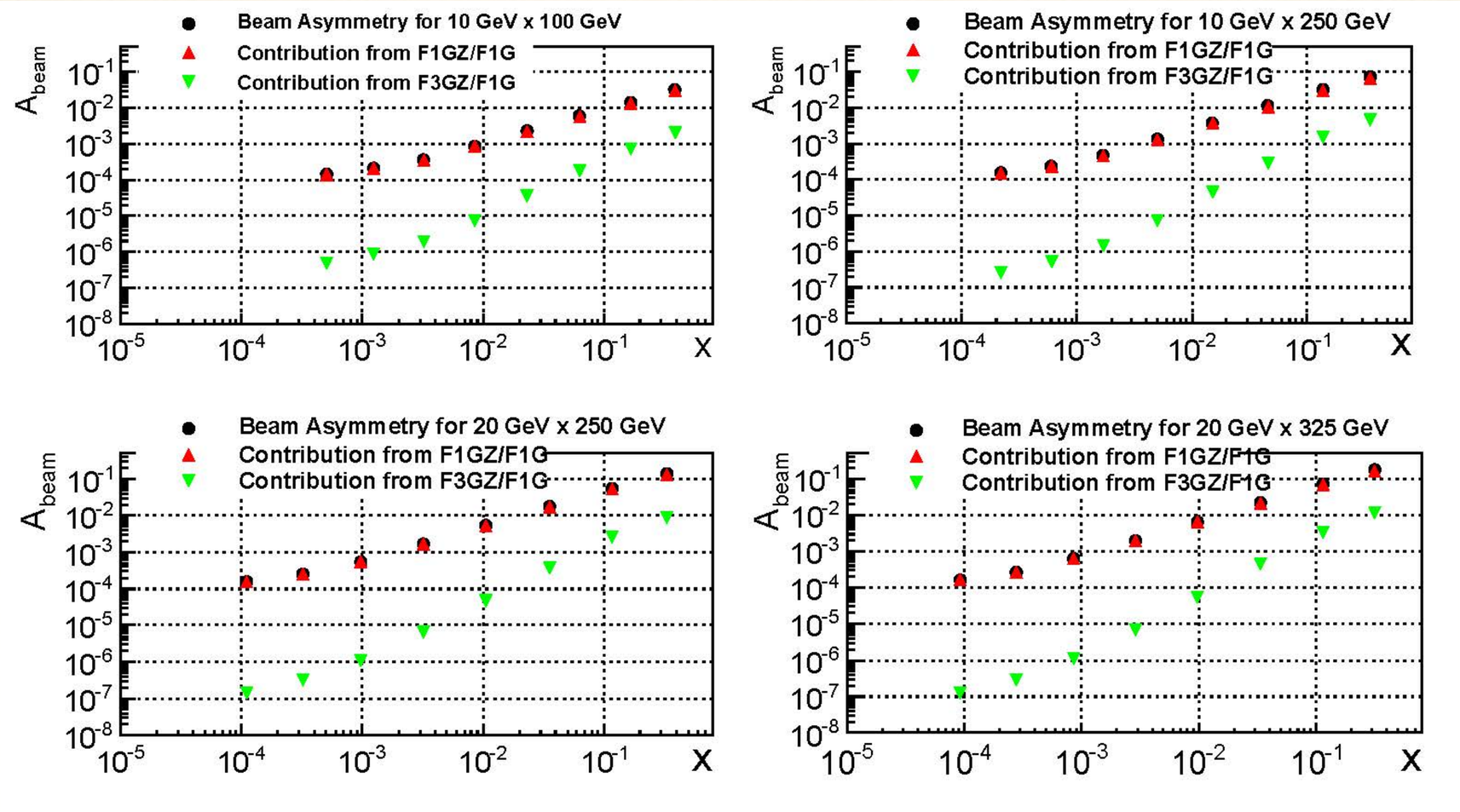
- **Electron Asymmetries are sensitive to the weak mixing angle**
  - *Deuteron is very clean but need a large data set going to be even part of the program*
  - *Must control pdf uncertainties well enough to use proton events (the main data sample at EIC)*
  - *Studies are required to use both low Q^2 (well-understood) and high Q^2*
  - *Over the next few years, QED and QCD radiative corrections will require a careful look*
- **Hadron Asymmetries**
  - *Access to entirely new set of structure functions*
  - *Can contribute to flavor separation of polarized pdfs*

Y. Zhao et al • *Eur.Phys.J.A* 53 (2017) 3, 55 • e-Print: 1612.06927 [nucl-ex]

Electron Asymmetry A_{PV}

polarized electron; unpolarized proton

$$A_{PV} = \frac{G_F Q^2}{2\sqrt{2}\pi\alpha}\left[g_A \frac{F_1^{\gamma Z}}{F_1^{\gamma}} + g_V \frac{f(y)}{2}\frac{F_3^{\gamma Z}}{F_1^{\gamma}}\right]$$



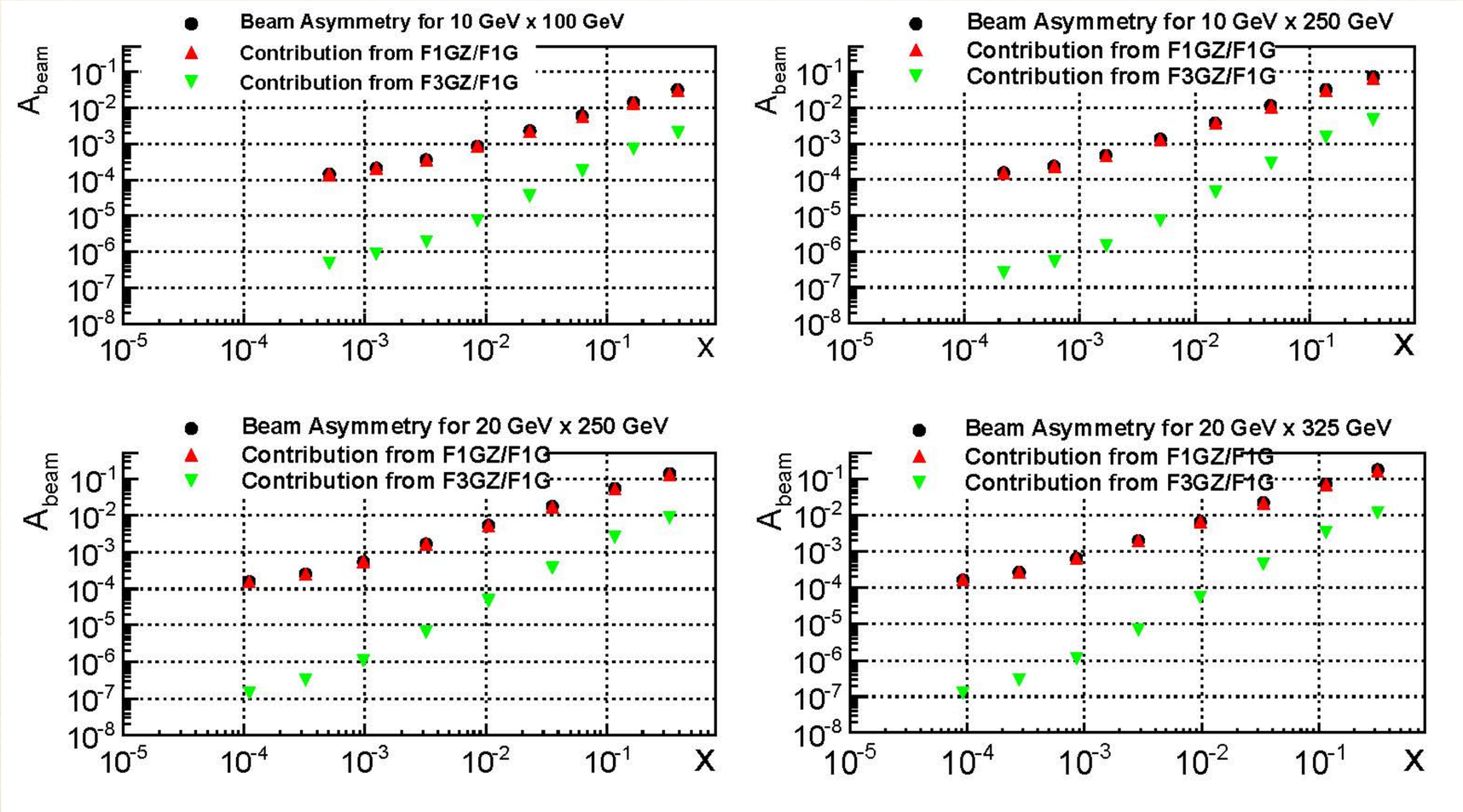
Y. Zhao et al • *Eur.Phys.J.A* 53 (2017) 3, 55 • e-Print: 1612.06927 [nucl-ex]

Y. Zhao (SBU)
A. Deshpande (SBU)
J. Huang (BNL)
K. Kumar (UMass)
S. Riordan (SBU)

Electron Asymmetry A_{PV}

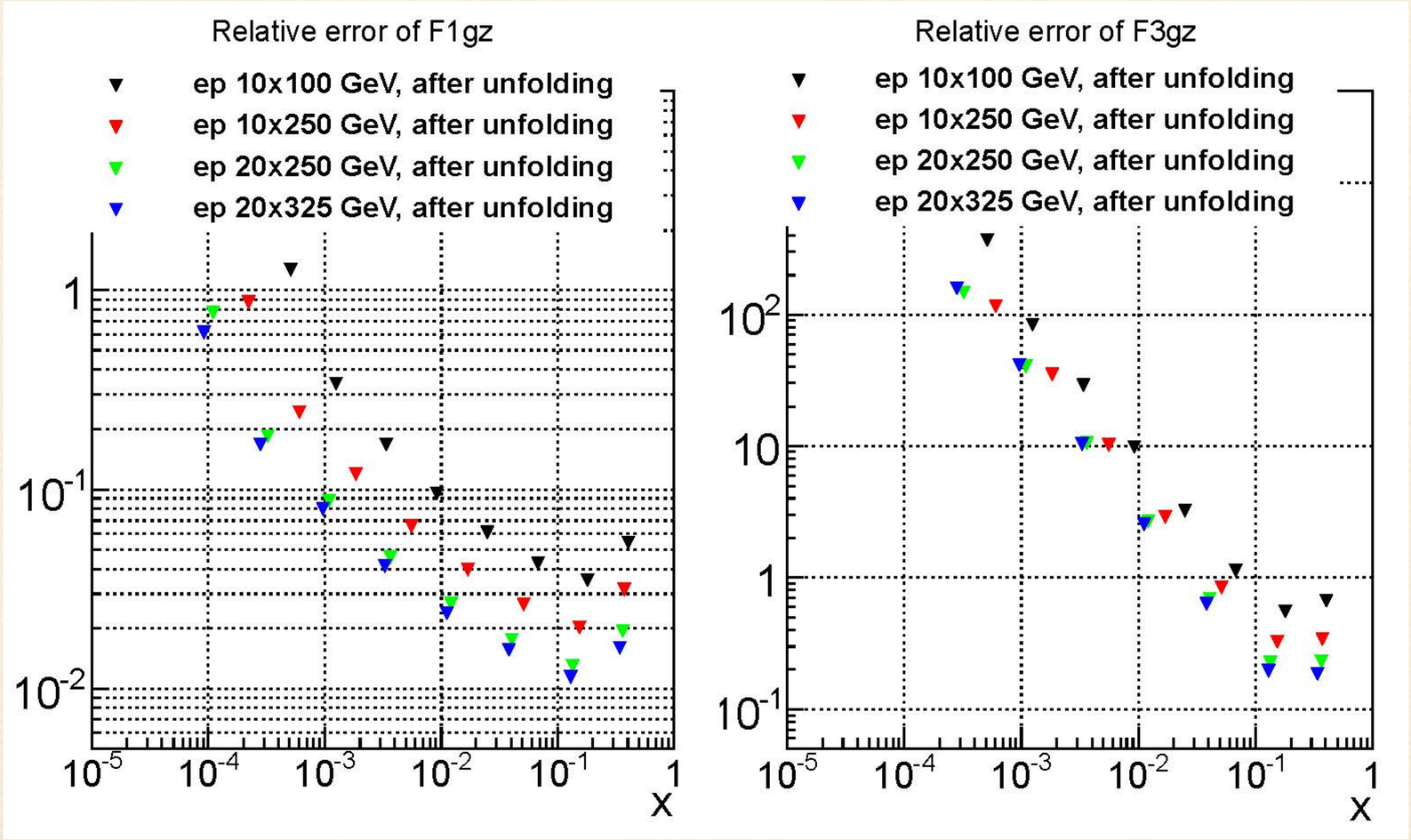
polarized electron; unpolarized proton

$$A_{PV} = \frac{G_F Q^2}{2\sqrt{2}\pi\alpha}\left[g_A \frac{F_1^{\gamma Z}}{F_1^{\gamma}} + g_V \frac{f(y)}{2}\frac{F_3^{\gamma Z}}{F_1^{\gamma}}\right]$$



Fraction Statistical Errors on Structure Functions

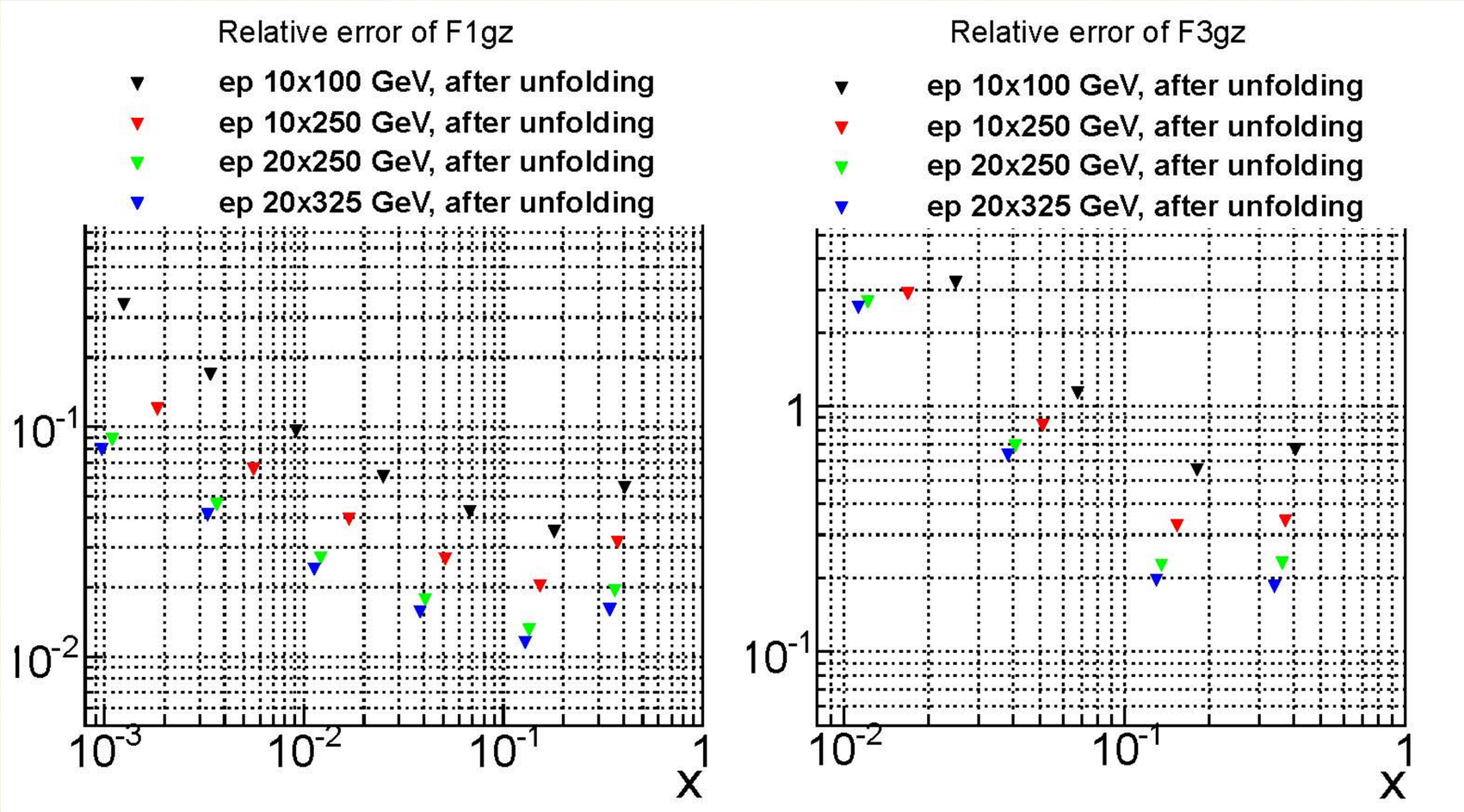
$$F_1^{\gamma Z} \propto u + d + s \qquad F_3^{\gamma Z} \propto 2u_v + d_v$$



Fraction Statistical Errors on Structure Functions

$$F_1^{\gamma Z} \propto u + d + s$$

$$F_3^{\gamma Z} \propto 2u_v + d_v$$

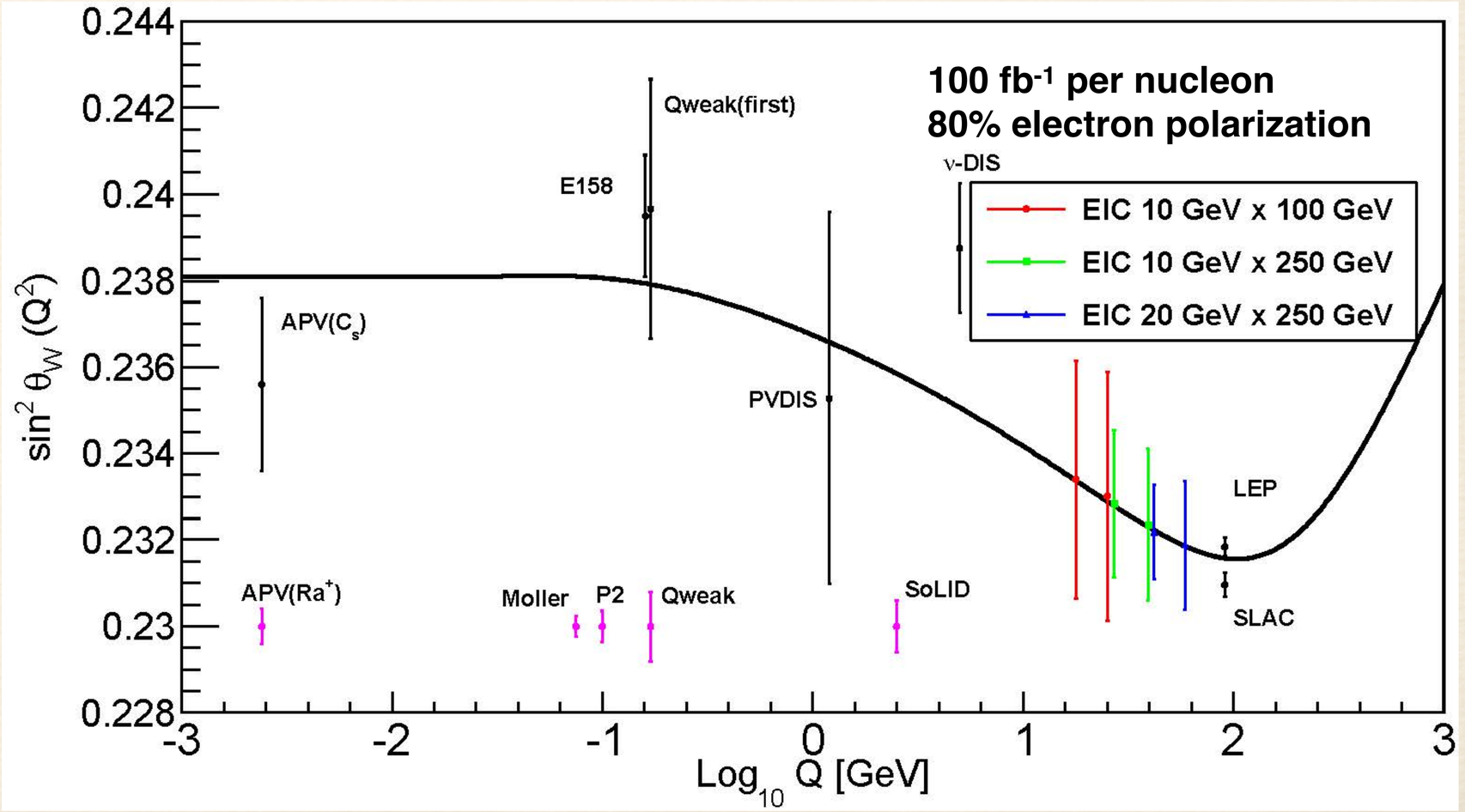


Y. Zhao et al • *Eur.Phys.J.A* 53 (2017) 3, 55 • e-Print: 1612.06927 [nucl-ex]

e-D: Weak Mixing Angle

$$g_A^e \frac{F_1^{\gamma Z}}{F_1^{\gamma}} \rightarrow g_A^e(2g_V^u - g_V^d) \propto \left(\frac{20}{3}\sin^2\theta_W - 1\right)$$

for a deuteron, structure functions cancel: assuming charge symmetry and neglecting strange quarks



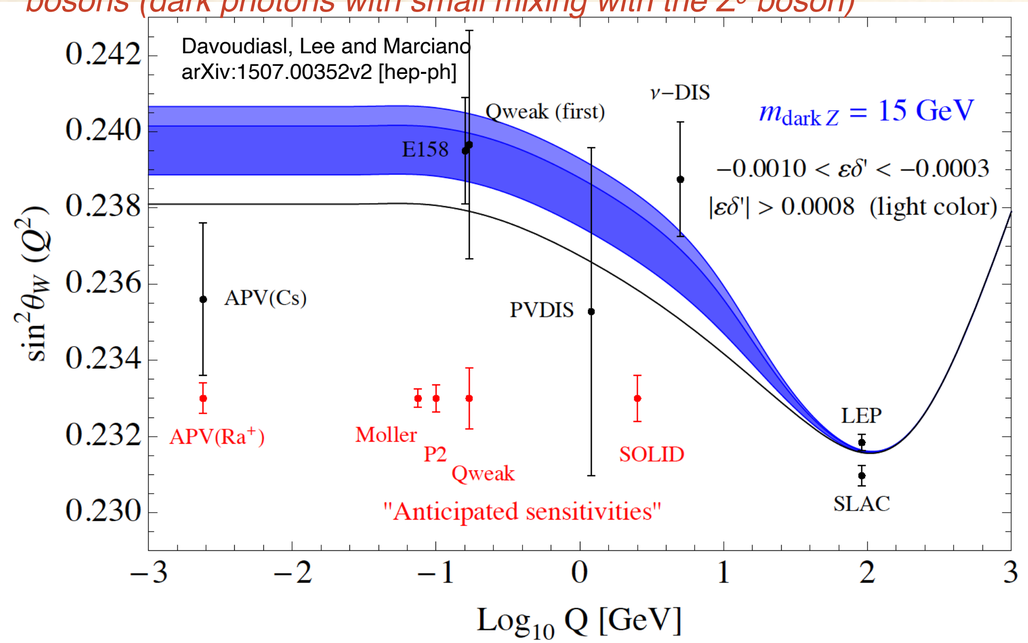
Implications of EIC Measurements

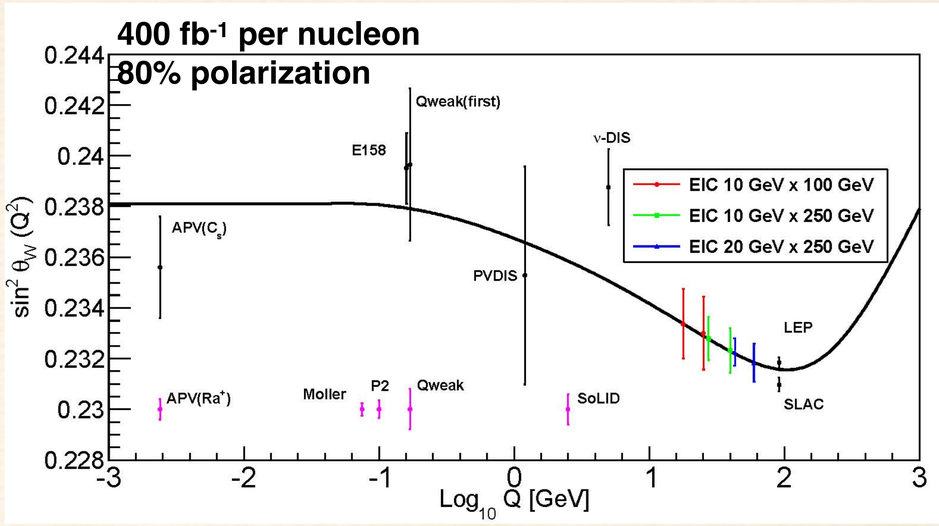
What will be the electroweak landscape in 2035?

Has LHC discovered new physics?

Presumably, the red projections below have been successful…

It has been pointed out that there are rather weak limits on "dark" Z bosons (dark photons with small mixing with the Z^0 boson)

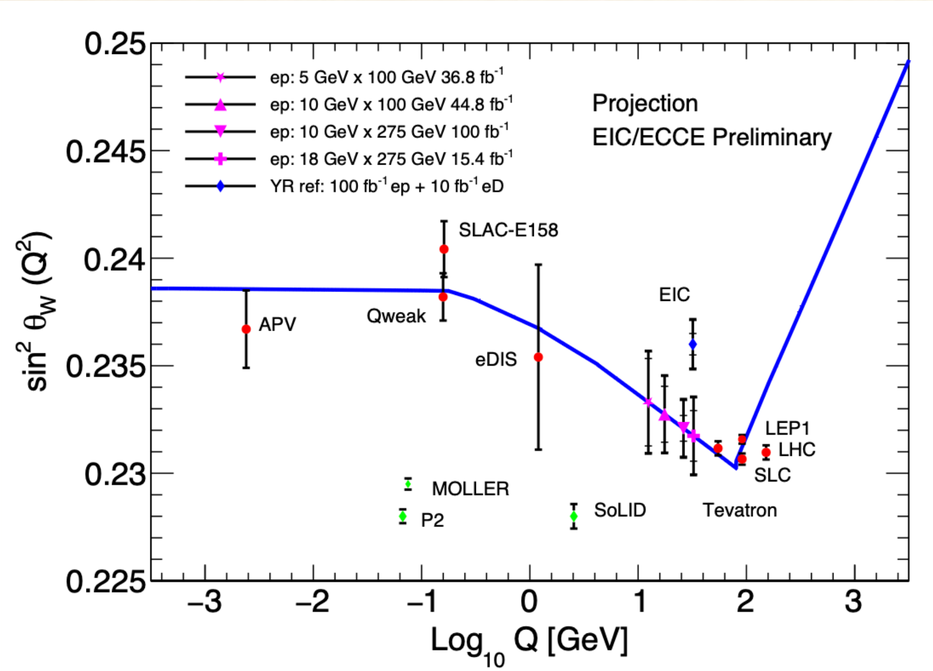




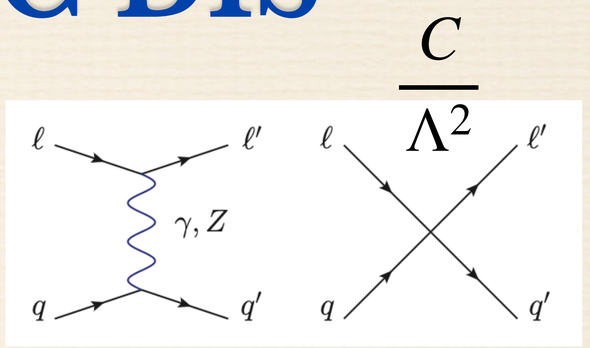
- **Do measurements help constrain *u*, *d*, *s* pdfs?**
- **Conversely, are *u*, *d*, *s* pdfs known well enough from other measurements so one can use electron-proton data at EIC to better constrain $\sin^2\theta_W$?**

Boughezal et al *Phys.Rev.D* 106 (2022) 1, 016006 · 2204.07557 [hep-ph]

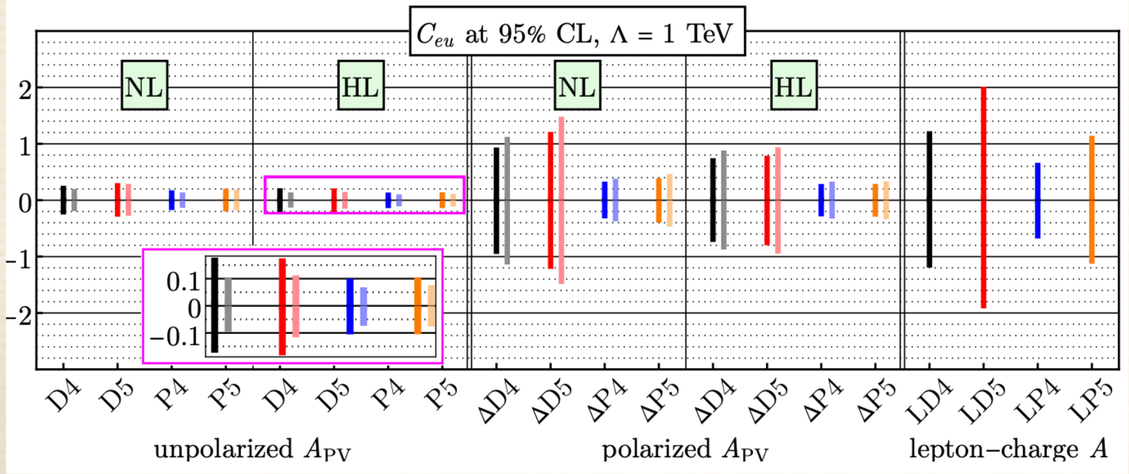
SMEFT Analysis of EIC NC DIS



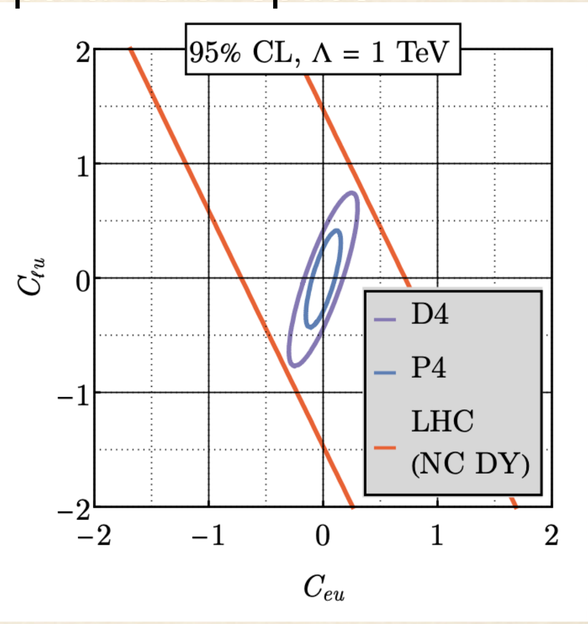
10 GeV ×137 GeV eD 100 fb^{-1}: D4, ΔD4, LD4 ,
18 GeV ×137 GeV eD 15.4 fb^{-1}: D5, ΔD5, LD5 ,
10 GeV ×275 GeV ep 100 fb^{-1}: P4, ΔP4, LP4 ,
18 GeV ×275 GeV ep 15.4 fb^{-1}: P5, ΔP5, LP5 .



- They find that proton asymmetries are more sensitive
- The can overcome pdf uncertainties via global fits
- They find no “flat” dimensions in the parameter space



The future strategy is to do combined fits LHC Drell-Yan data with EIC asymmetry data; the LHC data alone does have “flat” dimensions

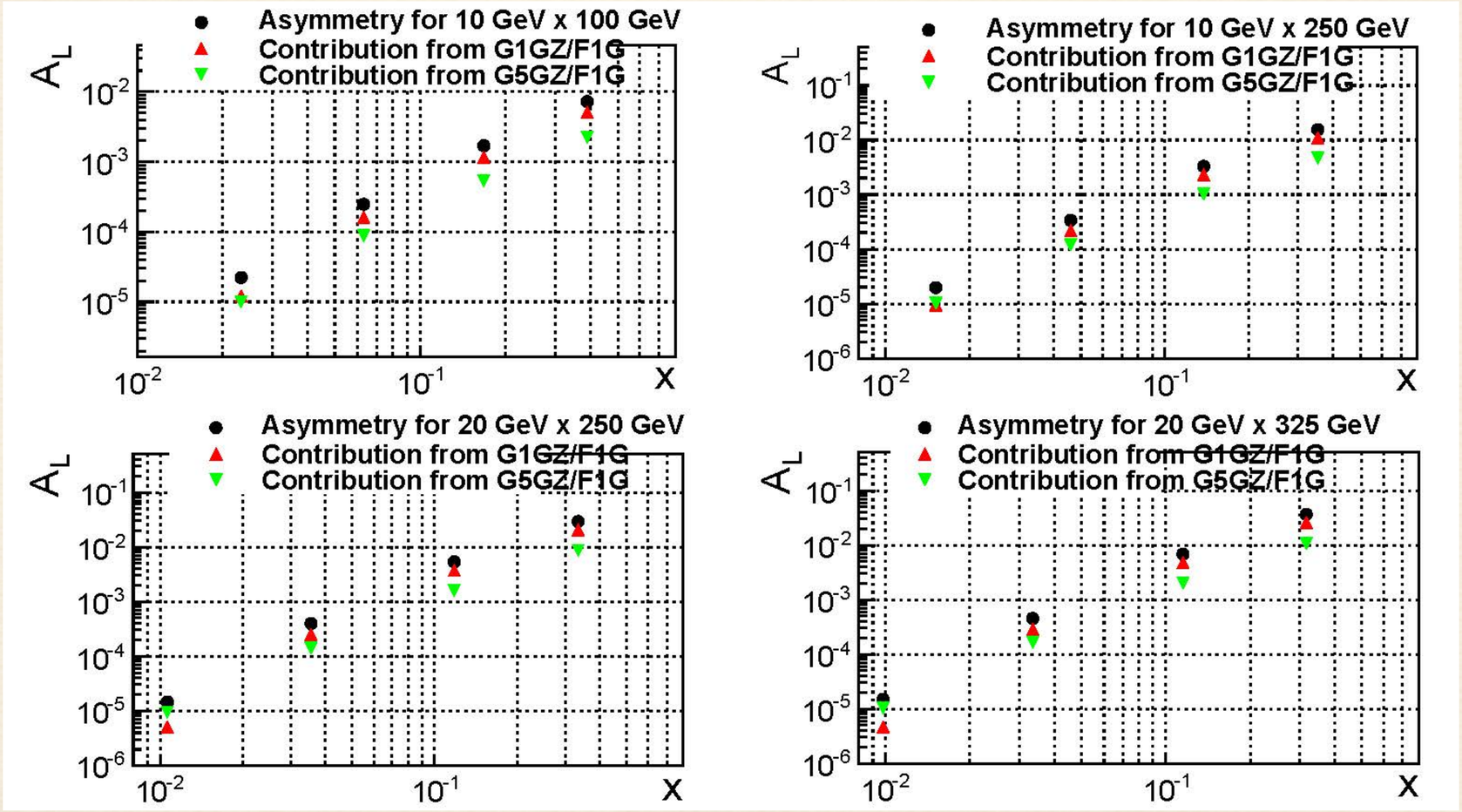


Y. Zhao et al • *Eur.Phys.J.A* 53 (2017) 3, 55 • e-Print: 1612.06927 [nucl-ex]

Hadron Asymmetry A_{TPV}

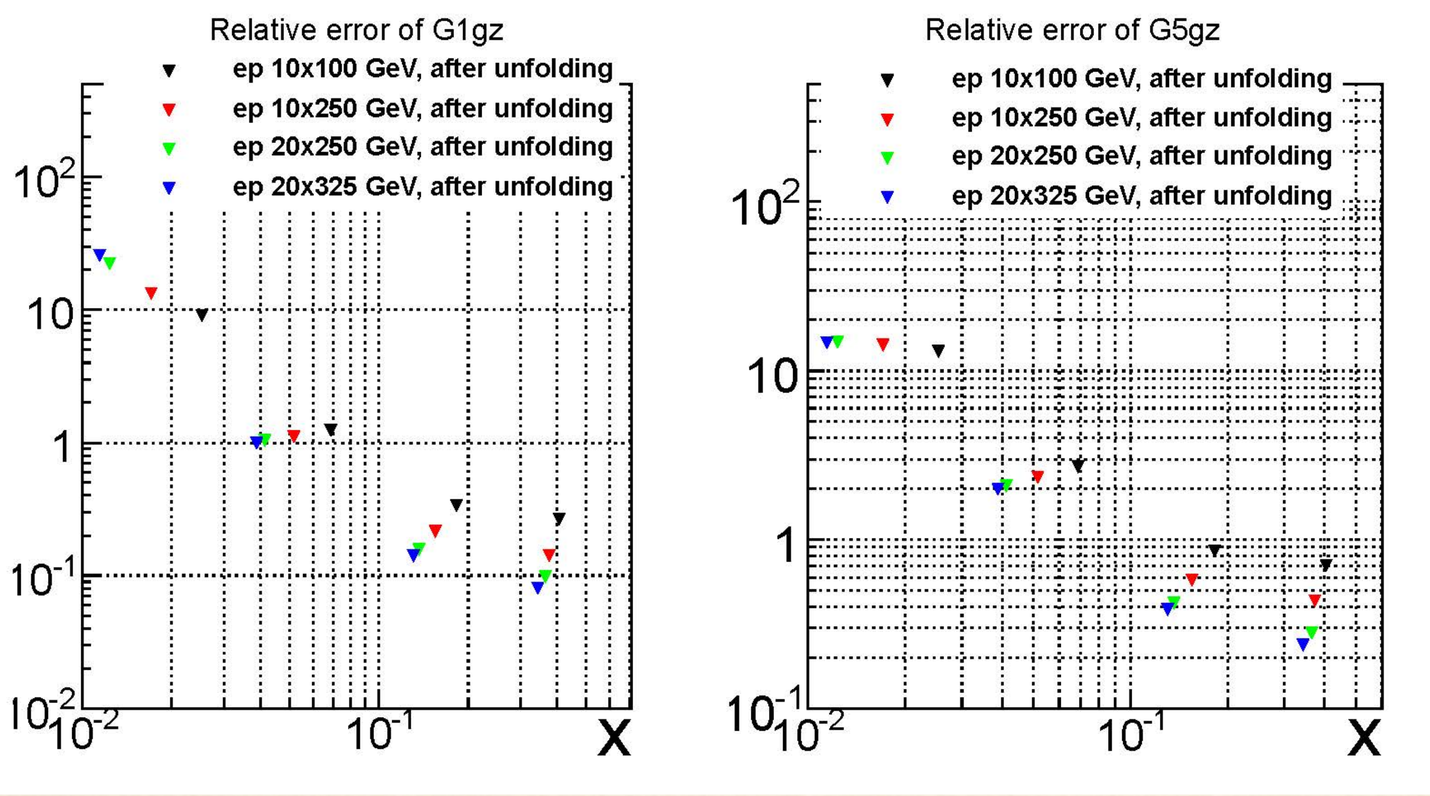
unpolarized electron; polarized proton

$$A_{TPV} = \frac{G_F Q^2}{2\sqrt{2}\pi\alpha}\left[g_V \frac{g_5^{\gamma Z}}{F_1^{\gamma}} + g_A f(y) \frac{g_1^{\gamma Z}}{F_1^{\gamma}}\right]$$



Fractional Statistical Errors on Structure Functions

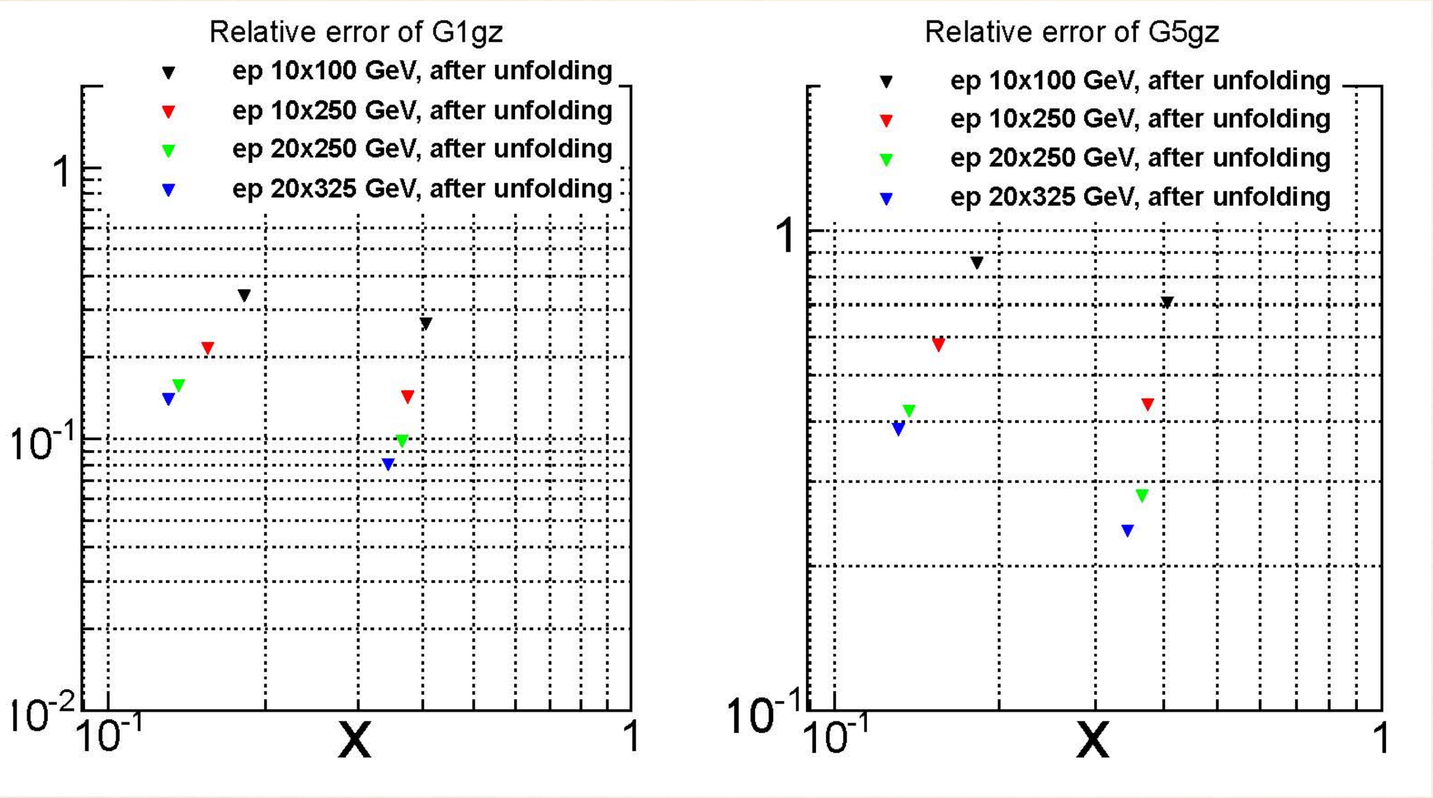
$$g_1^{\gamma Z} \propto \Delta u + \Delta d + \Delta s$$



Important input to the measurement of the strange quark polarization contribution to the proton spin from an inclusive measurement!

Fractional Statistical Errors on Structure Functions

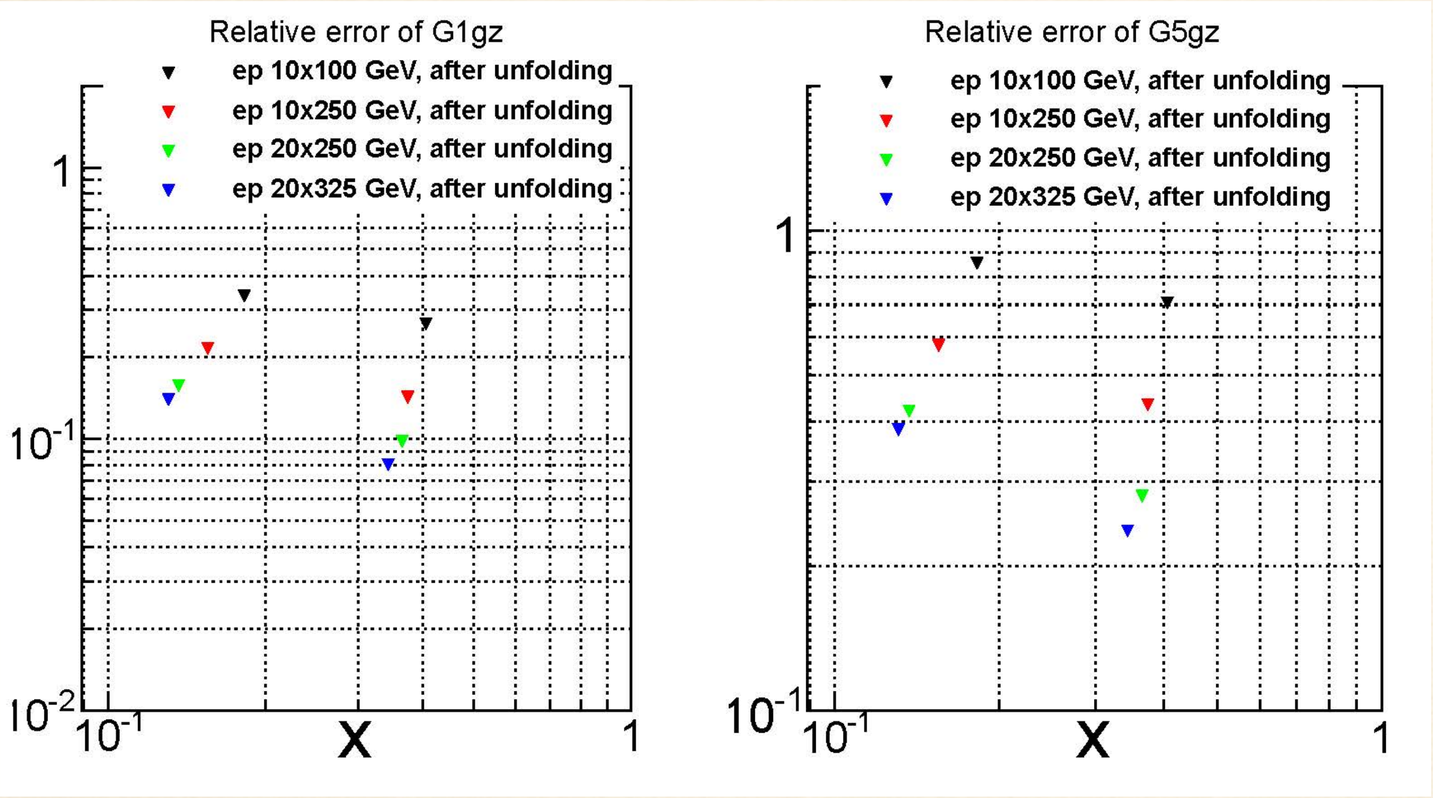
$$g_1^{\gamma Z} \propto \Delta u + \Delta d + \Delta s$$



Important input to the measurement of the strange quark polarization contribution to the proton spin from an inclusive measurement!

Fractional Statistical Errors on Structure Functions

$$g_1^{\gamma Z} \propto \Delta u + \Delta d + \Delta s$$



Important input to the measurement of the strange quark polarization contribution to the proton spin from an inclusive measurement!

Next Steps

- Generate pseudo data for polarized pdf constraints at various integrated luminosities
- Look at complementarity of proton, deuteron, helium-3 and charged current data

Summary: Lectures 3 and 4

Takeaway Message

- **Parity-Violating Electron Scattering**
  - ★ Enabled unique studies of the weak force
  - ★ Technical progress has enabled unprecedented precision
- **Fundamental Nuclear/Nucleon Physics**
  - ★ Strange quark electric and magnetic distributions in the proton
  - ★ Neutron RMS radii of heavy nuclei (PREX, CREX)
  - ★ valence quark structure of protons and neutrons (SOLID)
  - ★ New Structure Functions (EIC)
- **Fundamental Electroweak Physics**
  - ★ Search for new dynamics at the TeV scale (MOLLER, SOLID, P2)
    - *complementary to colliders; would help interpret potential anomalies*
    - *precision measurement of the weak mixing angle*

We anticipate the first physics results from MOLLER to start to flow by late next year

Backup

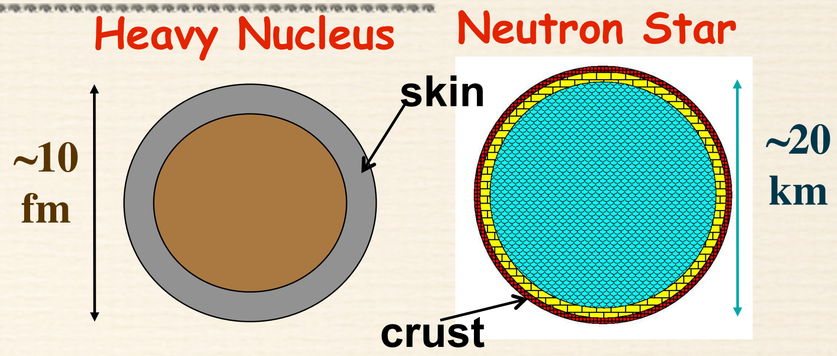
Neutron Skins and Neutron Stars

Horowitz and Piekarewicz, PRL 86 (2001)

Lattimer and Prakash, Science 304 (2004)

- Heavy nucleus has neutron skin
- Neutron star has solid crust over liquid core

Both neutron skin and neutron star crust are made out of neutron rich matter at similar densities.



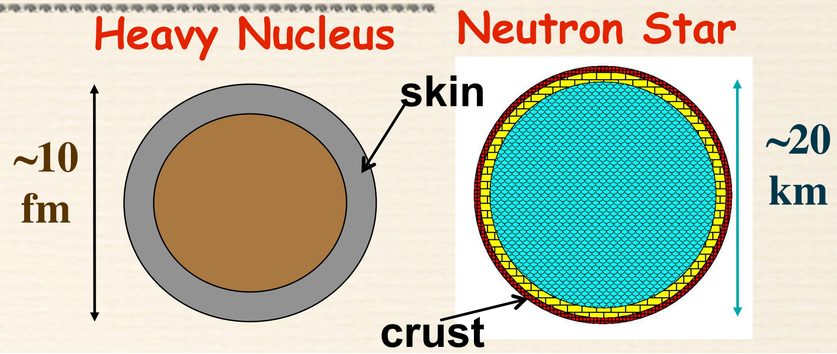
Neutron Skins and Neutron Stars

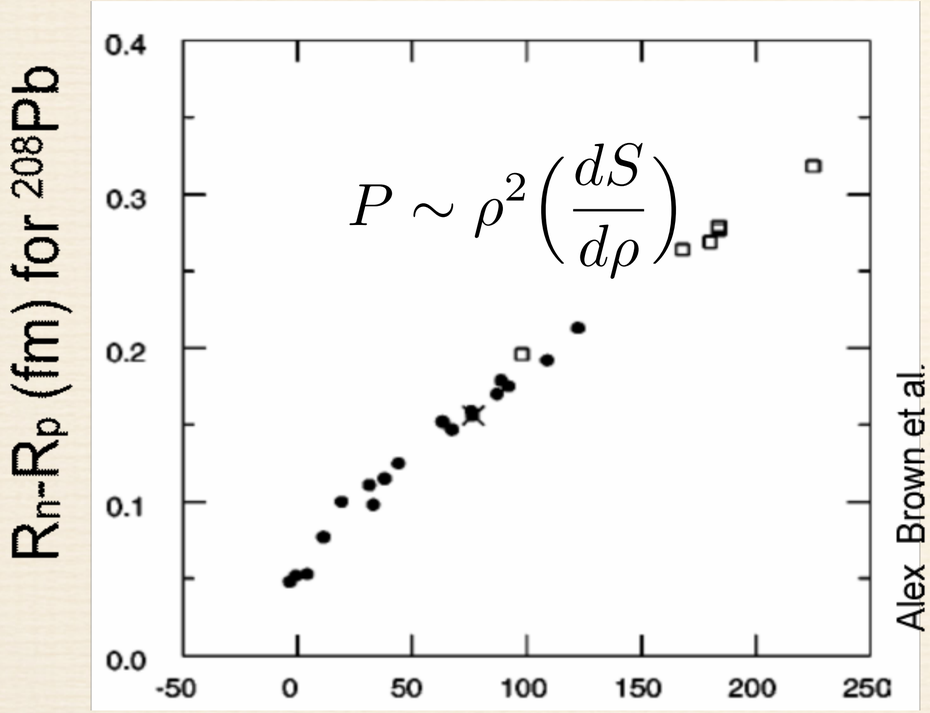
Horowitz and Piekarewicz, PRL 86 (2001)

Lattimer and Prakash, Science 304 (2004)

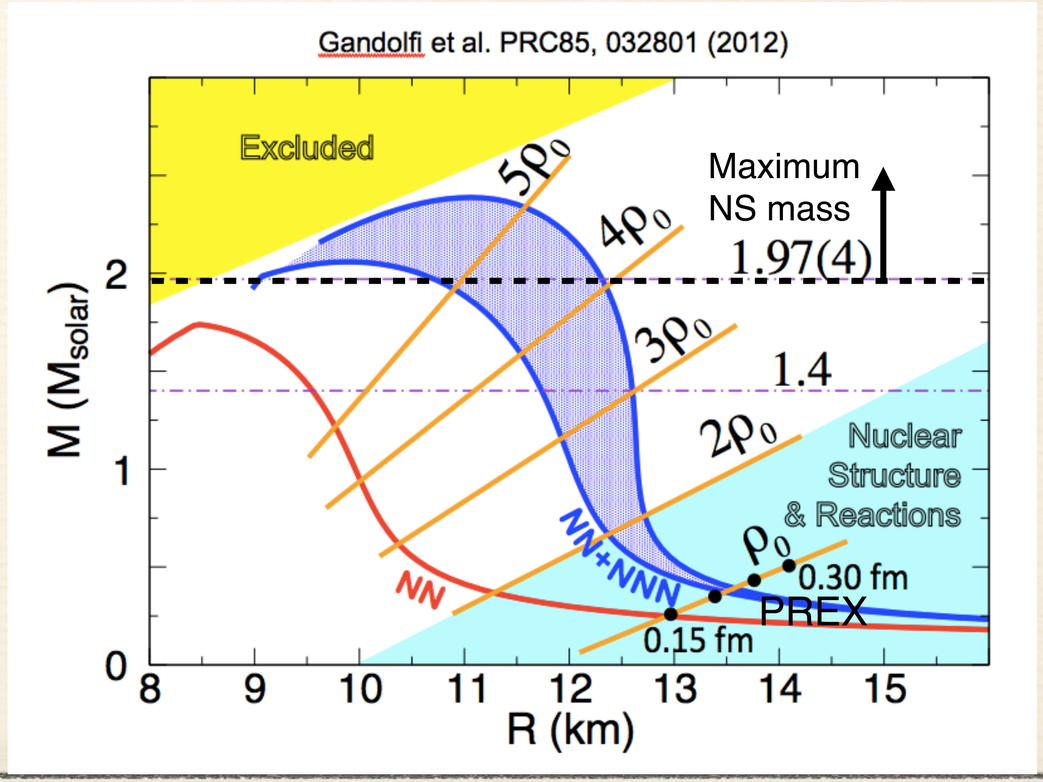
- Heavy nucleus has neutron skin
- Neutron star has solid crust over liquid core

Both neutron skin and neutron star crust are made out of neutron rich matter at similar densities.





Neutron matter P (MeV/fm^3) x100 at a density of 0.1 fm^{-3}.

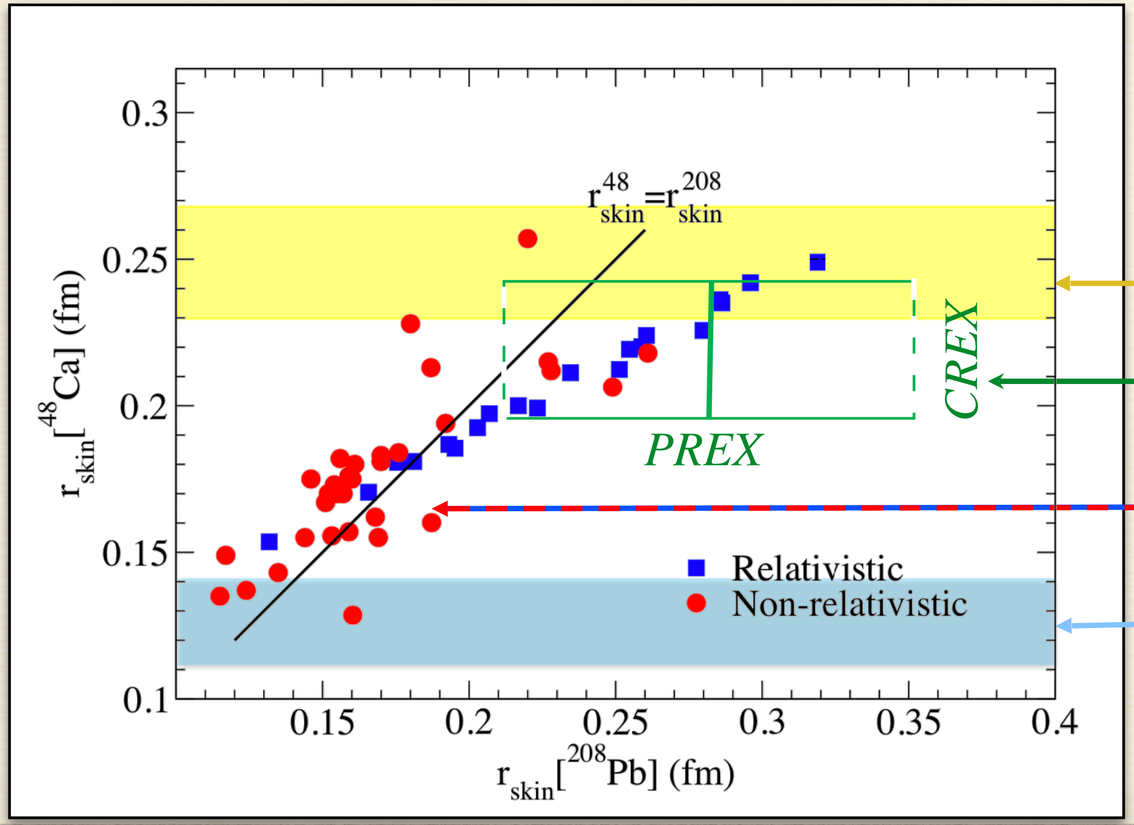


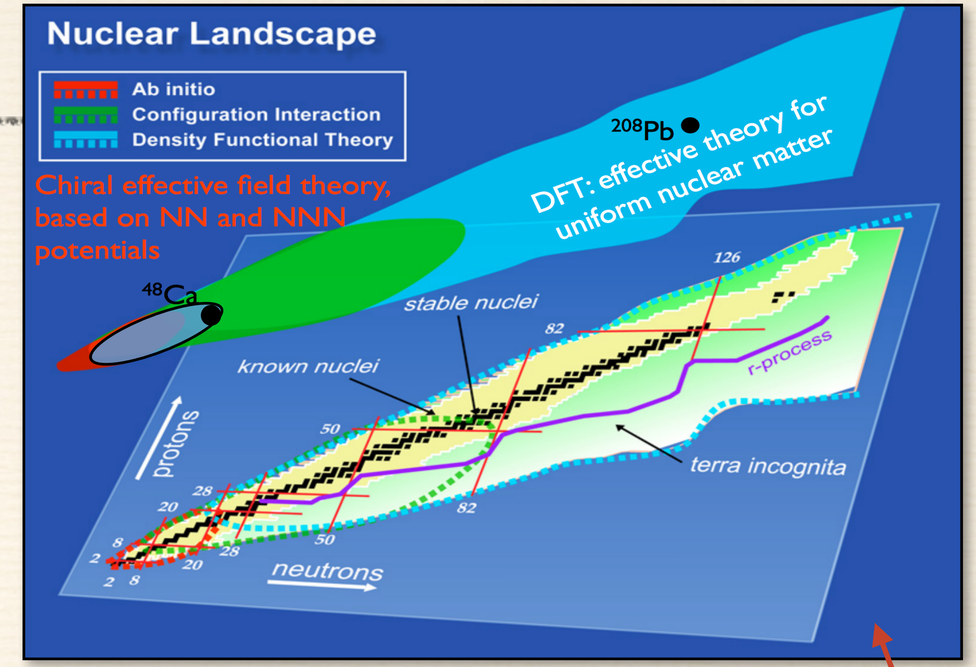
Motivation for Measuring a Second Nucleus

PREX: ^{208}Pb large, uniform nucleus, DFT

CREX: neutron FF ^{48}Ca

- moderate size system
- finite size effects
- Within reach of microscopic calculations (which suggest the importance of 3-nucleon forces)



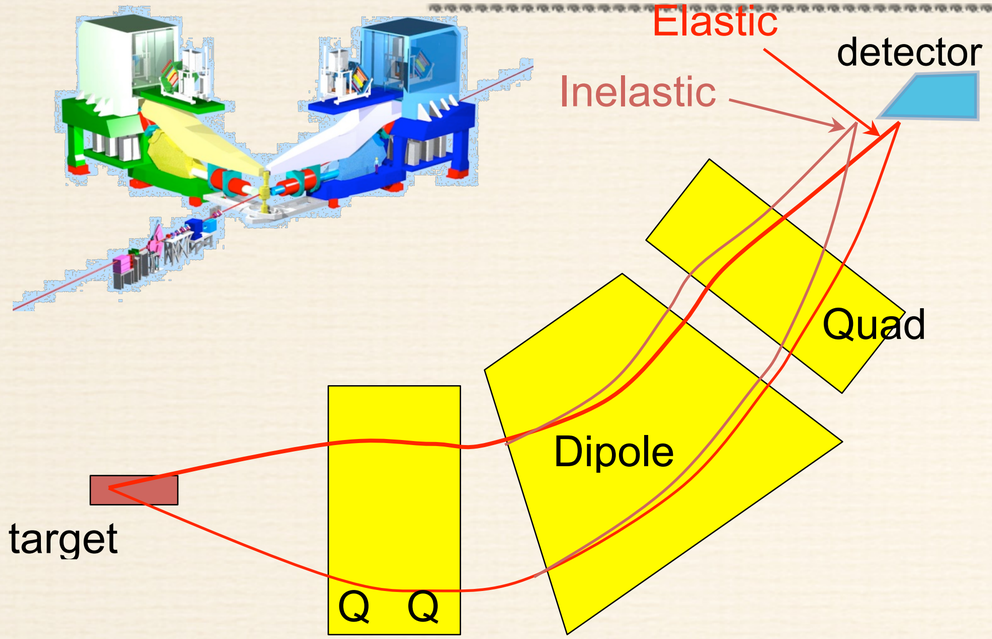


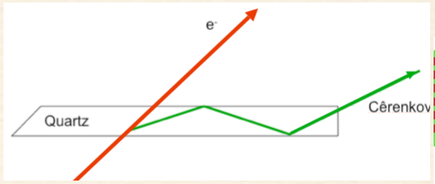
- DOM (Dispersive Optical Model)
  W. Dickoff *et al*, PRL 119, 222503(2017)
- *Arbitrary CREX central value*
- DFT (Relativistic, Non-relativistic)
  Fattoyev, Piekarewicz, PRC 85, 015802 (2012)
- Coupled cluster calculations predict a neutron skin of: $0.12 \leqq R_{skin} \leqq 0.15$ fm
  G. Hagen *et al*, Nature Physics **12**, 186–190 (2016)

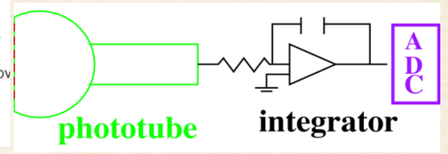
Picture likely "stolen" from someone in this audience!!

High Flux, Low Background

Hall A High Resolution Spectrometers







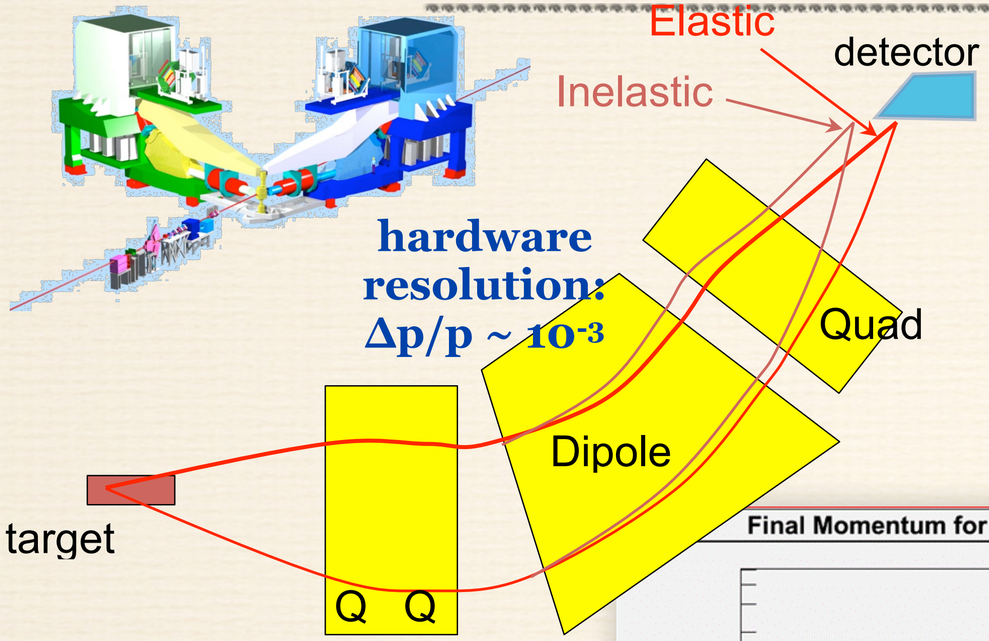
1 GHz scattered flux

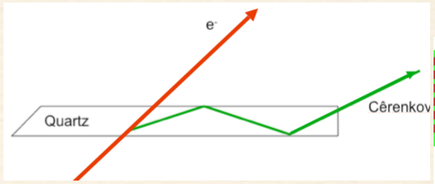
1 x 10^{-4} statistical uncertainty
30 times per second

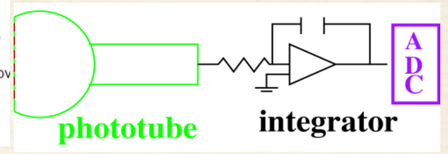
second major SLAC E122 innovation: “flux integration”

High Flux, Low Background

Hall A High Resolution Spectrometers

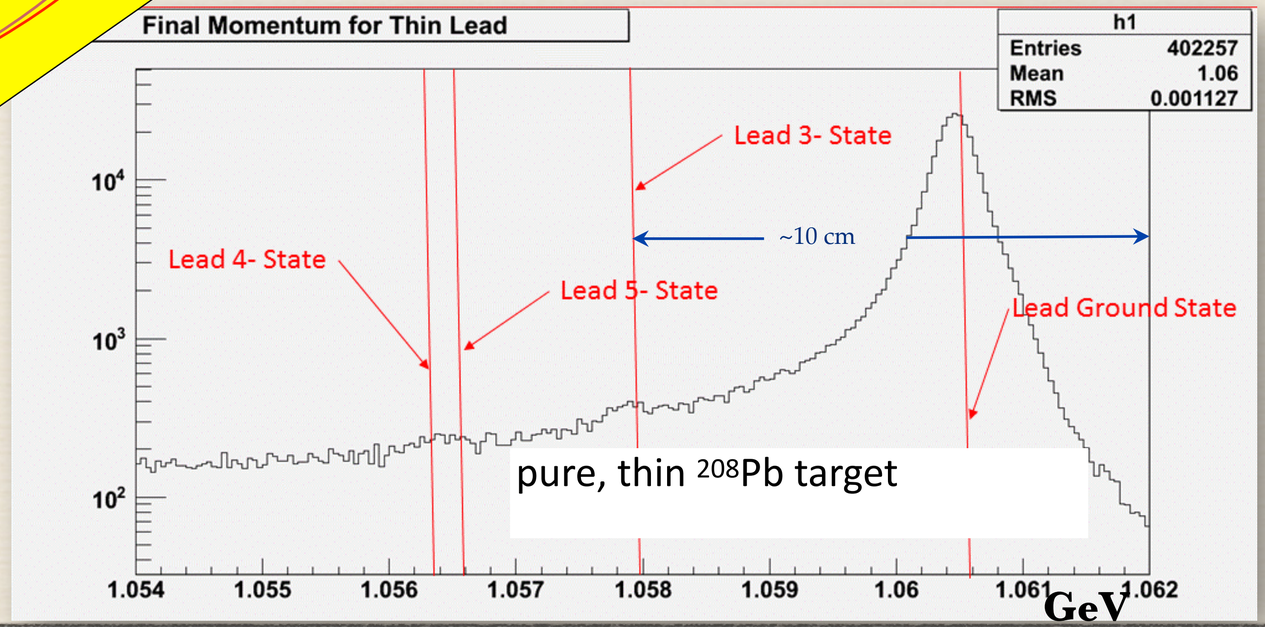






1 GHz scattered flux

1 x 10^{-4} statistical uncertainty
30 times per second



Inelastic backgrounds negligible

CREX Result Summary

Unblinded Corrected Asymmetry A_{corr}:

2336.0 ± 84.8ppb

$$A_{phys} = R_{radcorr}\, R_{accept}\, R_{Q^2} \frac{A_{corr} - P_L \sum_i f_i A_i}{P_L(1 - \sum_i f_i)}$$

$$A_{corr} = A_{det} - A_{beam} - A_{trans} - A_{nonlin} - A_{blind}$$

Unblinded A_{PV}:

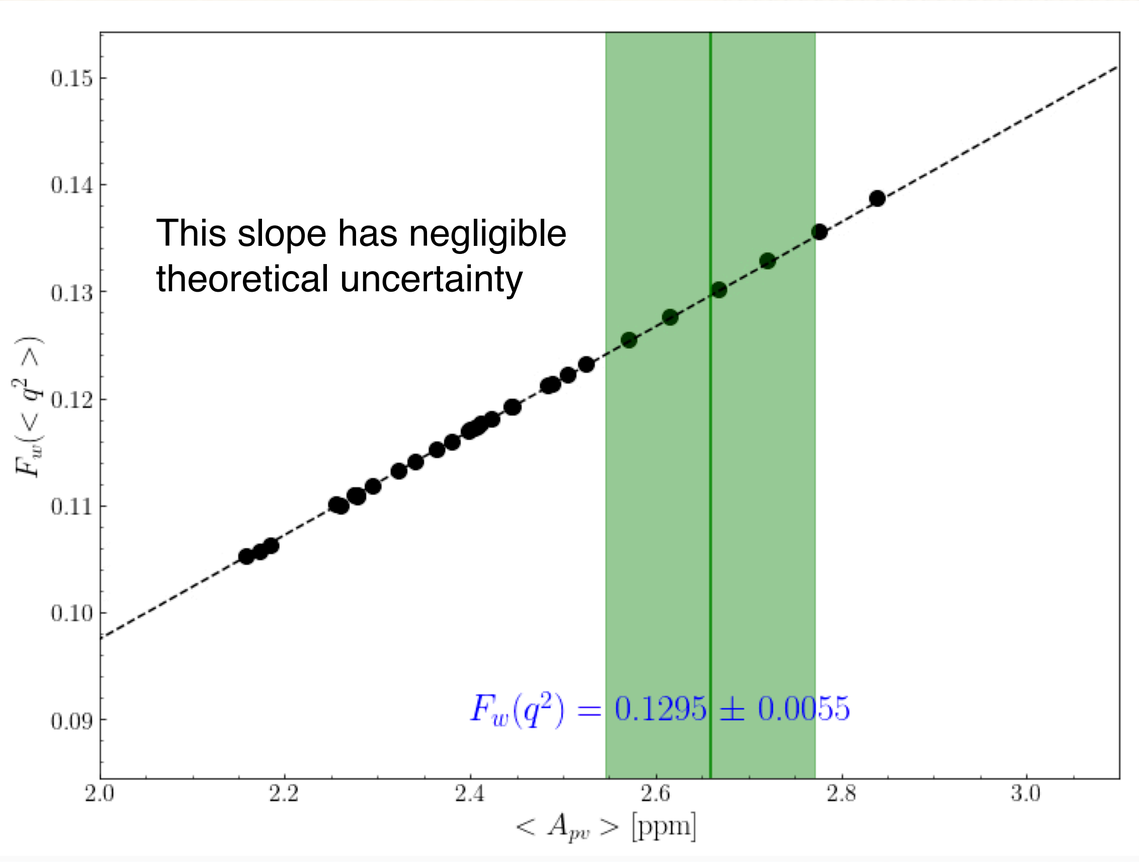
2658.6 ± 106.1(stat) ± 39.4(sys)ppb

[± 113.2ppb(tot) (4.3%)]

	A_{PV} uncertainty contribution [ppb]	A_{PV} uncertainty contribution [%]
Polarization	13.1	0.49%
Horizontal Polarization	12.7	0.48%
Vertical Polarization	0.9	0.03%
Acceptance normalization	23.9	0.90%
Beam correction	6.9	0.26%
Non-linear detector response	6.7	0.25%
Ca40 background	8.8	0.33%
Charge correction	1.1	0.04%
Inelastic contamination 2+	18.9	0.71%
Inelastic contamination 3-(1)	10.2	0.38%
Inelastic contamination 3-(2)	3.6	0.13%
Rescattering	0.5	0.02%
Total	**39.4**	**1.5%**

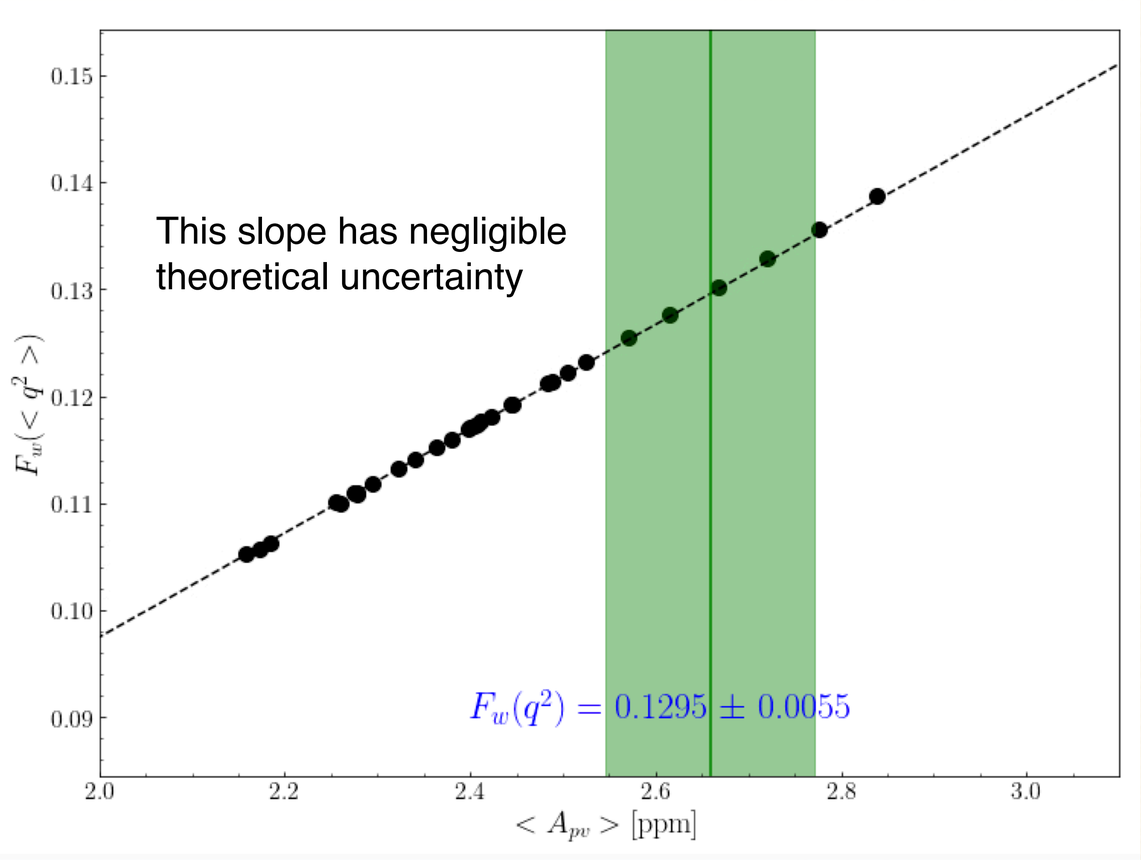
- When taken all into account the experimental systematic uncertainty comes to 1.5%, less than half the 4.0% statistical uncertainty
- Total uncertainty of is 113.2ppb (4.3%)

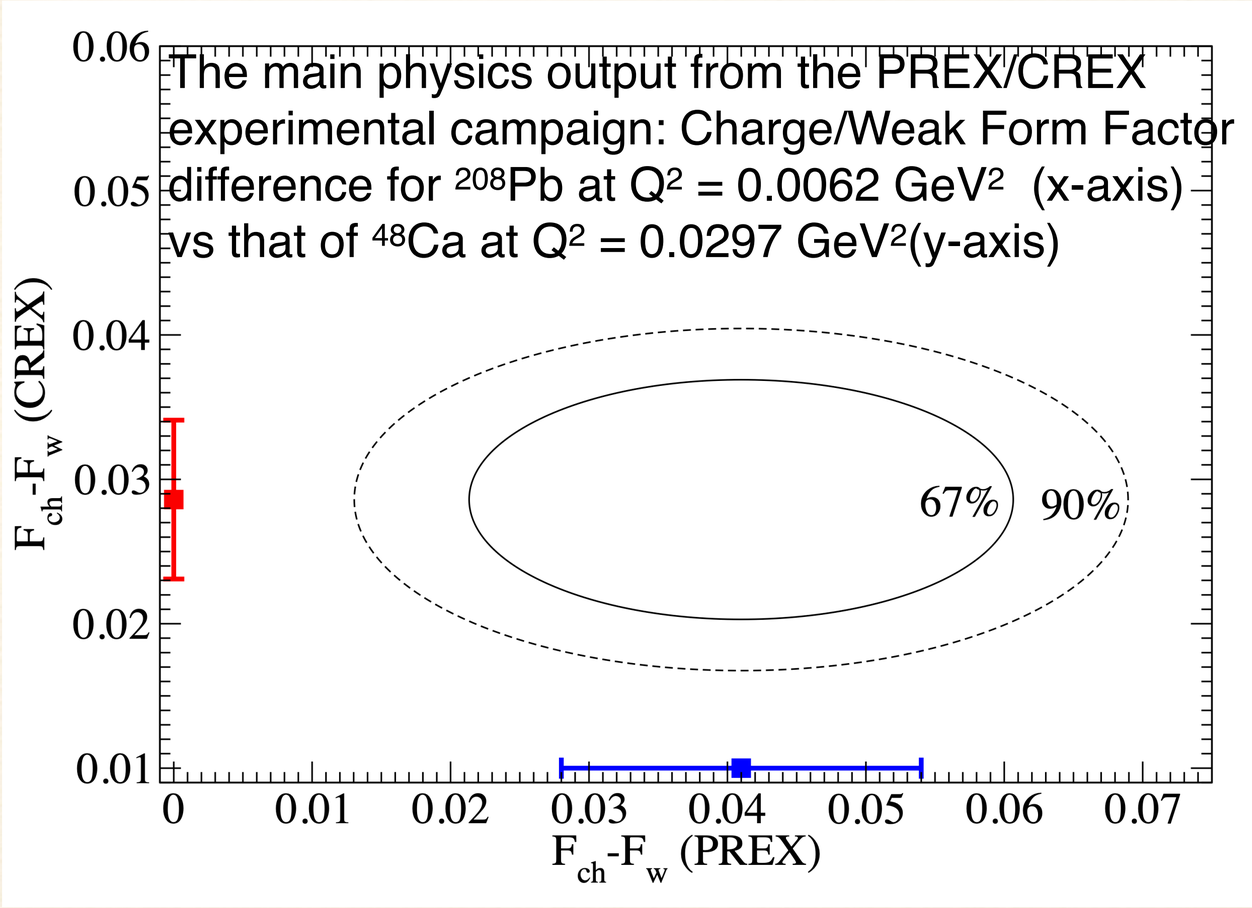
Main Derived Parameter: The Weak Form Factor at $Q^2 = 0.0297$ GeV^2



F_W: 0.1295 ± 0.0055

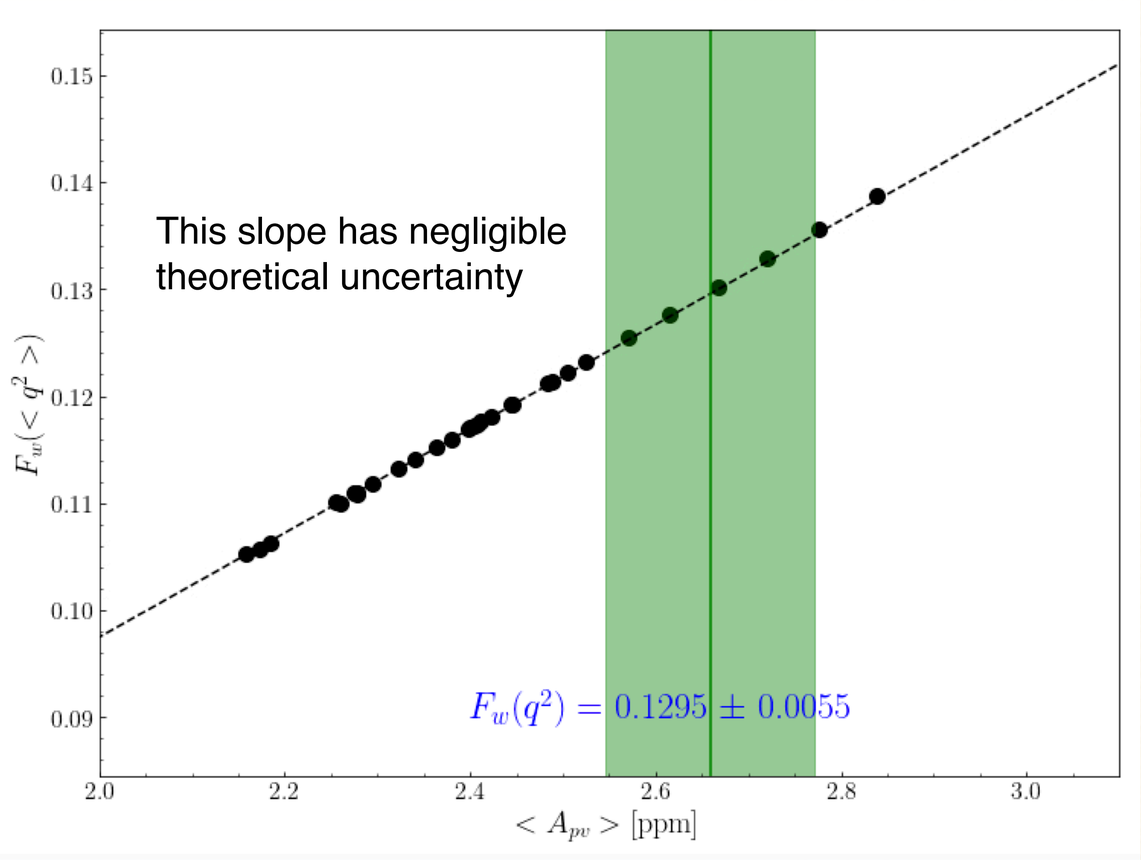
Main Derived Parameter: The Weak Form Factor at $Q^2 = 0.0297$ GeV^2

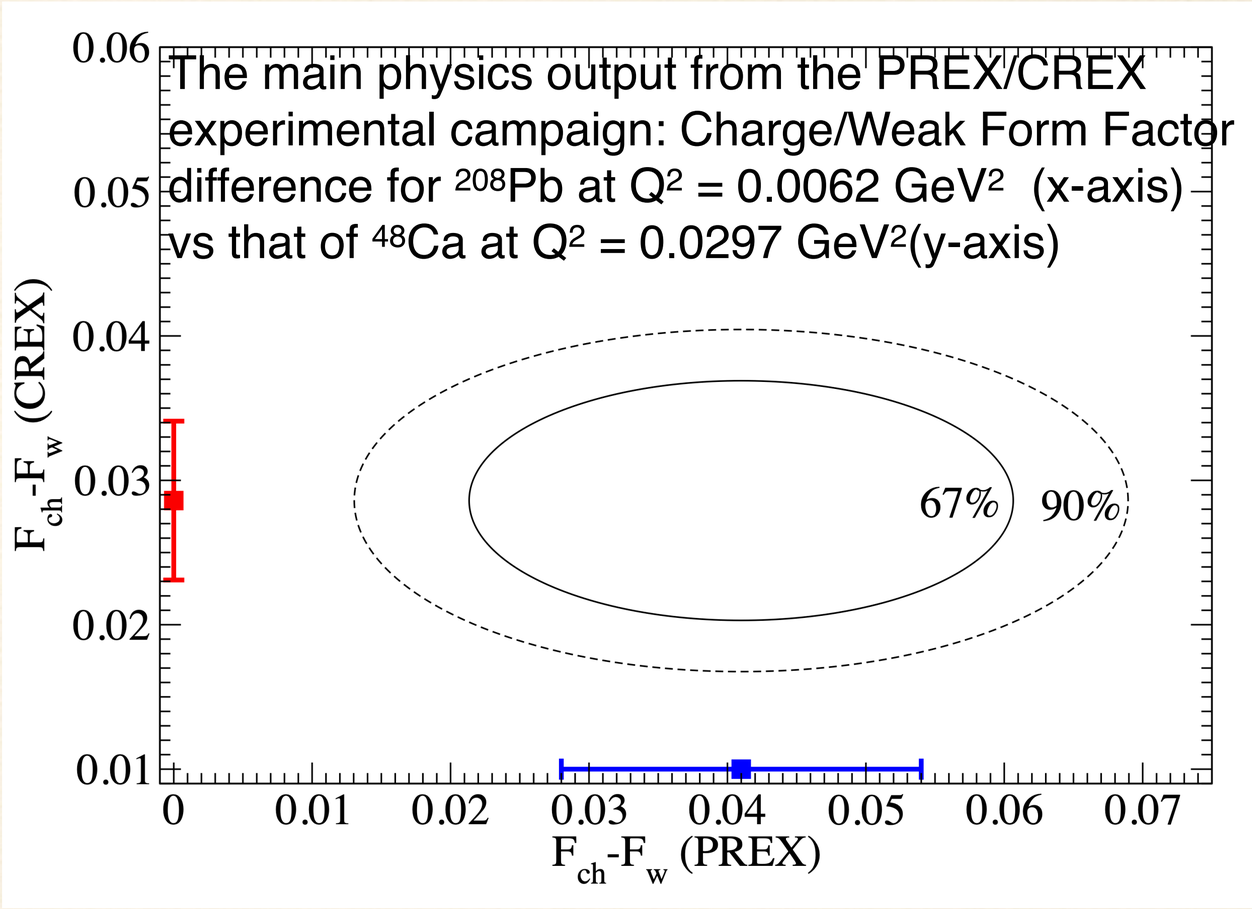




F_W: 0.1295 ± 0.0055

Main Derived Parameter: The Weak Form Factor at $Q^2 = 0.0297$ GeV^2

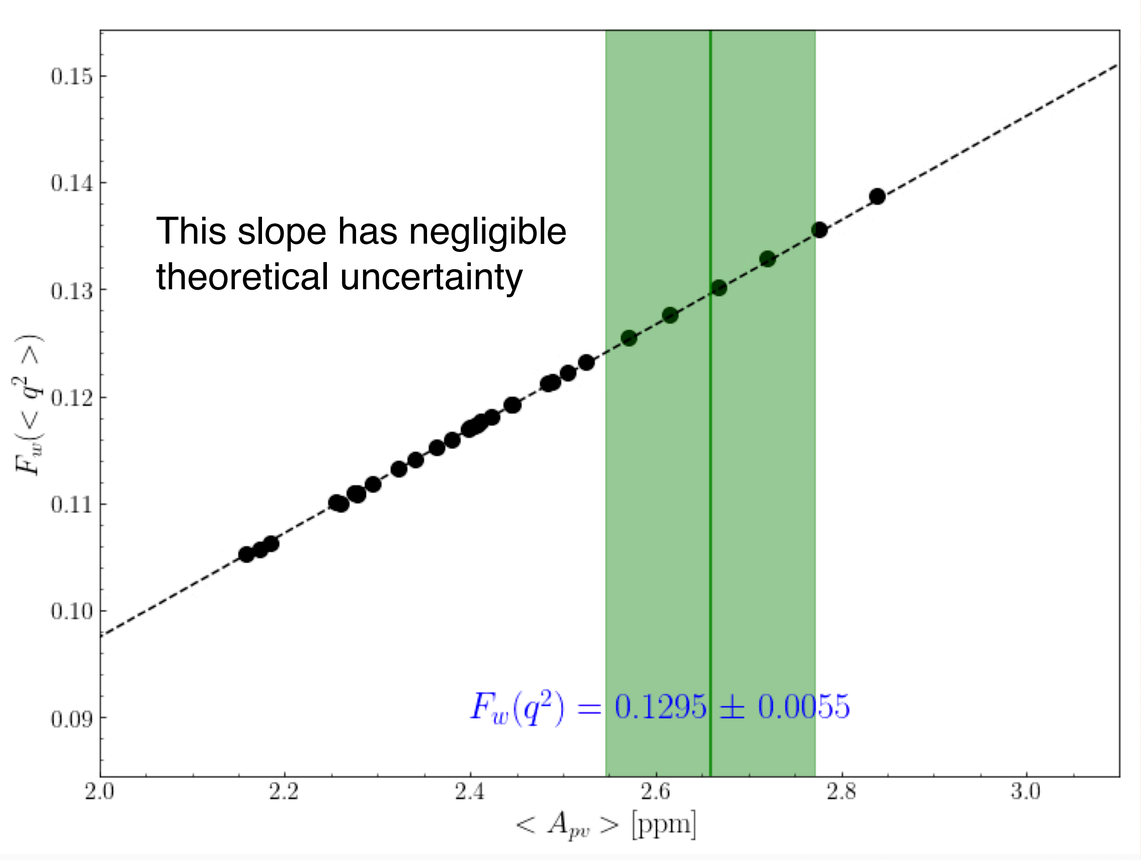


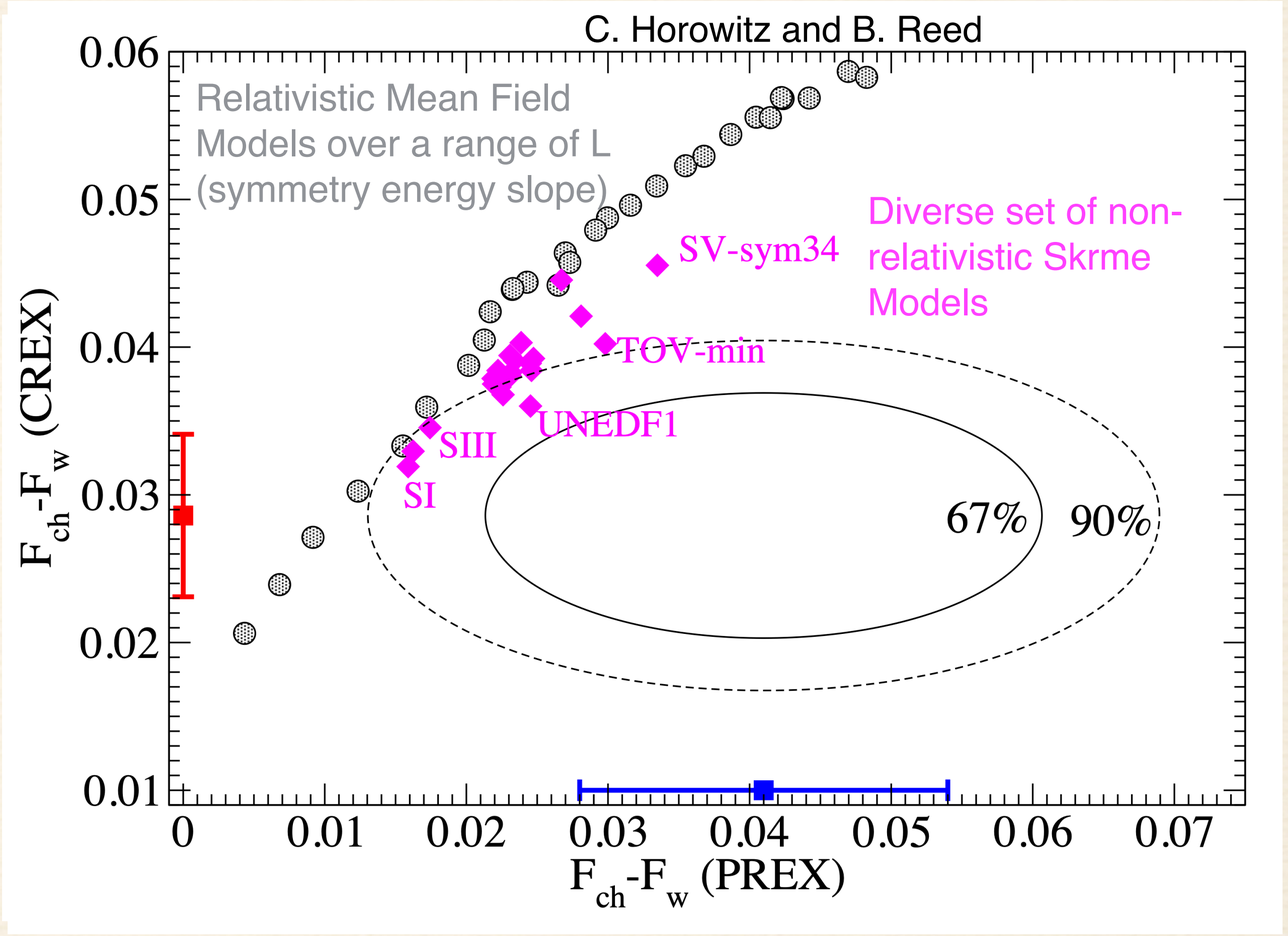


F_W: 0.1295 ± 0.0055

Observation:
CREX result is consistent with a thin neutron skin prediction (e.g. coupled cluster calculations) and is strongly inconsistent with predictions of a very thick skin

Main Derived Parameter: The Weak Form Factor at $Q^2 = 0.0297$ GeV^2

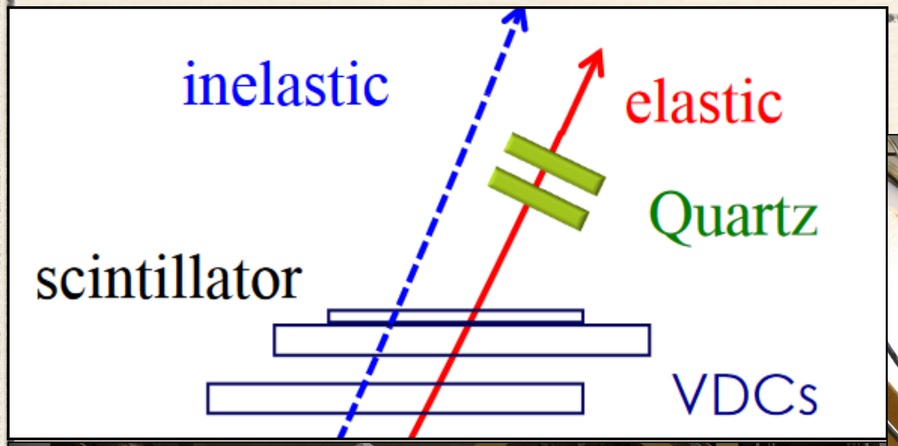




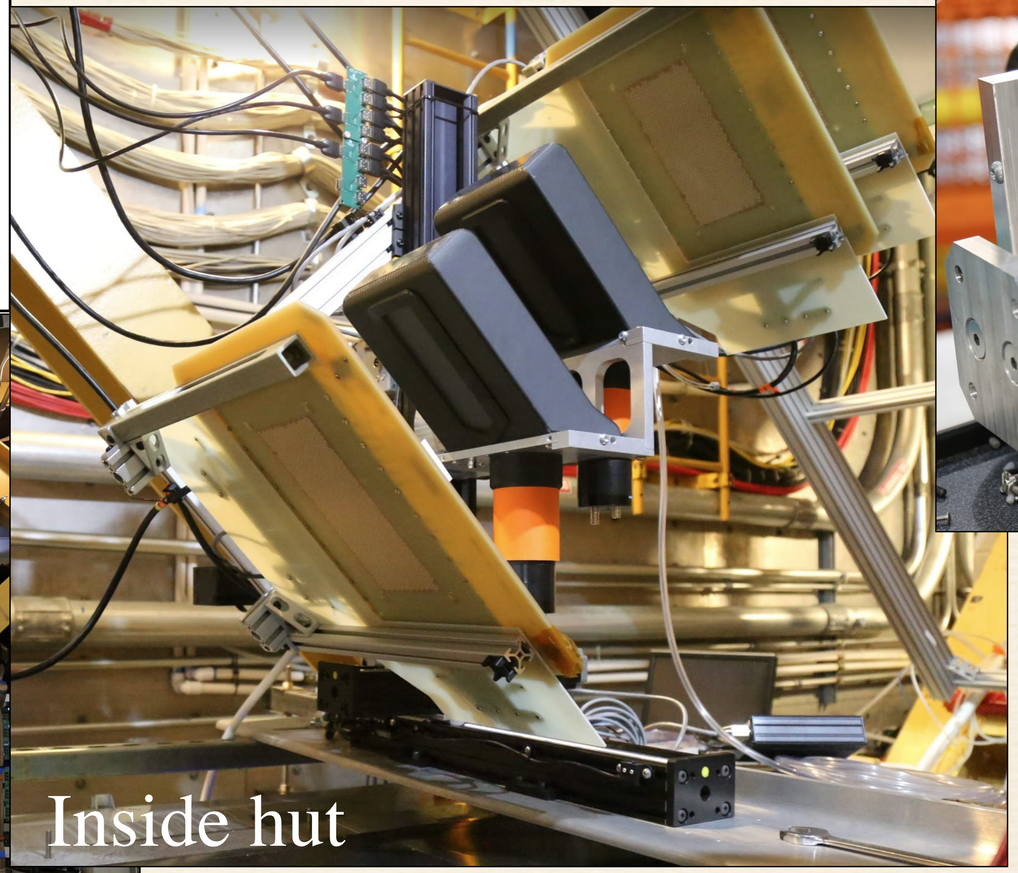
F_W: 0.1295 ± 0.0055

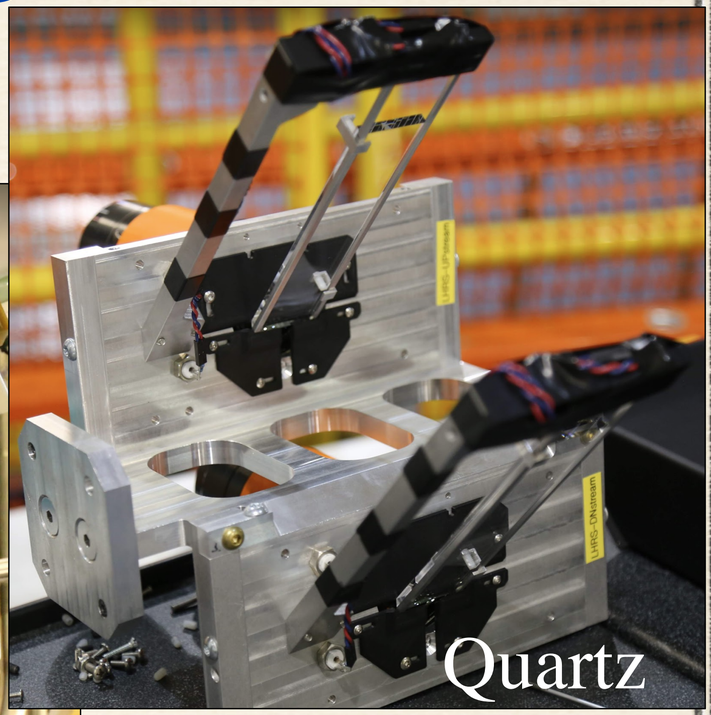
Observation:
CREX result is consistent with a thin neutron skin prediction (e.g. coupled cluster calculations) and is strongly inconsistent with predictions of a very thick skin

Inside the HRS "Counting Hut"



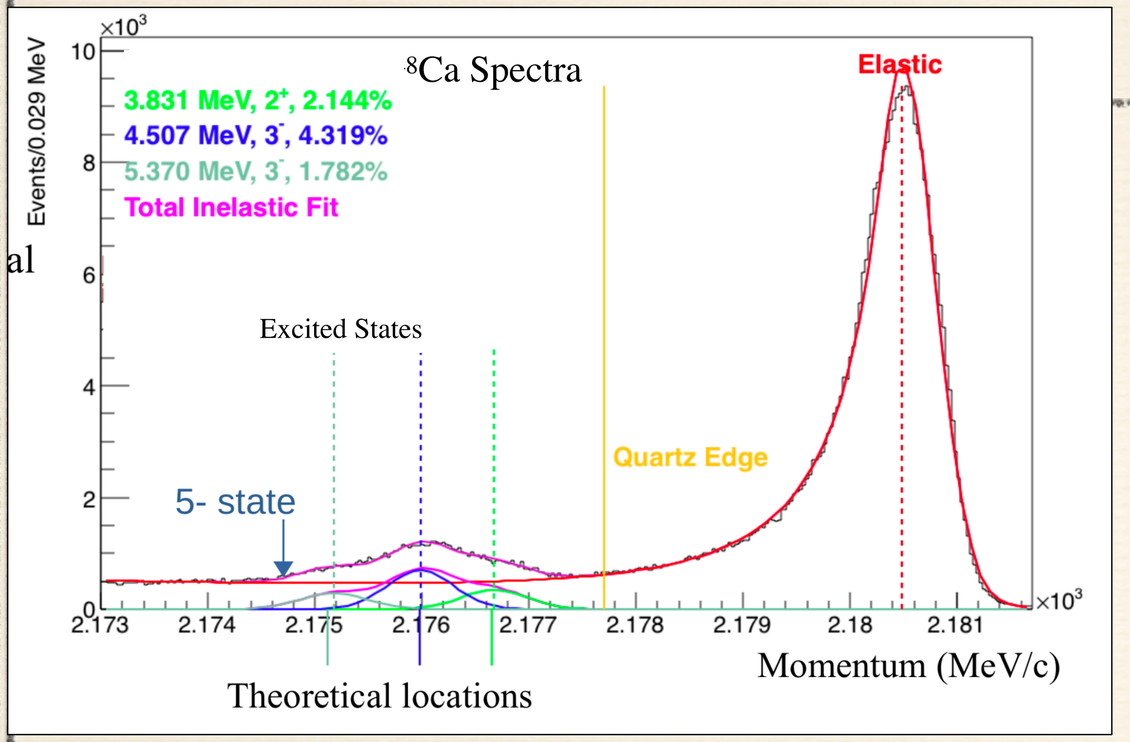






- Integrating detectors (reduce deadtime effects)
- Thick and thin quartz bars (different systematics)

^{48}Ca Target



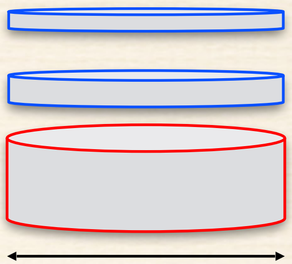
Target 1



Element: Calcium
Symbol: Ca
Isotope: 48
Series: LO
Batch: 140042

- Single puck
- 5mm thick
- 96% ^{48}Ca
- 3.84% ^{40}Ca

Target 2



Element: Calcium
Symbol: Ca
Isotope: 48
Series:
Batch: 900242

*Oak Ridge

- 1puck+2 foils sandwiched
- ~5.7mm thick total
- ~91.7% ^{48}Ca
- ~7.96% ^{40}Ca

Stored in mineral oil until installed
Protected against oxidation

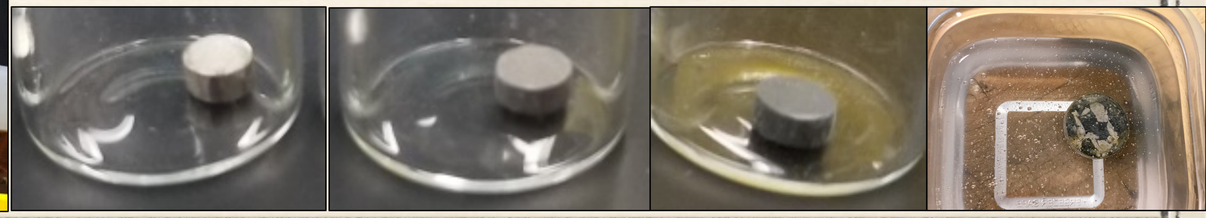
Delicate Installation



Cooled Copper Target Ladder



sanded | Oxidized 1hr | Oxidized 24hr | mineral oil



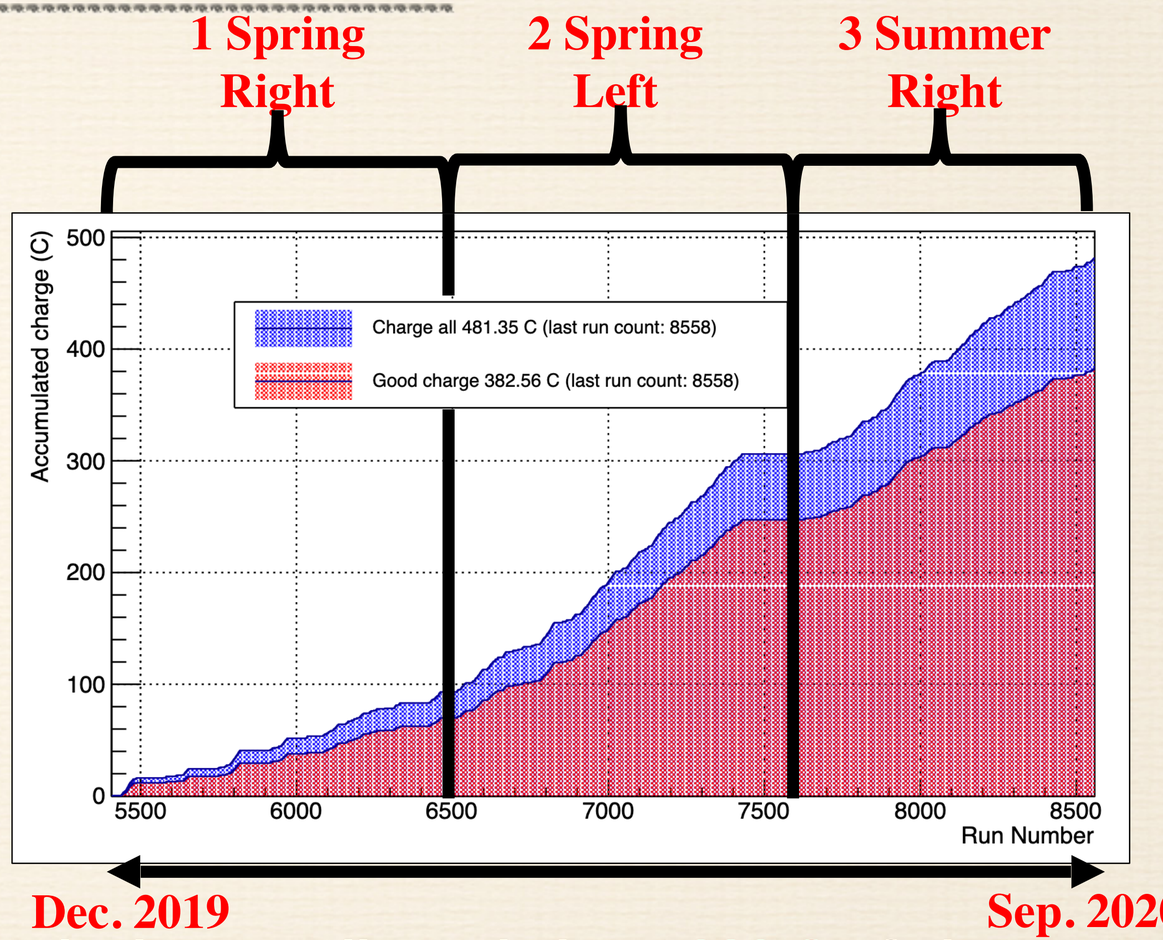
The CREX Physics Runs

13 Ph.D. students, 7 postdocs, a total of about 80 scientists

Data Divided Into 3 Run Periods

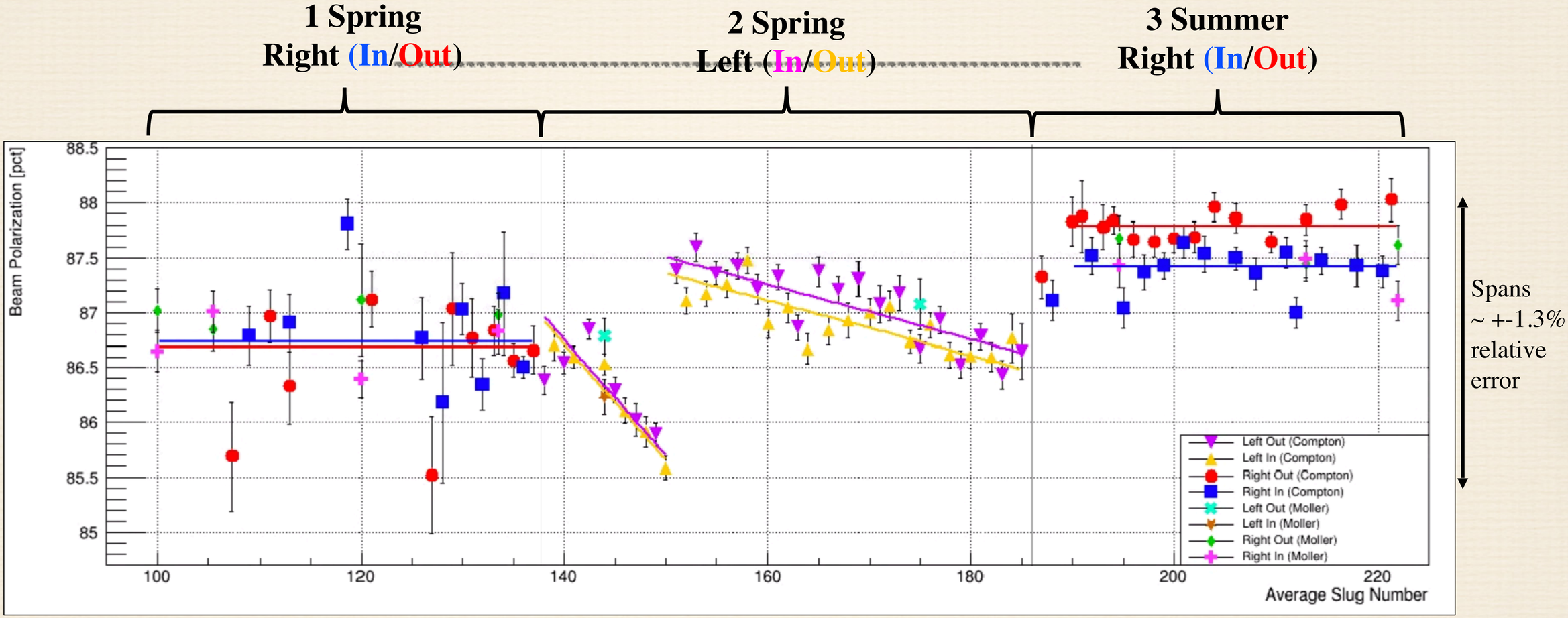
- Part 1) Wien* Right Spring
- Part 2) Wien* Left Spring
  …Covid hit….
- Part 3) Wien* Right Summer
- * “Wien” = Spin Manipulator

- Very close watch on-line data stream - beam conditions, detector response, etc.
- Frequent contact with MCC operators to maintain running conditions
- “prompt" analysis process flagged more subtle problems
- Daily grooming and review in "WAC" process
- (analysis development leader Paul King)



- **At the end of the experiment after our realtime analysis we collected about 383 C of charge on target which passed online analysis cuts(i.e. not excluded in calibrations or due to poor beam conditions, trip recovery, beam excursions, or beam monitor issues)**

Beam Polarimetry



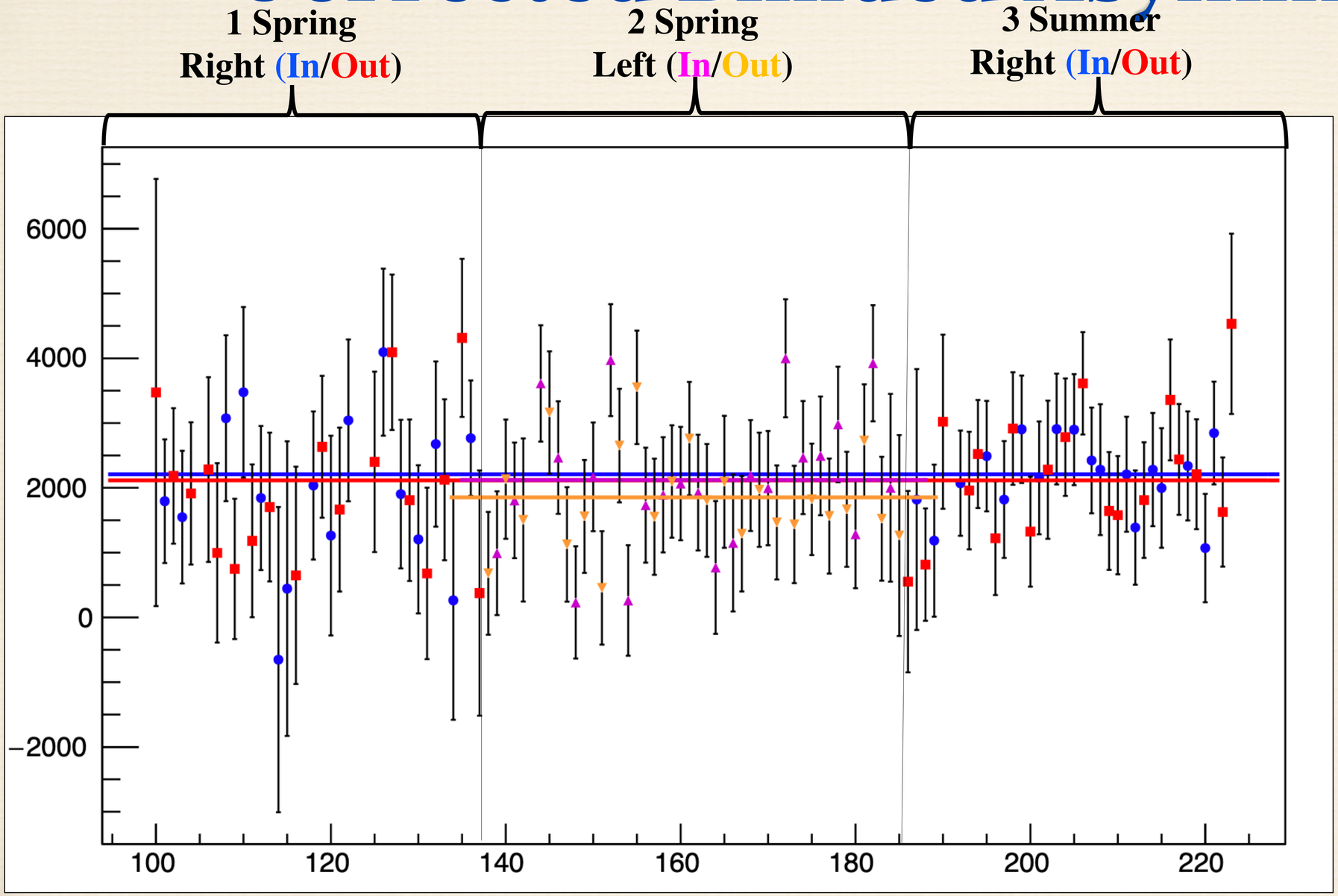
Acknowledgments: A.J. Zec, J. C. Cornejo, M. Dalton, C. Gal, D. Gaskell, C. Palatchi, K. Paschke, A. Premithilake, B. Quinn

Average Compton polarization:
87.10 ± (0.52% dP/P)

CREX Polarimetry Result:
P_e=87.09 +/- (0.44% dP/P)

Average Moller polarization:
87.06 ± (0.85% dP/P)

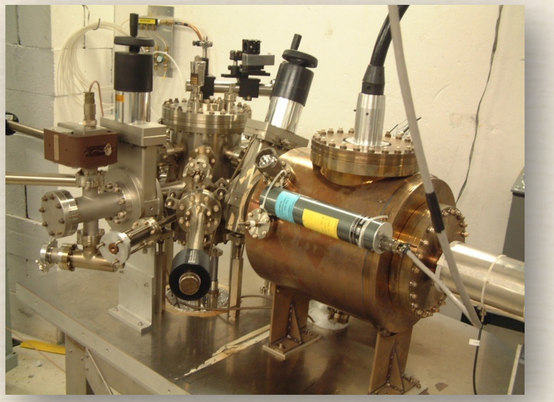
Corrected Blinded Asymmetries



We were looking at the final data set after carefully removing unstable run periods with multiple checks on log books by about the middle of Summer 2021

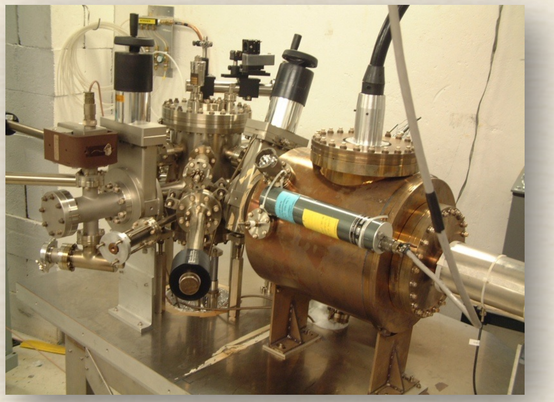
Statistical Uncertainty: 80 to 90 parts per billion

Stability of Polarized Beam at JLab

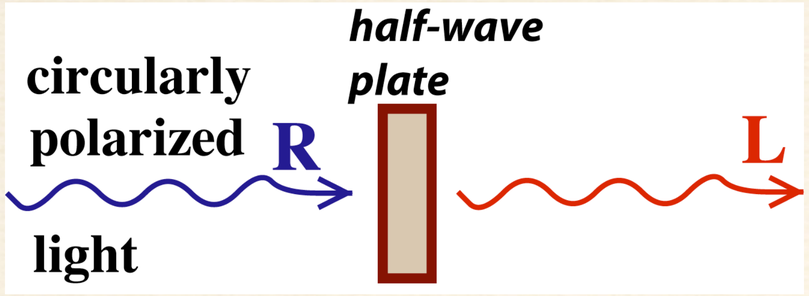


Beam helicity is chosen pseudo-randomly at 30 Hz

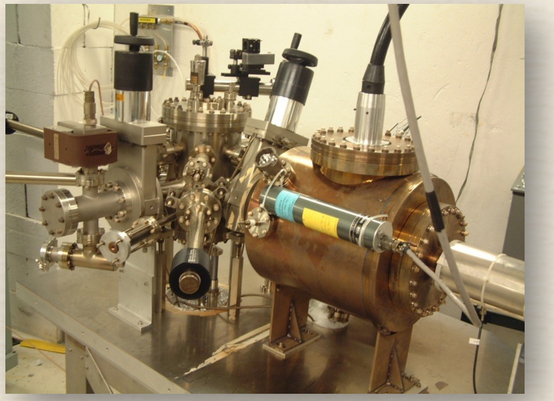
Stability of Polarized Beam at JLab



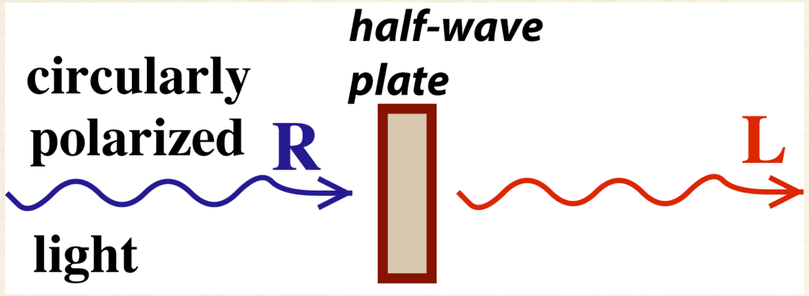
Beam helicity is chosen pseudo-randomly at 30 Hz

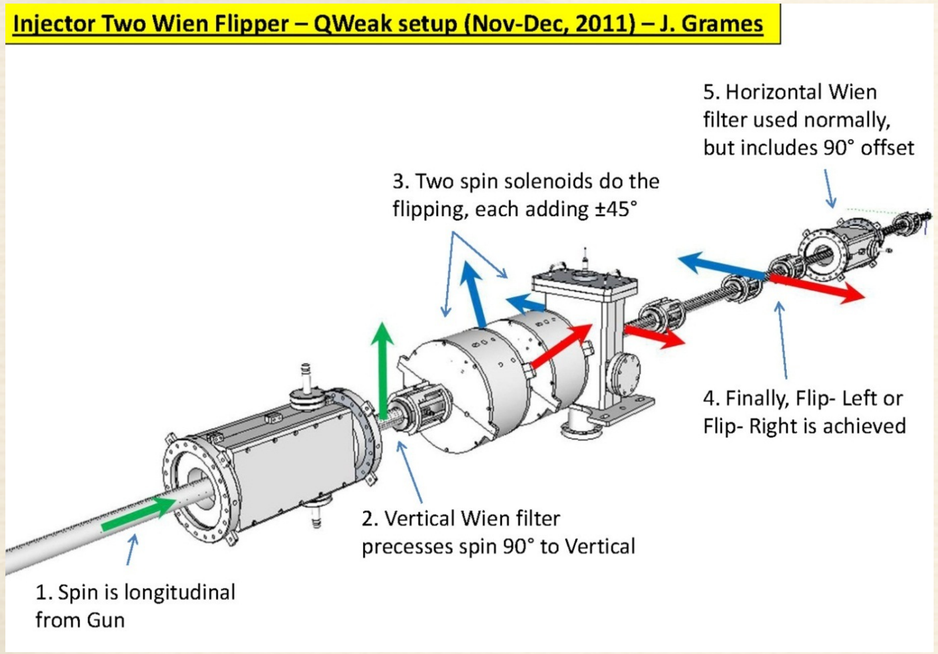


Stability of Polarized Beam at JLab

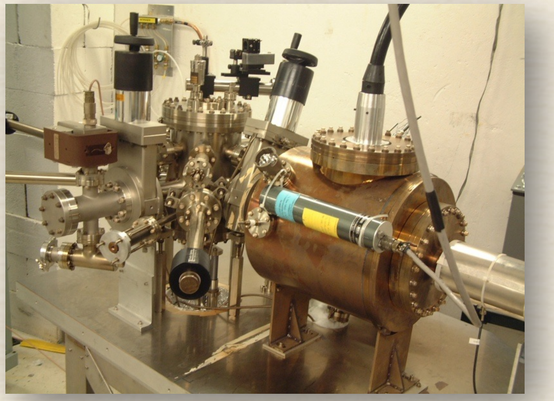


Beam helicity is chosen pseudo-randomly at 30 Hz

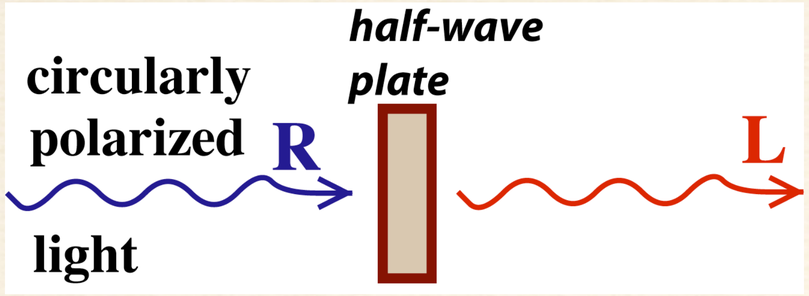




Stability of Polarized Beam at JLab

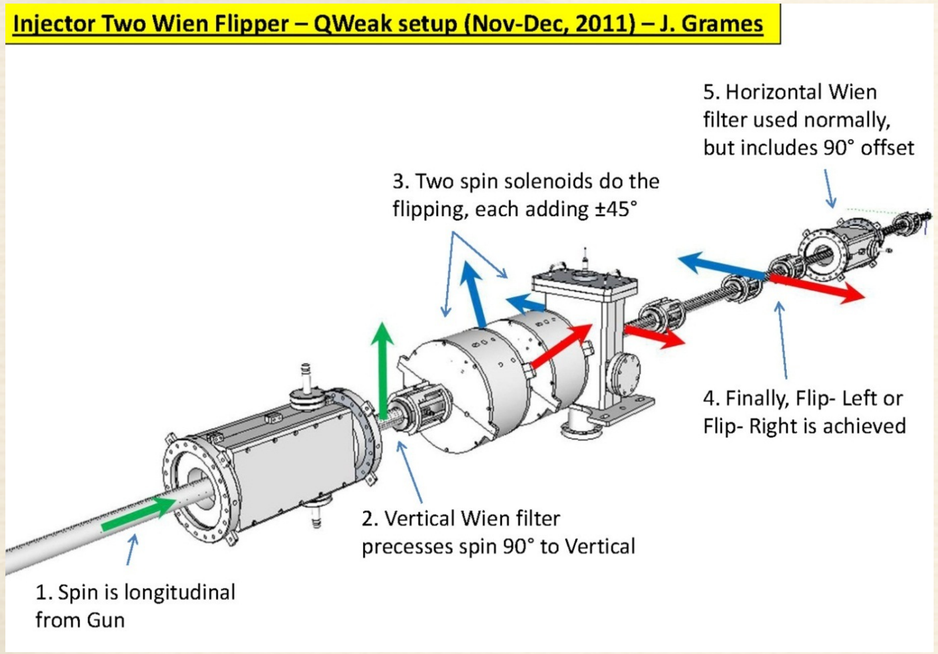


Beam helicity is chosen pseudo-randomly at 30 Hz

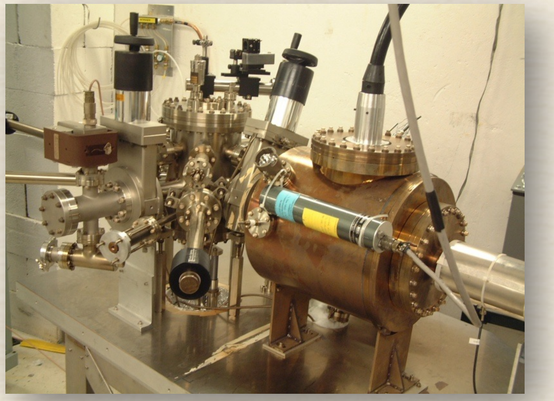


$$A_{corr} \sim 2000 \text{ ppb}$$

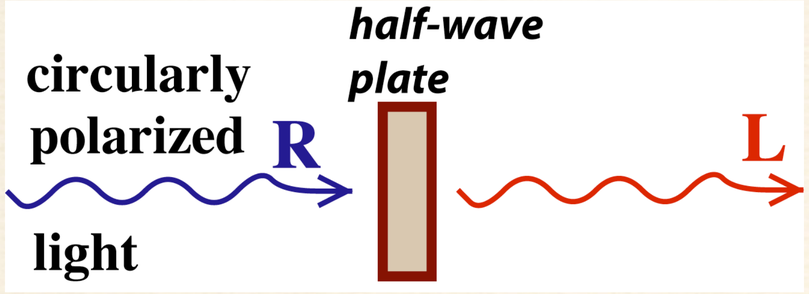
$$A_{corr} = A_{det} - A_Q + \alpha \Delta_E + \Sigma \beta_i \Delta x_i$$



Stability of Polarized Beam at JLab



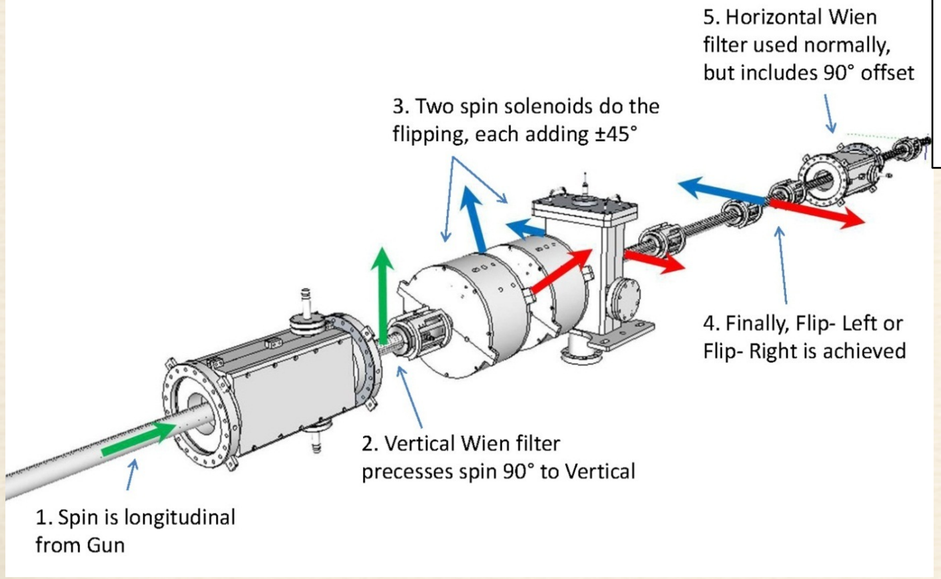
Beam helicity is chosen pseudo-randomly at 30 Hz



$$A_{corr} \sim 2000 \text{ ppb}$$

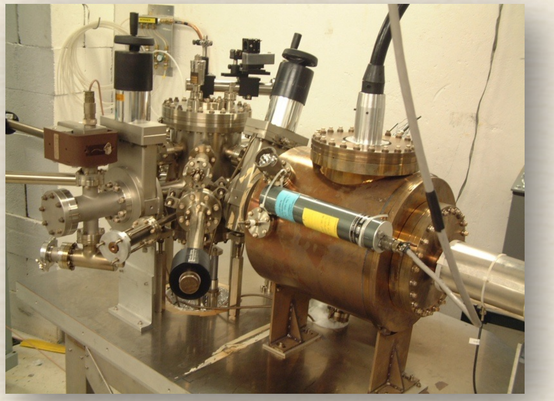
$$A_{corr} = A_{det} - A_Q + \alpha \Delta_E + \Sigma \beta_i \Delta x_i$$

Injector Two Wien Flipper – QWeak setup (Nov-Dec, 2011) – J. Grames

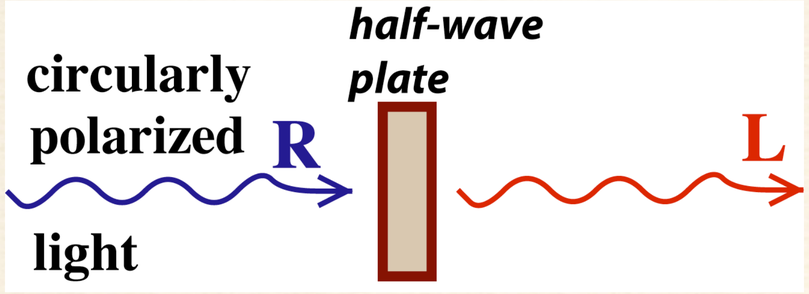


Wien	Weight	X (nm)	Y (nm)	θ X (nrad)	θ Y (nrad)	E dpp
R 1	18.0%	1.6 ± 3.7	-2.4 ± 2.0	-0.26 ± 0.17	-0.11 ± 0.12	$-2.0 \pm 2.0e^{-9}$
Left	45.2%	-4.1 ± 1.6	0.3 ± 1.1	0.08 ± 0.04	-0.024 ± 0.10	$0.32 \pm 1.5e^{-9}$
R 2	36.9%	-2.8 ± 4.1	-0.2 ± 1.7	-0.06 ± 0.09	-0.28 ± 0.17	$0.84 \pm 1.9e^{-9}$
	Avg	-2.6 ± 1.8	-0.4 ± 0.9	-0.03 ± 0.05	-0.13 ± 0.08	$0.09 \pm 1.0e^{-9}$

Stability of Polarized Beam at JLab

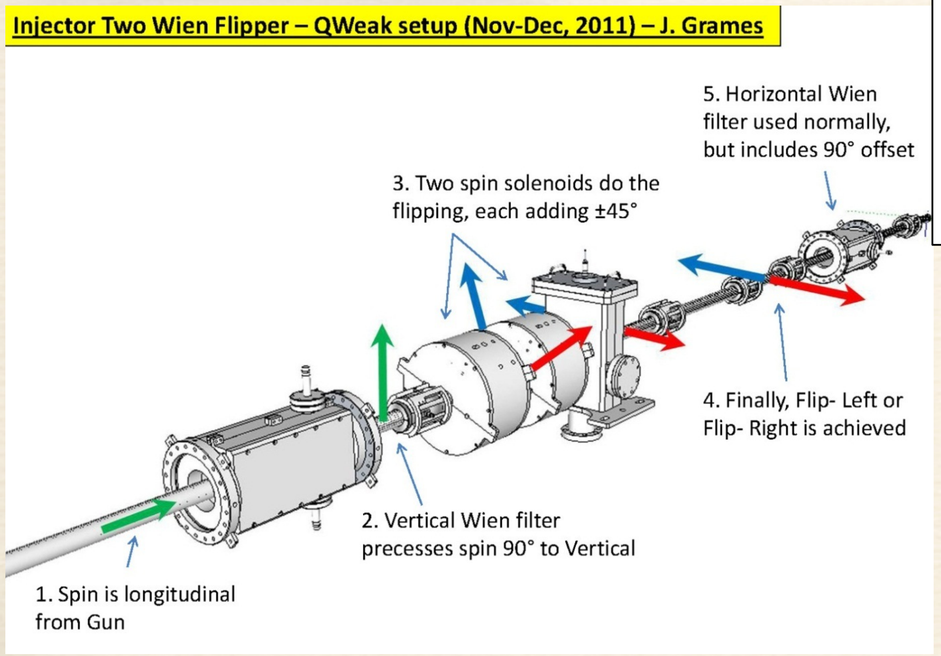


Beam helicity is chosen pseudo-randomly at 30 Hz



$$A_{corr} \sim 2000 \text{ ppb}$$

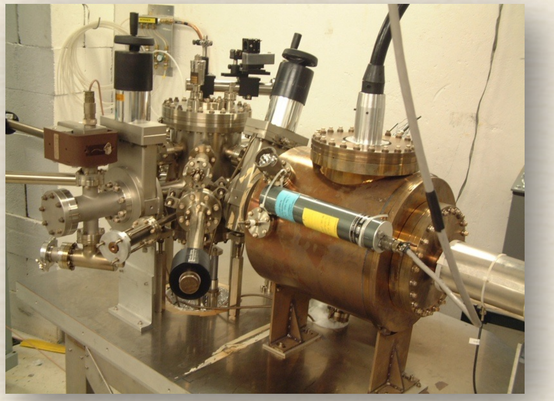
$$A_{corr} = A_{det} - A_Q + \alpha \Delta_E + \Sigma \beta_i \Delta x_i$$



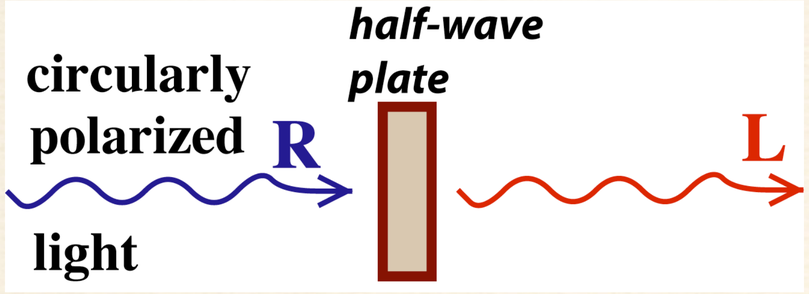
Wien	Weight	X (nm)	Y (nm)	θ X (nrad)	θ Y (nrad)	E dpp
R 1	18.0%	1.6 ± 3.7	-2.4 ± 2.0	-0.26 ± 0.17	-0.11 ± 0.12	$-2.0 \pm 2.0e^{-9}$
Left	45.2%	-4.1 ± 1.6	0.3 ± 1.1	0.08 ± 0.04	-0.024 ± 0.10	$0.32 \pm 1.5e^{-9}$
R 2	36.9%	-2.8 ± 4.1	-0.2 ± 1.7	-0.06 ± 0.09	-0.28 ± 0.17	$0.84 \pm 1.9e^{-9}$
	Avg	-2.6 ± 1.8	-0.4 ± 0.9	-0.03 ± 0.05	-0.13 ± 0.08	$0.09 \pm 1.0e^{-9}$

- Three independent techniques agree across 3-parts of data set
- For beam correction, decided to use 12 BPM Lagrange Multiplier 3-part eigenvector correction, 5% slope uncertainty
- Left/right symmetric detectors, so correction dominated by E

Stability of Polarized Beam at JLab



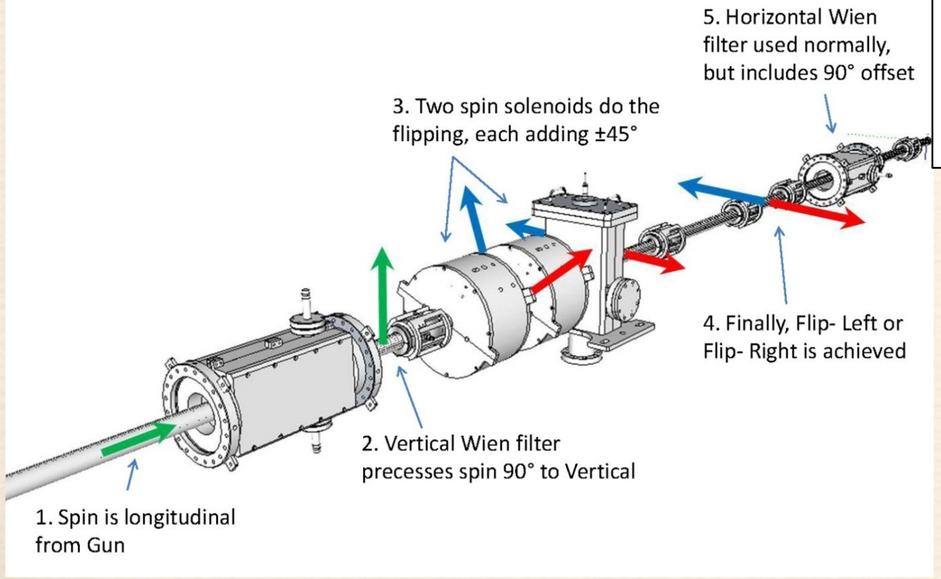
Beam helicity is chosen pseudo-randomly at 30 Hz



$$A_{corr} \sim 2000 \text{ ppb}$$

$$A_{corr} = A_{det} - A_Q + \alpha \Delta_E + \Sigma \beta_i \Delta x_i$$

Injector Two Wien Flipper – QWeak setup (Nov-Dec, 2011) – J. Grames



Wien	Weight	X (nm)	Y (nm)	θ X (nrad)	θ Y (nrad)	E dpp
R 1	18.0%	1.6 ± 3.7	-2.4 ± 2.0	-0.26 ± 0.17	-0.11 ± 0.12	$-2.0 \pm 2.0e^{-9}$
Left	45.2%	-4.1 ± 1.6	0.3 ± 1.1	0.08 ± 0.04	-0.024 ± 0.10	$0.32 \pm 1.5e^{-9}$
R 2	36.9%	-2.8 ± 4.1	-0.2 ± 1.7	-0.06 ± 0.09	-0.28 ± 0.17	$0.84 \pm 1.9e^{-9}$
	Avg	-2.6 ± 1.8	-0.4 ± 0.9	-0.03 ± 0.05	-0.13 ± 0.08	$0.09 \pm 1.0e^{-9}$

- Three independent techniques agree across 3-parts of data set
- For beam correction, decided to use 12 BPM Lagrange Multiplier 3-part eigenvector correction, 5% slope uncertainty
- Left/right symmetric detectors, so correction dominated by E

Total beam corrections:

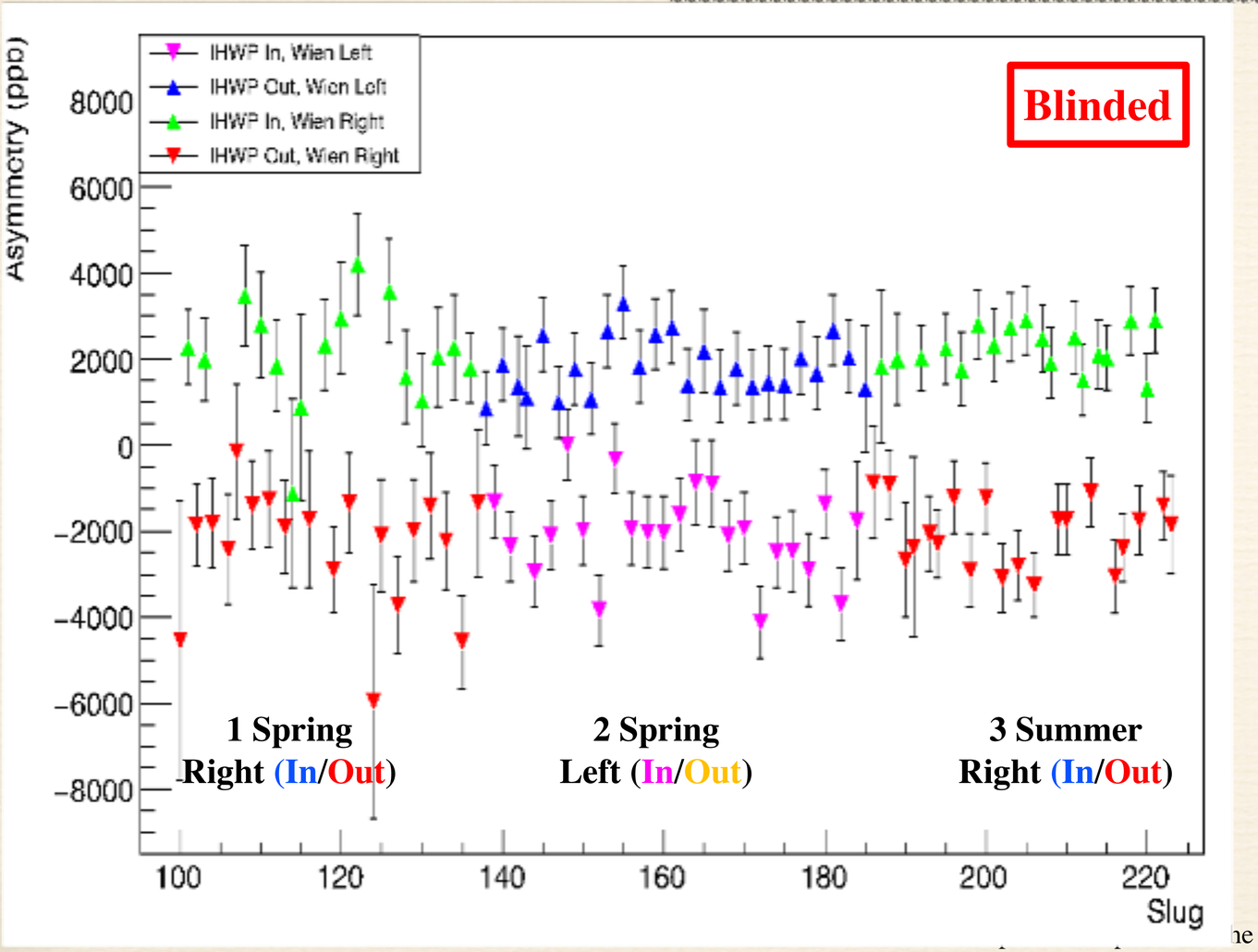
$A_{beam} = (53.5 \pm 5.4)$ ppb

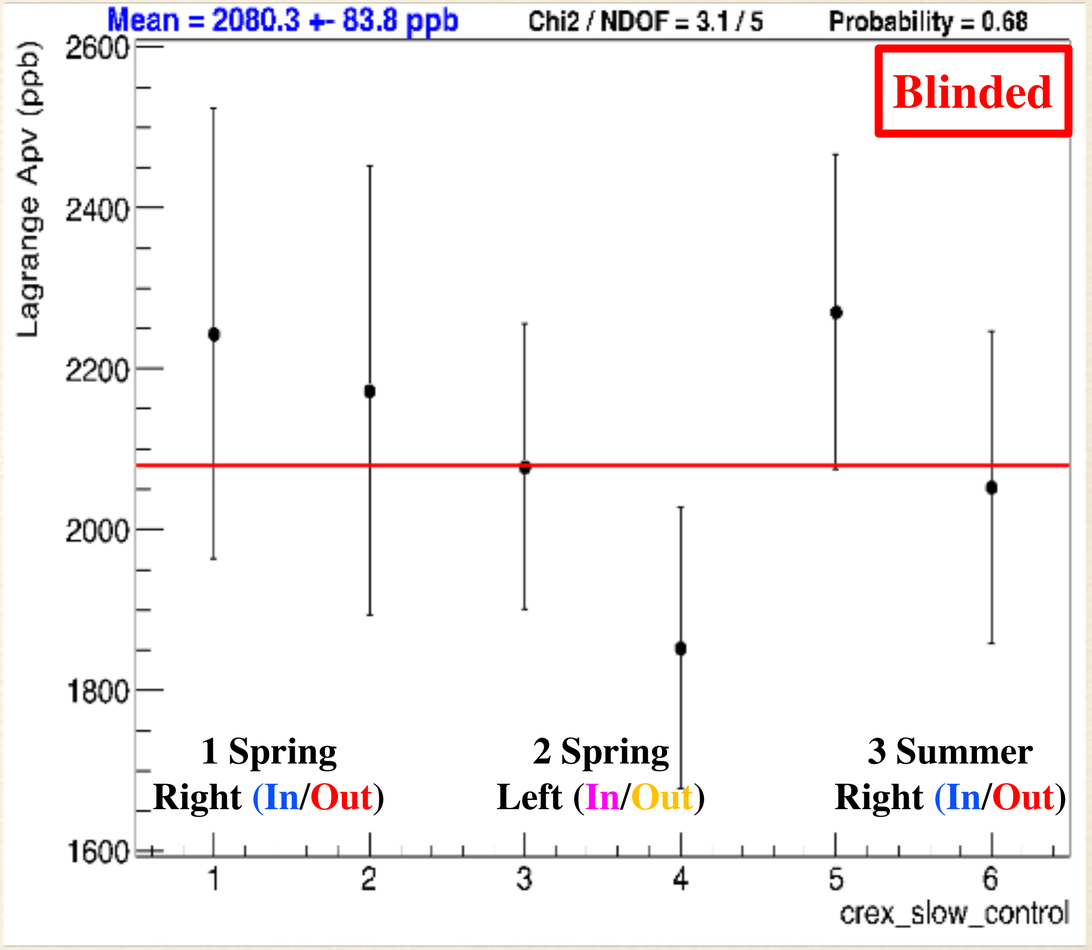
Half Wave Plate: IN/OUT Wien(Spin Manipulator): Left/Right

Demonstration of Systematic Control

Sign-uncorrected, Each point: 8h time-scale

Sign-corrected, Each point: ~1week time-scale





...e right (zoomed in y-scale)

- Measuring continuously flipping sign by 2 methods (IHWP, Wien)
- The corrected asymmetry removed effects from beam asymmetries and noise

Grand Corrected Asymmetry

Final result averaging over all IHWP and 3 Part Wien flip configurations

C. Clarke

Wien	Weight	A_{raw} (ppb)	A_{det} (ppb)	A_Q (ppb)
Right 1	17.9%	2460.15 ± 391.95	2207.90 ± 197.69	-94.1 ± 69.6
Left	45.2%	1871.06 ± 278.39	1963.65 ± 124.64	148.1 ± 40.1
Right 2	36.9%	2006.57 ± 335.29	2160.94 ± 137.95	-376.3 ± 38.7
Weighted Average		2026.81 ± 189.88	2080.26 ± 83.77	-88.8 ± 26.2

1 Right (In/Out)
2 Left (In/Out)
3 Right (In/Out)

Blinded Corrected Asymmetry A_{corr}:
2080.3 ± 83.8ppb

Grand Corrected Asymmetry

Final result averaging over all IHWP and 3 Part Wien flip configurations

C. Clarke

Wien	Weight	A_{raw} (ppb)	A_{det} (ppb)	A_Q (ppb)
Right 1	17.9%	2460.15 ± 391.95	2207.90 ± 197.69	-94.1 ± 69.6
Left	45.2%	1871.06 ± 278.39	1963.65 ± 124.64	148.1 ± 40.1
Right 2	36.9%	2006.57 ± 335.29	2160.94 ± 137.95	-376.3 ± 38.7
Weighted Average		2026.81 ± 189.88	2080.26 ± 83.77	-88.8 ± 26.2

1 Right (In/Out)
2 Left (In/Out)
3 Right (In/Out)

Blinded Corrected Asymmetry A_{corr}:
2080.3 ± 83.8ppb

Careful and painstaking analyses by multiple students on each of the small corrections to extract the physics asymmetry

$$A_{corr} = A_{det} - A_{beam} - A_{trans} - A_{nonlin} - A_{blind}$$

$$A_{phys} = R_{radcorr}\, R_{accept}\, R_{Q^2} \frac{A_{corr} - P_L \sum_i f_i A_i}{P_L(1 - \sum_i f_i)}$$

Grand Corrected Asymmetry

Final result averaging over all IHWP and 3 Part Wien flip configurations

C. Clarke

Wien	Weight	A_{raw} (ppb)	A_{det} (ppb)	A_Q (ppb)
Right 1	17.9%	2460.15 ± 391.95	2207.90 ± 197.69	-94.1 ± 69.6
Left	45.2%	1871.06 ± 278.39	1963.65 ± 124.64	148.1 ± 40.1
Right 2	36.9%	2006.57 ± 335.29	2160.94 ± 137.95	-376.3 ± 38.7
Weighted Average		2026.81 ± 189.88	2080.26 ± 83.77	-88.8 ± 26.2

1 Right (In/Out)
2 Left (In/Out)
3 Right (In/Out)

Blinded Corrected Asymmetry A_{corr}:
2080.3 ± 83.8ppb

Careful and painstaking analyses by multiple students on each of the small corrections to extract the physics asymmetry

$$A_{corr} = A_{det} - A_{beam} - A_{trans} - A_{nonlin} - A_{blind}$$

$$A_{phys} = R_{radcorr}\, R_{accept}\, R_{Q^2} \frac{A_{corr} - P_L \sum_i f_i A_i}{P_L(1 - \sum_i f_i)}$$

Unblinding!! Week before Fall DNP Meeting

Blinded A_{PV}:

2334.8 ± 112.4ppb (4.8%)

"Blinding box": an additive term on every quartet asymmetry, randomly selected (flat) at the start of the run, from ± 900 ppb

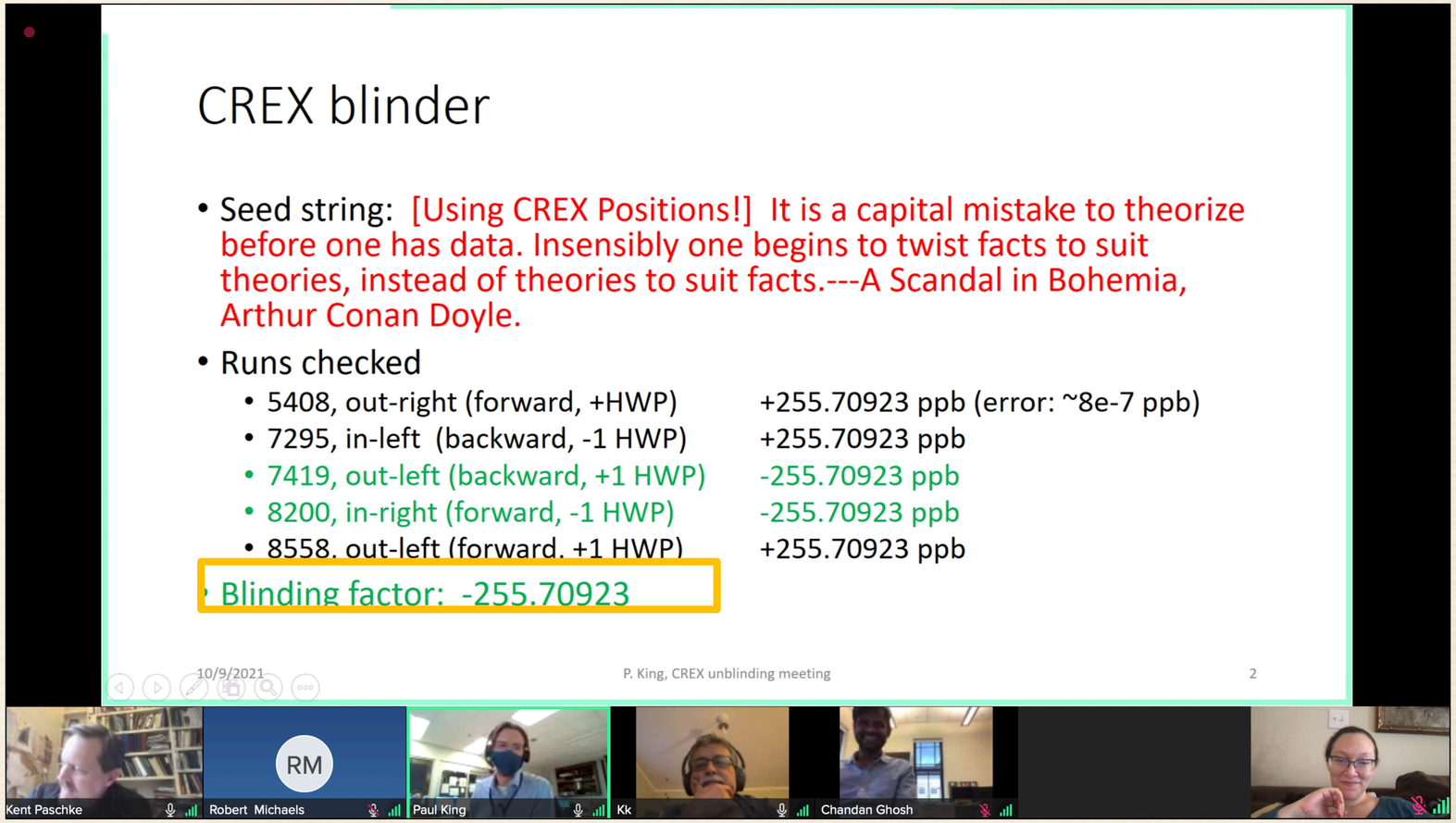
$$A_{phys} = R_{radcorr}\, R_{accept}\, R_{Q^2} \frac{A_{corr} - P_L \sum_i f_i A_i}{P_L(1 - \sum_i f_i)}$$

$$A_{corr} = A_{det} - A_{beam} - A_{trans} - A_{nonlin} - A_{blind}$$

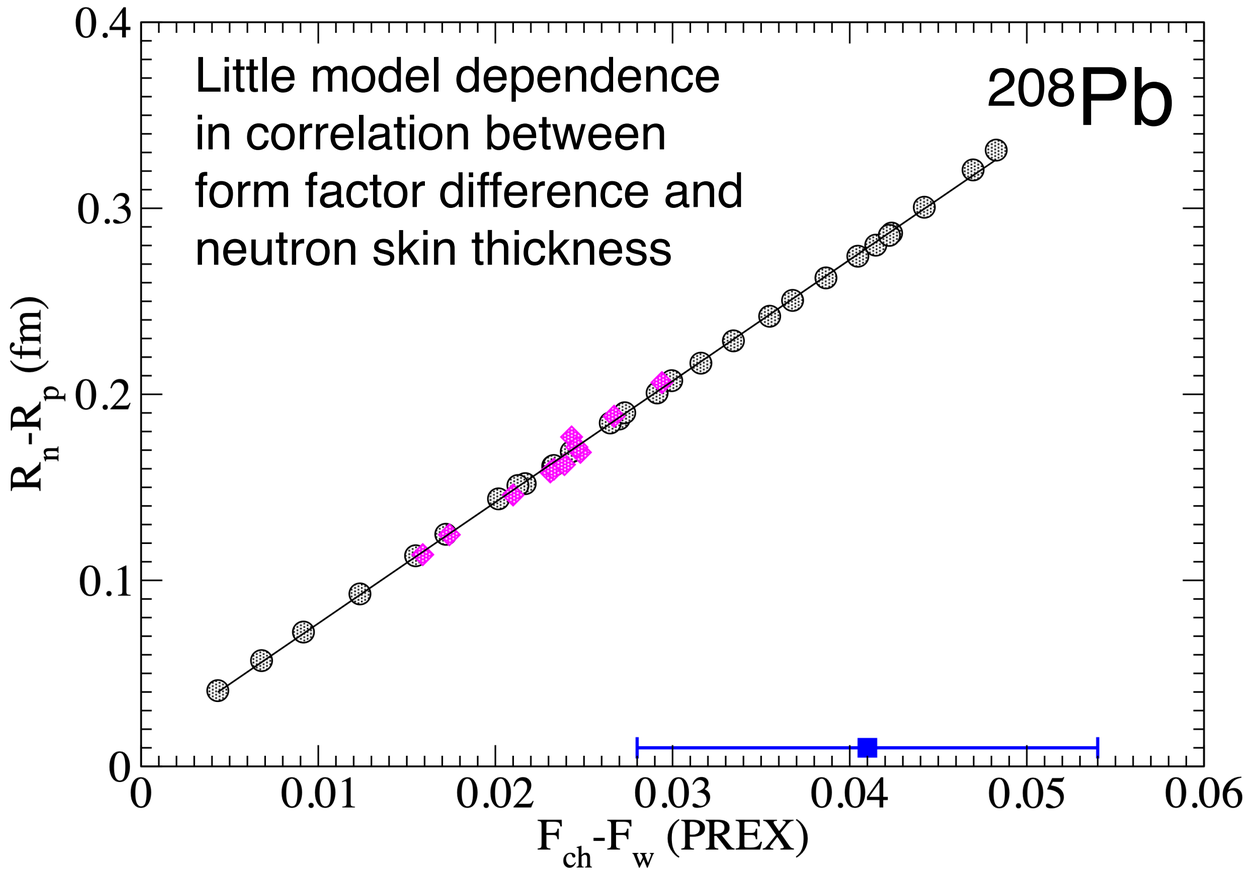
Unblinded A_{PV}:

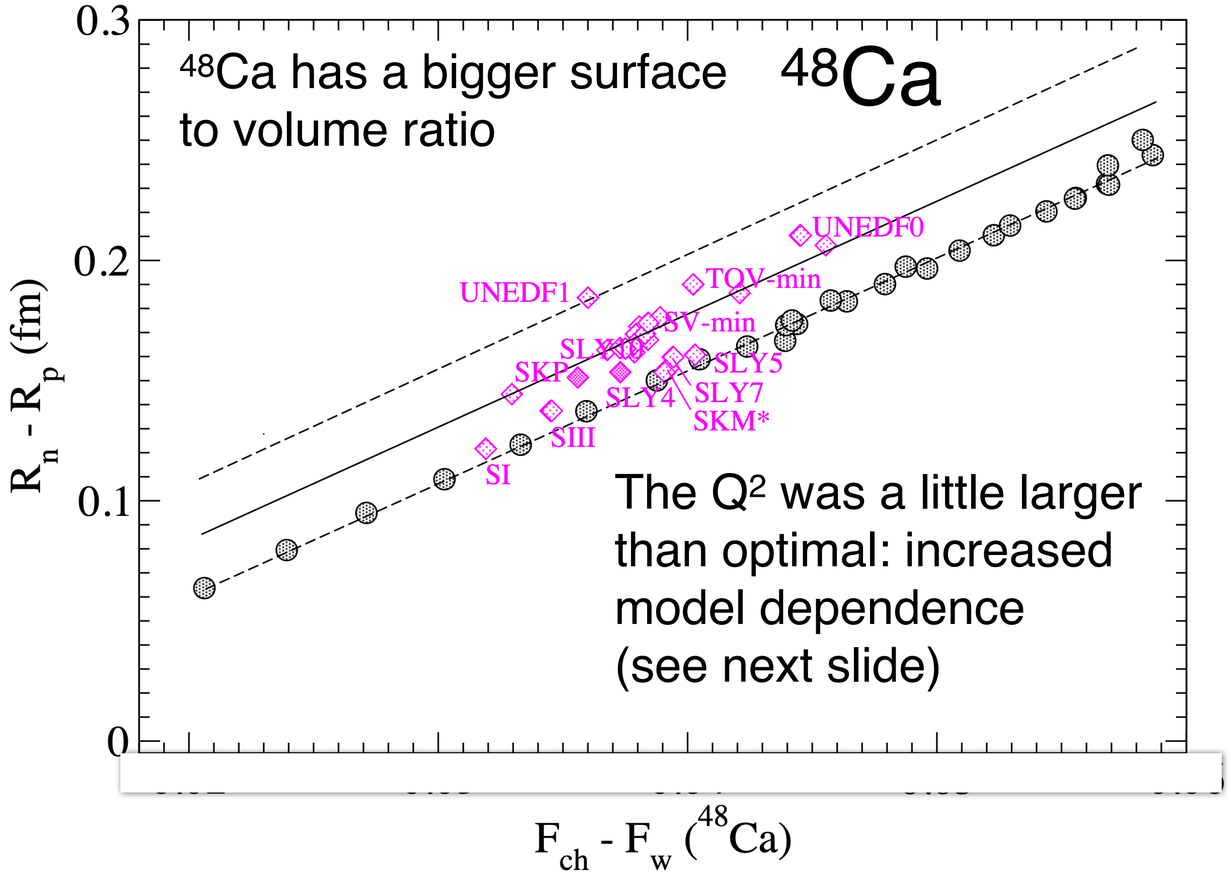
2658.6 ± 113.2ppb (4.3%)





Neutron Skin Extraction: Model Dependence





^{48}Ca: Projected experimental skin thickness uncertainty ~ 0.026 fm
Projected skin thickness model uncertainty ~ 0.023 fm

Outlook from PREX & CREX Campaigns

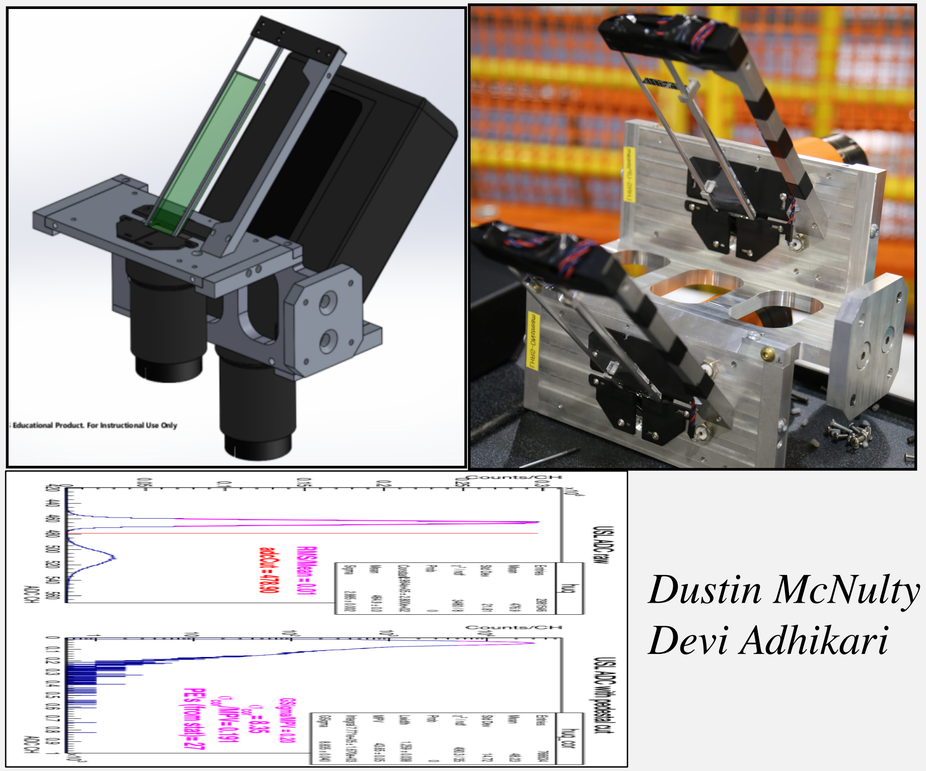
✦ The PREX measurement of the neutron skin thickness of ^{208}Pb has very little model uncertainty

- ★ There is a clear and transparent line from the statistical uncertainty in the experimental observable (A_{PV}) to the uncertainty in the neutron skin thickness and then on to slope of the symmetry energy: unique among all measurement techniques!
- ★ Given the above, improved A_{PV} uncertainty is desirable; a group of us have investigated a possible improved measurement at Mainz, targeting an uncertainty of +/- 0.04 fm

✦ The CREX measurement is likely the final statement at low Q for ^{48}Ca

- ★ Before extracting information on slope of the symmetry energy, the community must collaborate to carefully evaluate modeling modeling uncertainties
- ★ Given the focus of NSCL and FRIB measurements on a range of nuclei of similar A, reconciling all the experimental data is going to lead to important new insights. Exciting!
- ★ If found compelling, it might be feasible to devise a new A_{PV} measurement on ^{48}Ca at a different Q value at Mainz

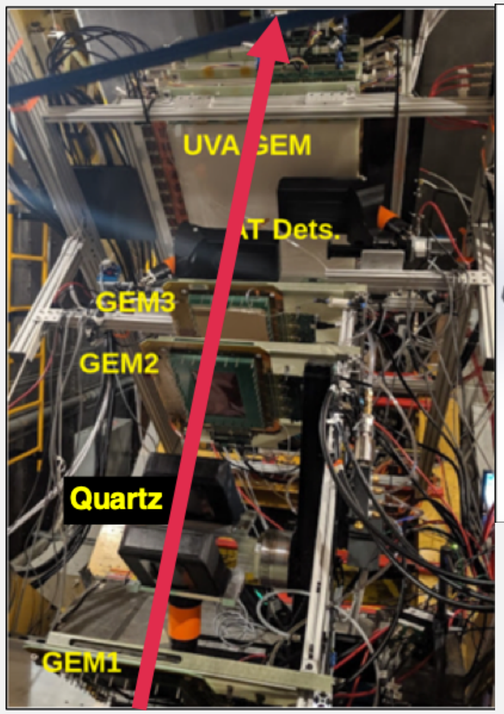
Integrating Detectors

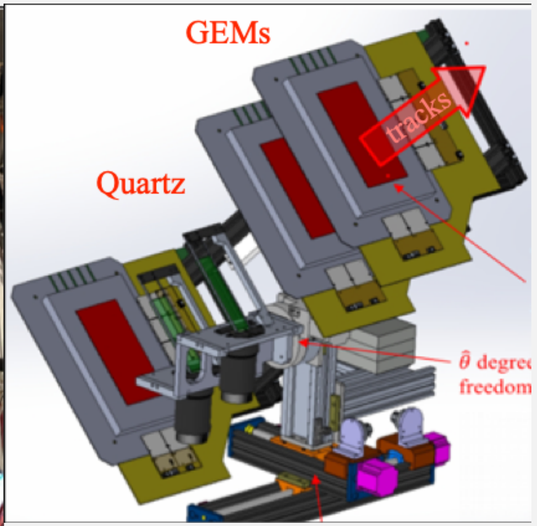


Dustin McNulty
Devi Adhikari

- The challenge: all electrons need to count the same - high photon statistics but low shower fluctuations
- Fused silica Cerenkov radiator, 5mm thick, 3.5x16 cm^2 area, mated to a single PMT
- ~56 MHz signal rate in a 3x3 cm^2 area at the end of the detector
- Non-linearity of detector response was tested on the bench and with beam during the experiment

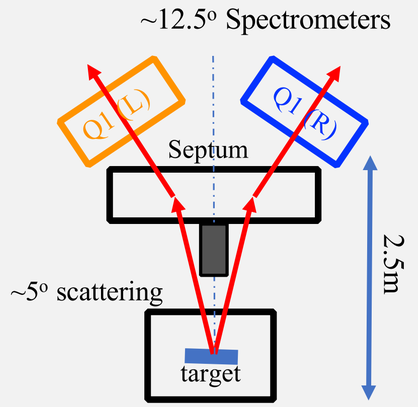
Counting Detectors



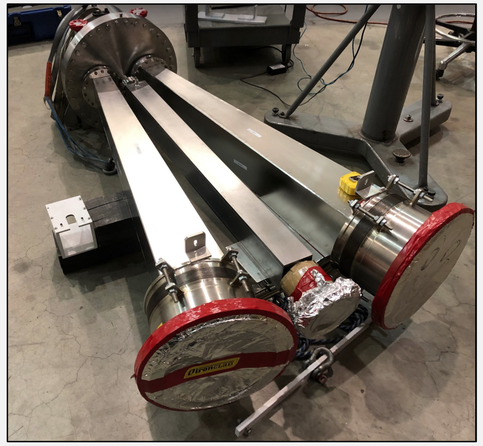


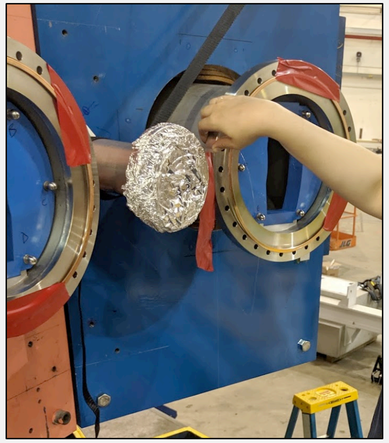
- The HRS Vertical Drift Chambers (VDCs) below the quartz detectors
- GEMs that we installed upstream and downstream of our quartz detectors (*N. Liyanage*)
- Used to align the elastic peak on the quartz and to measure accepted kinematics
- Used at very low beam currents (<1uA) “counting experimental mode”

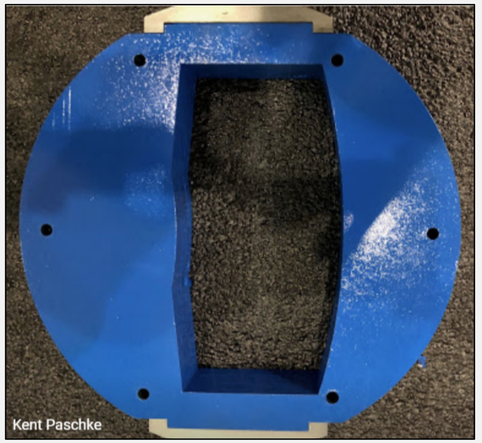
Hardware Downstream of Target

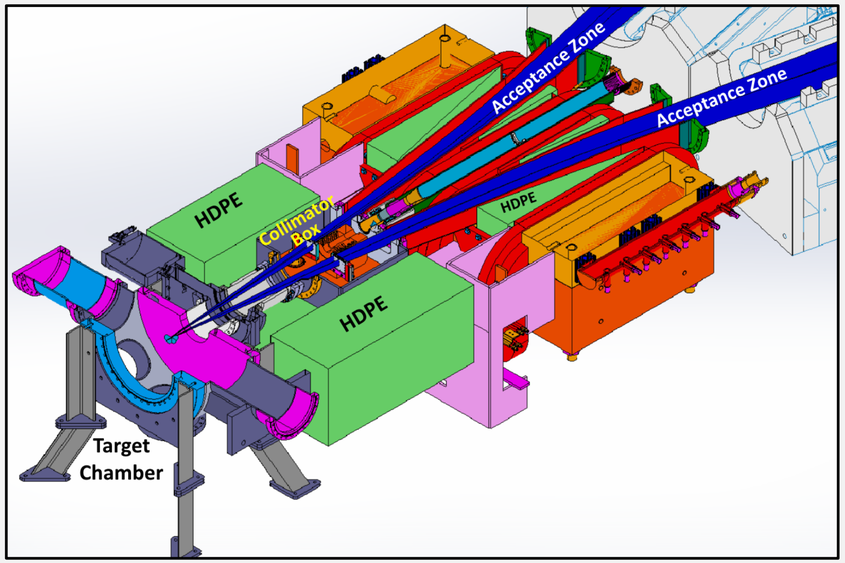










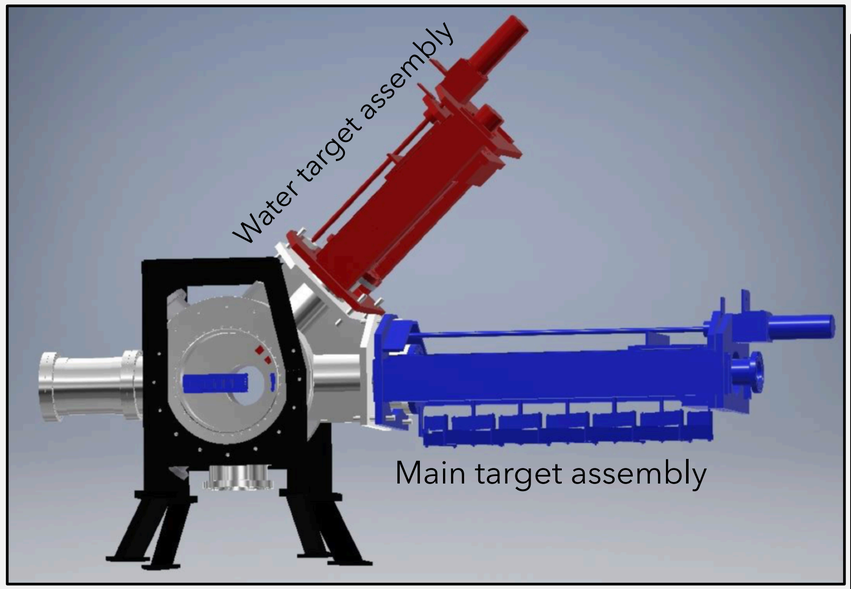


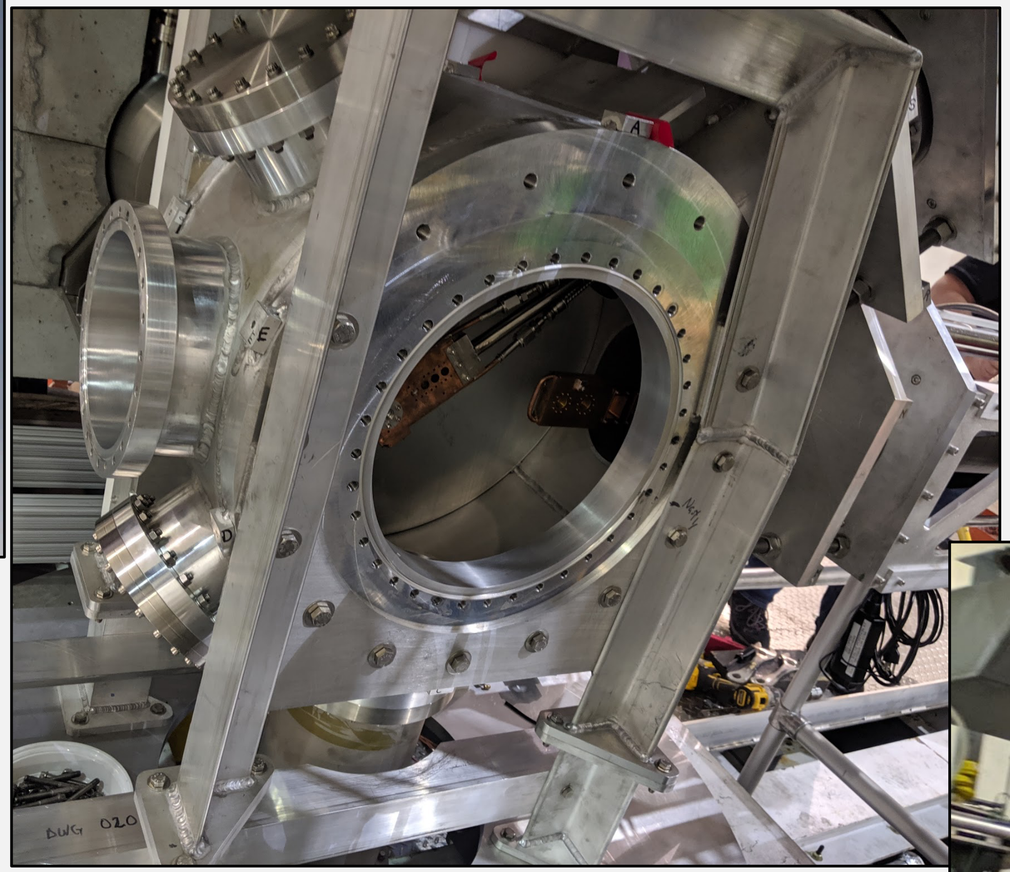
- Septum magnet needed to reach the low angles
- Vacuum vessel to transport scattered electrons in vacuum to detector hut
- Precision collimators to define the acceptance
- The experimental hall provides unique challenges for a high luminosity, high Z, low energy experiment
- Large angle scattered electrons need to be stopped close to the target and that region needs to be heavily shielded
- Electronics inside the hall need to be protected from both the electromagnetic and neutron radiation damage that will stop it from functioning properly

- Tight acceptance, space requirements, collimator power, shielding made for tricky installation

(acknowledgements to Hall A designers and the Hall A technical staff)

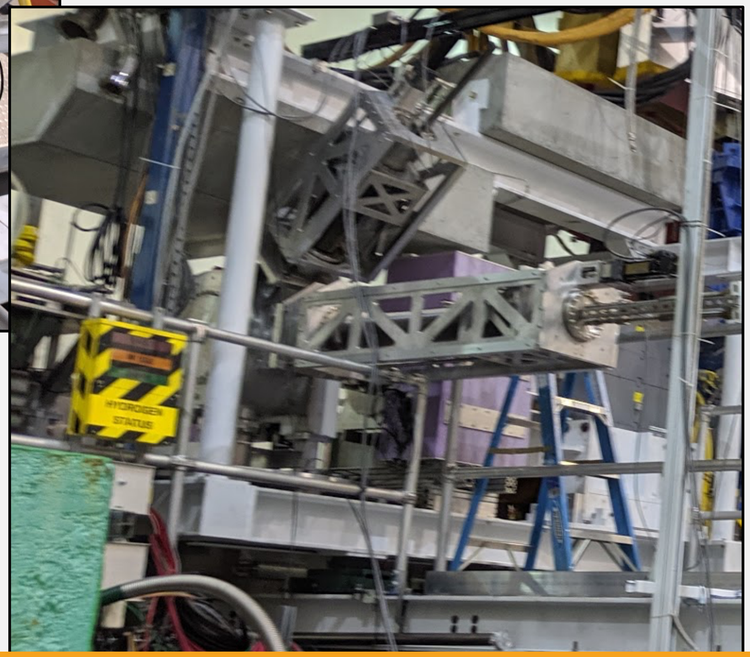
Target Chamber Design





Watercell target



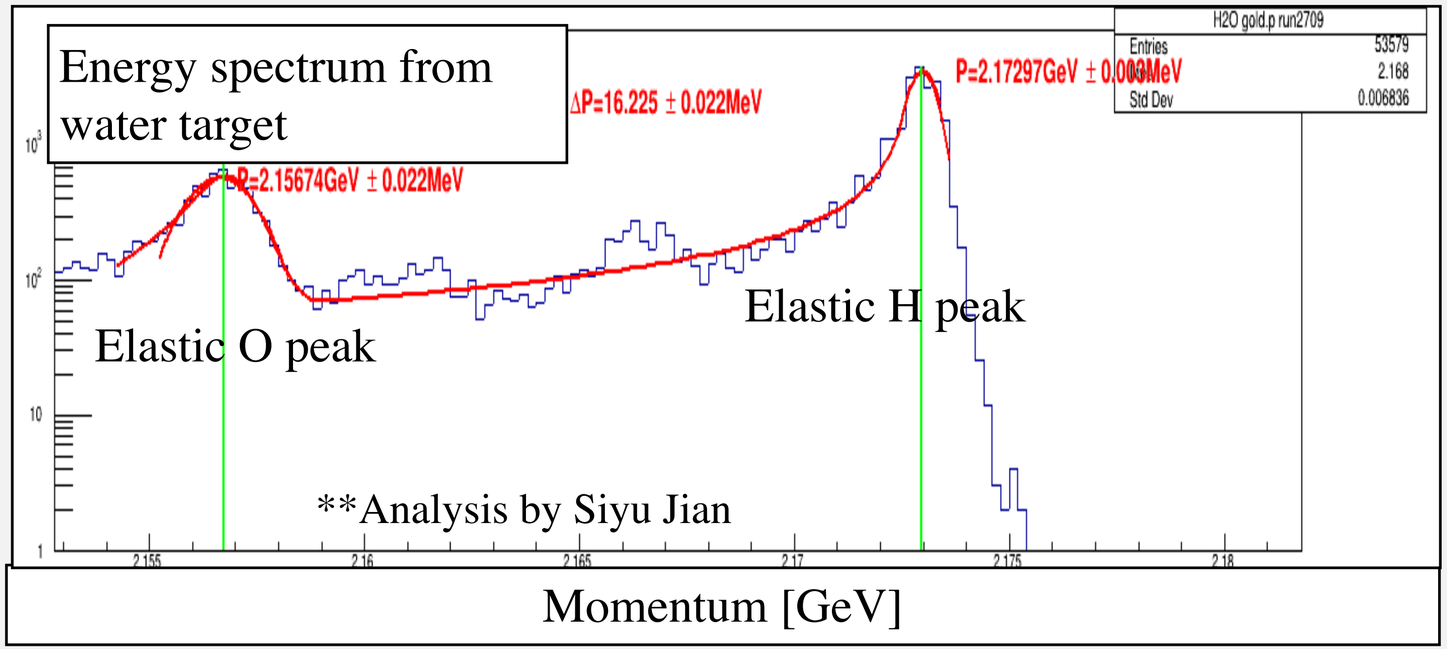


- Long horizontal target ladder
- 45^0 optics ladder

An important addition is the water cell absolute angle calibration

Challenging system, successfully implemented by the target group (esp. Dave Meekins)

Absolute Angle Calibration - Watercell



- Critical to measure the absolute scattering angle to high precision
- Nuclear recoil method
- ^{1}H and ^{16}O in one target (same E-loss) provides straightforward measurement of angle, insensitive to other calibrations

$$A_{PV} \approx \frac{G_F Q^2}{4\pi\alpha\sqrt{2}} \frac{Q_W F_W(Q^2)}{Z F_{ch}(Q^2)}$$

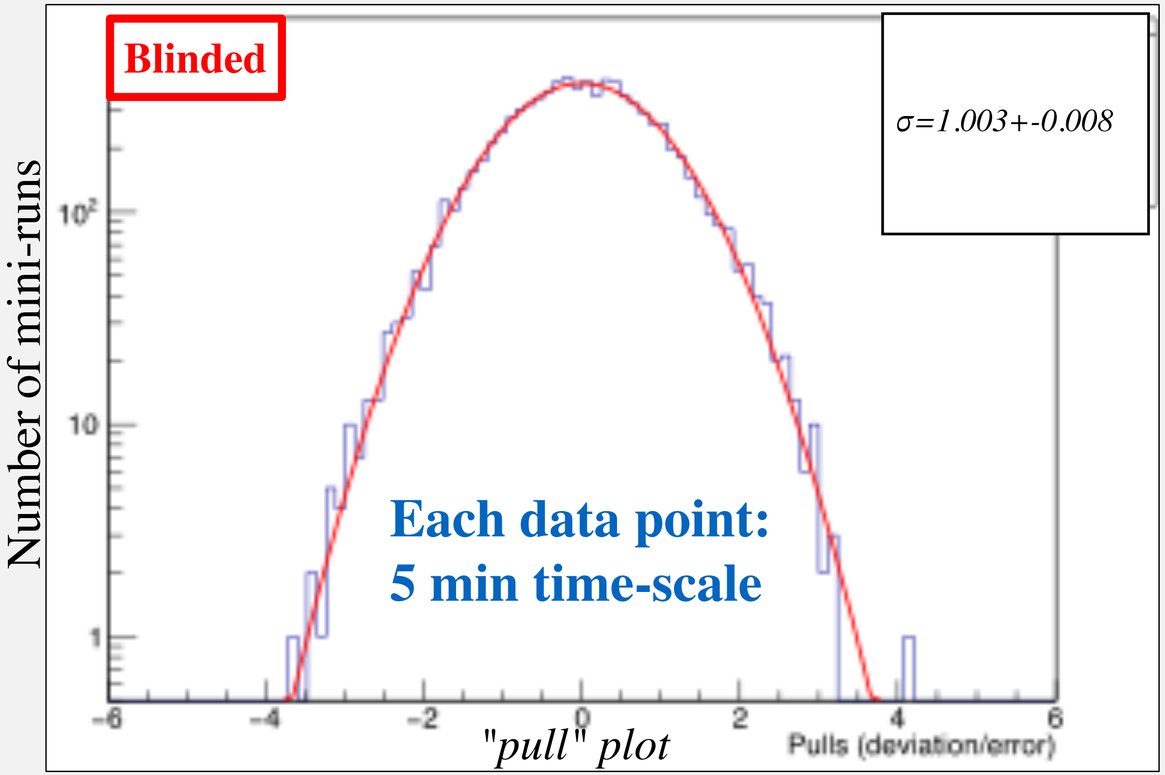
recoil momentum difference ⟶ scattering angle

$$\Delta E' = E'_O - E'_H = E\left(\frac{1}{1+\frac{2E\sin^2(\frac{\theta}{2})}{M_O}} - \frac{1}{1+\frac{2E\sin^2(\frac{\theta}{2})}{M_H}}\right)$$

Determined central angle with pointing with precision of
$\delta\theta = 0.02^0$ (0.45%)

Data Overview: Corrected Asymmetry

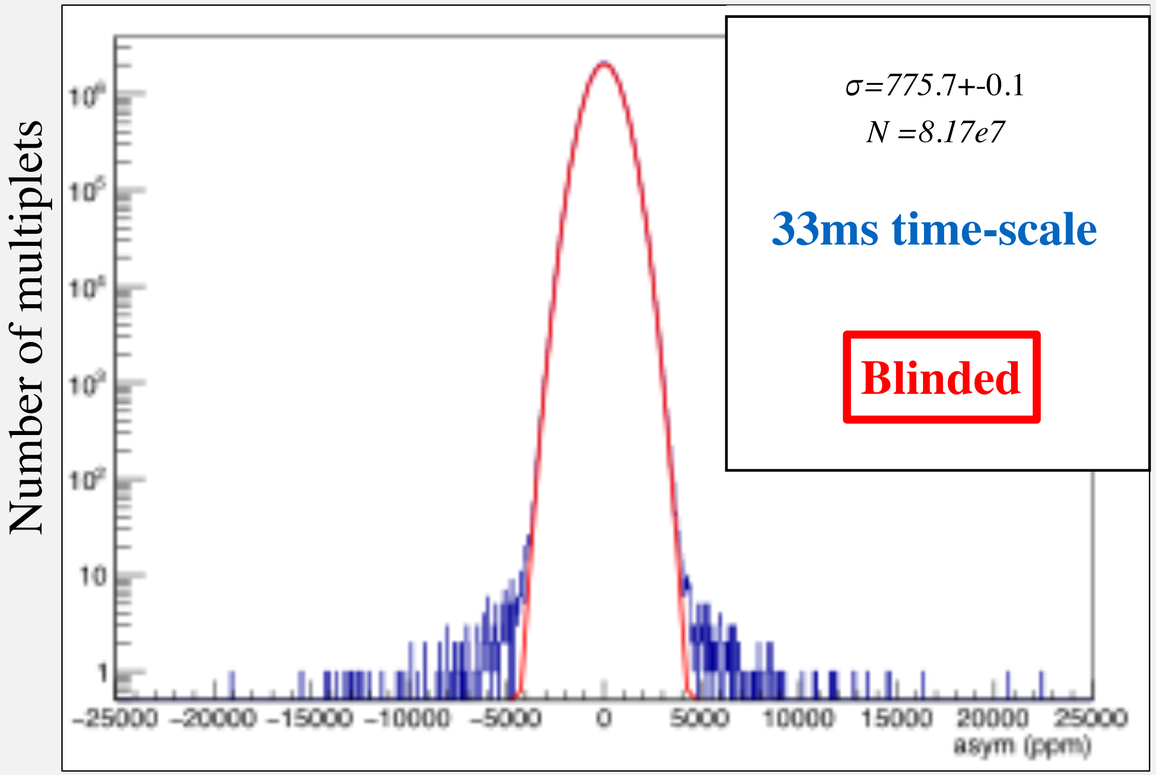
Miniruns



Normalized difference from average

- Check that we know how to calculate statistical errors
- 1σ pull plot width confirms we do

Individual quartets (>135μA, 120Hz)



Multiplet Asymmetry(ppm)

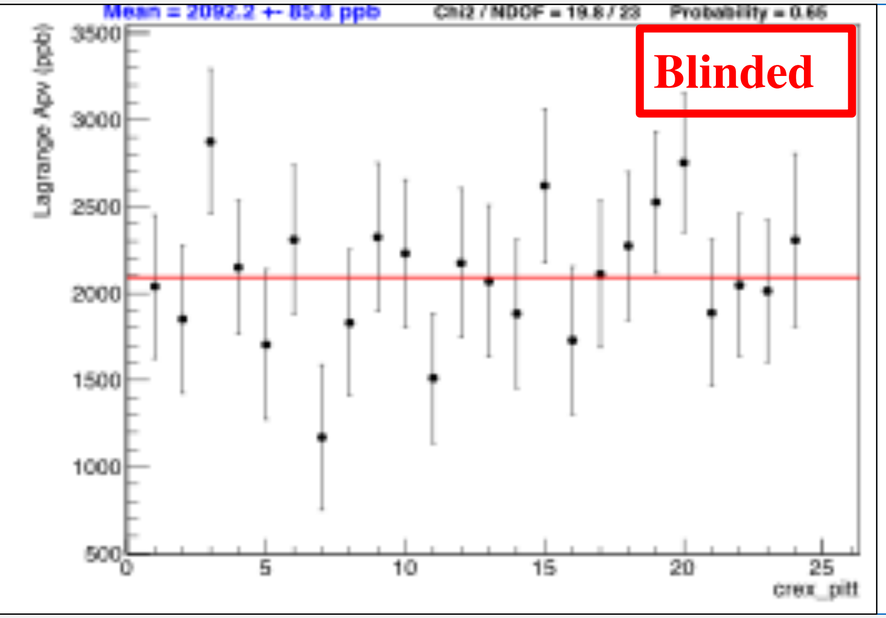
- Check at time scale of helicity flips, we don't have bizarre tails
- Extremely consistent widths, negligible tails, gaussian up to 5 OOM

Data Overview: Corrected & Null Asymmetry

Each data point: 2 days time-scale

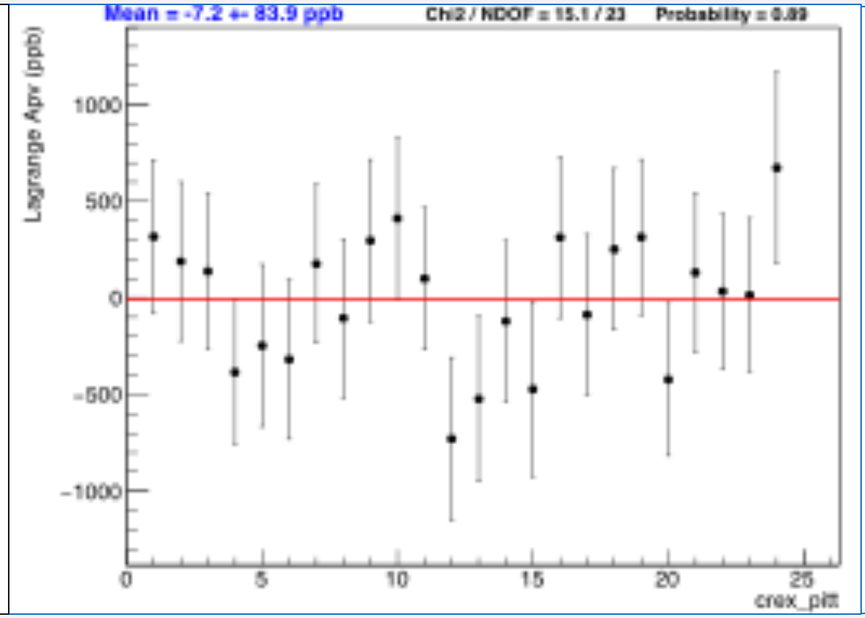
Corrected Asymmetry

Averaged over IHWP states

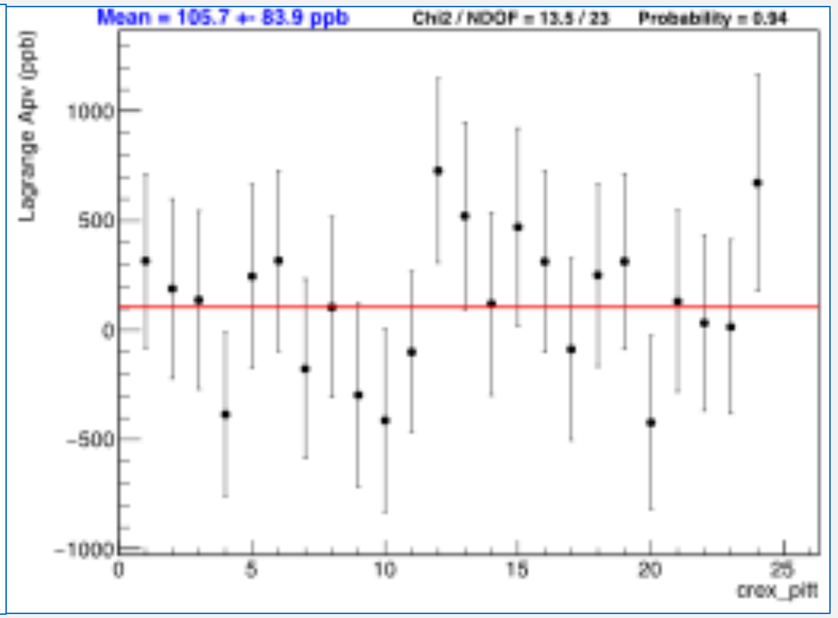


Null Asymmetry

Null Pitt (no Wien flip)



Null Pitt (Wien flip)



$$A_{null} = \frac{A_{IN} - A_{OUT}}{2}$$

Extracting A_{PV}

$$A_{phys} = R_{radcorr}\, R_{accept}\, R_{Q^2} \frac{A_{corr} - P_L \sum_i f_i A_i}{P_L(1 - \sum_i f_i)}$$

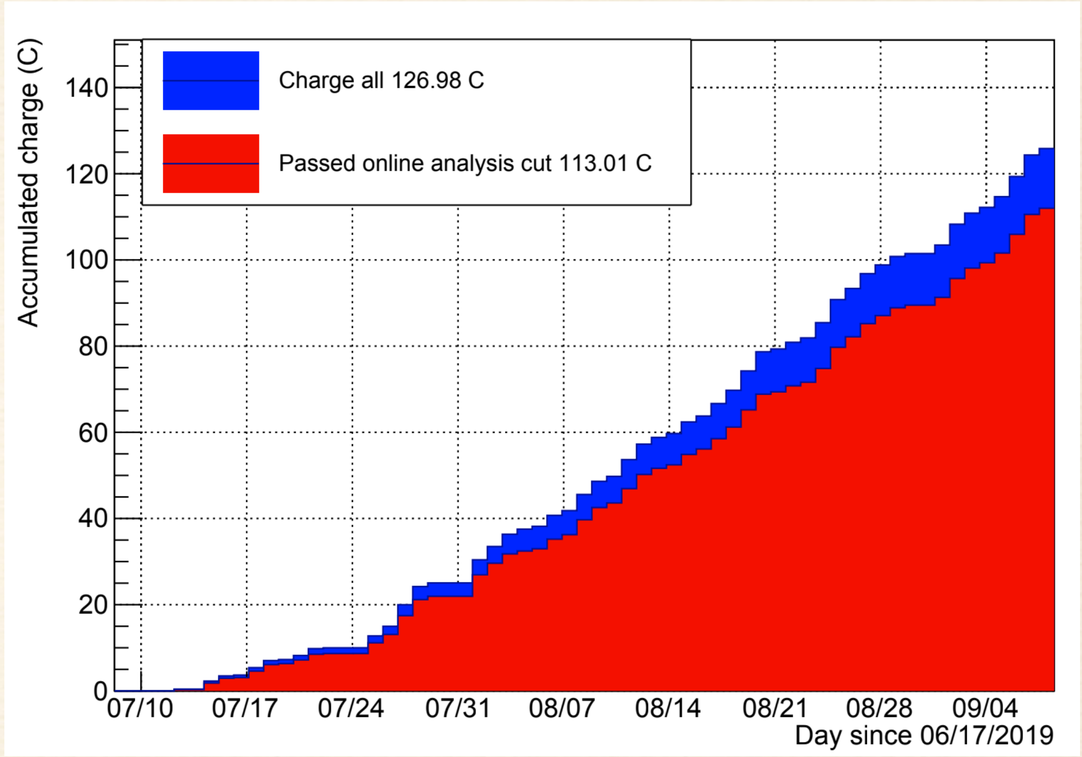
$$A_{corr} = A_{det} - A_{beam} - A_{trans} - A_{nonlin} - A_{blind}$$

A_{phys} extraction requires effort on multiple fronts:

- $R_{radcorr}$ (radiative correction)
- R_{accept} (acceptance)
- R_{Q2} (Q^2-scaling)
- P_L (beam polarization)
- $\frac{1}{1 - \sum_i f_i}$ (Overall background dilution)
- $P_L \sum_i f_i A_i$ (backgrounds)
- A_{corr} (Corrected Asymmetry)
- A_{beam} (Beam corrections)
- A_{trans} (Transverse asymmetry correction)
- A_{nonlin} (Detector nonlinearity)
- A_{blind} (Blinding factor)

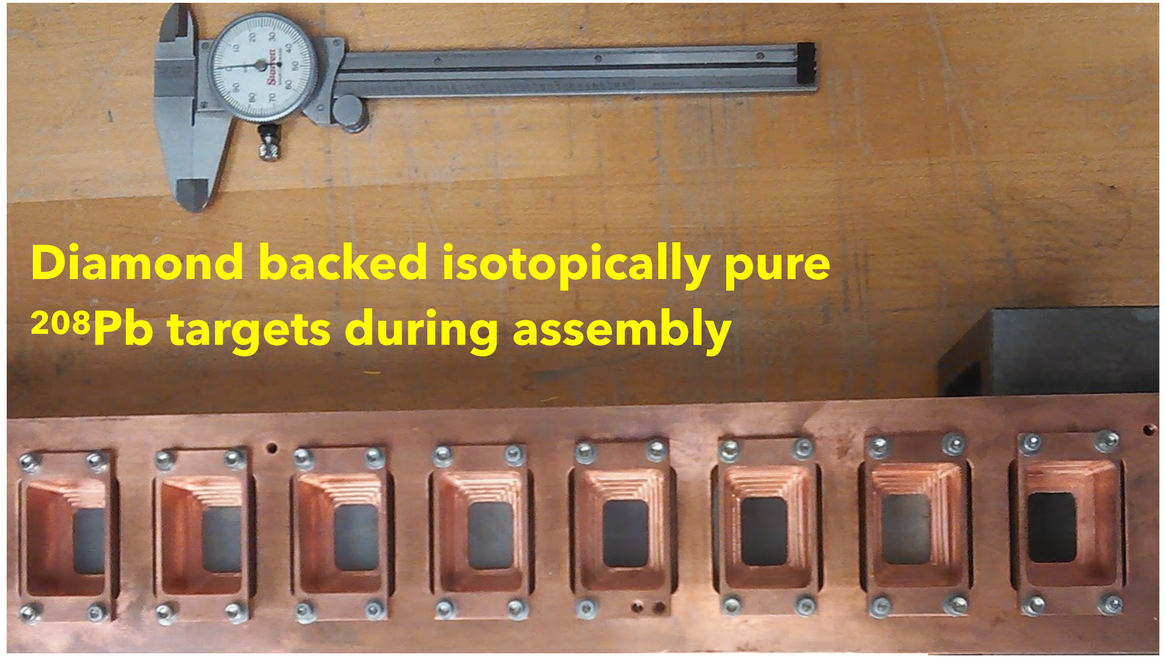
PREX-II Run: Summer 2019

- 13 Ph.D. students, 7 postdocs, a total of about 80 scientists
- Very close watch on-line data stream - beam conditions, detector response, etc.
- Frequent contact with machine operators to maintain running conditions
- “prompt" analysis flagged subtle problems: review of beam performance by PhD students in weekly shifts

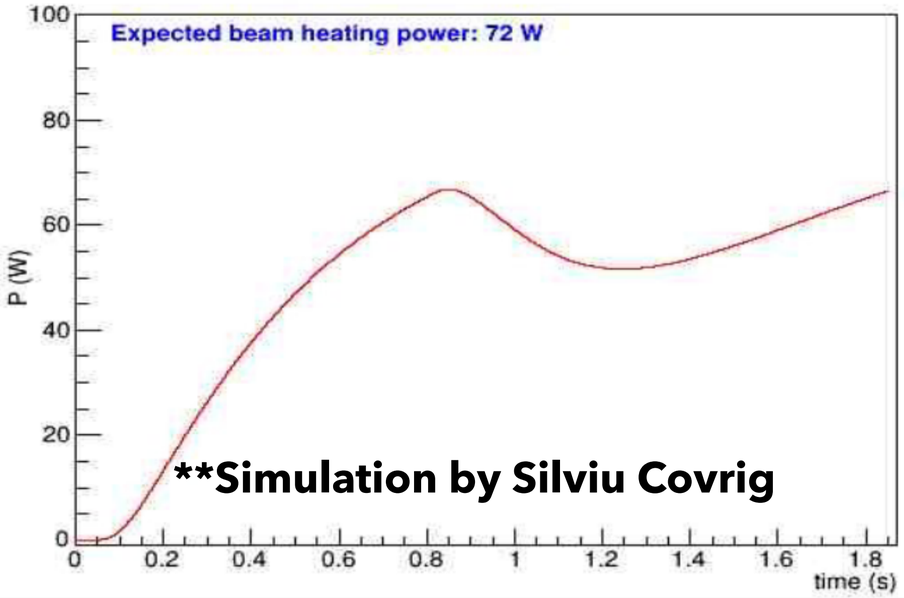


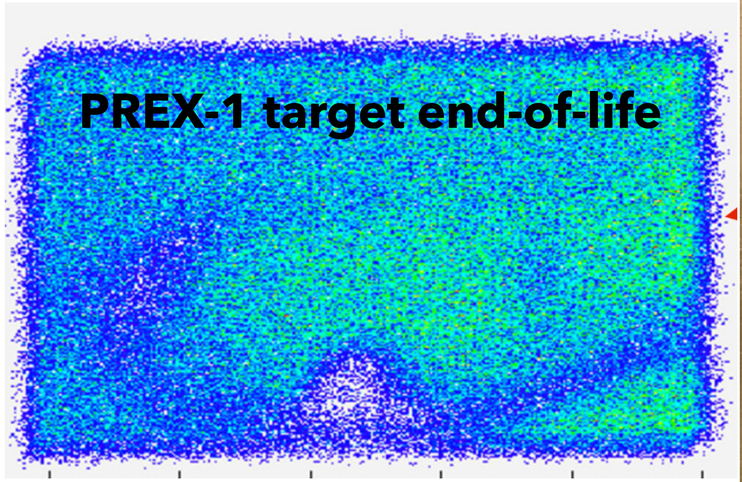
- At the end of the experiment after our realtime analysis we collected about 113 C of charge on target with only about 14 C being excluded in calibrations or due to poor beam conditions (mostly, trip recovery, beam excursions, or beam monitor issues)

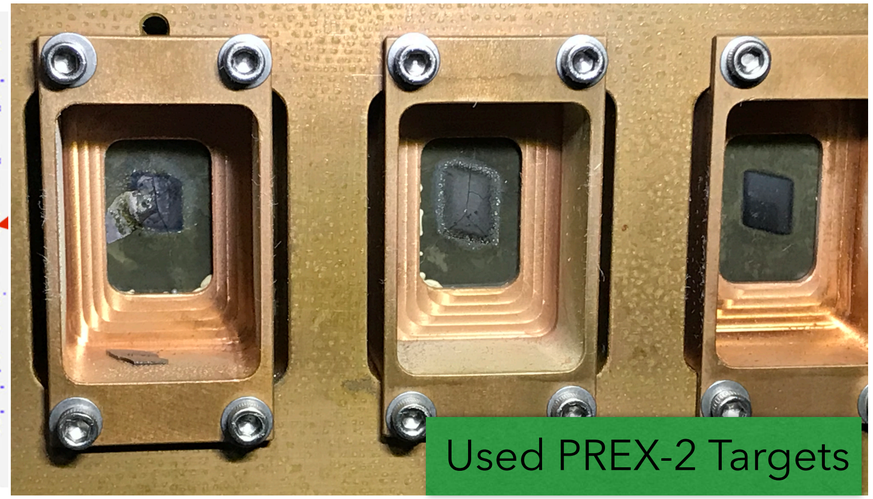
^{208}Pb Target



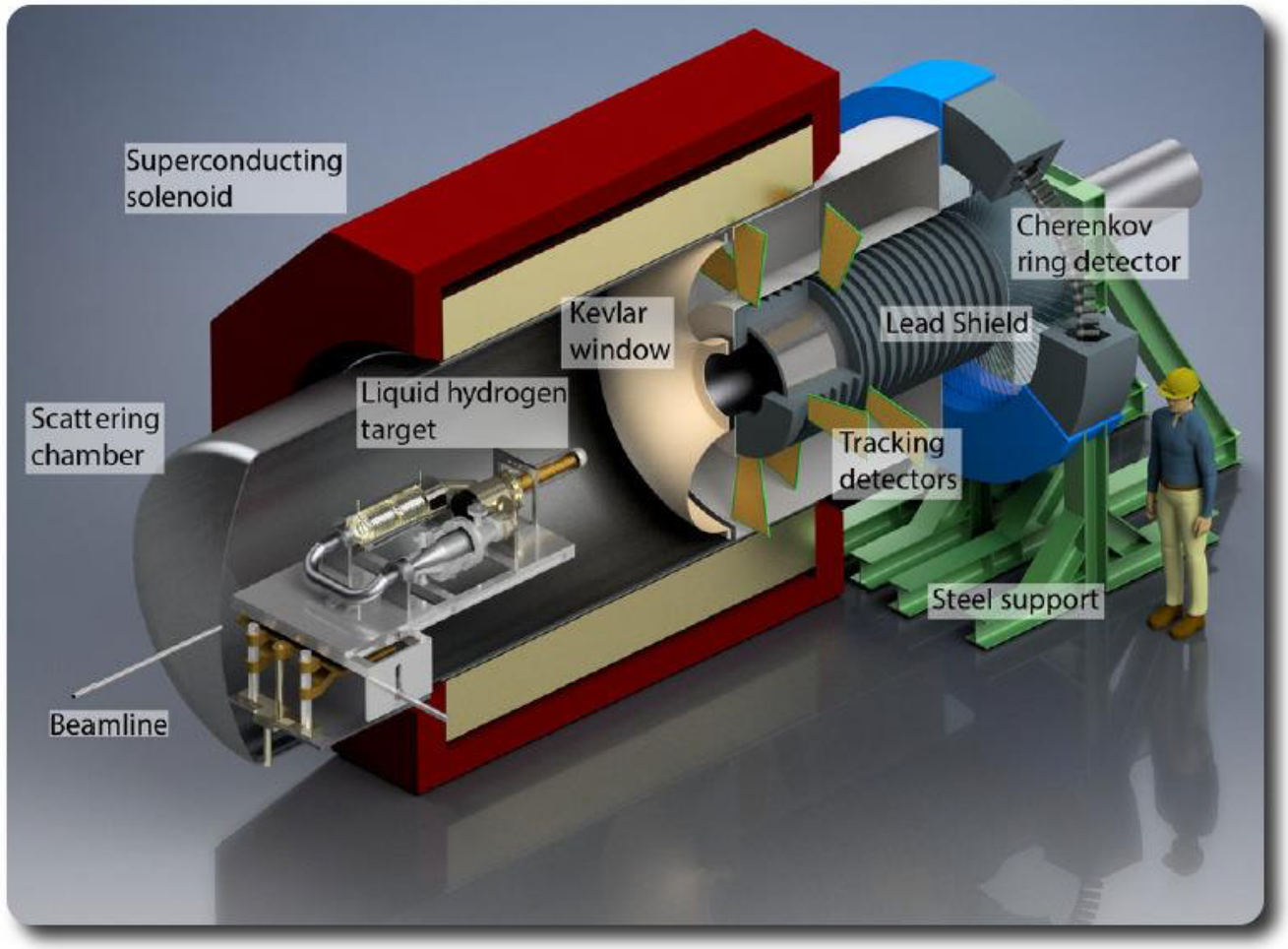
- Diamond-lead-diamond sandwich targets were used to get heat out of the target to cryocooling
- Diamond eventually breaks down, and lead is damaged
- PREX-1 proved concept and demonstrated target lifetime
- For PREX-2 we prepared a complement of 10 isotopically pure targets (used 6, as expected)
- Simulations predicted approximately 72 W of power deposition from the 70 μA rastered beam



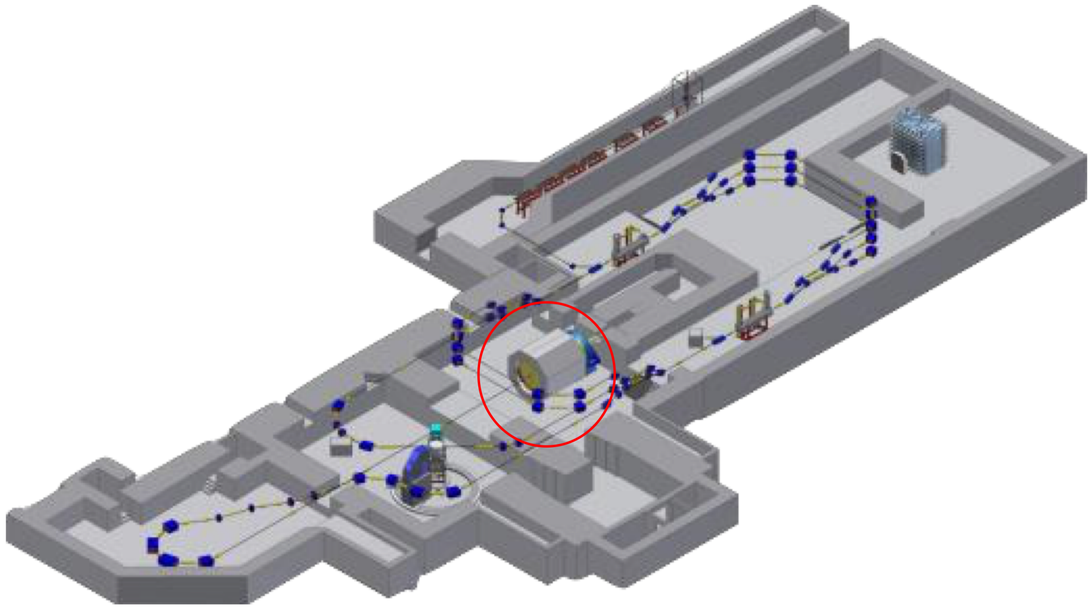




Future: MREX at MESA (Mainz)



MREX



$\Delta\theta$=4° : expected rate = 8.25 GHz, A_{pv} = 0.66 ppm, P = 85%, Q ≈ 86 MeV

1440h → $\delta R_n/R_n$ = 0.52% (^{208}Pb @ 155 MeV)

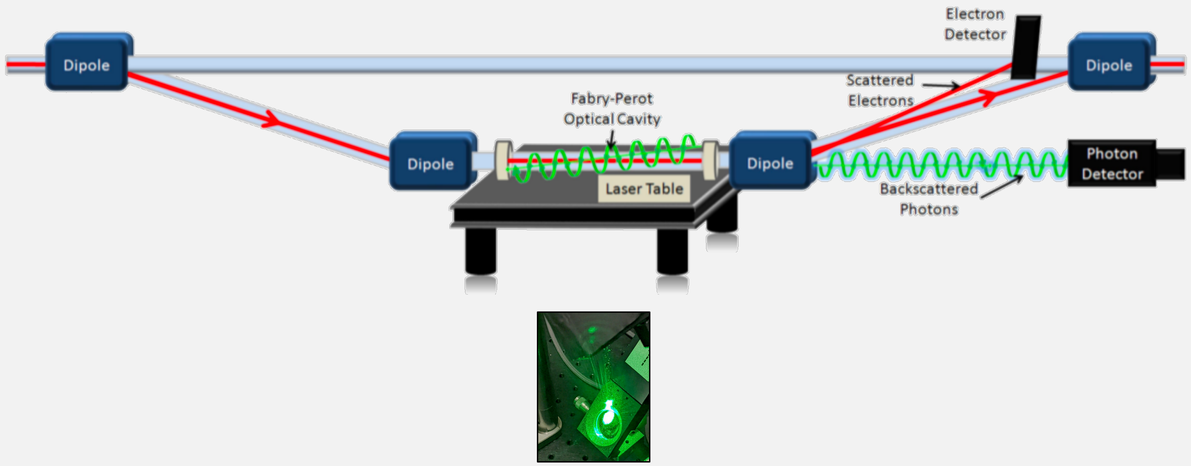
➢ $\delta R_n/R_n$ = 0.5%
→ L ± 20 MeV

Concettina Sfienti, Michaela Thiel

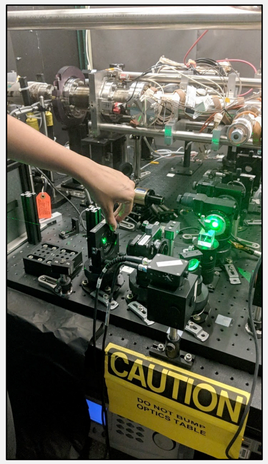
Goal: $\delta R_{n\text{-}p} \sim 0.03$ fm

Beam Polarization

Compton Polarimetry

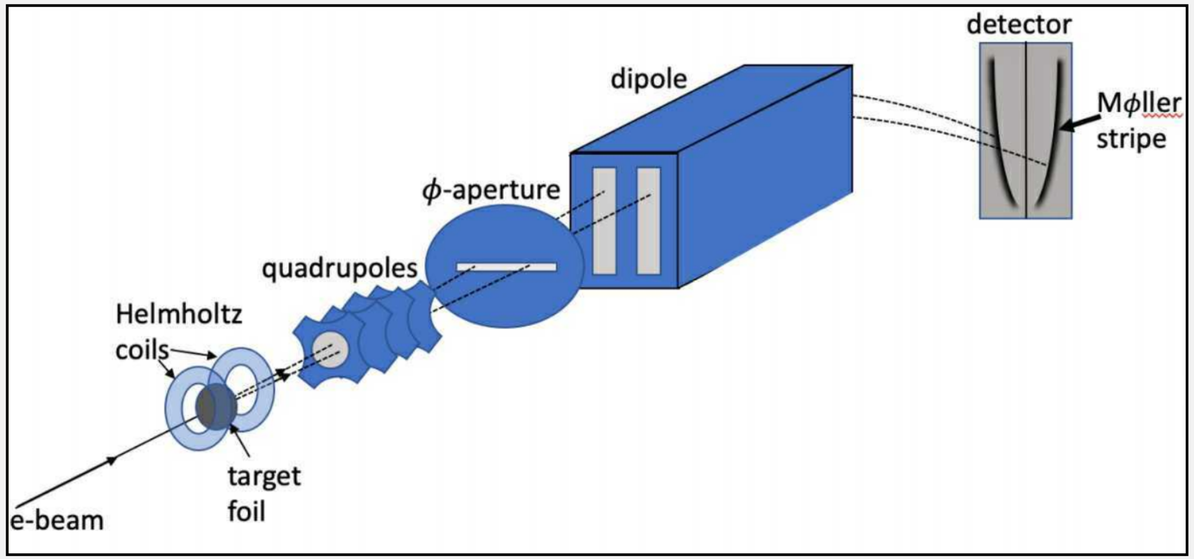


Acknowledgments: D. Gaskell, A. Premithilake A.J. Zec, J. C. Cornejo, M. Dalton, C. Gal, C. Palatchi, K. Paschke,, B. Quinn



- Continuous, non-invasive measurement
- Utilized integrating technique with photon detector
- Evaluated systematic uncertainty
- Polarimeter runs taken continuously alongside main detector data

Moller Polarimetry



Acknowledgments: S. Malace, E. King, D. Jones, P. Souder

- Low-current, invasive measurement
- 3-4T field provides saturated magnetization perpendicular to the foil
- Spectrometer redesigned for 11 GeV
- CREX reoptimized the spectrometer tune (and detector configuration), to provide high precision and sensitivity to systematic effects
- Polarimeter runs were taken approximately every week